Population ecology and decision analysis to inform seabird conservation

Amelia Jade DuVall

A dissertation

submitted in partial fulfillment of the

requirements for the degree of

Doctor of Philosophy

University of Washington

2025

Reading Committee:

Sarah J. Converse, Chair

Timothy E. Essington

T. Scott Sillett

Program Authorized to Offer Degree:

School of Aquatic and Fishery Sciences

University of Washington

Abstract

Population ecology and decision analysis
to inform seabird conservation

Amelia Jade DuVall

Chair of the Supervisory Committee:
Sarah J. Converse
School of Environmental and Forest Sciences, School of Aquatic and Fishery Sciences

Seabirds are among the most threatened vertebrate groups globally, facing a range of anthropogenic threats from invasive species and fisheries bycatch to increasingly pervasive climate-driven changes in ocean ecosystems. Despite the availability of proven conservation strategies, effective management of seabird populations is often constrained by ecological complexity, logistical challenges, and uncertainty in species-specific responses. Seabirds' long lifespans, low fecundity, and use of vast marine habitats create additional challenges for monitoring and decision-making. At the same time, these species play critical ecological roles as nutrient vectors and ecosystem indicators. As climate change alters the structure and productivity of marine environments, there is an urgent need to better understand how seabird populations

respond to environmental variability—and how that understanding can inform conservation decisions.

The research I present here explores the use of population ecology and decision analysis to evaluate seabird demography and improve conservation outcomes using case studies from the California Channel Islands, USA. First, I developed a novel daily nest survival model to assess how spatial and temporal variation in oceanographic conditions affect reproductive success for the Cassin's Auklet (*Ptychoramphus aleuticus*), a sentinel species of marine climate change (Chapter 2). I then extend this work by building an integrated population model to quantify how environmental drivers influence demographic rates, abundance, and population growth across two colonies and to determine the role of demographic buffering in population stability (Chapter 3). In a separate case study, I model marine and terrestrial drivers of nest survival for a rare seabird with a restricted breeding range, the Scripps's Murrelet (*Synthliboramphus scrippsi*), to support targeted management and conservation efforts (Chapter 4). Finally, I apply structured decision-making tools to evaluate uncertainty in seabird management and conservation, using constructed value of information to prioritize research and monitoring priorities across six species (Chapter 5). Together, this research shows how linking ecological modeling with decision analysis can improve seabird conservation under dynamic and uncertain conditions.

.

TABLE OF CONTENTS

Chapter 1. Introduction 13

1.1 Background 13

1.2 Research objectives 16

1.3 Broader impacts 18

1.4 References 21

Chapter 2. Differential Response of Nest Survival to Oceanographic Conditions for a Planktivorous Seabird 28

2.1 Abstract 28

2.2 Introduction 29

2.3 Methods 33

2.3.1 Study area and population 33

2.3.2 Nest monitoring 34

2.3.3 Daily nest survival model 35

2.3.4 Hypothesis testing 39

2.3.5 Model fitting and implementation 41

2.4 Results 42

2.5 Discussion 43

2.6 Acknowledgements 47

2.7 References 49

2.8 Tables and Figures 57

2.9 Appendix 2.1 65

2.10 Appendix 2.2 66

Chapter 3. Assessing the Impact of Ocean Climate Variability on Seabird Demography Using Integrated Population Modeling 68

3.1 Abstract 68

3.2 Introduction 69

3.3 Methods 74

3.3.1 Study area and population 74

3.3.2 Demographic data 75

3.3.3 Covariate data 76

3.3.4 Component models 77

3.3.5 Integrated population model 84
3.3.6 Model fitting and implementation 86
3.3.7 Population growth rate 87
3.3.8 Covariance between demographic parameters and population growth 88
3.4 Results 88
3.4.1 Survival model 89
3.4.2 Integrated population model 90
3.4.3 Population growth rate 92
3.4.4 Covariance between demographic parameters and population growth rate 93
3.5 Discussion 93
3.6 Acknowledgements 100
3.7 References 101
3.8 Tables and Figures 112
3.9 Appendix 3.1 123
3.10 Appendix 3.2 125
3.11 Appendix 3.3 128
Chapter 4. Disentangling Marine and Terrestrial Drivers of Nest Survival for a Rare Seabird 129
4.1 Abstract 129
4.2 Introduction 130
4.3 Methods 136
4.3.1 Study area and population 136
4.3.2 Nest monitoring 137
4.3.3 Covariate data 139
4.3.4 Daily nest survival model 140
4.3.5 Hypothesis testing 142
4.3.6 Model fitting and implementation 143
4.4 Results 143
4.5 Discussion 145
4.6 Acknowledgements 151
4.7 References 152
4.8 Tables and Figures 158

Chapter 5. Use of Constructed Value of Information to Identify Critical Uncertainties in Marine Bird Conservation 169

5.1 Abstract 169

5.2 Introduction 170

5.3 Methods 173

5.3.1 Participants and workshop format 173

5.3.2 Problem definition 174

5.3.3 Objectives 175

5.3.4 Alternatives 175

5.3.5 CVOI analysis 176

5.3.6 Sensitivity analysis 179

5.3.7 Personal confidence 180

5.4 Results 181

5.4.1 Ashy Storm-Petrel 181

5.4.2 California Brown Pelican 182

5.4.3 Cassin's Auklet 183

5.4.4 Scripps's Murrelet 184

5.4.5 Western Gull 185

5.4.6 Western Snowy Plover 186

5.4.7 Personal Confidence 187

5.5 Discussion 188

5.6 Acknowledgements 194

5.7 References 195

5.8 Tables and Figures 202

5.9 Appendix 5.1 230

5.10 Appendix 5.2 231

5.11 Appendix 5.3 234

LIST OF FIGURES

Figure 1.1 The eight islands that comprise the California Channel Islands archipelago in the Southern California Bight, USA. The five islands in Channel Islands National Park are San Miguel, Santa Rosa, Santa Cruz, Anacapa, and Santa Barbara islands. Santa Cruz Island is partly owned by The Nature Conservancy, and San Miguel Island is owned by the U.S. Navy but managed by Channel Islands National Park under agreement. 20

Figure 2.1 Daily values of z-scored oceanographic covariates included in the analysis during the study period, 1999 – 2022. Each panel shows a single year, with day-of-year on the x-axis and standardized z-scores on the y-axis. The regional covariate, Biologically Effective Upwelling Transport Index (BEUTI, purple), is the same at both colonies. The local covariates, sea surface temperature (SST), are different at each colony, Scorpion Rock (yellow) and Prince Island (blue). 61

Figure 2.2 Annual number of Cassin's Auklet nest attempts at Prince Island (blue) and Scorpion Rock (yellow), 1999–2022. Bars represent the total number of nest attempts each year colored by colony. There are more monitored artificial burrows at Prince Island (n = 72) than at Scorpion Rock (n = 35). 62

Figure 2.3 Posterior density plots from daily nest survival model, including: a) State-specific daily nest survival probability for egg and chick state; b) Probability of reproductive success for Scorpion Rock (yellow) and Prince Island (blue), defined as proportion of nests that fledged a chick relative to all nests that were monitored less those that were censored; and c) Average nest initiation dates (day of year) for Scorpion Rock (yellow) and Prince Island (blue). 63

Figure 2.4 Predicted daily nest survival probability for Cassin's Auklets as a function of sea surface temperature (°C) at Scorpion Rock (yellow) and Prince Island (blue). Solid lines represent chick-state survival; dotted lines represent egg-state survival. Shaded areas indicate 95% Bayesian credible intervals derived from posterior samples. Typical SSTs in Southern California range from 14–22°C. 64

Figure 3.1 State-transition diagram used in integrated population model. The model includes 11 discrete life history stages grouped into biologically meaningful categories: fledglings (stage 1), yearlings (stage 2), non-breeders (stages 3-4), breeders (stages 5-9), and skippers (stages 10-11). Transitions between stages are governed by survival probabilities for adults ϕ and juveniles ϕjuv and state transition probabilities ψ, including recruitment of pre-breeders to breeders ψnew, the probability of a breeder remaining as a breeder if they bred in the previous year ψII, and the probability of a skipper returning as a breeder ψOI. Individuals die with probability $1 - \phi *$, with the corresponding adult or juvenile survival rate depending on the life stage. See Table 3.2 for definition of demographic parameters. Here, the symbol for juvenile survival, $\phi juvenile$, and the pre-breeder

transition, $\psi newbreeder$, have been shortened to ϕjuv and ψnew, respectively, due to space constraints. 118

Figure 3.2 Estimated population structure and abundance of auklets at Scorpion Rock and Prince Island from 1999 – 2022. Stacked area plots show the posterior mean abundance of each stage (estimated number of auklets, identified by color in the legend) as estimated by the integrated population model. 119

Figure 3.3 Time series of fecundity and adult survival for auklet colonies at Scorpion Rock (yellow) and Prince Island (blue). Shaded bands represent 95% credible intervals from the integrated population model posterior distributions. Survival estimates represent annual adult survival from year *t* to *t*+1 and are plotted at the starting year of the interval (e.g., 1999 = survival from 1999 to 2000). Fecundity reflects the mean number of fledglings produced per breeding pair in year *t* and is plotted in the year observed. 120

Figure 3.4 Annual population growth rate λ of auklets at Scorpion Rock (yellow) and Prince Island (blue), 1999 – 2022. Lines represent the posterior mean annual population growth rate for each island, as estimated by the integrated population model, with shaded bands indicating the 95% Bayesian credible interval. The horizontal dashed line at $\lambda = 1.0$ represents stable growth (i.e., neither decreasing nor increasing). 121

Figure 3.5 Posterior distributions of correlations among demographic parameters and population growth rate (lambda, λ) for Scorpion Rock (yellow) and Prince Island (blue). Top: Correlation between fecundity in year *t* and λ in year *t*. Middle: Correlation between adult survival in year *t* to *t*+1 and λ in year t. Bottom: Correlation between survival and fecundity within the same year *t*. 122

Figure 4.1 Santa Barbara Island, Channel Islands National Park with the locations of long-term Scripps's Murrelet nest monitoring plots (*n* = 6): Arch Point North Cliffs, Bunkhouse, Cat Canyon, Dock, Landing Cove, and Nature Trail. 164

Figure 4.2 Scripps's Murrelet nest attempts at six monitoring plots on Santa Barbara Island over the study period, 1988 – 2019. Bars indicate the total number of monitored nest attempts, partitioned and colored by general nesting habitat: artificial/manmade habitat (orange), rocky crevice habitat (brown), and native shrub habitat (green). 165

Figure 4.3 Time series of continuous covariates used in the daily nest survival model. Values are z-scored within each covariate. Dotted lines represent linear trends over the time series period, 1988 – 2019. Variables include: *winter precipitation* (November in year *t*-1 to February in year *t*), *spring precipitation* (March to May in year *t*), *spring temperature* (March to May in year *t*), *pre-breeding season upwelling* (as measured by the Biologically Effective Upwelling Transport Index [Jacox et al. 2018]; January to March in year *t*), and *breeding season upwelling* (April to June in year *t*). See section 4.3.3 and Table 4.1 for more information on covariate data and hypotheses tested using covariate data. Note that we do not plot the covariate for the *previous winter precipitation*

hypothesis since it is the same as the data for the winter precipitation hypothesis but lagged by one year. 166

Figure 4.4 Posterior distributions of covariate effects on Scripps's Murrelet daily nest survival across six monitoring plots at Santa Barbara Island, 1988 – 2019. Plot are faceted by covariate type: weather (previous winter precipitation, winter precipitation, spring precipitation, spring temperature), marine (pre-breeding upwelling, breeding upwelling), and habitat (artificial habitat, crevice habitat). Note that covariate results for nesting habitat type variables are relative to the reference habitat type, native shrub habitat. Violin plots show the estimated effect sizes (posterior distributions) for each covariate, with black dots identifying the posterior means. Violin plots to the left of the dashed line (x = 0) indicates a negative relationship with daily nest survival; plots to the right indicate a positive relationship. 167

Figure 4.5 Posterior distribution of predicted hatching probability under three contrasting weather scenarios. Scenarios are created using standardized values (±2 standard deviations) for covariates reflecting *previous winter precipitation*, *winter precipitation*, *spring precipitation*, and *spring temperature*. The "Best Case" scenario reflects a dry previous winter, a dry recent winter, and warm and wet spring – conditions associated with higher nest survival. The "Worst Case" scenario reflects a wet previous winter, a wet recent winter, and a dry and cold spring – conditions associated with lower nest survival. The "Mean" scenario uses average conditions across all weather covariates (with the mean set to 0). Black dots indicate posterior means..... 168

Figure 5.1 Ashy Storm-Petrel (ASSP): Mean CVOI (constructed value of information; x-axis) and *reducibility* (y-axis) for each alternative threat hypothesis (n = 28). Each point represents the mean across experts with the horizontal bars representing estimated standard error for CVOI and the vertical bars representing estimated standard error for *reducibility*. Hypotheses are labeled by the hypothesis number, and colored based on the threat category shown in the legend. The vertical dashed black bar represents the median *reducibility* across all hypotheses for this species; the horizontal dashed black bar represents the median CVOI across all hypotheses for this species. See Table 5.2 for hypothesis names and descriptions. 222

Figure 5.2 California Brown Pelican (BRPE): Mean CVOI (constructed value of information; x-axis) and *reducibility* (y-axis) for each alternative threat hypothesis (n = 28). Each point represents the mean across experts with the horizontal bars representing estimated standard error for CVOI and the vertical bars representing estimated standard error for *reducibility*. Hypotheses are labeled by the hypothesis number, and colored based on the threat category shown in the legend. The vertical dashed black bar represents the median *reducibility* across all hypotheses for this species; the horizontal dashed black bar represents the median CVOI across all hypotheses for this species. See Table 5.2 for hypothesis names and descriptions. 223

Figure 5.3 Cassin's Auklet (CAAU): Mean CVOI (constructed value of information; x-axis) and *reducibility* (y-axis) for each alternative threat hypothesis (*n* = 28). Each point represents the mean across experts with the horizontal bars representing estimated standard error for CVOI and the vertical bars representing estimated standard error for *reducibility*. Hypotheses are labeled by the hypothesis number, and colored based on the threat category shown in the legend. The vertical dashed black bar represents the median *reducibility* across all hypotheses for this species; the horizontal dashed black bar represents the median CVOI across all hypotheses for this species. See Table 5.2 for hypothesis names and descriptions. 224

Figure 5.4 Scripps's Murrelet (SCMU): Mean CVOI (constructed value of information; x-axis) and *reducibility* (y-axis) for each alternative threat hypothesis (*n* = 28). Each point represents the mean across experts with the horizontal bars representing estimated standard error for CVOI and the vertical bars representing estimated standard error for *reducibility*. Hypotheses are labeled by the hypothesis number, and colored based on the threat category shown in the legend. The vertical dashed black bar represents the median *reducibility* across all hypotheses for this species; the horizontal dashed black bar represents the median CVOI across all hypotheses for this species. See Table 5.2 for hypothesis names and descriptions. 225

Figure 5.5 Western Gull (WEGU): Mean CVOI (constructed value of information; x-axis) and *reducibility* (y-axis) for each alternative threat hypothesis (*n* = 28). Each point represents the mean across experts with the horizontal bars representing estimated standard error for CVOI and the vertical bars representing estimated standard error for *reducibility*. Hypotheses are labeled by the hypothesis number, and colored based on the threat category shown in the legend. The vertical dashed black bar represents the median *reducibility* across all hypotheses for this species; the horizontal dashed black bar represents the median CVOI across all hypotheses for this species. See Table 5.2 for hypothesis names and descriptions. 226

Figure 5.6 Western Snowy Plover (WSPL): Mean CVOI (constructed value of information; x-axis) and *reducibility* (y-axis) for each alternative threat hypothesis (*n* = 28). Each point represents the mean across experts with the horizontal bars representing estimated standard error for CVOI and the vertical bars representing estimated standard error for *reducibility*. Hypotheses are labeled by the hypothesis number, and colored based on the threat category shown in the legend. The vertical dashed black bar represents the median *reducibility* across all hypotheses for this species; the horizontal dashed black bar represents the median CVOI across all hypotheses for this species. See Table 5.2 for hypothesis names and descriptions. 227

Figure 5.7 *Personal confidence* by hypothesis across all priority species. Hypotheses are on the x-axis and *personal confidence* scores on the y-axis, from low *personal confidence* to high *personal confidence*. Violin plots for each hypothesis are colored by threat category,

shown in the legend below. Mean *personal confidence* by hypothesis is represented by a black dot. 228

Figure 5.8 *Personal confidence* by priority species across all hypotheses. Species codes are on the x-axis (ASSP = Ashy Storm-Petrel, BRPE = California Brown Pelican, CAAU = Cassin's Auklet, SCMU = Scripps's Murrelet, WEGU = Western Gull, and WSPL = Western Snowy Plover) and *personal confidence* scores on the y-axis, from low *personal confidence* to high *personal confidence*. Mean *personal confidence* by priority species is represented by a black dot. 229

LIST OF TABLES

Table 2.1 Bayes Factors (BF) for each covariate in the Cassin's Auklet daily nest survival model, indicating relative support for the covariate as a predictor of daily nest survival. BFs < 3 indicate no support, while BF > 150 indicate very strong support. Island and sea surface temperature (SST; local covariate) had BF equal to infinity due to being sampled in every model. There was little support for the Biologically Effective Upwelling Transport Index (BEUTI; regional covariate) or the interaction covariate. 58

Table 2.2 Posterior model weights for each model of Cassin's Auklet nest survival sampled in the analysis. Covariates in the model set included: island, sea surface temperature (SST; local covariate), Biologically Effective Upwelling Transport Index (BEUTI; regional covariate), and an interaction covariate (SST*BEUTI). 59

Table 2.3 Parameter estimates from the top supported model with island and local sea surface temperature (SST) fixed effects and year (with SD = σy) and week of year (with SD = σw) random effects. See Eq. 7 for a full description of the parameters. Note that $\beta 0egg$ and $\beta 0chick$ are back transformed to the probability scale for ease of interpretation. 60

Table 3.1 Hypotheses on the relationship between oceanographic conditions and auklet adult survival and breeding probabilities, and covariates used to test hypotheses in survival model. The code used to reference the hypotheses in the text is included in parentheses under the corresponding hypothesis name. 113

Table 3.2 Demographic parameters (name, symbol, definition) estimated in the integrated population model across the study period (1999 – 2022). Each parameter represents a key demographic process influencing auklet population dynamics, including stage-specific survival and breeding transitions. Parameter symbols are consistent with those presented in the model description (section 3.3.5) and figures. 114

Table 3.3 Bayes Factors (BF) for each covariate in the survival model, indicating relative support for the covariate as a predictor of adult survival and breeding transition probabilities. BFs < 3 indicate no support, while BF > 150 indicate very strong support. See Table 3.1 for detailed hypothesis descriptions. 115

Table 3.4 Posterior model weights for top 10 of 32 candidate survival model sampled in the analysis. Oceanographic covariates hypotheses in the model set included three covariate hypotheses on annual survival probabilities (*annual survival* hypothesis, *southern winter* hypothesis, *northern winter* hypothesis) and three covariate hypotheses on breeding transition probabilities (*annual breeding* hypothesis, *pre-season breeding* hypothesis). See Table 3.1 for detailed hypothesis descriptions. 116

Table 3.5 Posterior mean estimates and 95% Bayesian credible intervals (BCIs) for parameters included in the integrated population model. Estimates are included separately by island

when parameters were modeled as island-specific; otherwise, a single estimate is shown for both islands combined. See Table 3.2 for definitions of demographic parameters. . 117

Table 4.1 Hypotheses on weather (*previous winter precipitation* hypothesis, *winter precipitation* hypothesis, *spring precipitation* hypothesis, *spring temperature* hypothesis), marine, and habitat (*habitat type* hypothesis) drivers of Scripps's Murrelet nest survival, and covariates used to test each hypothesis in the daily nest survival model..... 159

Table 4.2 Number of Scripps's Murrelet monitored nest attempts by year (1988 – 2019) and plot (n = 6) at Santa Barbara Island. Years or plots without any monitoring data are indicate by a dash (-). Nest attempts are summed across plots for each year and bolded and italicized in the last column, Total. 161

Table 4.3 Parameter mean estimates and lower and upper 95% Bayesian credible interval bounds from Scripps's Murrelet daily nest survival model. See Eq. 24 for a full description of the parameters and section 4.3.3 for information on covariate data. All parameters are reported on the logit scale. 163

Table 5.1 Breeding marine species at Channel Islands National Park. Species are noted with an X if they were included in the original 1983 monitoring plan as well as if they were selected as a priority species due to their conservation status for this analysis. 203

Table 5.2 Alternative threat hypotheses (n = 28) evaluated for six priority species across eight threat categories. Each hypothesis is identified by a number and includes the hypothesized driver(s) of population change. 204

Table 5.3. Experts that participated in expert elicitation (n = 12). Four individuals did not attend the November 2022 workshop. 207

Table 5.4 Scoring rubric for *relevance (a)*, *relevance (b)*, *magnitude of uncertainty*, and *reducibility* for constructed value of information (CVOI) expert elicitation. *Relevance* is calculated as *relevance (a)* multiplied by *relevance (b)* and rescaled to 0 – 4. CVOI is the product of *magnitude of uncertainty* and *relevance*. We also include a scoring rubric for *personal confidence*. 208

Table 5.5 Ashy Storm-Petrel (ASSP): Mean and estimated standard error (SE) for CVOI (constructed value of information; *relevance * magnitude of uncertainty*) and *reducibility* and percentage of 1,000 bootstrapped samples falling into each priority quadrat for each threat hypothesis (n = 28). Priority quadrats were assigned based on the median CVOI and *reducibility* scores across hypotheses. NA indicates experts unanimously agreed the hypothesis was not relevant for this species. Highest priority hypothesis names are bolded and italicized (n = 8); bolded percentages represent the priority ranking of each hypothesis. 210

Table 5.6 California Brown Pelican (BRPE): Mean and estimated standard error (SE) for CVOI (constructed value of information; *relevance * magnitude of uncertainty*) and *reducibility*

and percentage of 1,000 bootstrapped samples falling into each priority quadrat for each threat hypothesis (*n* = 28). Priority quadrats were assigned based on the median CVOI and *reducibility* scores across hypotheses. NA indicates experts unanimously agreed the hypothesis was not relevant for this species. Highest priority hypothesis names are bolded and italicized (*n* = 8); bolded percentages represent the priority ranking of each hypothesis. 212

Table 5.7 Cassin's Auklet (CAAU): Mean and estimated standard error (SE) for CVOI (constructed value of information; *relevance * magnitude of uncertainty*) and *reducibility* and percentage of 1,000 bootstrapped samples falling into each priority quadrat for each threat hypothesis (*n* = 28). Priority quadrats were assigned based on the median CVOI and *reducibility* scores across hypotheses. NA indicates experts unanimously agreed the hypothesis was not relevant for this species. Highest priority hypothesis names are bolded and italicized (*n* = 8); bolded percentages represent the priority ranking of each hypothesis. 214

Table 5.8 Scripps's Murrelet (SCMU): Mean and estimated standard error (SE) for CVOI (constructed value of information; *relevance * magnitude of uncertainty*) and *reducibility* and percentage of 1,000 bootstrapped samples falling into each priority quadrat for each threat hypothesis (*n* = 28). Priority quadrats were assigned based on the median CVOI and *reducibility* scores across hypotheses. NA indicates experts unanimously agreed the hypothesis was not relevant for this species. Highest priority hypothesis names are bolded and italicized (*n* = 8); bolded percentages represent the priority ranking of each hypothesis. 216

Table 5.9 Western Gull (WEGU): Mean and estimated standard error (SE) for CVOI (constructed value of information; *relevance * magnitude of uncertainty*) and *reducibility* and percentage of 1,000 bootstrapped samples falling into each priority quadrat for each threat hypothesis (*n* = 28). Priority quadrats were assigned based on the median CVOI and *reducibility* scores across hypotheses. NA indicates experts unanimously agreed the hypothesis was not relevant for this species. Highest priority hypothesis names are bolded and italicized (*n* = 8); bolded percentages represent the priority ranking of each hypothesis. 218

Table 5.10 Western Snowy Plover (WSPL): Mean and estimated standard error (SE) for CVOI (constructed value of information; *relevance * magnitude of uncertainty*) and *reducibility* and percentage of 1,000 bootstrapped samples falling into each priority quadrat for each threat hypothesis (*n* = 28). Priority quadrats were assigned based on the median CVOI and *reducibility* scores across hypotheses. NA indicates experts unanimously agreed the hypothesis was not relevant for this species. Highest priority hypothesis names are bolded and italicized (*n* = 8); bolded percentages represent the priority ranking of each hypothesis. 220

DEDICATION

To Aadu Prakash,

who brought much-needed engineering expertise to wildlife research

and radiated joy and love for birds. We miss you.

Chapter 1. Introduction

1.1 Background

Seabirds are among the world's most threatened groups of vertebrates. Global populations have declined by nearly 70% since the mid-20th century (Paleczny et al. 2015), and nearly one-third of species are at imminent risk of extinction (Croxall et al. 2012, Dias et al. 2019). Broadly defined as avian species that breed on land and forage at sea, seabirds comprise more than 350 species inhabiting environments that span from the Arctic to the Antarctic (Young and Ballance 2023). Across their breeding colonies and foraging ranges, seabirds face a suite of anthropogenic pressures, such as invasive species at nesting sites (e.g., Spatz et al. 2023), fisheries bycatch (e.g., Anderson et al. 2011), and the accelerating impacts of climate change and extreme weather (e.g., Holt and Boersma 2022). Addressing these threats alone could help conserve an estimated 45% of the global seabird population and benefit millions of individual seabirds worldwide (Dias et al. 2019).

In many cases, management solutions that are effective for conserving seabird populations are already known. Though logistically challenging, the removal of invasive species at breeding colonies can improve reproductive success (Whitworth et al. 2013, Oppel et al. 2022) and adult survival (Nur et al. 2019), as well as facilitate recolonization of historic breeding sites or the establishment of new colonies (Whitworth et al. 2013, Bedolla-Guzmán et al. 2019, Barbraud et al. 2021). While implementing conservation actions at sea is often more challenging, mitigation measures such as bird-scaring lines (e.g., Melvin et al. 2014) to reduce fisheries bycatch can effectively increase seabird survival (Dasnon et al. 2022). In contrast, climate-driven threats remain especially difficult to manage directly, suggesting that the most effective strategy

may be to buffer populations against climate impacts using other proven conservation actions (Dias et al. 2019).

Despite the availability of proven conservation strategies, effective seabird conservation is often constrained by ecological complexity and practical limitations, such as the high costs of managing remote breeding grounds. For example, demographic parameters can respond slowly to management interventions, as seabirds are typically long-lived, late-maturing, and have low fecundity (Young and Ballance 2023). As a result, even when threats are reduced, population recovery can take decades (Jones 2010), and evidence of success may be difficult to detect in the short-term. Different life stages (e.g., egg, chick, fledgling, juvenile, adult, etc.) are also often vulnerable to different threats, meaning that conservation actions must address multiple demographic stages simultaneously. Compounding this, many seabird species disperse thousands of kilometers from their breeding grounds and use both national and international waters, requiring coordinated, cross-jurisdictional management to ensure protection throughout the full life cycle.

Seabird conservation is further complicated by limited accessibility for monitoring. Most seabird species return to land only to breed, which is when they are most available for study. Even then, many species nest on remote islands, cliffs, or offshore rocks that are difficult for humans to access and often can only be accessed during favorable weather conditions. In addition, species in several families (e.g., Procellariidae, Hydrobatidae, Alcidae) nest underground or in cavities, making direct observation challenging. These logistical constraints limit data collection and complicate long-term monitoring. The slow life histories of seabirds also require extended monitoring to estimate survival and detect population trends. Monitoring efforts are often hindered by low recapture rates and imperfect detection, leading to sparse

encounter histories and increased uncertainty in demographic estimates. Moreover, seabird reproduction can fluctuate widely from year to year due to environmental variability (Young and Ballance 2023). Distinguishing long-term trends from short-term stochasticity requires consistent, multi-year data.

Bayesian hierarchical modeling offers a powerful framework for analyzing seabird demographic data. Given the challenges of seabird monitoring, datasets often include incomplete observations, are missing observations entirely, or depend on information from various sources. Bayesian models provide a flexible framework for ecological systems characterized by sparse, noisy, and multi-stream data (Clark 2004) and can be used to estimate latent (i.e., unknown) variables that are only partially informed by data. By explicitly separating the biological (i.e., state) and observation processes (Hobbs and Hooten 2015), hierarchical models can be particularly useful for species with low or variable detection probabilities, where raw data would otherwise underestimate parameters such as abundance. Finally, the full posterior distributions obtained from Bayesian modeling allow uncertainty to be carried through all stages of inference, from parameter estimation to forecasting.

Similarly, the field of decision analysis is well suited for seabird management and conservation. Structured decision making (SDM) supports transparent, objective-driven decision processes in complex and uncertain contexts with multiple competing objectives (Runge et al. 2020, Hemming et al. 2022). SDM emphasizes the clear articulation of management goals, the systematic evaluation of alternative actions, and the explicit incorporation of uncertainty. It also facilitates value of information analysis (Williams and Johnson 2015), which can help determine whether it is better to act immediately or to invest in reducing uncertainty through additional data

collection – an especially important consideration in seabird management, where fieldwork is often expensive and logistically constrained.

1.2 Research objectives

Here, I use Bayesian hierarchical modeling and decision analysis to inform the conservation and management of seabirds. My research aims to evaluate how seabird monitoring data can be used across a range of applications—from guiding species-specific conservation actions to serving as indicators of broader marine ecosystem conditions.

The California Channel Islands, off the Southern California coast in the USA, provide an ideal location for this work (Figure 1.1). Five of the archipelago's eight islands fall wholly or partially within Channel Islands National Park (CHIS), and the National Park Service's Inventory and Monitoring Program has identified seabirds as key indicators of natural resource conditions (Cameron et al. 2005). Ecologically, the region is highly productive due to its location at the confluence of the cold California Current and the warm Southern California countercurrent. This dynamic transition zone supports a uniquely diverse assemblage of breeding seabirds associated with both cold-water and warm-water systems – a combination found nowhere else (Hunt Jr. et al. 1980).

At least sixteen seabird species with diverse foraging ecologies and life histories currently breed on the islands. The number of breeding species here is increasing, as tropical species expand their ranges northward and colonize new breeding sites, likely in response to ongoing marine climate change (Howard et al. 2024). In contrast, cold-water breeding species such as the Tufted Puffin (*Fratercula cirrhata*) and Rhinoceros Auklet (*Cerorhinca monocerata*) were likely occasional or intermittent breeders on the California Channel Islands during the 20th century (Hunt Jr. et al. 1980, McChesney et al. 1995) but have not been observed breeding there

for a few decades (NPS unpublished data). The California Channel Islands thus offer a valuable setting to investigate how seabird monitoring can inform conservation and long-term ecological assessment in the face of increasing oceanographic variability.

In Chapter 2, I develop a multi-event daily nest survival model for a planktivorous seabird, the Cassin's Auklet (*Ptychoramphus aleuticus)*, which has been identified as an ecosystem sentinel for the California Current system because it exhibits demographic responses to ocean conditions, such as sea surface temperature and upwelling, before other marine species (Wolf et al. 2010, Hazen et al. 2019, Clark-Wolf et al. 2024). To better understand spatial variation in demographic responses to environmental variability, I evaluate relationships between nest survival and oceanographic drivers for auklets at two colonies in CHIS that, while similar, are subject to differing marine conditions.

Since reproductive success tends to be more responsive to oceanographic variability but survival tends to be a more important parameter for seabird population viability (Young and Ballance 2023), I compare overall demographic viability of the two auklet colonies in Chapter 3 by building an integrated population model that links demographic rates (e.g., survival and fecundity) to abundance in a unified analysis (Besbeas et al. 2002). I evaluate hypotheses regarding the oceanographic drivers of adult survival and breeding transitions (i.e., the probability of breeding each year), and integrate the most supported model with results from Chapter 2 to model demographic parameters and abundance over time as a function of oceanographic variability.

In Chapter 4, I investigate marine and terrestrial drivers of nest survival for the Scripps's Murrelet (*Synthliboramphus scrippsi*), a rare seabird with a limited breeding range that is highly vulnerable to nest predation via an endemic mouse and other native avian species. Given the

limited management options available to mitigate oceanographic variability, I use a multi-state daily nest survival model to examine whether terrestrial factors, such as precipitation, can help predict years of elevated predation risk. By evaluating how murrelet nest success varies with environmental conditions, I aim to inform the use of targeted, proactive predator management in years where high predation risk is anticipated.

Finally, in Chapter 5, I use an SDM process to identify critical structural uncertainties regarding current and potential threats to seabirds across multiple islands within CHIS, and the potential of monitoring and management actions to address these threats. Using expert elicitation, I calculate constructed value of information (CVOI), a relatively new method for assessing value of information in data-poor situations (Runge et al. 2023), for six priority species and 28 hypotheses regarding threats. I then combine CVOI with information on the degree to which hypotheses may be reducible to identify the highest priority hypotheses that can be targeted through research and monitoring to most effectively improve conservation outcomes.

1.3 Broader impacts

Beyond their intrinsic value, seabirds play important ecological roles as nutrient vectors and ecological indicators of marine ecosystems (Young and Ballance 2023). Seabirds transport marine-derived nutrients via guano to land and nearshore environments, where such nutrients are often scarce or limiting, thereby providing a critical link between marine and terrestrial ecosystems. Nesting seabirds in mangrove ecosystems, for example, were shown to significantly enrich local food webs by delivering marine-derived nitrogen, resulting in broader dietary niches and increased body size for macroinvertebrate communities (Appoo et al. 2024). The recovery of seabird colonies following the eradication of invasive predators has similarly been associated with the restoration of nutrient subsidies and cascading ecological benefits in both terrestrial and

nearshore marine ecosystems, particularly in oligotrophic tropical systems (Graham et al. 2018, Benkwitt et al. 2021). Recent evidence shows that the return of seabird-derived nutrients can double coral reef growth rates and accelerate reef recovery, likely enhancing coral reef resilience to climate-driven disturbances (Benkwitt et al. 2023). Even in temperate ecosystems, where nutrient limitation is generally less pronounced, seabird-derived inputs appear to enhance ecosystem function and community composition (Healing et al. 2024). Together, these examples highlight that conserving seabird populations is not only essential for biodiversity, but also for sustaining key nutrient flows that underpin ecosystem resilience and productivity across land–sea boundaries.

Seabirds can also serve as ecological indicators for marine ecosystem health because their demography, behavior, and diet can reflect changes in ocean conditions before such changes are detectable in other components of the ecosystem (Piatt and Sydeman 2007, Parsons et al. 2008, Velarde et al. 2019). For example, the first clear signal of ecosystem disruption during the anomalously delayed upwelling in the California Current in 2005 was widespread breeding failure and colony abandonment of the Cassin's Auklet (Sydeman et al. 2006). Seabirds have also been used as indicators of fish stocks (Piatt and Sydeman 2007, Velarde et al. 2019). In the Gulf of California, seabird diet has been strongly correlated with commercial fish landings (Velarde et al. 1994) and can be used to predict catch-per-unit-effort for sardine and anchovy fisheries (Velarde et al. 2015). Likewise, Roth et al. (2007) found that reproductive success of seabirds at Southeast Farallon Island covaried with Chinook salmon (*Oncorhynchus tshawytscha*) abundance off central California, likely driven by a shared dependence on common prey. Understanding seabird relationships with forage fish dynamics or other commercially important species enhances their utility as indicators of ecosystem change and offers critical

insights for ecosystem-based fisheries management and conservation decision-making (Sydeman et al. 2017). However, seabirds are likely reflecting prey availability, not necessarily absolute abundance, and their responses are often non-linear, species-specific, and modulated by foraging constraint, life-history trade-offs, and lagged demographic effects (Cairns 1987, Piatt et al. 2007b). Thus, while seabirds hold promise as sentinels of marine ecosystem change, care must be taken to contextualize their responses within appropriate ecological, spatial, and temporal frameworks.

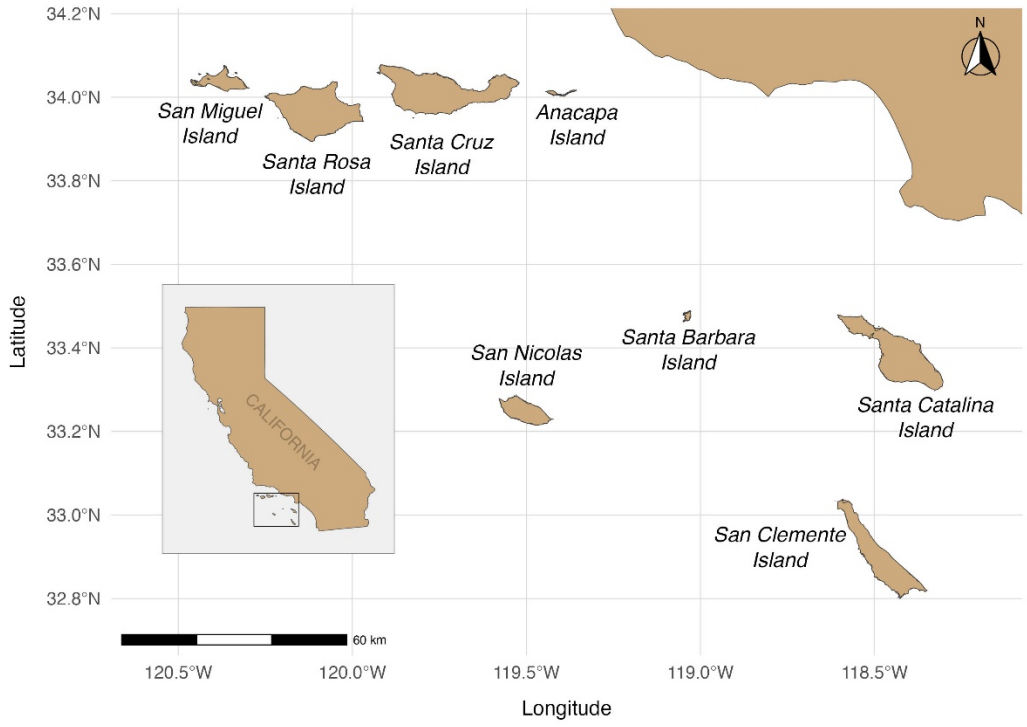

Figure 1.1 The eight islands that comprise the California Channel Islands archipelago in the Southern California Bight, USA. The five islands in Channel Islands National Park are San Miguel, Santa Rosa, Santa Cruz, Anacapa, and Santa Barbara islands. Santa Cruz Island is partly owned by The Nature Conservancy, and San Miguel Island is owned by the U.S. Navy but managed by Channel Islands National Park under agreement.

1.4 References

Anderson, O. R., C. J. Small, J. P. Croxall, E. K. Dunn, B. J. Sullivan, O. Yates, and A. Black. 2011. Global seabird bycatch in longline fisheries. Endangered Species Research 14:91–106.

Appoo, J., N. A. J. Graham, C. W. Jones, S. Jaquemet, and N. Bunbury. 2024. Seabird nutrient subsidy alters size and resource use of functionally important mangrove macroinvertebrates. Ecosphere 15:e70121.

Barbraud, C., K. Delord, F. Le Bouard, R. Harivel, J. Demay, A. Chaigne, and T. Micol. 2021. Seabird population changes following mammal eradication at oceanic Saint-Paul Island, Indian Ocean. Journal for Nature Conservation 63:126049.

Bedolla-Guzmán, Y., F. Méndez-Sánchez, A. Aguirre-Muñoz, M. Félix-Lizárraga, A. Fabila-Blanco, E. Bravo-Hernández, A. Hernández-Ríos, M. Corrales-Sauceda, A. Aguilar-Vargas, A. Aztorga-Ornelas, F. Solís-Carlos, F. Torres-García, L. Luna-Mendoza, A. Ortiz-Alcaraz, J. Hernández-Montoya, M. Latofski-Robles, E. Rojas-Mayoral, and A. Cárdenas-Tapia. 2019. Recovery and current status of seabirds on the Baja California Pacific Islands, Mexico, following restoration actions. Pages 531–538 in C. R. Veitch, M. N. Clout, A. R. Martin, J. C. Russell, and C. J. West, editors. Island invasives: scaling up to meet the challenge. Occasional Paper of the IUCN Species Survival Commission No. 62. IUCN, Gland, Switzerland.

Benkwitt, C. E., R. L. Gunn, M. Le Corre, P. Carr, and N. A. J. Graham. 2021. Rat eradication restores nutrient subsidies from seabirds across terrestrial and marine ecosystems. Current Biology 31:2704–2711.e4. https://doi.org/10.1016/j.cub.2021.03.104.

Benkwitt, C. E., C. D'Angelo, R. E. Dunn, R. L. Gunn, S. Healing, M. L. Mardones, J. Wiedenmann, S. K. Wilson, and N. A. J. Graham. 2023. Seabirds boost coral reef resilience. Science Advances 9:eadj0390. https://doi.org/10.1126/sciadv.adj0390.

Besbeas, P., S. N. Freeman, B. J. T. Morgan, and E. A. Catchpole. 2002. Integrating mark–recapture–recovery and census data to estimate animal abundance and demographic parameters. Biometrics 58:540–547.

Cairns, D. K. 1987. Seabirds as indicators of marine food supplies. Biological Oceanography 5(4):261–271.

Cameron, J. L., R. Sauvajot, D. Kamradt, and L. Lee. 2005. Mediterranean Coast Network Vital Signs Monitoring Plan. National Park Service. 102 pp.

Clark, J. S. 2005. Why environmental scientists are becoming Bayesians. Ecology Letters 8:2–14.

Clark-Wolf, T. J., K. A. Holt, E. Johansson, A. C. Nisi, K. Rafiq, L. West, P. D. Boersma, E. L. Hazen, S. E. Moore, and B. Abrahms. 2024. The capacity of sentinel species to detect changes in environmental conditions and ecosystem structure. Journal of Applied Ecology 61:1074–1086.

Croxall, J. P., S. H. M. Butchart, B. Lascelles, A. J. Stattersfield, B. Sullivan, A. Symes, and P. Taylor. 2012. Seabird conservation status, threats and priority actions: a global assessment. Bird Conservation International 22:1–34.

Dasnon, A., K. Delord, A. Chaigne, and C. Barbraud. 2022. Fisheries bycatch mitigation measures as an efficient tool for the conservation of seabird populations. Journal of Applied Ecology 59:1674–1685.

Dias, M. P., R. Martin, E. J. Pearmain, I. J. Burfield, C. Small, R. A. Phillips, O. Yates, B. Lascelles, P. G. Borboroglu, and J. P. Croxall. 2019. Threats to seabirds: A global assessment. Biological Conservation 237:525–537.

Graham, N. A. J., S. K. Wilson, P. Carr, A. S. Hoey, S. Jennings, and M. A. MacNeil. 2018. Seabirds enhance coral reef productivity and functioning in the absence of invasive rats. Nature 559:250–253.

Hazen, E. L., B. Abrahms, S. Brodie, G. Carroll, M. G. Jacox, M. S. Savoca, K. L. Scales, W. J. Sydeman, and S. J. Bograd. 2019. Marine top predators as climate and ecosystem sentinels. Frontiers in Ecology and the Environment 17:565–574.

Healing, S., C. E. Benkwitt, R. E. Dunn, and N. A. J. Graham. 2024. Seabird-vectored pelagic nutrients integrated into temperate intertidal rocky shores. Frontiers in Marine Science 11:1292484.

Hemming, V., A. E. Camaclang, M. S. Adams, M. Burgman, K. Carbeck, J. Carwardine, I. Chadès, L. Chalifour, S. J. Converse, L. N. K. Davidson, G. E. Garrard, R. Finn, J. R. Fleri, J. Huard, H. J. Mayfield, E. M. Madden, I. Naujokaitis-Lewis, H. P. Possingham, L. Rumpff, M. C. Runge, D. Stewart, V. J. D. Tulloch, T. Walshe, and T. G. Martin. 2022. An introduction to decision science for conservation. Conservation Biology 36:e13868.

Hobbs, N. T., and M. B. Hooten. 2015. Bayesian models: a statistical primer for ecologists. Princeton University Press, Princeton, New Jersey.

Holt, K. A., and P. D. Boersma. 2022. Unprecedented heat mortality of Magellanic penguins. The Condor 124:duab052.

Howard, J. A., A. J. DuVall, D. M. Pereksta, D. M. Mazurkiewicz, A. J. Searcy, P. J. Capitolo, and T. M. Russell. 2024. Northern breeding range expansion of two Sula species at Sutil Island, California, USA. Western North American Naturalist 84:223–231.

Hunt, G. L., Jr., R. L. Pitman, and H. L. Jones. 1980. Distribution and abundance of seabirds breeding on the California Channel Islands. Pages 443–459 in D. M. Power, editor. The California Islands: Proceedings of a multidisciplinary symposium. Santa Barbara Museum of Natural History, Santa Barbara, California.

Jones, H. P. 2010. Seabird islands take mere decades to recover following rat eradication. Ecological Applications 20:2075–2080.

McChesney, G. J., H. R. Carter, and D. L. Whitworth. 1995. Reoccupation and extension of southern breeding limits of Tufted Puffins and Rhinoceros Auklets in California. Colonial Waterbirds 18:79–90.

Melvin, E. F., T. J. Guy, and L. B. Read. 2014. Best practice seabird bycatch mitigation for pelagic longline fisheries targeting tuna and related species. Fisheries Research 149:5–18.

Nur, N., R. W. Bradley, L. Salas, P. Warzybok, and J. Jahncke. 2019. Evaluating population impacts of predation by owls on storm petrels in relation to proposed island mouse eradication. Ecosphere 10:e02878.

Oppel, S., B. L. Clark, M. M. Risi, C. Horswill, S. J. Converse, C. W. Jones, A. M. Osborne, K. Stevens, V. Perold, A. L. Bond, R. M. Wanless, R. Cuthbert, J. Cooper, and P. G. Ryan. 2022. Cryptic population decrease due to invasive species predation in a long-lived seabird supports need for eradication. Journal of Applied Ecology 59:2059–2070.

Paleczny, M., E. Hammill, V. Karpouzi, and D. Pauly. 2015. Population trend of the world's monitored seabirds, 1950–2010. PLOS ONE 10:e0129342.

Parsons, M., I. Mitchell, A. Butler, N. Ratcliffe, M. Frederiksen, S. Foster, and J. B. Reid. 2008. Seabirds as indicators of the marine environment. ICES Journal of Marine Science 65:1520–1526.

Piatt, I., and W. Sydeman. 2007. Seabirds as indicators of marine ecosystems. Marine Ecology Progress Series 352:199–204.

Piatt, J. F., A. M. A. Harding, M. Shultz, S. G. Speckman, T. I. Van Pelt, G. S. Drew, and A. B. Kettle. 2007b. Seabirds as indicators of marine food supplies: Cairns revisited. Marine Ecology Progress Series 352:221–234.

Roth, J. E., K. L. Mills, and W. J. Sydeman. 2007. Chinook salmon (Oncorhynchus tshawytscha)–seabird covariation off central California and possible forecasting applications. Canadian Journal of Fisheries and Aquatic Sciences 64:1080–1090.

Runge, M. C., S. J. Converse, J. E. Lyons, and D. R. Smith, editors. 2020. Structured decision making: case studies in natural resource management. Johns Hopkins University Press, Baltimore, Maryland.

Runge, M. C., C. S. Rushing, J. E. Lyons, and M. A. Rubenstein. 2023. A simplified method for value of information using constructed scales. Decision Analysis 20:220–230. https://doi.org/10.1287/deca.2023.0474.

Sydeman, W. J., R. W. Bradley, P. Warzybok, J. Jahncke, K. D. Hyrenbach, V. Kousky, J. A. Perlwitz, and M. D. Shulz. 2006. Planktivorous auklet Ptychoramphus aleuticus responses to ocean climate, 2005: Unusual atmospheric blocking? Geophysical Research Letters 33:L22S09.

Sydeman, W. J., S. A. Thompson, T. Anker-Nilssen, M. Arimitsu, A. Bennison, S. Bertrand, P. Boersch-Supan, C. Boyd, N. C. Bransome, R. J. M. Crawford, F. Daunt, R. W. Furness,

D. Gianuca, A. Gladics, L. Koehn, J. W. Lang, E. Logerwell, T. L. Morris, E. M. Phillips, J. Provencher, A. E. Punt, C. Saraux, L. Shannon, R. B. Sherley, A. Simeone, R. M. Wanless, S. Wanless, and S. Zador. 2017. Best practices for assessing forage fish fisheries–seabird resource competition. Fisheries Research 194:209–221.

Spatz, D. R., H. P. Jones, E. Bonnaud, P. Kappes, N. D. Holmes, and Y. B. Guzmán. 2023. Invasive species threats to seabirds. Pages 97–130 in L. Young and E. VanderWerf, editors. Conservation of marine birds. Academic Press, San Diego, California, USA.

Velarde, E., M. S. Tordesillas, L. Vieyra, and R. Esquivel. 1994. Seabirds as indicators of important fish populations in the Gulf of California. California Cooperative Oceanic Fisheries Investigations Reports 35:137–143.

Velarde, E., E. Ezcurra, and D. W. Anderson. 2015. Seabird diet predicts following-season commercial catch of Gulf of California Pacific Sardine and Northern Anchovy. Journal of Marine Systems 146:82–88.

Velarde, E., D. W. Anderson, and E. Ezcurra. 2019. Seabird clues to ecosystem health. Science 365:3.

Whitworth, D. L., H. R. Carter, and F. Gress. 2013. Recovery of a threatened seabird after eradication of an introduced predator: Eight years of progress for Scripps's murrelet at Anacapa Island, California. Biological Conservation 162:52–59.

Williams, B. K., and F. A. Johnson. 2015. Value of information and natural resources decision-making. Wildlife Society Bulletin 39:488–496.

Wolf, S. G., M. A. Snyder, W. J. Sydeman, D. F. Doak, and D. A. Croll. 2010. Predicting population consequences of ocean climate change for an ecosystem sentinel, the seabird Cassin's auklet. Global Change Biology 16:1923–1935.

Young, L., and L. T. Ballance. 2023. Ecology of marine birds. In L. Young and E. VanderWerf, editors. Conservation of marine birds. Academic Press, San Diego, California, USA.

Chapter 2. Differential Response of Nest Survival to Oceanographic Conditions for a Planktivorous Seabird

Publication history: This study was co-authored with Josh Adams, David M. Mazurkiewicz, Catherine A. Carter, and Sarah J. Converse. At the time this dissertation was published, this chapter was not in review with a journal.

2.1 Abstract

A greater understanding of temporal and spatial variation among demographic rates and environmental conditions is key for predicting climate change impacts on wildlife species. The Cassin's Auklet (*Ptychoramphus aleuticus*) has been identified as an ecosystem sentinel of ocean climate change for the California Current system, but the strength of the relationship between reproductive success and oceanographic conditions differs throughout its extensive breeding range. We investigated this relationship in the California Channel Islands, where auklets breed at two colonies that, although close to each other, can experience different oceanographic conditions. We analyzed 989 nest records collected between 1999 and 2022 and hypothesized that nest survival was driven by either local oceanographic conditions (as measured by satellite-derived sea surface temperature), regional oceanographic conditions (as indicated by the Biologically Effective Upwelling Transport Index), or an interaction between local and regional oceanographic conditions. We also hypothesized that there may be island-specific differences that affect reproductive success and are not captured by oceanographic covariates. We developed a daily multievent nest survival model to estimate state-specific survival probabilities in the face of uncertain observations of nest state and age. We modeled survival as a function of covariates and conducted model selection using Bayes Factors. The overall probability of reproductive success was higher for Scorpion Rock (0.448 [95% BCI: 0.414, 0.481]), the colony subjected to

warmer waters, than Prince Island (0.439 [95% BCI: 0.417, 0.462]). The most supported model only included the island effect and sea surface temperature, which indicated auklets were most influenced by marine conditions within core foraging zones near their breeding colonies. In addition, we found the relationship between sea surface temperature and nest survival differed between the colonies, suggesting that auklets may not respond uniformly to ocean climate change across their range. Despite these nuances, our findings offer broader insight into how seabirds breeding in dynamic upwelling systems may respond to climate-driven changes in marine conditions.

2.2 Introduction

We are experiencing rapid effects of global climate change on ocean ecosystems (e.g., Werb and Rudnick 2023), and seabirds can help inform our understanding of these effects. Seabirds are highly visible predators in the ocean food web, and they have been identified as important indicators of marine conditions (Piatt et al. 2007, Parsons et al. 2008, Velarde et al. 2019). Seabirds tend to be long-lived with delayed sexual maturity, and reproductive success has frequently been linked with metrics of marine productivity that reflect prey availability (e.g., Baird 1990, Lee et al. 2007, Bond et al. 2011). However, there are over 350 different seabird species that vary widely in terms of size, life history, diet, and foraging habits (Young and Ballance 2023). Given this diversity, the strength and character of relationships between reproductive success and marine conditions, and how this relationship may be mediated by climate change, will vary depending on species and location (Oro 2014).

The Cassin's Auklet (*Ptychoramphus aleuticus*, hereafter “auklet”) exemplifies how species-specific traits can influence the strength of ecological responses to climate variability. Auklets are small (164 ± 12 g) zooplanktivorous seabirds that feed at lower trophic levels,

making them closely linked to primary productivity and upwelling-driven dynamics in the marine environment (Manuwal 1974, Abraham and Sydeman 2004, Adams et al. 2004b). They are sensitive to ocean warming events that may disrupt prey availability, as illustrated by the 2013 – 2015 marine heatwave in the northeast Pacific Ocean, during which thousands of auklets were found dead on beaches along the west coast of North America (Jones et al. 2018). Auklet diet and foraging behavior can also vary in response to marine conditions (Ainley et al. 1996, Hedd et al. 2002, Adams et al. 2004a, 2004b). Although auklets can travel 30-75 km to provision chicks using specialized throat pouches (Adams et al. 2004a, Bertram et al. 2017), their flight is energetically costly (Hodum et al. 1998). As such, auklets tend to concentrate foraging within 30 km of breeding colonies in southern California (Adams et al. 2004a), and forage relatively closer to colonies in British Columbia when copepod prey are sufficiently abundant, even when prey availability is greater farther offshore (Bertram et al. 2017). Because auklets have shown measurable demographic responses to changing ocean conditions, they have been identified as ecosystem sentinels of ocean climate change in the California Current System (Wolf et al. 2010, Hazen et al. 2019, Clark-Wolf et al. 2024), a dynamic and diverse oceanographic system with wind-driven upwelling that varies in intensity as a function of latitude (Checkley and Barth 2009).

Auklets exhibit substantial geographic and ecological variation across their range, reflecting regional differences in diet, oceanography, and genetic structure. They nest throughout a range of wind-driven coastal upwelling systems along the west coast of North America, from the Aleutian Islands in Alaska to Baja California, Mexico. Most of the global breeding population occurs on the Scott Islands off British Columbia, Canada, with over one million individuals on Triangle Island alone (Bertram et al. 2005). Two subspecies are recognized: a

northern group (*P. a. aleuticus*) that primarily consumes copepods, euphausiids, and amphipods in British Columbia (Vermeer 1984) and euphausiids off northern California (Abraham and Sydeman 2004, 2006) and a southern group (*P. a. australe*) that may rely more heavily on larval fishes and exhibit greater dietary diversity (Adams et al. 2004b). Although auklets in the California Channel Islands were once considered part of the northern group, recent genetic analyses indicate they are more closely related to the southern group, and that Point Conception – a prominent headland and biogeographic boundary where ocean currents shift and upwelling dynamics change – may represent a barrier to gene flow (Wallace et al. 2015).

Wolf et al. (2009) examined covariance in auklet breeding phenology and productivity in British Columbia, central California, and northern Mexico and related these parameters to local and regional oceanographic conditions over a six-year period. A local variable, satellite-derived sea surface height, which characterizes the heat content and flow in the water column and can indicate upwelling, best explained breeding phenology and productivity, but the strength of this relationship differed among populations. Whereas auklets of the northern subspecies appear to time breeding with seasonal productivity peaks, there was no relationship detected between ocean conditions and breeding phenology for auklets breeding in the southern portion of the species' range, where upwelling can be more aseasonal and less predictable (Wolf et al. 2009). Differences in the strength of the relationship between upwelling and reproductive success indicated localized, regional adaptations may be aligned with the identified subspecies.

While the relationships between marine productivity and reproductive success are well established for the northern subspecies of Cassin's Auklet, much less is known about how oceanographic variability affects reproduction at the southern extent of the species' range (e.g., Wolf et al. 2009). Most research has focused on colonies in British Columbia and northern

California (e.g., Manuwal 1974, Hodum et al. 1998, Ainley and Boekelheide 1990, Pyle et al. 2001, Hedd et al. 2002, Abraham and Sydeman 2004, Bertram et al. 2005, Abraham and Sydeman 2006, Sydeman et al. 2006, Lee et al. 2007, Bertram et al. 2017, Johns et al. 2017, Johns et al. 2018, Hipfner et al. 2020). The California Channel Islands, located within the Southern California Bight just south of the subspecies boundary, provide an opportunity to investigate this question in a region with highly variable oceanographic conditions. Here, complex topography and coastline orientation shape local patterns of wind forcing, while the interaction between the equatorward-flowing California Current and the poleward Davidson Current creates a dynamic, seasonally variable system characterized by upwelling, convergence, and relaxation (Winant et al. 2003). We test the hypothesis that oceanographic conditions influence reproductive success in Cassin's Auklets by comparing two colonies, separated by 90 km, that experience different marine conditions. By evaluating this relationship in a transitional and understudied portion of the species' range, our study provides new insight into the flexibility of auklet reproductive responses and contributes to a broader understanding of how planktivorous seabirds may function as ecosystem sentinels in spatially heterogeneous systems.

We aimed to evaluate how local and regional oceanographic variability influences auklet reproductive success across a 24-year period (1999 – 2022). Given auklets' foraging ecology and the oceanographic complexity of the Southern California Bight, we considered three hypotheses related to reproductive success: (1) Auklets have restricted foraging areas due to high energetic cost of foraging and flight; thus, reproductive success is driven by local (i.e., within 30 km of breeding colony) marine conditions (*local effect hypothesis*); (2) Auklets will shift foraging areas in response to marine conditions; thus, reproductive success is driven by regional (i.e., within the Santa Barbara Channel) marine influences (*regional effect hypothesis*); and, (3) Auklet

reproductive success is a function of both local and regional marine influences, given some but relatively limited flexibility in foraging areas (*interaction effect hypothesis*). We also developed a fourth hypothesis orthogonal to the first three hypotheses: (4) There are inherent differences between the colony locations that are not fully captured by marine conditions and result in colony-specific differences in reproductive success (*island effect hypothesis*).

To evaluate these hypotheses, we built a multi-event daily nest survival model (Mayfield 1961, Rotella et al. 2004, Converse et al. 2013) in a Bayesian framework that allows daily nest survival to vary by nest state (egg or chick) while accounting for uncertainty in nest age and state (sensu Pradel 2005; see also Warlick 2022, Bratt 2023). This model is adaptable for modeling daily nest survival when state-specific survival is of interest, but nest age and state are uncertain.

2.3 METHODS

2.3.1 STUDY AREA AND POPULATION

The California Channel Islands are an archipelago of eight islands located in the Southern California Bight in an ecologically distinct marine region that extends from Point Conception, California (34.4°N) southward to Punta Banda, Mexico (31.7°N). Channel Islands National Park (CHIS) includes five islands: Anacapa, Santa Cruz (with the majority of the island owned and managed by The Nature Conservancy), Santa Rosa, San Miguel (owned by the US Navy and managed by CHIS under agreement), and Santa Barbara islands (Figure 1.1). Auklets are known to breed on all park islands except Santa Rosa. Two of the largest colonies are located on offshore islands 90 km apart in CHIS: Prince Island (34˚05’ N, 120˚20’ W; 0.16 km2) located 2 km northeast of San Miguel Island, and Scorpion Rock (34˚05’ N, 119˚30’ W; < 0.01 km2) located <1 km northeast of Santa Cruz Island. At the last survey effort in 1991, colony size was estimated at 8,922 and 546 individuals for Prince Island and Scorpion Rock, respectively (Carter

et al. 1992). Prince Island is located approximately 90 km west of Scorpion Rock and generally experiences cooler and more mixed waters through spring and summer, while marine conditions at Scorpion Rock tend to be less directly affected by upwelling off Point Conception, warmer, and more stratified (Adams et al. 2004a).

2.3.2 NEST MONITORING

Auklets were monitored in artificial nest burrows at Scorpion Rock and Prince Island as part of a long-term effort. During the study period (1999 – 2022), there were 72 artificial burrows at the southeast corner of Prince Island and 35 dispersed across Scorpion Rock for a total of 107 monitored burrows. Survey effort varied greatly across years and sites due to variable funding and weather limitations (Appendix 2.1). During each survey, researchers checked burrows and recorded nest contents as egg, chick, adult in nest, dead egg/chick, or empty. Due to the accessible nature of the artificial burrows, researchers could generally determine the state of any nest in the burrow without error. However, to limit disturbance when an adult was present in the burrow, researchers did not always remove the adult to determine the nest contents. In these cases, it was not possible to determine if the adult was incubating an egg, a chick, or neither (i.e., the nest had not been initiated). In this situation, the state of the nest was unknown.

Females lay one egg that is incubated during alternating 24-hour shifts by both parents (range 37 to 57 days, Ainley and Boekelheide 1990); if an egg is lost, females may lay a second replacement egg. Chicks are semi-precocial and independent of adults when they fledge (range 38 to 57 days, Ainley and Boekelheide 1990); fledgling age can vary by year (Hedd et al. 2002). In some cases, pairs known as “double brooders” will lay a second egg within the same breeding season after successfully fledging a first chick (Adams et al. 2004b).

We identified all nest attempts in which either an egg or a chick was first observed in a nest burrow. To ensure sufficient data quality for estimating nest fate, we then retained only those nest encounter histories for which all subsequent observations occurred no more than 37 days apart. This threshold corresponds to the minimum estimated incubation period and was used to reduce the likelihood of missing or conflating a second nest attempt in the same burrow following a nest failure. We further restricted the dataset to nest attempts with at least a minimum of two observations. Given that multiple nest attempts sometimes occurred within the same burrow, we needed to be able to separate these into distinct attempts. We identified new nest attempts occurring in a previously occupied burrow based on the following criteria: (1) the observation of a failed egg or chick or an empty nest preceding a new nest attempt, or (2) the observation of an egg over a period greater than the estimated maximum incubation period (57 days) followed by observation of a chick. In the second circumstance, we assumed that the first nest attempt failed, and we estimated the initiation of the second nest attempt by backdating the first observation of the chick by the estimated minimum incubation period. If the last observation of the nest included an egg or chick, the nest was censored at the last observation.

We analyzed 989 nest attempts from 20 years in this 24-year period (1999 – 2022; Figure 2.2), ten of which had data from both locations. In the remaining years, nest observations either did not occur or occurred too far apart in time to satisfy our criteria for inclusion. Approximately 70% (705) of the nest attempts included in the analysis were from Prince Island, which can be explained, in part, by the greater number of artificial nest burrows installed and monitored there.

2.3.3 Daily nest survival model

We developed a daily nest survival model (Mayfield 1961) that allowed us to evaluate differences in survival between the egg and chick states while accounting for uncertainty in nest

age and state (Pradel 2005). The true state of nest *n* at survey day *d*, $Z_{n,d}$, was modeled as categorically distributed with transition probabilities, $\boldsymbol{\theta}$**,** that are a function of the state in the previous time step, nest, and day:

$$Z_{n,d}|Z_{n,d-1} \sim \text{Categorical}(\boldsymbol{\theta_{n,d}}) \quad (1)$$

where $\boldsymbol{\theta_{n,d}}$ =

$$\begin{bmatrix} & \textbf{egg} & \textbf{chick} & \textbf{fledged} & \textbf{dead} \\ \textbf{egg} & \phi^{e}_{n,d}(1-\psi^{ec}_{n,d}) & \phi^{e}_{n,d}(\psi^{ec}_{n,d}) & 0 & 1-\phi^{e}_{n,d} \\ \textbf{chick} & 0 & \phi^{c}_{n,d}(1-\psi^{cf}_{n,d}) & \phi^{c}_{n,d}(\psi^{cf}_{n,d}) & 1-\phi^{c}_{n,d} \\ \textbf{fledged} & 0 & 0 & 0 & 1 \\ \textbf{dead} & 0 & 0 & 0 & 1 \end{bmatrix} \quad (2)$$

with state(*s*)-specific survival, $\phi^{s}_{n,d}$, and transition probabilities, $\psi^{sr}_{n,d}$ (for states *s* and *r*). We use the following notation for states: *e* for egg, *c* for chick, *f* for fledged.

Transition probabilities were modeled as age-dependent, with transitions allowed across the range of egg ages at which eggs can hatch (for transitions from egg to chick) and the range of chick ages at which chicks can fledge (for transitions from chick to fledged). We set these age ranges to 37 to 57 days for eggs and 38 to 58 days for chicks (Ainley and Boekelheide 1990). Within these ranges, we modeled the prior probability of transitioning as equal across days, i.e.,

$$\psi^{ec}_{n,d} \sim Dirichlet\ (min_e{:}\,max_e), \quad (3)$$

where min_e is the minimum egg age at hatching and max_e is the maximum egg age at hatching; the formulation for the transition $\psi^{cf}_{n,d}$ was equivalent. We modeled latent nest age by modeling

the age in state *s* at first observation, $a^{s}_{n,first_n}$ as a random variable, with age thereafter deterministic, i.e.,

$$a^{e}_{n,first_n} \sim Dirichlet(1{:}\,max_e),$$

$$a^{e}_{n,first_n+1} = a^{e}_{n,first_n} + 1. \quad (4)$$

Again, the formulation for the age of chicks was equivalent. We conditioned on the state in which the nest was first observed, i.e., if the nest was first observed in the chick state, we did not model the latent age of the egg that preceded the chick. When an egg transitioned into the chick state, we modeled the age of the chick based on the (latent) date of hatching.

We modeled daily nest survival probabilities, ϕ^{e} and ϕ^{c} as a function of oceanographic conditions, island effects, and random effects of time, to test our primary hypotheses. See details below in *Hypothesis testing*.

The observation of nest n at survey occasion day *d*, $y_{n,d}$, was modeled as categorically distributed with probabilities, **Ω,** that are modeled as a function of the state of nest *n* on day *d,* $Z_{n,d}$:

$$y_{n,d}|Z_{n,d} \sim \text{Categorical}(\boldsymbol{\Omega}) \quad (5)$$

where **Ω** =

$$\begin{bmatrix} & \textbf{A: egg} & \textbf{B: chick} & \textbf{C: adult} & \textbf{D: dead} & \textbf{E: empty} \\ \textbf{egg} & \gamma_1 & 0 & 1-\gamma_1 & 0 & 0 \\ \textbf{chick} & 0 & \gamma_2 & 1-\gamma_2 & 0 & 0 \\ \textbf{fledged} & 0 & 0 & 0 & 0 & 1 \\ \textbf{dead} & \gamma_3 & 0 & \gamma_4 & \gamma_5 & 1-\gamma_3-\gamma_4-\gamma_5 \end{bmatrix} \quad (6)$$

In this matrix, γ represents the state-specific probability of being observed in a certain event ($y = \{A, \ldots, E\}$) conditional on the state of the nest, $Z_{n,d}$. We accounted for uncertainty in the following observations: (1) an observation of an egg could indicate a nest in *s* = egg or *s* = dead (i.e., a dead embryo in an egg); (2) an observation of an adult could indicate a nest in *s* = egg, *s* = chick, or *s* = dead (again, because a bird may continue to incubate a dead egg); and, (3) an observation of an empty burrow could indicate a nest in *s* = fledged or *s* = dead. Only observations of a live chick, a definitively dead (e.g., broken) egg, or a dead chick were made without any resultant uncertainty in state. Appropriate uninformative priors were used for state-specific probabilities of observation: γ_1 and γ_2 had prior probabilities that were beta(1,1). The remaining γ probabilities were modeled using a multinomial logit link function (to constrain the sum of the probabilities of all observations conditional on a state to 1), with the link-scale parameters given normal(0, standard deviation [SD] = 1) priors.

Overall reproductive success is the probability that an initiated nest reaches the fledged state. This also represents the per-nest fecundity rate, given birds lay only one egg in a nest. We estimated overall reproductive success by summing the number of nests that reached the fledged state, based on the matrix $Z_{n,d}$, divided by the total number of nests that were monitored less those that were censored. We further summarized this by island. We also used the estimated latent nest age at first observation of an egg, $a^{e}_{n,first_n}$, to estimate nest initiation dates by island by taking the date of first observation less the estimated age at first observation. We used the mean nest initiation dates by island to examine differences in breeding phenology between Prince Island and Scorpion Rock.

2.3.4 HYPOTHESIS TESTING

To test our hypotheses, we modeled state-specific survival ϕ as a function of island and oceanographic covariates:

$$logit(\phi^{s}_{n,d}) = \beta^{s}_{0} + \beta_{island} * island_{n}$$
$$+ \beta_{local[island]} * local_{island_{n},d} + \beta_{regional[island]} * regional_{d}$$
$$+ \beta_{interaction[island]} * local_{island_{n},d} * regional_{d} + \delta_{y} + \delta_{w}$$
$$\delta_{y} \sim N(0, \sigma_{y})$$
$$\delta_{w} \sim N(0, \sigma_{w}) \quad (7)$$

where β^{s}_{0} is a state-specific intercept term; β_{island} is the coefficient for the island effect for each nest *n*; $\beta_{local[island]}$ is the island-specific coefficient associated with an island-specific local oceanographic covariate, $local_{island_{n},d}$ for each nest *n* on day *d*; $\beta_{regional[island]}$ is the island-specific coefficient associated with a regional oceanographic covariate that is the same for both islands, $regional_{d}$ on day *d*; and $\beta_{interaction[island]}$ is the island-specific coefficient associated with the interaction between the local and regional covariates.

To estimate the difference in survival between the two islands, we used a centered parameterization in which each island was given an effect, but these effects were constrained to be equal in magnitude and opposite in direction. With this approach, the island effects are centered around zero, allowing the intercept to represent the average across islands, and each island-specific effect captures the magnitude and direction of deviation from the average.

To account for repeated measures and residual variation, we included random effects for year (δ_{y}) with SD = σ_{y}, and week of year (δ_{w}) with SD = σ_{w}. We gave these SDs uniform(0, 5)

priors. We gave the state-specific intercept terms, β_0^s, normal(0,1) priors. The priors for all other parameters in the survival model – β_{island}, β_{local}, $\beta_{regional}$, and $\beta_{interaction}$ – are explained below.

For the local oceanographic covariate, we used the National Oceanic and Atmospheric Administration (NOAA) 0.25-degree Daily Optimum Interpolation Sea Surface Temperature (SST) Version 2.1 (Huang et al. 2020). We established core foraging areas located within 30 km of each breeding colony, supported by tracking data collected during 1999 – 2001 (Adams et al. 2004a). We then averaged across four to five daily sea surface temperature values within each buffer for a colony-specific daily SST value for each colony. For the regional oceanographic covariate, we used the 1.0-degree daily Biologically Effective Upwelling Transport Index (BEUTI) at 34°N, which provides an estimate of vertical nitrate flux, or the amount of nitrate that is upwelled or downwelled along the coast (Jacox et al. 2018). We checked for correlation and *Z*-scored all covariates prior to analysis (Figure 2.1).

To evaluate support for our hypotheses, we conducted model selection using the indicator-variable approach (Kuo and Mallick 1998; see also Link and Barker 2006, Smith et al. 2011, Converse et al. 2013). Here, each covariate *m* is associated with a Bernoulli variable, w_m, that is either a 0 (covariate excluded) or a 1 (covariate included) for each Markov chain Monte Carlo (MCMC) sample. This resulted in 10 candidate models: $2^3 = 8$ models given all possible combinations of island, local, and regional covariates, and two additional models (one with and one without the island effect) that included the interaction between local and regional covariates. Each model in this implied model set was given equal prior probability by adjusting prior probabilities associated with the Bernoulli distributions governing the w_m (see Smith et al. 2011, Appendix 2.2).

We calculated the Bayes Factor (BF; Hooten and Hobbs 2015) for each covariate, calculated as the ratio of the posterior odds to the prior odds of inclusion (Smith et al. 2011):

$$\mathrm{BF} = \frac{\frac{\Pr(A|\mathrm{data})}{(1-\Pr(A|\mathrm{data}))}}{\frac{\Pr(A)}{(1-\Pr(A))}} \quad (8)$$

where $\Pr(A|\mathrm{data})$ is the mean of the posterior distribution of the indicator variable for covariate *A*, i.e., $\Pr(w_m = 1|data)$, and $\Pr(A)$ is the prior probability for covariate *A*, i.e., $\Pr(w_m = 1)$. The BF provides a weight of evidence for the inclusion of the associated covariate in the model. Since the prior distributions of covariates can affect model selection results (Link and Barker 2006), we scaled the variance of the prior distributions for the model coefficients β_{island}, β_{local}, $\beta_{regional}$, and $\beta_{interaction}$ such that the total prior uncertainty in the linear predictor was constant regardless of the model (Link and Barker 2006). Each covariate had a normal prior probability with a mean of 0 and a precision of V/K. Here, *K* is the number of covariates (i.e., 4) in the model (determined by the sum of the w_m in a given MCMC sample) and *V* is Gamma distributed with α = 3.29 and β = 7.8, which results in a marginal distribution for the linear predictor that is approximately uniform(0,1) (Link and Barker 2006; see also Smith et al. 2011). We considered a BF value < 3 indicative of no support for the covariate, >3 and <20 indicative of positive support; >20 and <150 indicative of strong support; and >150 indicative of very strong support (Kass and Raftery 1995).

2.3.5 Model fitting and implementation

Models were fit using NIMBLE (Valpine et al. 2017) executed through R (v4.4.1; R Core Team 2024). We found that initialization errors occurred under some sets of initial values; we

therefore identified a set of seeds that generated compatible initial values and used these values to run the analysis. We ran 28,000 iterations across three independent Markov chains after discarding the first 3,000 samples, for a total of 75,000 samples. We assessed convergence of the chains by visually inspecting trace plots and based on Brooks-Gelman-Rubin statistics $\hat{R}$ <1.1 (Gelman and Rubin 1992, Brooks and Roberts 1998). All materials and code developed for the analysis can be found on GitHub (https://github.com/ameliaduvall/Dissertation_Chapter2).

2.4 RESULTS

Of the four covariates we considered as predictors of daily nest survival, both island and the SST covariate had BF of infinity due to being included in every model that was sampled (Table 2.1); this signifies very strong support for these two predictors. The BEUTI covariate and the interaction between local and regional conditions covariate had BF < 1, which indicates little support for these two predictors. Out of the 10 candidate models, only two models were sampled through the indicator variable model selection process, in which covariates are selected dynamically during MCMC: one with the island and SST covariate and one with the island, SST, and BEUTI covariate. See Table 2.2 for posterior model probabilities. Because over 97% of the weight was on the model with the island and SST effect only, we used this model for inference and all estimates presented are based on this model.

Auklet reproductive success varied by nest state, colony, and environmental conditions. Daily nest survival probabilities were lower for the egg state (β_0^{egg} = 0.939, 95% Bayesian credible interval [BCI]: 0.862, 0.966) than the chick state (β_0^{chick} = 0.982, 95% BCI: 0.954, 0.990), reflecting increased vulnerability earlier in the nesting period (Figure 2.3A; Table 2.3). Among monitored nests that were not censored, the overall probability of success (i.e., fledging) was similar at the two sites: 44.8% at Scorpion Rock (95% BCI: 0.414, 0.481) for Scorpion Rock

and 43.9% at Prince Island (95% BCI: 0.417, 0.462; Figure 2.3B). However, posterior estimates of coefficients revealed notable differences in survival patterns between colonies. Daily nest survival was higher at Scorpion Rock relative to Prince Island (β_{island} = 0.515, 95% BCI: 0.334, 0.707), and more negatively affected by increasing sea surface temperature at Prince Island ($\beta_{SST}^{Prince\ Island}$ = -1.353 (95% BCI: -1.734, -0.987) compared to Scorpion Rock ($\beta_{SST}^{Scorpion\ Rock}$ = -0.538, 95% BCI: -0.883, -0. 193; Figure 2.4). Finally, we observed slight differences in breeding phenology between the sites, with auklets initiating nests marginally earlier at Prince Island (day of year 83.9, 95% BCI: 81.2, 86.8) than Scorpion Rock (day of year 84.8, 95% BCI: 82.0, 87.8; Figure 2.3C), though there was substantial overlap in the posterior distributions.

2.5 Discussion

Here, we built a multi-event daily nest survival model that accounts for both state uncertainty and unknown nest age, enabling us to leverage a multi-year dataset to investigate oceanographic drivers of reproductive success at two Cassin's Auklet colonies located in proximity but often influenced by contrasting marine conditions. Overall, reproductive success was higher, eggs were laid later, and sensitivity to warming waters was reduced at Scorpion Rock, a colony influenced by warmer oceanographic conditions, compared to Prince Island, which is located near cooler, upwelled waters.

Auklet nest survival in the California Channel Islands appears to be closely tied to local oceanographic conditions and inherent island-specific differences that were not captured by the oceanographic covariates. These results indicate that breeding auklets, which are largely restricted to foraging in proximity to their breeding colonies, are sensitive to oceanographic variability within a relatively small spatial area (<3,000 km^2). Notably, auklets appear to respond differently to local conditions at the two colonies. Auklet daily nest survival at Prince Island, a

location influenced by cooler, more dynamic upwelling conditions, exhibited a stronger negative relationship with sea surface temperature than did Scorpion Rock, which is characterized by warmer, more stratified waters and had overall higher nest survival. This difference may reflect variability in local prey composition and/or availability, differences in foraging habitat or quality, or other factors such as colony density, adult body condition, or mismatches between peak prey availability and breeding phenology. Future research that incorporates individual tracking, prey availability, and colony-specific habitat-characteristics could help disentangle the ecological drivers of these spatial differences.

Our results are broadly consistent with the range-wide results of Wolf et al. (2009), who reported that auklet breeding phenology and reproductive success were best explained by local oceanographic conditions, but that the strength of the relationship differed throughout their range – generally being less pronounced at the southern, warmer part of the range. In our analysis, the "warmer" colony (Scorpion Rock), which is more representative of environmental conditions fond in the southern extent of the species' range, exhibited a less pronounced response to rising sea surface temperature compared to the "cooler" colony (Prince Island; Figure 2.4). These findings reinforce the idea that auklet populations may exhibit site-specific responses to oceanographic variability and continued work comparing colonies across latitudinal and oceanographic gradients will be important for understanding population-specific vulnerabilities to ocean climate change.

Robust demographic analyses require long-term monitoring data, which can be difficult, time-intensive, and expensive to collect, often resulting in variable data quality across sites and years, which can create challenges with analyses. We were able to use 20 years of inconsistent nest monitoring data from two colonies over a 24-year period to build a novel multi-event daily

nest survival model that accounts for uncertainty in nest age and nest state. We used monitoring data to estimate the latent age of nests, which allowed us to model state-specific survival probabilities using a multi-state formulation of daily nest survival with transitions dependent on egg or chick age (Warlick 2022, Bratt 2023). However, even when we observed a nest, we could not always be certain of its state, so we handled uncertainty in nest state by developing a multi-event model (sensu Pradel 2005) that allowed uncertain observations to map to different true nest states (Warlick 2022). Our model can be adapted for use in similar situations to estimate daily nest survival where the age of a nest is unknown and the state of the nest cannot be observed perfectly (e.g., contents may be obscured or unobservable during part of the breeding season).

Despite the challenges we overcame with our modeling framework to leverage this long-term monitoring dataset, there was meaningful uncertainty in nest outcomes due to the relatively long intervals between monitoring visits, especially in some years. Only a subset of failed nests was observed with certainty (i.e., when a definitively dead egg or dead chick was observed), and fledging was entirely latent (i.e., an unobservable state), with information on nest age and state-specific survival probabilities informing it. As such, interpretations of reproductive success should be made cautiously, and future efforts to reduce observation gaps could help refine estimates of reproductive outcomes.

Modeling demographic outcomes as a function of oceanographic covariates for seabirds poses a variety of challenges and often requires assumptions depending on the spatial and temporal availability of covariates. For example, one assumption of our analysis is that auklet prey abundance is a function of oceanographic conditions, which is supported by Fisher at al. (2015). However, changes in prey quality as a result of oceanographic conditions (e.g., Heneghan et al. 2023) could also be a contributing factor in this system. We also assumed that

changes in upwelling and/or sea surface temperature would impact prey quickly and that auklets would respond quickly to changes in the foraging conditions, which is supported by research at other auklet colonies (e.g., Sydeman et al. 2006). Although we did not model the temporal scale of oceanographic covariates as a lagged and/or cumulative response, this could be investigated in the future.

Most studies involving seabirds and oceanographic climate change focus on species-level rather than population-level responses (see Oro 2014). It is well established that auklet demography is negatively impacted by warmer ocean conditions (e.g., Abraham and Sydeman 2004, Bertram et al. 2005, Sydeman et al. 2006, Lee et al. 2007, Ainley and Hyrenbach 2010, Johns et al. 2017, Hipfner et al. 2020); however, our results add to an increasing body of evidence that not all auklet populations will respond similarly to ocean climate change. This is relevant when considering conservation efforts across the species' range to mitigate impacts from climate change and when evaluating auklets as "ecosystem sentinels." Although the demography of several auklet populations appears to serve as an indicator of marine productivity, the relationship between these factors differs somewhat depending on the population that is being studied. We suggest, therefore, that interpreting demographic signals in terms of changes in the ocean is complex and will benefit from further study.

Despite these nuances, our results can be used more broadly to anticipate seabird responses in dynamic upwelling systems to changing marine conditions due to climate change. The California Current has been warming since the 1970s due to the large-scale climatic changes in the Pacific Ocean (Levitus et al. 2000). Shifts in seabird ranges, apparently in response to warming, have already occurred (Hyrenbach and Veit 2003, Russell et al. 2025). Cold-water-affiliated breeding species such as the Tufted Puffin (*Fratercula cirrhata*) and Rhinoceros

Auklet (*Cerorhinca monocerata*) appear to have been extirpated from the California Channel Islands, which once represented the southernmost extent of their breeding range. Both species were last suspected to breed at Prince Island in the early 1990s (McChesney et al. 1995) but have not been observed as breeders for decades (NPS unpublished data). In contrast, the archipelago has gained two new sub-tropical species (*Sula leucogaster, S. nebouxii)* as breeders on one of the southern islands (Santa Barbara Island; Figure 1.1) in recent years (Howard et al. 2024). Cassin's Auklets are another cold-water affiliated species that is likely to be negatively impacted by ocean climate change in the California Current (Wolf et al. 2010), but our results suggest fine-scale variation in response to warming may occur across their breeding range. As climate change continues to restructure marine ecosystems, understanding how populations respond at fine spatial scales will be critical to anticipating demographic tipping points, implementing conservation strategies, and evaluating the utility of seabirds as ecosystem indicators.

2.6 Acknowledgements

We acknowledge the Montrose Trustee Council, whose funding and support were critical to the collection of these data. We thank and acknowledge several others who have contributed to this work, including but not limited to: H. Carter, J. Felis, A. Hebshi, J. Howard, E. Kelsey, P. Larramendy, J. Takekawa, A. Yamagiwa. We owe deep thanks to A. Bratt, N. Hostetter, and A. Warlick for assistance with the analysis. We are grateful for feedback and improvements by T. Essington and T.S. Sillett. AJD was supported by funding from Channel Islands National Park, National Park Service Inventory & Monitoring Division, and the U.S. Geological Survey Natural Resource Preservation Program, facilitated by the Washington Cooperative Fish and Wildlife Research Unit. JA was supported in part by U.S. Geological Survey Ecosystem Mission Area.

Any use of trade, firm, or product names is for descriptive purposes only and does not imply endorsement by the U.S. Government.

2.7 References

Abraham, C. L., and W. J. Sydeman. 2004. Ocean climate, euphausiids and auklet nesting: inter-annual trends and variation in phenology, diet and growth of a planktivorous seabird, Ptychoramphus aleuticus. Marine Ecology Progress Series 274:235–250.

Abraham, C. L., and W. J. Sydeman. 2006. Prey-switching by Cassin's Auklet Ptychoramphus aleuticus reveals seasonal climate-related cycles of Euphausia pacifica and Thysanoessa spinifera. Marine Ecology Progress Series 313:271–283.

Adams, J., J. Y. Takekawa, and H. R. Carter. 2004a. Foraging distance and home range of Cassin's Auklets nesting at two colonies in the California Channel Islands. The Condor 106:618–637.

Adams, J., J. Y. Takekawa, and H. R. Carter. 2004b. Stable foraging areas and variable chick diet in Cassin's Auklets (Ptychoramphus aleuticus) off southern California. Canadian Journal of Zoology 82:1578–1595.

Ainley, D. G., and R. J. Boekelheide. 1990. Seabirds of the Farallon Islands: Ecology, dynamics, and structure of an upwelling-system community. Stanford University Press, Stanford, California, USA.

Ainley, D., L. Spear, and S. Allen. 1996. Variation in the diet of Cassin's Auklet reveals spatial, seasonal, and decadal occurrence patterns of euphausiids off California, USA. Marine Ecology Progress Series 137:1–10.

Ainley, D. G., L. B. Spear, C. T. Tynan, J. A. Barth, S. D. Pierce, R. G. Ford, and T. J. Cowles. 2005. Physical and biological variables affecting seabird distributions during the upwelling season of the northern California Current. Deep Sea Research Part II: Topical Studies in Oceanography 52:123–143.

Ainley, D. G., and K. D. Hyrenbach. 2010. Top-down and bottom-up factors affecting seabird population trends in the California Current System (1985–2006). Progress in Oceanography 84:242–254.

Baird, P. H. 1990. Influence of abiotic factors and prey distribution on diet and reproductive success of three seabird species in Alaska. Ornis Scandinavica 21:224–235.

Bertram, D. F., A. Harfenist, and B. D. Smith. 2005. Ocean climate and El Niño impacts on survival of Cassin's Auklets from upwelling and downwelling domains of British Columbia. Canadian Journal of Fisheries and Aquatic Sciences 62:2841–2853.

Bertram, D. F., D. L. Mackas, D. W. Welch, W. S. Boyd, J. L. Ryder, M. Galbraith, A. Hedd, K. Morgan, and P. D. O'Hara. 2017. Variation in zooplankton prey distribution determines marine foraging distributions of breeding Cassin's Auklet. Deep Sea Research Part I: Oceanographic Research Papers 129:32–40.

Bond, A. L., I. L. Jones, W. J. Sydeman, H. L. Major, S. Minobe, J. C. Williams, and G. V. Byrd. 2011. Reproductive success of planktivorous seabirds in the North Pacific is related to ocean climate on decadal scales. Marine Ecology Progress Series 424:205–218.

Bratt, A. E. 2023. From mark-resight to management: Bayesian hierarchical models for endangered bird populations. University of Washington Libraries, Seattle, Washington, USA.

Brooks, S. P., and G. O. Roberts. 1998. Convergence assessment techniques for Markov chain Monte Carlo. Statistics and Computing 8:319–335.

Carter, H. R., G. J. McChesney, D. L. Jaques, C. S. Strong, M. W. Parker, J. E. Takekawa, D. L. Jory, and D. L. Whitworth. 1992. Breeding populations of seabirds in California, 1989–

1991. Volume I – Population estimates. Unpublished draft final report. U.S. Fish and Wildlife Service, Northern Prairie Wildlife Research Center, Dixon, California.

Checkley, D. M., and J. A. Barth. 2009. Patterns and processes in the California Current System. Progress in Oceanography 83:49–64.

Clark-Wolf, T. J., K. A. Holt, E. Johansson, A. C. Nisi, K. Rafiq, L. West, P. D. Boersma, E. L. Hazen, S. E. Moore, and B. Abrahms. 2024. The capacity of sentinel species to detect changes in environmental conditions and ecosystem structure. Journal of Applied Ecology 61:1074–1086.

Converse, S. J., J. A. Royle, P. H. Adler, R. P. Urbanek, and J. A. Barzen. 2013. A hierarchical nest survival model integrating incomplete temporally varying covariates. Ecology and Evolution 3:4439–4447.

Fisher, J. L., W. T. Peterson, and R. R. Rykaczewski. 2015. The impact of El Niño events on the pelagic food chain in the northern California Current. Global Change Biology 21:4401–4414.

Gelman, A., and D. B. Rubin. 1992. Inference from iterative simulation using multiple sequences. Statistical Science 7:457–472.

Hazen, E. L., B. Abrahms, S. Brodie, G. Carroll, M. G. Jacox, M. S. Savoca, K. L. Scales, W. J. Sydeman, and S. J. Bograd. 2019. Marine top predators as climate and ecosystem sentinels. Frontiers in Ecology and the Environment 17:565–574.

Hedd, A., J. L. Ryder, L. L. Cowen, and D. F. Bertram. 2002. Inter-annual variation in the diet, provisioning and growth of Cassin's Auklet at Triangle Island, British Columbia: Responses to variation in ocean climate. Marine Ecology Progress Series 229:221–232.

Heneghan, R. F., J. D. Everett, J. L. Blanchard, P. Sykes, and A. J. Richardson. 2023. Climate-driven zooplankton shifts cause large-scale declines in food quality for fish. Nature Climate Change 13:1–8.

Hipfner, J. M., M. Galbraith, D. F. Bertram, and D. J. Green. 2020. Basin-scale oceanographic processes, zooplankton community structure, and diet and reproduction of a sentinel North Pacific seabird over a 22-year period. Progress in Oceanography 182:102290.

Hodum, P. J., W. J. Sydeman, G. H. Visser, and W. W. Weathers. 1998. Energy expenditure and food requirement of Cassin's Auklets provisioning nestlings. The Condor 100:546–550.

Hooten, M. B., and N. T. Hobbs. 2015. A guide to Bayesian model selection for ecologists. Ecological Monographs 85:3–28.

Howard, J. A., A. J. DuVall, D. M. Pereksta, D. M. Mazurkiewicz, A. J. Searcy, P. J. Capitolo, and T. M. Russell. 2024. Northern breeding range expansion of two Sula species at Sutil Island, California, USA. Western North American Naturalist 84:223–231.

Huang, B., C. Liu, V. F. Banzon, E. Freeman, G. Graham, W. Hankins, T. M. Smith, and H.-M. Zhang. 2020. NOAA 0.25-degree Daily Optimum Interpolation Sea Surface Temperature (OISST), Version 2.1. NOAA National Centers for Environmental Information. https://doi.org/10.25921/RE9P-PT57. Accessed October 2023.

Hyrenbach, K. D., and R. R. Veit. 2003. Ocean warming and seabird communities of the southern California Current System (1987–98): Response at multiple temporal scales. Deep Sea Research Part II: Topical Studies in Oceanography 50:2537–2565.

Jacox, M. G., C. A. Edwards, E. L. Hazen, and S. J. Bograd. 2018. Coastal upwelling revisited: Ekman, Bakun, and improved upwelling indices for the U.S. West Coast. Journal of Geophysical Research: Oceans 123:7332–7350.

Johns, M., P. Warzybok, R. Bradley, J. Jahncke, M. Lindberg, and G. Breed. 2017. Age, timing, and a variable environment affect double brooding of a long-lived seabird. Marine Ecology Progress Series 564:187–197.

Johns, M. E., P. Warzybok, R. W. Bradley, J. Jahncke, M. Lindberg, and G. A. Breed. 2018. Increased reproductive investment associated with greater survival and longevity in Cassin's Auklets. Proceedings of the Royal Society B: Biological Sciences 285:20181464.

Jones, T., J. K. Parrish, W. T. Peterson, E. P. Bjorkstedt, N. A. Bond, L. T. Ballance, V. Bowes, J. M. Hipfner, H. K. Burgess, J. E. Dolliver, K. Lindquist, J. Lindsey, H. M. Nevins, R. R. Robertson, J. Roletto, L. Wilson, T. Joyce, and J. Harvey. 2018. Massive mortality of a planktivorous seabird in response to a marine heatwave. Geophysical Research Letters 45:3193–3202.

Kass, R. E., and A. E. Raftery. 1995. Bayes factors. Journal of the American Statistical Association 90:773–795.

Kuo, L., and B. Mallick. 1998. Variable selection for regression models. Sankhyā: The Indian Journal of Statistics, Series B (1960–2002) 60:65–81.

Lee, D. E., N. Nur, and W. J. Sydeman. 2007. Climate and demography of the planktivorous Cassin's Auklet Ptychoramphus aleuticus off northern California: Implications for population change. Journal of Animal Ecology 76:337–347.

Levitus, S., J. I. Antonov, T. P. Boyer, and C. Stephens. 2000. Warming of the world ocean. Science 287:2225–2229.

Link, W. A., and R. J. Barker. 2006. Model weights and the foundations of multimodel inference. Ecology 87:2626–2635.

Manuwal, D. A. 1974. The natural history of Cassin's Auklet (Ptychoramphus aleuticus). The Condor 76:421–431.

Mayfield, H. 1961. Nesting success calculated from exposure. The Wilson Bulletin 73:8.

McChesney, G. J., H. R. Carter, and D. L. Whitworth. 1995. Reoccupation and extension of southern breeding limits of Tufted Puffins and Rhinoceros Auklets in California. Colonial Waterbirds 18:79–90.

Oro, D. 2014. Seabirds and climate: knowledge, pitfalls, and opportunities. Frontiers in Ecology and Evolution 2:79.

Parsons, M., I. Mitchell, A. Butler, N. Ratcliffe, M. Frederiksen, S. Foster, and J. B. Reid. 2008. Seabirds as indicators of the marine environment. ICES Journal of Marine Science 65:1520–1526.

Piatt, J. F., A. M. A. Harding, M. Shultz, S. G. Speckman, T. I. van Pelt, G. S. Drew, and A. B. Kettle. 2007. Seabirds as indicators of marine food supplies: Cairns revisited. Marine Ecology Progress Series 352:221–234.

Pradel, R. 2005. Multievent: An extension of multistate capture-recapture models to uncertain states. Biometrics 61:442–447.

Pyle, P., W. J. Sydeman, and M. Hester. 2001. Effects of age, breeding experience, mate fidelity and site fidelity on breeding performance in a declining population of Cassin's Auklets. Journal of Animal Ecology 70:1088–1097.

R Core Team. 2024. R: A language and environment for statistical computing. R Foundation for Statistical Computing, Vienna, Austria.

Rotella, J. J., S. J. Dinsmore, and T. L. Shaffer. 2004. Modeling nest–survival data: A comparison of recently developed methods that can be implemented in MARK and SAS. Animal Biodiversity and Conservation 27:187–205.

Russell, T. M., D. M. Pereksta, J. R. Tietz, M. Vernet, J. Jahncke, and L. T. Ballance. 2025. Increase of tropical seabirds (Sula) in the California Current Ecosystem with warmer ocean conditions. Frontiers in Marine Science 12:1561438.

Smith, D. H. V., S. J. Converse, K. W. Gibson, A. Moehrenschlager, W. A. Link, G. H. Olsen, and K. Maguire. 2011. Decision analysis for conservation breeding: Maximizing production for reintroduction of whooping cranes. The Journal of Wildlife Management 75:501–508.

Sydeman, W. J., R. W. Bradley, P. Warzybok, J. Jahncke, K. D. Hyrenbach, V. Kousky, J. A. Perlwitz, and M. D. Shulz. 2006. Planktivorous auklet Ptychoramphus aleuticus responses to ocean climate, 2005: Unusual atmospheric blocking? Geophysical Research Letters 33:L22S09.

Valpine, P. de, D. Turek, C. J. Paciorek, C. Anderson-Bergman, D. T. Lang, and R. Bodik. 2017. Programming with models: Writing statistical algorithms for general model structures with NIMBLE. Journal of Computational and Graphical Statistics 26:403–413.

Velarde, E., D. W. Anderson, and E. Ezcurra. 2019. Seabird clues to ecosystem health. Science 365:116–117.

Vermeer, K. 1984. The diet and food consumption of nestling Cassin's Auklets during summer, and a comparison with other plankton-feeding alcids. Murrelet 65:65–77.

Wallace, S. J., S. G. Wolf, R. W. Bradley, A. L. Harvey, and V. L. Friesen. 2015. The influence of biogeographical barriers on the population genetic structure and gene flow in a coastal Pacific seabird. Journal of Biogeography 42:390–400.

Warlick, A. 2022. Understanding the effects of environmental variability on demography in species with complex life histories through integrated population modeling. University of Washington Libraries, Seattle, Washington, USA.

Werb, B. E., and D. L. Rudnick. 2023. Remarkable changes in the dominant modes of North Pacific sea surface temperature. Geophysical Research Letters 50:e2022GL101078.

Winant, C. D., E. P. Dever, and M. C. Hendershott. 2003. Characteristic patterns of shelf circulation at the boundary between central and southern California. Journal of Geophysical Research: Oceans 108:3021.

Wolf, S. G., W. J. Sydeman, J. M. Hipfner, C. L. Abraham, B. R. Tershy, and D. A. Croll. 2009. Range-wide reproductive consequences of ocean climate variability for the seabird Cassin's Auklet. Ecology 90:742–753.

Wolf, S. G., M. A. Snyder, W. J. Sydeman, D. F. Doak, and D. A. Croll. 2010. Predicting population consequences of ocean climate change for an ecosystem sentinel, the seabird Cassin's Auklet. Global Change Biology 16:1923–1935.

Young, L., and L. T. Ballance. 2023. Ecology of marine birds. In L. Young and E. VanderWerf, editors. Conservation of marine birds. Academic Press, San Diego, California, USA.

2.8 Tables and Figures

Table 2.1 Bayes Factors (BF) for each covariate in the Cassin's Auklet daily nest survival model, indicating relative support for the covariate as a predictor of daily nest survival. BFs < 3 indicate no support, while BF > 150 indicate very strong support. Island and sea surface temperature (SST; local covariate) had BF equal to infinity due to being sampled in every model. There was little support for the Biologically Effective Upwelling Transport Index (BEUTI; regional covariate) or the interaction covariate.

Predictor	**BF**
Island	Inf
SST	Inf
BEUTI	0.019
Interaction (SST*BEUTI)	0

Table 2.2 Posterior model weights for each model of Cassin's Auklet nest survival sampled in the analysis. Covariates in the model set included: island, sea surface temperature (SST; local covariate), Biologically Effective Upwelling Transport Index (BEUTI; regional covariate), and an interaction covariate (SST*BEUTI).

Model	**Weight**
Island + SST	0.972
Island + SST + BEUTI	0.028
Island + SST + BEUTI + Interaction	0.000 [a]
NULL	0.000 [a]
Island	0.000 [a]
Island + BEUTI	0.000 [a]
SST	0.000 [a]
BEUTI	0.000 [a]
Local + BEUTI	0.000 [a]
SST + BEUTI + Interaction	0.000 [a]

[a] These models were never sampled in the MCMC chains and therefore have weights of 0.

Table 2.3 Parameter estimates from the top supported model with island and local sea surface temperature (SST) fixed effects and year (with SD = σ_y) and week of year (with SD = σ_w) random effects. See Eq. 7 for a full description of the parameters. Note that β_0^{egg} and β_0^{chick} are back transformed to the probability scale for ease of interpretation.

Parameter	**Mean**	**Lower 95% Credible Interval**	**Upper 95% Credible Intervals**
β_0^{egg}	0.939	0.862	0.966
β_0^{chick}	0.982	0.954	0.990
$\beta_{island}^{Scorpion\ Rock}$	0.515	0.334	0.707
$\beta_{island}^{Prince\ Island}$	-0.515	-0.334	-0.707
$\beta_{SST}^{Scorpion\ Rock}$	-0.538	-0.883	-0.193
$\beta_{SST}^{Prince\ Island}$	-1.353	-1.734	-0.987
σ_y	1.080	0.650	1.902
σ_w	0.711	0.410	1.169

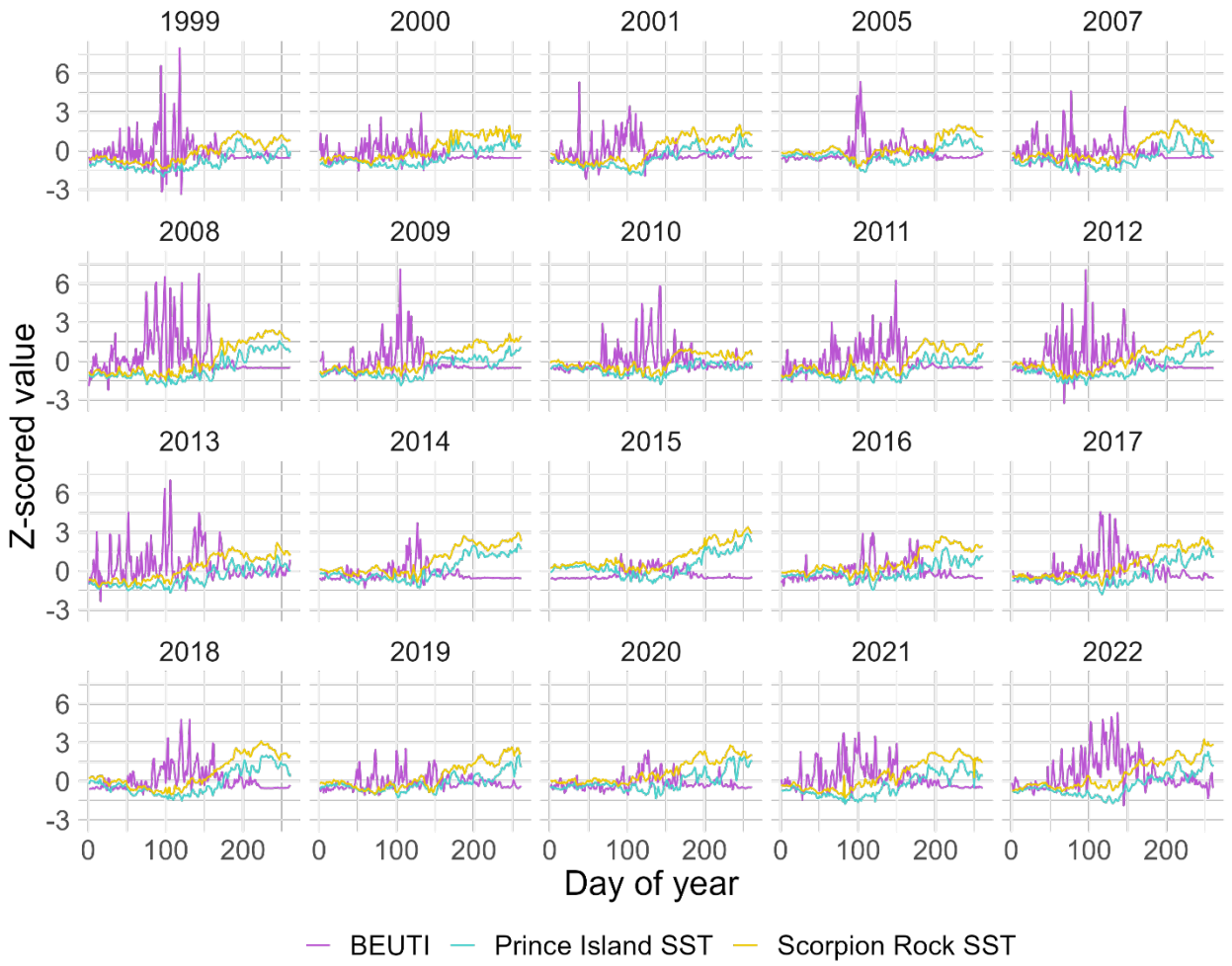

Figure 2.1 Daily values of z-scored oceanographic covariates included in the analysis during the study period, 1999 – 2022. Each panel shows a single year, with day-of-year on the x-axis and standardized z-scores on the y-axis. The regional covariate, Biologically Effective Upwelling Transport Index (BEUTI, purple), is the same at both colonies. The local covariates, sea surface temperature (SST), are different at each colony, Scorpion Rock (yellow) and Prince Island (blue).

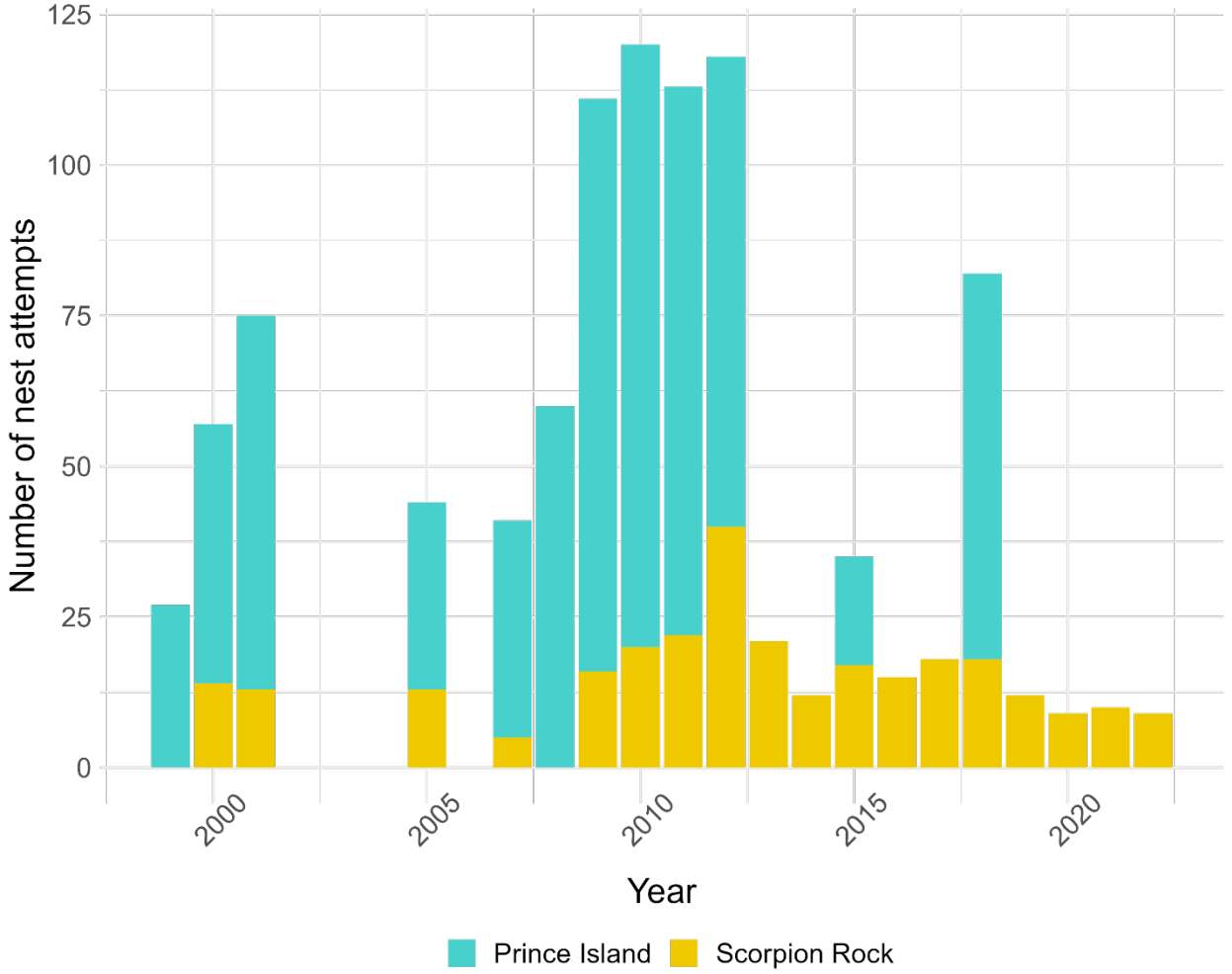

Figure 2.2 Annual number of Cassin's Auklet nest attempts at Prince Island (blue) and Scorpion Rock (yellow), 1999–2022. Bars represent the total number of nest attempts each year colored by colony. There are more monitored artificial burrows at Prince Island (n = 72) than at Scorpion Rock (n = 35).

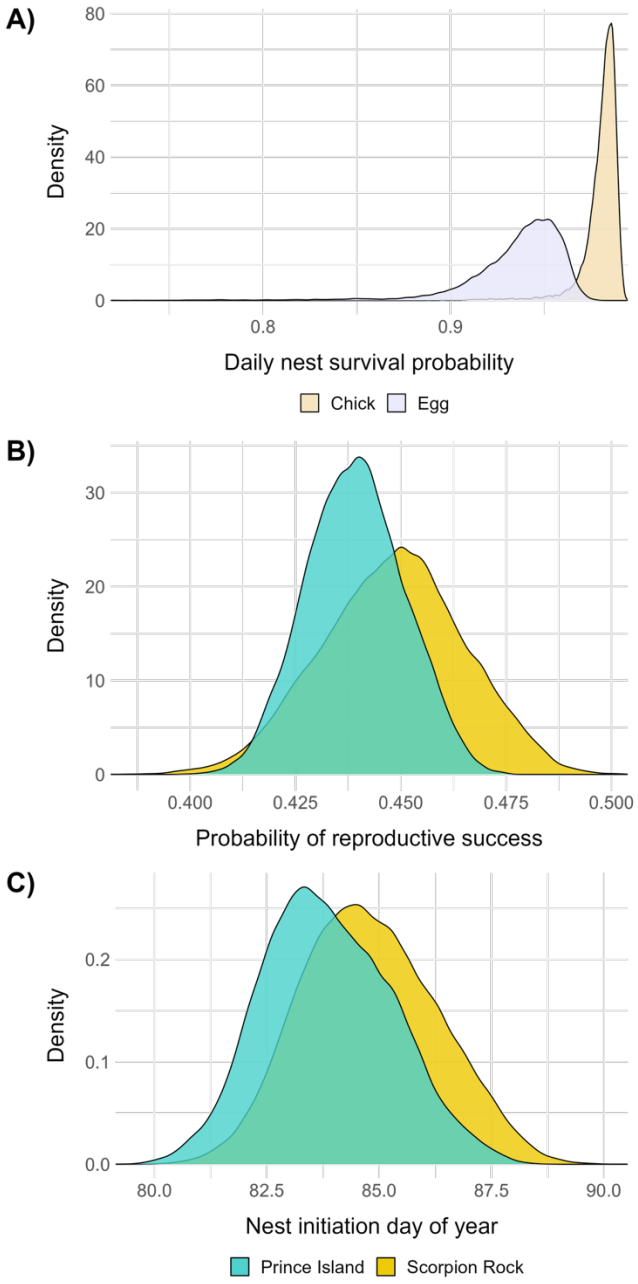

Figure 2.3 Posterior density plots from daily nest survival model, including: a) State-specific daily nest survival probability for egg and chick state; b) Probability of reproductive success for Scorpion Rock (yellow) and Prince Island (blue), defined as proportion of nests that fledged a chick relative to all nests that were monitored less those that were censored; and c) Average nest initiation dates (day of year) for Scorpion Rock (yellow) and Prince Island (blue).

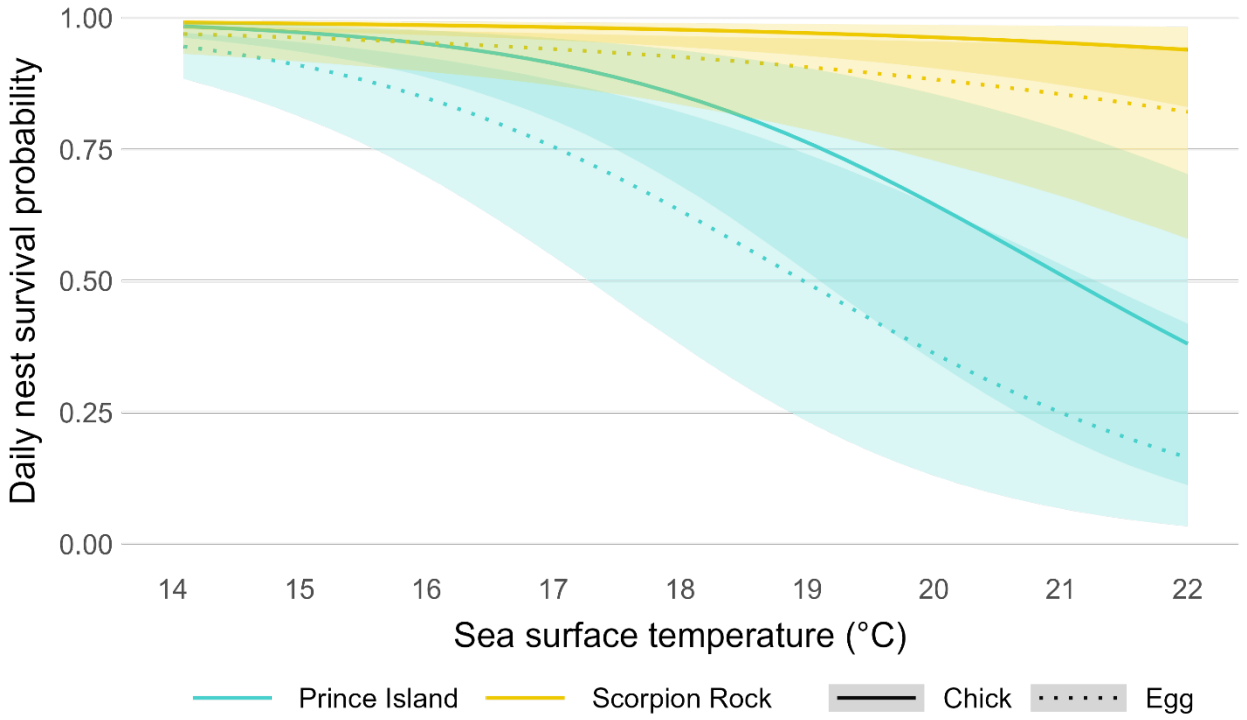

Figure 2.4 Predicted daily nest survival probability for Cassin's Auklets as a function of sea surface temperature (°C) at Scorpion Rock (yellow) and Prince Island (blue). Solid lines represent chick-state survival; dotted lines represent egg-state survival. Shaded areas indicate 95% Bayesian credible intervals derived from posterior samples. Typical SSTs in Southern California range from 14–22°C.

2.9 APPENDIX 2.1

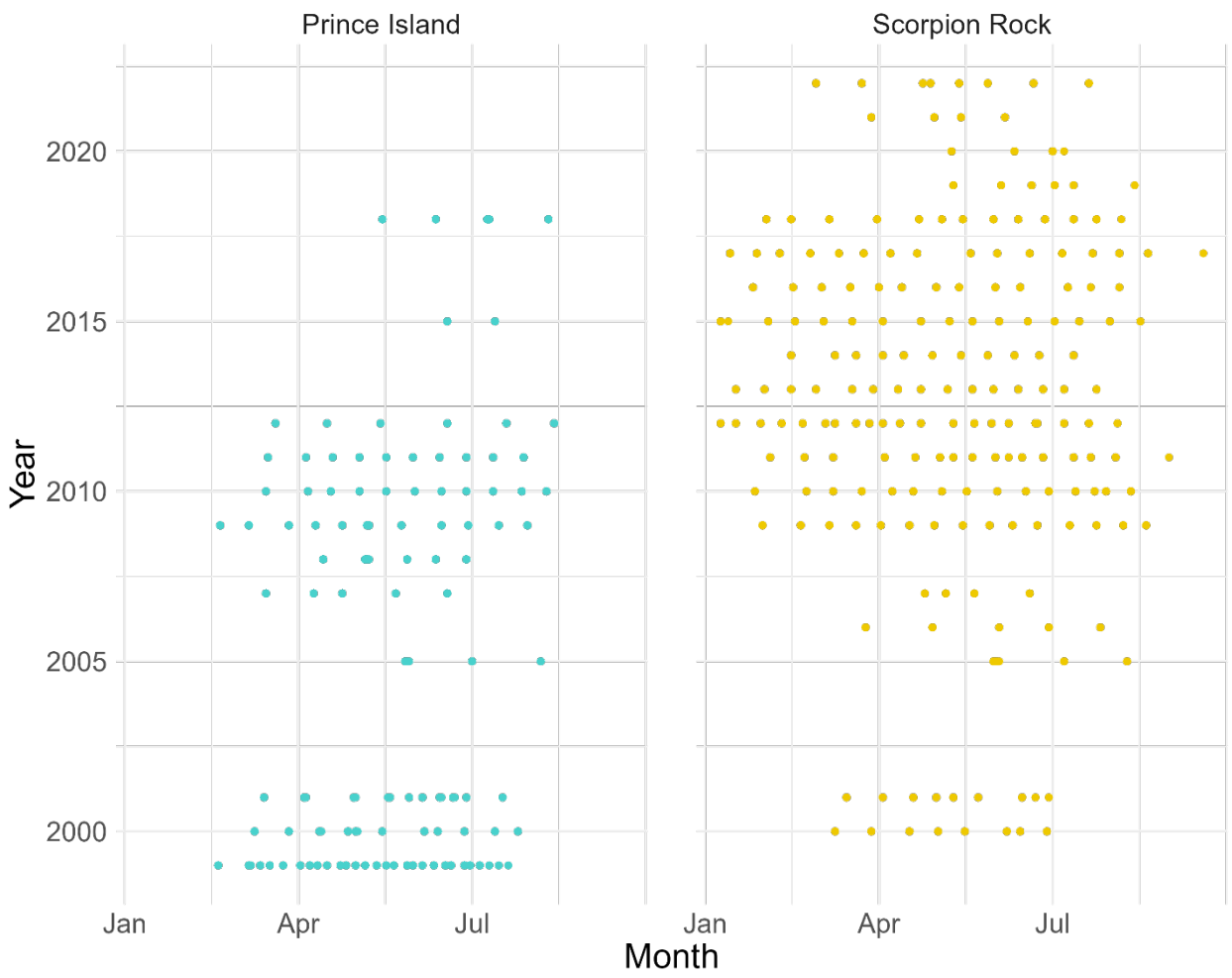

Temporal distribution of nest monitoring for Cassin's Auklets at Prince Island (left, blue) and Scorpion Rock (right, yellow), 1999–2022. Each point represents a nest visit, with visit dates plotted by day-of-year (x-axis) and year (y-axis).

2.10 APPENDIX 2.2

To give each model in the model set an equal prior probability, we used the following equations to adjust prior probabilities associated with the Bernoulli probabilities governing the variables w_m, associated with each covariate m. We had 10 candidate models: 2^3 = 8 models given all possible combinations of island, local, and regional covariates, and two additional models (one with and one without the island effect) that included the interaction between local and regional covariates. For each covariate, we calculated the probability of inclusion for each candidate model in the model set.

Model Set

1) Null
2) Island
3) Island + MENSO
4) Island + SST
5) Island + SST + MENSO
6) MENSO
7) SST
8) SST + MENSO
9) Island + SST + MENSO + SST *MENSO
10) SST + MENSO + SST*MENSO

$$\Pr(Island) = \frac{5}{10}$$

$$\Pr(BEUTI) = \left(\Pr(Island) * \frac{3}{5}\right) + \left((1 - \Pr(Island) * \frac{3}{5})\right)$$

$$\begin{aligned}\Pr(SST) = &\left((\Pr(Island) * \Pr(BEUTI) * \frac{2}{3}\right) + \left(\Pr(Island) * (1 - \Pr(BEUTI)) * \frac{1}{2}\right) \\ &+ \left((1 - \Pr(Island) * \Pr(BEUTI) * \frac{2}{3}\right) \\ &+ \left((1 - \Pr(Island)) * (1 - \Pr(BEUTI)) * \frac{1}{2}\right)\end{aligned}$$

$$\Pr(Interaction) = \left(\Pr(Island) * \Pr(SST) * \Pr(BEUTI) * \frac{1}{2}\right) +$$

$$\left((1 - \Pr(Island)) * \Pr(SST) * \Pr(BEUTI) * \frac{1}{2}\right) \quad (9)$$

Chapter 3. Assessing the Impact of Ocean Climate Variability on Seabird Demography Using Integrated Population Modeling

Publication history: This study was co-authored with Josh Adams, David M. Mazurkiewicz, Catherine A. Carter, and Sarah J. Converse. At the time this dissertation was published, this chapter was not in review with a journal.

3.1 Abstract

Understanding how environmental variability affects population dynamics benefits from integrating multiple demographic responses, yet most studies of seabird ecology examine vital rates in isolation. Here, we developed an integrated population model for Cassin's Auklets (*Ptychoramphus aleuticus*) at two colonies in the California Channel Islands from 1999 to 2022 to jointly evaluate how oceanographic conditions influence adult survival, fecundity, and population growth. The colonies—Prince Island and Scorpion Rock—lie along a natural oceanographic gradient, offering contrasting marine conditions that likely affect foraging success and reproductive output. We tested hypotheses linking survival and breeding probabilities to regional and seasonal oceanographic drivers. Our survival model provided strong support for the *southern winter* hypothesis, indicating that auklet survival is primarily driven by wintertime conditions in the southern California Current, but the direction of the effect was opposite from what we expected with greater survival associated with decreased upwelling. In contrast, we found no evidence that environmental variability influenced breeding probability. Posterior estimates of population size revealed that while both colonies remained small, Prince Island exhibited modest growth over the study period, whereas Scorpion Rock remained relatively stable. Overall, adult survival was relatively high and less variable compared to fecundity, providing evidence for demographic buffering. Across colonies, survival and fecundity were

positively correlated, suggesting an increased demographic sensitivity to environmental variability. This study highlights the value of integrated demographic modeling in capturing complex responses to environmental change and provides new insights into the mechanisms by which climate variability influences seabird demography and viability.

3.2 Introduction

Global seabird populations have declined by nearly 70% since 1950 (Paleczny et al. 2015), with climate change increasingly recognized as a key driver of this trend. Shifting oceanographic conditions affect the abundance and distribution of marine prey, which in turn influence the foraging success of marine predators such as seabirds. These changes can impact key demographic rates, including survival and fecundity. Due to the logistical challenges of collecting long-term demographic data, most studies examine oceanographic effects on individual parameters in isolation. As a result, we have a limited understanding of how multiple demographic responses interact to influence population dynamics, or the extent to which seabirds are robust to environmental variability through plasticity in life history traits.

Seabirds are typically long-lived, with delayed maturity, high adult survival, and low annual fecundity (Young and Ballance 2023). Many species also skip breeding in some years, often in response to factors such as food availability, body condition, or prior reproductive effort. Survival in seabirds is expected to be relatively invariant in the face of oceanographic variability; the demographic buffering hypothesis (Pfister 1998, Gaillard et al. 2000) predicts that life-history traits to which individual fitness, and thereby population growth, are more sensitive (Saether and Bakke 2000) will be relatively insensitive to environmental variability. In contrast, the effects of oceanographic variability on reproductive output in seabirds are well-documented: seabirds often exhibit reduced reproductive success in years with low prey availability or weak

marine productivity (Sydeman et al. 2006, Bond et al. 2011). During the breeding season, seabirds are central place foragers, constrained to repeatedly return to their nest site to provision chicks, which limits their foraging range to nearby prey resources—even when local conditions are suboptimal. In response to poor foraging conditions, many species reduce clutch size (Regehr and Montevecchi 1997, Mills et al. 2008, Tomita et al. 2009, Blight 2011), abandon nesting attempts (Sydeman et al. 2006, Montevecchi et al. 2020), or skip breeding altogether (Reed et al. 2015). Conversely, during favorable conditions, some species may increase reproductive investment via double-brooding, where pairs initiate another nesting attempt following a successful nest attempt (Adams et al. 2004b, Johns et al. 2017).

While survival, as predicted by the demographic buffering hypothesis, tends to be less variable in long-lived species than fecundity (e.g., Schmidt et al. 2015, Rotella et al. 2012), it can still be sensitive to oceanographic variation and climate variability (Sandvik et al. 2012). In extreme cases, hundreds of thousands to millions of individuals can be lost in mass mortality events due to marine heat waves driven by ocean climate conditions (Jones et al. 2018, Jones et al. 2024, Renner et al. 2024). In particular, winter tends to be a challenging time for seabirds in terms of survival (Barbraud and Weimerskirch 2003, Votier et al. 2005), seemingly due to harsher ocean and weather conditions (e.g., Boano et al. 2010, Laurenson et al. 2024).

With rapid environmental change, species' tolerance of environmental variability via demographic buffering could become insufficient, as conditions push populations past ecological thresholds. Given that overall extinction risk is inversely related to variability in population growth (Lewontin and Cohen 1969), this has important implications for biodiversity. For example, Lunn et al. (2016) found that polar bear survival, rather than breeding probability, was most tightly linked with sea ice conditions from 1984 – 2011 in western Hudson Bay, Canada.

However, populations may be able to respond to environmental variability via demographic compensation, where declines in some vital rates are offset by increases in others, resulting in stability in overall population growth (Morris and Doak 2004, Villellas et al. 2015).

The Cassin's Auklet (*Ptychoramphus aleuticus*) is a small, zooplanktivorous alcid endemic to the North Pacific. It is the most widely distributed auklet species, with a breeding range extending from the Aleutian Islands of Alaska, USA to Baja California, Mexico. In the California Current, a large-scale, cold eastern boundary current that flows southward along the western coast of North America, their demography is influenced by upwelling-driven variation in zooplankton availability that reflects ocean productivity (Abraham and Sydeman 2004, Abraham and Sydeman 2006, Adams et al. 2004b). As such, their population dynamics are tightly linked to ocean productivity with only short temporal lags, making them an ideal species for examining demographic responses to oceanographic variability. Previous studies have linked reproductive success and survival to oceanographic variability at multiple colonies (e.g., Bertram et al. 2005, Lee et al. 2007, Wolf et al. 2009, Johns et al. 2017), with both vital rates declining in years of lower marine productivity.

The Channel Islands in southern California, USA, are a model system for examining the relationship between auklet demography and marine conditions across a natural environmental gradient of oceanographic variability (Figure 1.1). At Point Conception, where the coastline shifts sharply from a north–south to an east–west orientation, the cold, nutrient-rich California Current meets the warmer, poleward-flowing Davidson Current. This interaction creates a cyclonic circulation pattern in the Santa Barbara Channel, characterized by dynamic seasonal upwelling, surface convergence, and relaxation events (Winant et al. 2003). The Channel Islands are situated within this transition zone, resulting in a spatial and temporal mosaic of

oceanographic conditions. Cassin's Auklets breed at colonies located across this gradient, where differing oceanographic influences may present distinct foraging opportunities and constraints.

We developed an integrated population model (IPM; Besbeas et al. 2002) for two Cassin's Auklet breeding colonies in the Channel Islands, with the goal of comprehensively evaluating the effects of oceanographic variability on both survival and reproduction in an area with substantial inter- and intra-annual variability in ocean conditions. We leveraged results from a previous analysis in the Channel Islands, in which DuVall (Chapter 2, this dissertation) evaluated the influence of local and regional oceanographic conditions on Cassin's Auklet fecundity. By integrating these findings into the current IPM, we were able to develop a holistic evaluation of the effect of oceanographic variability on demographic parameters and population growth. IPMs offer a powerful framework for jointly estimating demographic parameters by combining multiple data sources—typically those relevant to estimating reproductive success, survival, and abundance—into a single hierarchical analysis. Thus, we were able to evaluate the effects of oceanographic variability on survival, multiple aspects of reproduction, and population growth in tandem.

DuVall (Chapter 2, this dissertation) found that fecundity in Cassin's Auklets in the Channel Islands was primarily influenced by local sea surface temperature, suggesting that auklets are most responsive to marine conditions within their core foraging areas during the breeding season. Building on this finding, we developed a set of hypotheses regarding effects of temporal and spatial oceanographic variability on annual adult survival and breeding probabilities (Table 3.1). For adult survival, we developed three hypotheses: (1) Adult survival is driven by Pacific Ocean basin-wide oceanographic conditions throughout the course of the year, reflecting consistent, year-round sensitivity to large-scale processes (*annual effect on survival*

hypothesis; hereafter, *annual survival*); (2) Adult survival is driven by conditions in the southern California Current during winter, reflecting overwintering sensitivity and a tendency to remain in southern waters (*southern winter effect on survival hypothesis*; hereafter, *southern winter*); and, (3) Adult survival is driven by conditions in the northern California Current during winter, reflecting overwintering sensitivity and a tendency to remain in northern waters (*northern winter effect on survival hypothesis*; hereafter, *northern winter*).

We similarly proposed two hypotheses regarding effects of environmental variability on the probability of breeding in a given year. These were: (1) Breeding probability is driven by Pacific Ocean basin-wide oceanographic conditions throughout the course of the prior year, reflecting cumulative, long-term effects on decisions to initiate breeding (*annual effect on breeding hypothesis;* hereafter, *annual breeding*); and, (2) Breeding probability is driven by conditions just prior to breeding, reflecting short-term effects on decisions regarding whether to initiate breeding (*pre-season effect on breeding hypothesis*; hereafter, *pre-season breeding*). Across all hypotheses, we expected that oceanographic conditions indicative of greater marine productivity (i.e., more prey availability) would lead to increased survival and an increased probability of breeding in a given year.

After testing these hypotheses, we undertook a sensitivity analysis to evaluate the sensitivity of population growth to demographic parameters. This allowed us to understand how the effects of oceanographic variability may impact population growth through multiple demographic pathways. The IPM we developed provided a single, unified framework, facilitating a comprehensive analysis of the impacts of oceanographic variability on Cassin's Auklets at two colonies within a highly dynamic oceanographic region. Through this approach,

we aimed to quantify fine-scale demographic responses to environmental variability and improve our understanding of seabird viability under marine climate change.

3.3 METHODS

3.3.1 STUDY AREA AND POPULATION

The California Channel Islands are an archipelago of eight islands located in the Southern California Bight, a biogeographically distinct marine region that extends from Point Conception, California (34.4°N) south to Punta Banda, Mexico (31.7°N). Channel Islands National Park (CHIS) encompasses five of these islands—Anacapa, Santa Cruz (co-owned with The Nature Conservancy), Santa Rosa, San Miguel (owned by the US Navy and managed by CHIS under agreement), and Santa Barbara (Figure 1.1). Cassin's Auklets (hereafter, "auklets") are known to breed on all park islands except Santa Rosa. Two of the largest colonies are located on offshore islets approximately 90 km apart: Prince Island (34°05'N, 120°20'W; 0.16 km^2), situated 2 km northeast of San Miguel Island, and Scorpion Rock (34°05'N, 119°30'W; <0.01 km^2), located <1 km northeast of Santa Cruz Island. The most recent colony size estimates, from a 1991 survey, were 8,922 individuals at Prince Island and 546 at Scorpion Rock (Carter et al. 1992); however, monitoring indicated the population at Scorpion Rock dropped to a maximum of 120 in 2000 (NPS unpublished data). Prince Island typically experiences cooler, more mixed waters during spring and summer due to stronger exposure to upwelling off Point Conception, whereas Scorpion Rock experiences warmer and more stratified marine conditions (Adams et al. 2004a).

Most of the global breeding population of auklets is found on the Scott Islands off British Columbia, Canada, with the largest colony (>1 million) found on Triangle Island (Bertram et al. 2005). Other large colonies exist at the Farallon Islands in central California, USA; the California Channel Islands; and islands in Baja California, Mexico (Ainley et al. 2020). Auklets

can live over 20 years, with an average lifespan of at least 6 years (Ainley et al. 2020) and a mean age of first breeding around 3 years (Pyle 2001). Females lay a single egg per breeding attempt, and both parents share incubation duties in alternating 24-hour shifts for approximately 38 days (Manuwal 1974). Pairs are known to sometimes double brood, where they initiate another nesting attempt following a successful nest attempt (Adams et al. 2004b, Johns et al. 2017). Chicks are semi-precocial and fledge independently about 41 to 51 days after hatching (Ainley et al. 2020).

3.3.2 Demographic data

CHIS staff and collaborators have monitored auklets intermittently in artificial burrows at Prince Island and Scorpion Rock as funding and logistics have allowed. During the period covered by this study (1999 – 2022), there were 72 artificial burrow sites at the southeast corner of Prince Island and 35 dispersed across Scorpion Rock, for a total of 107 monitored sites. During this period, auklets were monitored intermittently, with survey effort varying substantially—from no surveys in some years to over ten surveys per island in other years. See DuVall (Chapter 2, this dissertation) for details on nest monitoring protocols and effort. During visits, when adult auklets were encountered inside nest burrows, individuals were banded with uniquely numbered US Geological Survey #3 metal leg bands. Recaptures or re-sightings of banded individuals were also recorded. Chicks were typically banded once they reached 100 grams. In some cases, individuals were not banded or handled, such as when adults were incubating newly hatched chicks or during 2006 – 2011 at Scorpion Rock to limit disturbance during native habitat restoration efforts that were then underway.

3.3.3 COVARIATE DATA

We obtained covariate data from the California Current Integrated Ecosystem Assessment Program, part of the National Oceanic and Atmospheric Administration (NOAA) interdisciplinary research along the US West Coast (NOAA 2024). We used Oceanic Niño Index (ONI), which is a measure of air pressure fluctuations and sea surface temperature anomalies in the El Niño 3.4 region, as an annual Pacific basin-wide covariate for testing *annual survival* and *annual breeding hypotheses* (Table 3.1). Lower ONI values correspond to La Niña conditions, which are generally associated with increased upwelling along the west coast of North America (Amos and Castelao 2022). We extracted and averaged ONI values from July in year *t*-1 to June in year *t* to model survival from year *t*-1 to year *t*, and values from April in year *t*-1 to March in year *t* to model breeding state transitions (i.e., the probability of breeding) in year *t*. We did not include a separate winter ONI covariate (October of year *t*-1 to January of year *t*) because it was highly correlated with annual ONI ($r > 0.9$).

For all other hypotheses (*southern winter*, *northern winter*, and *pre-season breeding hypotheses*; Table 3.1), we used the Biologically Effective Upwelling Transport Index (BEUTI), which estimates vertical nitrate flux, the amount of nitrate upwelled or downwelled near the west coast of the US (higher values indicate stronger upwelling; Jacox et al. 2018). BEUTI values were obtained at two latitudes: 36°N to reflect northern oceanographic conditions and 34°N to represent conditions at the auklet breeding grounds in southern California. We extracted and averaged monthly BEUTI values from October of year *t*-1 to January of year *t* to model the effects of winter on survival from *t*-1 to *t*, and from January to March of year *t* to model pre-breeding effects on breeding probability in year *t*.

While ONI and BEUTI reflect distinct oceanographic processes – basin-scale equatorial Pacific climate variability versus regional coastal upwelling dynamics – both were included to broadly characterize marine productivity as a proxy for auklet prey availability. Conditions that are indicative of greater upwelling (lower ONI, higher BEUTI) are expected to supporter greater zooplankton biomass and higher forage availability (Messié and Chavez 2017). In contrast to ONI's broad spatial scale, BEUTI offers final spatial resolution (1° latitude), enabling more localized hypothesis testing.

We checked all covariates for correlation and *z*-scored each prior to inclusion in the model.

3.3.4 Component models

The IPM we constructed integrated component models for fecundity, survival and breeding state transitions, and abundance, respectively. These component models were linked via a series of stage-specific population growth equations. We step through each of these models in turn.

3.3.4.1 Fecundity model

DuVall (Chapter 2, this dissertation) developed a daily nest survival model to estimate annual reproductive success, defined as the probability that a nest attempt results in a successfully fledged chick. The model accounts for differential survival between egg and chick stages and incorporates state uncertainty for observations that cannot be linked definitively to a nest state (e.g., when it is not possible to see under an adult on a nest; Pradel 2005).

To inform annual, island-specific fecundity (defined as the probability that a breeding bird fledges a chick), we used posterior samples from the top-supported nest survival model to derive informative priors for fecundity at each island. Because individual breeding birds could

not be uniquely linked to specific nest attempts, we assumed that each breeder attempted only a single brood per year. This assumption is supported by low hatching and fledging successes in second clutches (Ainley and Boekelheide 1990) and the rarity of double-brooding (Johns et al. 2017), suggesting that its contribution to annual reproductive output is low. Given the time required to complete Markov chain Monte Carlo (MCMC) sampling for the fecundity model, integrating the results as informative priors was substantially more efficient than modeling fecundity directly in the IPM. For each posterior sample, we calculated the proportion of successful nests, defined as the number of nests with a final fate indicating successful fledging, divided by the total number of nests that reached a terminal state (i.e., were not censored at the egg or chick stage due to incomplete monitoring). We used the moment-matching method to convert posterior samples from the nest survival model into beta-distributed fecundity priors for the IPM. For each island-year combination, we calculated the posterior mean and standard deviation of posterior samples and used these to estimate the parameters, α and β, of the beta distributions (see Appendix 3.1 for density plots of the derived beta priors for each island-year combination). For year and island combinations with no nest monitoring data, we used the mean and standard deviation of posterior samples for that island across all available years.

3.3.4.2 Survival model

To estimate adult survival and breeding state transitions, we developed a multistate mark-recapture model (Arnason 1972, 1973) with an unobservable state for individuals, known as "skippers" (Converse et al. 2009), that did not return to breed in a given year (Fujiwara and Caswell 2002, Kendall and Nichols 2002). We assumed that bands were not lost or misread, that individuals were independent, and that there was no unmodeled heterogeneity in individual survival, state transition, or detection probabilities. To meet the closure assumption of the

multistate model, we restricted the encounter data to the core breeding season by subsetting annual captures to March through June, inclusive.

Our multistate model includes adult birds only, and conditions on first capture. Because all captured adults are breeders, all birds enter the model in the breeder state. For all future time steps, the state *z* of individual *i* at time *t* is a categorical random variable following a Markov process, such that

$$z_{i,t}|z_{i,t-1} \sim \text{Categorical}(\boldsymbol{\Omega}_{i,t-1,z_{i,t-1}}), \quad (10)$$

where the state $z_{i,t}$ of an individual *i* at time *t* is a function of a transition probability matrix $\boldsymbol{\Omega}_{i,t-1,z_{i,t-1}}$, which depends on individual, time, and the individual's previous state $z_{i,t-1}$. We included three states: (1) alive and available for detection (breeders), (2) alive and unavailable (skippers), and (3) dead. We defined the state transition matrix as

$$\boldsymbol{\Omega}_{i,t-1,z_{i,t-1}} = \begin{bmatrix} & \mathbf{breeder}_{\boldsymbol{t}} & \mathbf{skipper}_{\boldsymbol{t}} & \mathbf{dead}_{\boldsymbol{t}} \\ \mathbf{breeder}_{\boldsymbol{t-1}} & \phi_{island,t}\psi^{II}_{island,t} & \phi_{island,t}(1-\psi^{II}_{island,t}) & 1-\phi_{island,t} \\ \mathbf{skipper}_{\boldsymbol{t-1}} & \phi_{island,t}\psi^{OI}_{island,t} & \phi_{island,t}(1-\psi^{OI}_{island,t}) & 1-\phi_{island,t} \\ \mathbf{dead}_{\boldsymbol{t-1}} & 0 & 0 & 1 \end{bmatrix}, \quad (11)$$

where rows represent the state in year $t-1$ and columns represent the state in year t. Individuals survive with probability $\phi_{island,t}$ (where island is either Prince Island or Scorpion Rock and is known and fixed for individual *i*); remain in the breeder state with repeat breeding probability $\psi^{II}_{island,t}$; transition to the skipper state with complementary probability $1-\psi^{II}_{island,t}$; transition from skipping to breeding with return breeding probability $\psi^{OI}_{island,t}$; and remain in the skipper state with complementary probability $1-\psi^{OI}_{island,t}$. Models for these survival and state transition probabilities are described below.

The observed capture history, $y_{i,t}$, for individual *i* at time *t* is also a categorical random variable,

$$y_{i,t}|z_{i,t} \sim \text{Categorical}(\boldsymbol{\Theta}_{i,t-1,z_{i,t}}), \quad (12)$$

with observation matrix $\boldsymbol{\Theta}_{i,t-1,z_{i,t}}$, which is conditional on individual, time, and the individual's current state $z_{i,t}$. We define this observation matrix as:

$$\boldsymbol{\Theta}_{i,t-1,z_{i,t}} = \begin{bmatrix} & \textbf{observed}_t & \textbf{unobserved}_t \\ \textbf{breeder}_t & p_{island,t} & 1 - p_{island,t} \\ \textbf{skipper}_t & 0 & 1 \\ \textbf{dead}_t & 0 & 1 \end{bmatrix} \quad (13)$$

with individuals in the breeder state detected with probability $p_{island,t}$, where again island is known and fixed for individual *i*. Note that, because there are only two observation types in this case, the categorical distribution is equivalent here to a Bernoulli distribution. Individuals in the skipper (and dead) states are unobservable. We modeled the detection probability for breeders, using a logit link, as a function of log(effort) for island and year *t*, with effort measured in days, thereby accounting for variation in the time devoted to monitoring at a given island and year. Thus,

$$\text{logit}(p_{island,t}) = \beta_0 + \beta_1 * \log(\text{effort}_{island,t}). \quad (14)$$

When there was no effort at a given island and year, detection probability was forced to 0 by this model.

We analyzed encounter histories for 558 adult individuals (450 from Prince Island, 108 from Scorpion Rock) during the study period, 1999 – 2022. We had 8 years of recapture data

from both islands (2000, 2001, 2005, 2012, 2015, 2016, 2018, 2021); 8 years from Prince Island only (1999, 2002, 2006, 2007, 2008, 2009, 2010, 2011); 2 years from Scorpion Rock only (2019, 2022), and 6 years without data from either island (2003, 2004, 2013, 2014, 2017, 2020).

To test our hypotheses regarding survival, we modeled adult survival, $\phi_{island,t}$, for each island and year *t* as a function of oceanographic covariates. We implemented a logit-linear model,

$$\begin{aligned}\text{logit}\left(\phi_{island,t}\right) = \alpha_0^{\phi} \; + \; \alpha_1^{\phi}[I_{island}] \\ + \beta^{\phi}_{annual\_survival} * ONI_t \\ + \beta^{\phi}_{southern\_winter} * winterBEUTI33_t \\ + \beta^{\phi}_{northern\_winter} * winterBEUTI39_t\end{aligned} \quad (15)$$

where α_0^{ϕ} is a global intercept; α^{ϕ}_{island} is an island-specific fixed effect with island indicator I_{island} = 1 for Scorpion Rock and 0 for Prince Island; and $\beta^{\phi}_{annual\_survival}$, $\beta^{\phi}_{southern\_winter}$, and $\beta^{\phi}_{northern\_winter}$ represent coefficients on time-varying covariates $ONI_t, winterBEUTI33_t$, and $winterBEUTI39_t$, which reflect our hypotheses on *annual survival* (ONI_t), *southern winter* ($winterBEUTI33_t$), and *northern winter* ($winterBEUTI39_t$) conditions.

To test our hypotheses on breeding transitions, we modeled breeding transition probabilities $\psi^{II}_{island,t}$ and $\psi^{OI}_{island,t}$, or generally $\psi^{SI}_{island,t}$, using an analogous structure,

$$\begin{aligned}\text{logit}\left(\psi^{SI}_{island,t}\right) = \alpha_0^{\psi} + \alpha_1^{\psi}[I_{island}] \\ + \beta^{\psi}_{annual\_breeding} * ONI_{t-1} \\ + \beta^{\psi}_{prebreeding} * preBEUTI33_t,\end{aligned} \quad (16)$$

where α_0^{ψ} are transition-specific intercepts, i.e., separate for $\psi_{island,t}^{II}$ and $\psi_{island,t}^{OI}$; α_1^{ψ} is an island-specific fixed effect that is shared across $\psi_{island,t}^{II}$ and $\psi_{island,t}^{OI}$; and $\beta_{annual\_breeding}^{\psi}$ and $\beta_{prebreeding}^{\psi}$ are coefficients, also shared across $\psi_{island,t}^{II}$ and $\psi_{island,t}^{OI}$, for time-varying covariates ONI_{t-1} and $preBEUTI33_t$ reflect our hypotheses on *annual breeding* (ONI_{t-1}) and *pre-season breeding* ($preBEUTI33_t$) conditions. See section 3.3.3 *Covariate data* for information on how covariates were prepared and indexed by time.

To account for unmeasured annual variation in demographic rates, we fit alternative models that included random time effects in the survival and breeding transition probability equations (Appendix 3.2). These models were structurally identical to the primary models described above except for the inclusion of the random effect terms. Model selection and fitting procedures remained the same (see below), allowing for direct comparison of support for covariates with and without accounting for unexplained temporal variation.

To evaluate the adequacy of model assumptions, we performed goodness-of-fit tests using the R2ucare package in R (Gimenez et al. 2018). We applied four standard component tests designed to identify violations in capture–recapture data: test 2.CL (assesses heterogeneity in capture probability among individuals not captured in the previous occasion); test 2.CT (tests for behavioral trap-dependence); test 3.SR (evaluates the presence of transient individuals by comparing apparent survival between newly marked and previously marked individuals); and test 3.SM (extends test 3.SR to a time-specific assessment across sampling occasions). These tests were applied separately to each island dataset using encounter histories and encounter frequencies, with Fisher's exact test substituted where expected cell counts were low.

To evaluate support for our hypotheses, we conducted model selection prior to integrating the survival model into the IPM using the indicator-variable approach (Kuo and

Mallick 1998; see also Link and Barker 2006; Smith et al. 2011; Converse et al. 2013). Here, each covariate *m* is associated with a Bernoulli variable, w_m, that is either a 0 (covariate excluded) or a 1 (covariate included) for each MCMC sample. This resulted in 32 candidate models and each model in this implied model set was given equal prior probability (e.g., $w_m \sim \text{dbern}(0.5)$; see details in Smith et al. 2011; Chapter 2, this dissertation). We calculated the Bayes Factor (BF; Hooten and Hobbs 2015) for each covariate as the ratio of the posterior odds to the prior odds of inclusion (Smith et al. 2011). The BF provides a weight of evidence for the inclusion of the associated covariate in the model. Because BF is sensitive to parameter priors, we restricted the total prior variance in the linear predictor and then apportioned that variance to all predictors in the model for any given MCMC sample (see details in Link and Barker 2006; Smith et al. 2011; Converse et al. 2013; Chapter 2, this dissertation). We considered a BF value < 3 indicative of no support for the covariate, >3 and <20 indicative of moderate support; >20 and <150 indicative of strong support; and >150 indicative of very strong support (Kass and Raftery 1995).

To conduct model selection on the survival model outside of the IPM, we fit the model in a Bayesian framework using NIMBLE (Valpine et al. 2017) in R (v4.4.1; R Core Team 2024). We drew 800,000 samples across three independent Markov chains from the joint posterior distribution and discarded 200,000 as burn-in. We assessed model convergence both visually using traceplots and by ensuring that the Brooks-Gelman-Rubin statistic ($\hat{R}$; Gelman and Rubin 1992) was <1.1.

Priors used for model selection on the survival model are described above. For the remaining priors on detection, (e.g., β_0, β_1), we used normal(0,1).

3.3.4.3 ABUNDANCE MODEL

To estimate annual abundance of breeders, we modeled count data collected from artificial burrows at each island and year. The observed counts represent the number of breeding pairs (and therefore the number of breeding females) detected in year *t* at each island. We modeled the log-transformed counts as normally distributed around the log of the true number of breeders, with a constant observation error shared across islands and years, such that:

$$\log\left(\text{Count}_{island,t}\right) \sim \text{Normal}(\log\left(N_{island,t}^{breeders}\right), \sigma) \quad (17)$$

where $N_{island,t}^{breeders}$ is the latent number of breeding pairs on island at year *t*, and σ is the standard deviation of the observation error on the log scale. Here, we are only modeling abundance of breeders available in artificial nest burrows, and we assume that the nest boxes are representative of trends in the larger island-wide auklet population (Johns 2020).

3.3.5 INTEGRATED POPULATION MODEL

The IPM integrates the three component models in a unified hierarchical framework by specifying a joint likelihood and shared latent variables. Fecundity, survival, and breeding state transition probabilities inform the stage-specific abundances, while counts of occupied nest boxes are linked to the abundance of the breeding population.

We used a female-only post-breeding census model, where the census is assumed to occur immediately after the annual breeding pulse (Caswell 2001). The population matrix model includes 11 stages: fledglings, yearlings, 2-year-old pre-breeders, 2-year-old first-time breeders, 3 year-old pre-breeders, 3 year-old first-time breeders, 4 year-old first-time breeders, established breeders (breeders that were breeders in the previous year), return breeders (breeders that were

skippers in the previous year), new skippers (skippers that were breeders in the previous year), and established skippers (skippers that were skippers in the previous year; Figure 3.1).

Annual transitions between stages were governed by survival probabilities, breeding probabilities, and recruitment probabilities for new breeders. Fledglings, yearlings, and pre-breeders survived with probability $\phi_{juvenile}$, a parameter that was not informed by data but was given an informed prior (see *Model fitting and implementation* for information on priors). Pre-breeders aged 2 and 3 transitioned to a first-time breeding state with probability $\psi_{newbreeder}$, which was not informed by data and was given a vague prior. All 4-year-olds that had not bred previously were assumed to become breeders with probability = 1. After first breeding, transitions between the breeding and skipping states were based on $\psi^{II}_{island,t}$, $\psi^{OI}_{island,t}$, and their associated complementary probabilities. Breeders and skippers survived with island-specific, time-varying probability ϕ. A list of demographic parameters and definitions can be found in Table 3.2.

Our analysis made several simplifying assumptions, largely due to data limitations. First, we assumed an equal sex ratio in the adult population, a common assumption in seabird demographic models (Lahoz-Monfort et al. 2017, Horswill et al. 2022, Bratt 2023, Frederiksen et al. 2024). Second, we assumed density-independent population dynamics. We believe this assumption is supported because monitored sites (artificial burrows and natural nest burrows) were never fully occupied during the study period (i.e., we did not observe limitations in nest habitat) and colony sizes are believed to be below historic levels (NPS unpublished data). Third, we assumed that individuals exhibit site fidelity, a common assumption for seabird species (Young and Ballance 2023) and for this species in particular (Ainley and Boekelheide 1990, Pyle et al. 2001). Additionally, we assumed homogeneity in adult survival across ages and breeding

states (i.e., breeders and non-breeders), and, due to data limitations, we assumed uniform juvenile survival across fledglings, yearlings, and pre-breeders. Finally, we assumed that four-year-olds that have not previously bred become breeders, i.e., all birds breed at or before age four, an assumption supported by Pyle et al. 2001 and Lee et al. 2012.

3.3.6 Model fitting and implementation

The likelihood of the integrated population model is the product of the component likelihoods. Estimating survival, productivity, and abundance from the same sample of individuals violates the assumption that the data sets in an integrated population model are independent, an assumption required for correct variance estimation. However, IPMs have been shown to be robust to violations of the independence assumption (Abadi et al. 2010, Weegman et al. 2021) and the benefits of an IPM have the potential to outweigh the risks of violating this assumption.

We fit the model in a Bayesian framework using NIMBLE (Valpine et al. 2017) in R (v4.4.1; R Core Team 2024). We drew 350,000 samples across three independent Markov chains from the joint posterior distribution and discarded 50,000 as burn-in. We assessed model convergence both visually using traceplots and by ensuring that the Brooks-Gelman-Rubin statistic ($\hat{R}$; Gelman and Rubin 1992, Brooks and Roberts 1998) was <1.1. Posterior summaries and diagnostics were based on MCMC samples thinned by retaining every third iteration.

We largely used weakly informative priors in the IPM. For all breeding transition probabilities ($\psi_{newbreeder}$, $\psi^{II}_{island,t}$, $\psi^{OI}_{island,t}$), we used uniform(0,1). For priors on detection, survival, and breeding transition intercepts and covariates (e.g., β_0, β_1, α_0^{ϕ}, α_1^{ϕ}, α_1^{ψ}, α_1^{ψ}), we used normal(0,1). The observation error for the log-transformed count data was modeled using a normal distribution with shared precision $\tau = {}^{1}/_{\sigma^2}$, where σ had a gamma(1,0.001) prior. Given

the lack of data to inform juvenile survival, we used an informed prior of beta(2,3) for a mean of 0.40, informed by Lee et al. (2012), who estimated survival of auklets from ages 0 to 2 at Southeast Farallon Island at 0.381.

The population structure in the first year was drawn from a multinomial distribution using a probability vector equal to an approximate stable age distribution, based on exploratory simulations. The total population in the first year was drawn from a discrete uniform distribution bounded between 70 and 200 individuals per island.

All materials and code developed for the analysis can be found on GitHub (https://github.com/ameliaduvall/Dissertation_Chapter3).

3.3.7 Population growth rate

To quantify trends in overall population dynamics, we estimated both annual and long-term population growth rates using posterior samples of total population size from the IPM. For each MCMC iteration, we summed the estimated number of individuals across all life stages to calculate total population size for each island and year t, $N_{island,t}^{total}$. Annual population growth rates were computed as:

$$\bar{\lambda}_{island,t} = \frac{N_{island,t+1}^{total}}{N_{island,t}^{total}} \quad (18)$$

representing the year-to-year proportional change in total abundance. These values were calculated across all posterior samples to produce a full posterior distribution of $\lambda_{island,t}$ for each island and year.

To assess long-term trends, we also calculated the geometric mean population growth rate across the entire time series for each island:

$$\bar{\lambda}_{island,t} = \left(\prod_{t=1}^{T-1} \lambda_{island,t}\right)^{1/(T-1)} \quad (19)$$

where *T* is the total number of years of abundance estimates. The geometric mean was computed for each MCMC iteration, allowing the propagation of uncertainty from the posterior distributions of abundance and annual growth. We summarized both the annual and geometric mean growth rates by posterior means and 95% credible intervals to assess whether populations were, on average, increasing ($\bar{\lambda} > 1.0$), declining ($\bar{\lambda} < 1.0$), or stable ($\bar{\lambda} = 1.0$).

3.3.8 Covariance between demographic parameters and population growth

To evaluate the sensitivity of population growth rate ($\bar{\lambda}$) to variation in key demographic parameters and assess evidence for demographic compensation, we calculated posterior distributions of correlations among survival, fecundity, and $\bar{\lambda}$ across years. Specifically, for each island, we computed correlations: (1) adult survival in year *t* (representing survival from year *t* to *t+1*) and $\bar{\lambda}$ in year *t*, (2) fecundity in year *t* and $\bar{\lambda}$ in year *t*, and (3) survival in year *t* and fecundity in year *t*. For each MCMC iteration, we calculated $\bar{\lambda}$ as the ratio of total population size at each island in year *t* + 1 to the population size in year *t*, based on posterior samples of age-structured abundance (see *Population growth rate*). We then extracted corresponding samples of survival and fecundity and computed Pearson correlation coefficients across years within each iteration.

3.4 Results

Below, we present results from the component survival model, followed by estimates from the integrated population model and results on population growth rate and covariance between demographic parameters and population growth.

3.4.1 SURVIVAL MODEL

For model selection conducted on the adult survival and breeding state transition model, outside of the IPM, only the covariate associated with the *southern winter* hypothesis was indicative of very strong support with a BF value of 38296.87 (Table 3.3). All other covariates had BF<1, indicating no support for inclusion of these covariates in the model (Table 3.3). These results support our *southern winter* hypothesis that adult survival is driven by southern winter conditions, reflecting a sensitivity to overwintering conditions and a tendency to remain in the southern California Current during winter. See Table 3.1 for information on all hypotheses tested.

Out of the 32 candidate models, the model with the most weight (28.3%) had the *southern winter* hypothesis covariates on survival and none on the breeding transition probabilities (Table 3.4). We used the model with the *southern winter* hypothesis covariate on annual adult survival only and no oceanographic covariates on breeding transition probabilities for inference and integration into the IPM. The alternative model structure with the inclusion of time random effects, explored in Appendix 3.2, found no support for any covariates, suggesting that temporal variation could explain much of the variation in demographic rates that was otherwise attributed to oceanographic covariates in the primary models.

We assessed the fit of the mark-recapture model for each island using component goodness-of-fit tests implemented in the R2ucare package (Gimenez et al. 2018). At Scorpion Rock, none of the tests indicated a violation of model assumptions. Specifically, there was no evidence for heterogeneity in capture probability among individuals not seen at the previous occasion (test 2.CL: $\chi^2 = 0$, degrees of freedom [df] = 2, p = 1.00), nor for behavioral responses to capture (test 2.CT: $\chi^2 = 0$, df = 1, p = 1.00). Likewise, we detected no evidence of transients

using either the time-specific (test 3.SM: χ^2 = 0, df = 1, p = 1.00) nor overall transience test (test 3.SR: χ^2 = 2.74, df = 5, p = 0.740). At Prince Island, three of the four tests similarly supported the assumptions of the model (Test 2.CL: χ^2 = 3.02, df = 8, p = 0.933; test 2.CT: χ^2 = 5.20, df = 6, p = 0.518; Test 3.SM: χ^2 = 0.668, df = 9, p = 1.00). However, the overall transience test (test 3.SR) yielded a borderline significant result (χ^2 = 19.67, df = 11, p = 0.050), largely driven by a single interval (component 2: χ^2 = 12.34, p < 0.001), suggesting possible presence of transient individuals in the early part of the time series. Across both islands, many time intervals could not be evaluated due to sparse data or low cell counts, which limited the number of component tests that could be performed.

3.4.2 Integrated population model

3.4.2.1 Population size and structure

Posterior estimates of stage-structured abundance indicate both similarities and differences in the magnitude and timing of population growth and structure over the past two decades (Figure 3.2). At Prince Island, total population size increased steadily from fewer than 40 individuals in the early 2000s to nearly 100 by 2022. In contrast, Scorpion Rock exhibited slower growth, with initial fluctuations and a smaller net increase, stabilizing below 50 individuals in recent years. Both populations experienced an early decline in estimated abundance during the early 2000s. The overall larger population size observed at Prince Island likely reflects, at least in part, the greater availability of artificial nesting habitat (n = 72) compared to Scorpion Rock (n = 35).

Estimated stage-specific abundances revealed consistent population structure at both colonies (Figure 3.2). The skipped breeder stage was the dominant component in later years at both sites. Despite increases in this stage, the number of active breeders remained relatively

stable across the time series, generally ranging from 1 to 10 individuals per year. The non-breeder stage (pre-breeders aged 2–3) was the smallest across years, with estimated annual abundances below three individuals per site. Fledgling and yearling stages showed the most interannual variability, consistent with expectations for stages influenced by fecundity and early-life survival. The highest estimated number of fledglings occurred in 1999, with approximately 17 individuals fledged from both colonies, whereas no fledglings were estimated in 2007, indicating reproductive failure that year for the study population. This was followed by no yearling estimated in 2008.

3.4.2.2 Parameter estimates

Fecundity and survival probabilities exhibited notable differences in magnitude, variability, and temporal pattern between Scorpion Rock and Prince Island (Table 3.5; Figure 3.3). Fecundity varied substantially across years on both islands. On average, Scorpion Rock (0.430 [95% Bayesian credible interval, BCI: 0, 0.761]) exhibited slightly higher fecundity than Prince Island (0.401 [95% BCI: 0, 0.682]), although both islands experienced episodic declines. In contrast, survival was consistently higher and more stable across time. Survival at both islands was similar: Scorpion Rock at 0.810 (95% BCI: 0.542, 0.939) and Prince Island at 0.788 (95% BCI: 0.520, 0.911). Mean juvenile survival was lower than annual adult survival probabilities at both islands and had high uncertainty (0.624 [95% BCI: 0.281, 0.889]), which is expected given that there was not any data available to inform this parameter. Likewise, the probability of a pre-breeder transitioning to a breeder, which was also uninformed and had a vague prior, had high uncertainty (0.633 [95% BCI: 0.162, 0.979]).

Breeding transition probabilities varied substantially by island. The repeat breeding probability (ψ_{II}) was much higher for Prince Island (0.791 [95% BCI: 0.657, 0.957]) than

Scorpion Rock (0.288 [95% BCI: 0.123, 0.518]). Skipped breeders were slightly more likely to return to breeding (return breeding probability, ψ_{OI}) on Prince Island (0.254 [95% BCI: 0.084, 0.445]) than Scorpion Rock (0.165 [95% BCI: 0.079, 0.291]), although, the probability was low at both islands.

The posterior estimate for the *southern winter* hypothesis coefficient $\beta_{southern\_winter}$ was -0.557 [95% BCI: -0.799, -0.338]), indicating lower survival with stronger southern upwelling (higher BEUTI) in the winter.

Annual detection probabilities (p) for breeding individuals varied over time as a function of monitoring effort and differed between Scorpion Rock and Prince Island (Appendix 3.3). In years without monitoring effort, detection probability was fixed to zero, resulting in intermittent gaps in the time series and contributing to low mean detection probabilities at both Scorpion Rock (0.285 [95% BCI: 0, 0.892]) and Prince Island (0.361 [95% BCI: 0, 0.895]) with substantial interannual variation.

3.4.3 Population growth rate

Annual population growth rates ($\bar{\lambda}$) varied across years and between islands, with fluctuations in both the point estimates and associated uncertainty (Figure 3.4). At Scorpion Rock, $\bar{\lambda}$ was generally close to 1.0, with a minimum of 0.967 observed in 2001 and a peak of 1.070 in 2020. In contrast, Prince Island exhibited consistently higher annual $\bar{\lambda}$ values than Scorpion Rock, particularly during the early and mid-2000s, with growth rates frequently exceeding 1.0. A minimum $\bar{\lambda}$ of 0.990 was observed in 2006, followed by a maximum of 1.132 shortly thereafter in 2009.

Geometric mean population growth rates indicate consistent increases at both colonies, but more pronounced at Prince Island. At Scorpion Rock, the posterior mean $\bar{\lambda}$ was 1.023 (95%

BCI: 1.010, 1.036), while Prince Island exhibited slightly higher growth at 1.056 (95% BCI: 1.039, 1.076). The credible intervals for both islands excluded 1, indicating strong evidence for positive population growth over the study period.

3.4.4 Covariance between demographic parameters and population growth rate

For Scorpion Rock, the correlation coefficient between survival in year *t* to year *t*+1 and population growth rate in year *t* to year *t*+1 was 0.316 (95% BCI: -0.078, 0.596; Figure 3.5). Correlation between fecundity in year *t* and population growth rate in year *t* to year *t*+1 was 0.152 (95% BCI: -0.219, 0.468). Correlation between the two demographic parameters, fecundity in year *t* and survival in year *t* to year *t*+1, was 0.474 (95% BCI: 0.310, 0.635).

For Prince Island, the correlation coefficient between survival in year *t* to year *t*+1 and population growth rate in year *t* to year *t*+1 was 0.124 (95% BCI: -0.278, 0.465; Figure 3.5). Correlation between fecundity in year *t* and population growth rate in year *t* to year *t*+1 was -0.025 (95% BCI: -0.393, 0.341). Correlation between the two demographic parameters, fecundity in year *t* and survival in year *t* to year *t*+1, was 0.219 (95% BCI: 0.098, 0.330).

3.5 Discussion

We developed an IPM to evaluate how oceanographic variability influences Cassin's Auklet population dynamics through multiple demographic pathways. By modeling survival, fecundity, and abundance using data from two colonies situated across a natural oceanographic gradient, our IPM provided a unified framework for quantifying fine-scale demographic responses to environmental change. Our results reveal that auklet demography is sensitive to environmental variability in ways that reflect both life history and site-specific responses.

We found evidence largely consistent with the demographic buffering hypothesis at both Scorpion Rock and Prince Island. As predicted by this hypothesis (Pfister 1998, Gaillard et al. 2000), adult survival, a vital rate with strong influence on population viability for seabirds, was higher and less variable than fecundity at both colonies (Figure 3.3). Mean fecundity was slightly higher at Scorpion Rock (0.430 [95% BCI: 0, 0.761]) than at Prince Island (0.401 [95% BCI: 0, 0.682]), but survival estimates were similar at both locations and relatively high and stable (Scorpion Rock: 0.810 [95% BCI: 0.542, 0.939], Prince Island: 0.788 [0.520, 0.912]). The island-specific fixed effect for survival (0.164 [95% BCI: -0.454, 0.882]) was centered near zero with a wide credible interval overlapping zero, indicating no strong evidence for a difference in survival between the two colonies. Despite considerable variability in fecundity, and years with reproductive failure, neither colony appears to be decreasing, with Prince Island showing slightly more growth than Scorpion Rock (Figure 3.4).

Oceanographic drivers of vital rates differed between survival and fecundity and, to some extent, by colony. Fecundity was best explained by local sea surface temperature and inherent site-specific differences that were not fully captured by oceanographic covariates (DuVall, Chapter 2, this dissertation). Reproductive success at Prince Island also appeared more sensitive to warming sea surface temperatures than at Scorpion Rock, suggesting differential susceptibility to warming via ocean climate change at the two colonies. In contrast, the strongest predictor of adult survival was winter ocean conditions in the southern California Bight, providing support for the *southern winter* hypothesis and highlighting the importance of winter ocean productivity and conditions in shaping survival outcomes for seabirds. However, the direction of the effect was opposite of what we expected, where lower adult survival was associated with conditions indicative of greater upwelling, and therefore marine productivity and prey availability. This may

be explained, in part, because winter is not a major upwelling period in the California Current, instead peaking in late spring and summer (Bograd et al. 2009). While it warrants further investigation, it is possible that BEUTI was a proxy for storminess at this time, which is known to negatively impact seabird survival (Boano et al. 2010, Laurenson et al. 2024). At other northern colonies, reduced auklet survival has been associated with El Niño events, periods associated with warm sea surface temperatures and suppressed upwelling in the California Current (Bertram et al. 2005), particularly during the winter (Lee et al. 2007).

Our results also offer new insights into non-breeding season movement patterns. Although some auklets at CHIS are known to disperse northward to central California post-breeding (Adams et al. 2004a), we found no support for the *northern winter* hypothesis, which posits that auklets move north in the California Current during the winter. Instead, our findings suggest that individuals are likely to remain in southern California region during winter. This contrasts with geolocator data showing that auklets from Southeast Farallon Island primarily use waters between Cape Mendocino and Point Conception in winter (Johns et al. 2020), supporting the idea that Point Conception may serve as a barrier to gene flow between the northern and southern auklet subspecies (Wallace et al. 2015). Similar survival rates between Scorpion Rock and Prince Island also suggest that individuals from both colonies may occupy overlapping wintering areas during this time, making them equally susceptible to environmental variability during the non-breeding season.

To evaluate the robustness of our findings, we also fit an alternative model that included random time effects on the survival and breeding transition probabilities. These random time effects account for unmeasured temporal variation across years or time intervals, helping to reduce bias and improve model flexibility. However, they can also absorb variation that might

otherwise be attributed to oceanographic covariates, potentially limiting the ability to detect fixed effects. In our analysis, the inclusion of random time effects eliminated support for all oceanographic covariates. It is unclear whether this reflects truly weak associations or whether meaningful relationships were obscured by temporal variation, a challenge that was compounded by spotty mark-recapture data across years. This ambiguity underscores the difficulty of detecting climate-demography linkages in systems with limited or uneven data and highlights both the utility and limitations of including random effects when covariate signals are subtle.

The positive correlation between fecundity and survival at both colonies indicates that these vital rates often co-vary in response to ocean conditions (Figure 3.5). Such synchrony can increase population-level sensitivity to environmental variability, as multiple demographic processes may decline simultaneously during unfavorable years. Similar patterns of positive covariation have been reported for auklets at Southeast Farallon Island, where survival, breeding probability, and reproductive success were all positively correlated (Lee et al. 2007), as well as in other seabird species (Nur and Sydeman 1999, Jenouvrier et al. 2003). A stronger correlation between survival and fecundity ($r = 0.474$) at Scorpion Rock as compared to Prince Island ($r = 0.219$), suggests Scorpion Rock may be more sensitive to oceanographic variability. While auklet reproductive success at Scorpion Rock seemed more robust to oceanic warming (DuVall, Chapter 2), the tighter coupling between demographic rates may render the colony at Scorpion Rock more vulnerable to oceanographic variability.

Despite positive covariation between vital rates, neither survival nor fecundity was strongly correlated with annual population growth rate, suggesting that these parameters alone do not fully explain changes in annual population growth. Since both colonies appear to be stable or increasing (Figures 3.2, 3.4), other demographic processes, such as recruitment and breeding

transitions, may play an influential role. Recruitment has been identified as a key demographic buffer in other auklet populations (Johns et al. 2022). At both colonies, the number of individuals in the skipper stage increased over time, yet the number of active breeders remained relatively consistent (Figure 3.2). Recruitment of new breeders may be offsetting the rising prevalence of non-breeding adults as abundance increasing, indicating the importance of population structure in overall dynamics.

Differences in population growth rates between the colonies could be explained, in part, by a much lower repeat breeding probability for Scorpion Rock (0.288 [95% BCI: 0.123, 0.518]) as compared to Prince Island (0.791 [95% BCI: 0.520, 0.912]). Likewise, skipped breeders were less likely to return to breed at Scorpion Rock (0.165 [95% BCI: 0.079, 0.291]) than Prince Island (0.254 [95% BCI: 0.084, 0.445]), but the probability remained low at both sites. We did not find support for the inclusion of oceanographic covariates in explaining variation in breeding transition probabilities, leaving the drivers of these differences unresolved. This may indicate that environmental cues relevant to breeding transition probabilities occur on finer temporal or spatial scales than our covariates captured, or that individual decisions to skip breeding are more influenced by intrinsic factors such as body condition or age (e.g., Johns et al. 2017). However, these results could also suggest dispersal or recruitment outside of the study area, which would challenge our assumption of site fidelity. Alternatively, individuals may have site fidelity to an island, but not a nest site (i.e., individuals move between natural and artificial nest burrows). Finally, we cannot rule out the possibility that it could reflect some confounding between mortality and skip breeding probability, especially given the sparse data (Kendall and Nichols 2002, Bailey et al. 2010).

Our findings are broadly consistent with auklet demography studies from elsewhere in the species' range. Auklet survival tends to be lower than in other seabirds (Young and Ballance 2023) and varies both spatially and temporally. Survival was estimated at 0.71 (standard error [SE] = .02) in 1994 – 2000 at Triangle Island and 0.80 (SE = 0.02) at a nearby colony, Frederick Island (Bertram et al. 2005). At Southeast Farallon Island from 1986 – 2002, survival ranged from 0.789 for males (SE = 0.040; males) to 0.774 for females (SE = 0.036; Lee et al. 2007). Annual survival can be as great as 0.96 (95% confidence interval: 0.84, 0.99) for high-quality, older individuals (Johns et al. 2018). From 2000 – 2005, reproductive success at three major auklet breeding colonies varied from 0.54 (standard deviation [SD] = 0.25) chicks per breeding pair/year at Triangle Island, to 0.77 (SD = 0.42) at Southeast Farallon Island, and 0.54 (SD = 0.23) at San Benito Island in Baja California (Wolf et al. 2009). While our estimates are on the lower end of this range, apparent nest success can often overestimate true success because it does not account for variation in exposure time or the higher likelihood of detecting nests that survive longer (Mayfield 1961).

Our analysis had some limitations, largely due to data availability, that should be further explored. First, we were not able to account for multiple nests in a season associated with one female (i.e., double-brooding) due to an inability to definitively associate clutches with uniquely identified individuals. While hatching and fledging success tends to be low for second clutches (Ainley and Boekelheide 1990) and overall double-brooding is rare (Johns et al. 2017), it appears to be driven by a subset of high-quality, older individuals that produce substantially more offspring over the course of their lifetimes (Johns et al. 2017). At Southern Farallon Island, double-brooding helps buffer the effects of climate-driven mass mortality events by increasing the likelihood of high recruitment episodes, which replenish the breeding population in

subsequent years and help maintain long-term population stability despite periods of high adult mortality (Johns et al. 2022).

Another limitation of our analysis is that it relied on a comparison between only two colonies. While these islands offer a compelling natural contrast, the small sample size limited our ability to disentangle the effects of oceanographic drivers from other site-specific influences such as colony history, predator pressure, or habitat quality. Although auklets have bred at both islands for decades (and likely longer; NPS unpublished data), the artificial habitat at Scorpion Rock was installed more recently than at Prince Island, where monitoring of auklets in artificial burrows began in 1975. At both sites, the design and installation of artificial habitats have gone through several iterations, though some form of artificial structure has consistently been present and occupied during the breeding season. Another site-level difference is the initiation of a native habitat restoration project at Scorpion Rock in 2007, undertaken in part due to observed auklet mortality. The project aimed to reduce avian predation and enhance natural burrow habitat by increasing native shrub cover. These context-specific factors could contribute to the observed demographic differences between islands. For example, lower breeding probabilities at Scorpion Rock may reflect a less established or more disturbed colony. Finally, our analyses were limited to individuals using artificial nest burrows, which may introduce bias or fail to fully capture population-wide dynamics if artificial habitat users differ in behavior or demography from those in natural burrows; although, research at another colony suggests that individuals in artificial nest burrows can act as proxies for those in natural nest burrows (Johns 2022).

By integrating fecundity, survival, and abundance into a unified population model, this study offers one of the first comprehensive assessments of Cassin's Auklet demography in the southern portion of their range. These findings contribute to a growing understanding of seabird

responses to ocean climate variability and can help inform range-wide conservation strategies in dynamic and vulnerable ecosystems like the California Current.

3.6 Acknowledgements

We acknowledge the Montrose Trustee Council, whose funding and support were critical to the collection of these data. We thank and acknowledge several others who have contributed to this work, including but not limited to: H. Carter, J. Felis, A. Hebshi, J. Howard, E. Kelsey, P. Larramendy, J. Takekawa, A. Yamagiwa. We owe deep thanks to N. Hostetter and A. Warlick for assistance with the analysis. Any use of trade, firm, or product names is for descriptive purposes only and does not imply endorsement by the U.S. Government.

3.7 References

Abadi, F., O. Gimenez, R. Arlettaz, and M. Schaub. 2010. An assessment of integrated population models: bias, accuracy, and violation of the assumption of independence. Ecology 91:7–14.

Adams, J., J. Y. Takekawa, and H. R. Carter. 2004a. Foraging distance and home range of Cassin's Auklets nesting at two colonies in the California Channel Islands. The Condor 106:618–637.

Adams, J., J. Y. Takekawa, and H. R. Carter. 2004b. Stable foraging areas and variable chick diet in Cassin's Auklets (Ptychoramphus aleuticus) off southern California. Canadian Journal of Zoology 82:1578–1595.

Ainley, D. G., and R. J. Boekelheide. 1990. Seabirds of the Farallon Islands: Ecology, dynamics, and structure of an upwelling-system community. Stanford University Press, Stanford, California, USA.

Ainley, D. G., D. A. Manuwal, J. Adams, and A. C. Thoresen. 2020. Cassin's Auklet (Ptychoramphus aleuticus), version 1.0. In A. F. Poole, editor. Birds of the World. Cornell Lab of Ornithology, Ithaca, New York, USA. https://doi.org/10.2173/bow.casauk.01

Amos, C. M., and R. M. Castelao. 2022. Influence of the El Niño-Southern Oscillation on SST fronts along the west coasts of North and South America. *Journal of Geophysical Research: Oceans* 127:e2022JC018479.

Arnason, A. N. 1972. Parameter estimates from mark-recapture experiments on two populations subject to migration and death. Population Ecology 13:97–113.

Arnason, A. N. 1973. The estimation of population size, migration rates and survival in a stratified population. Researches on Population Ecology 15:1–8.

Barbraud, C., and H. Weimerskirch. 2003. Climate and density shape population dynamics of a marine top predator. Proceedings of the Royal Society of London. Series B: Biological Sciences 270:2111–2116.

Bailey, L. L., S. J. Converse, and W. L. Kendall. 2010. Bias, precision, and parameter redundancy in complex multistate models with unobservable states. Ecology 91:1598–1604.

Bertram, D. F., A. Harfenist, and B. D. Smith. 2005. Ocean climate and El Niño impacts on survival of Cassin's Auklets from upwelling and downwelling domains of British Columbia. Canadian Journal of Fisheries and Aquatic Sciences 62:2841–2853.

Besbeas, P., S. N. Freeman, B. J. T. Morgan, and E. A. Catchpole. 2002. Integrating mark–recapture–recovery and census data to estimate animal abundance and demographic parameters. Biometrics 58:540–547.

Blight, L. K. 2011. Egg production in a coastal seabird, the Glaucous-Winged Gull (Larus glaucescens), declines during the last century. PLOS ONE 6:e22027.

Boano, G., P. Brichetti, and U. Foschi. 2010. 'La Niña'-driven Atlantic storms affect winter survival of Mediterranean Cory's Shearwaters. Italian Journal of Zoology 77:460–468.

Bograd, S. J., I. Schroeder, N. Sarkar, X. Qiu, W. J. Sydeman, and F. B. Schwing. 2009. Phenology of coastal upwelling in the California Current. Geophysical Research Letters 36.

Bond, A. L., I. L. Jones, W. J. Sydeman, H. L. Major, S. Minobe, J. C. Williams, and G. V. Byrd. 2011. Reproductive success of planktivorous seabirds in the North Pacific is related to ocean climate on decadal scales. Marine Ecology Progress Series 424:205–218.

Bratt, A. E. 2023. From mark-resight to management: Bayesian hierarchical models for endangered bird populations. University of Washington Libraries, Seattle, Washington, USA.

Brooks, S. P., and G. O. Roberts. 1998. Convergence assessment techniques for Markov chain Monte Carlo. Statistics and Computing 8:319–335.

Caswell, H. 2001. Matrix population models: Construction, analysis, and interpretation. 2nd edition. Sinauer Associates, Sunderland, Massachusetts, USA.

Converse, S. J., W. L. Kendall, P. F. Doherty, and P. G. Ryan. 2009. Multistate models for estimation of survival and reproduction in the grey-headed albatross (Thalassarche chrysostoma). The Auk 126:77–88.

Converse, S. J., J. A. Royle, P. H. Adler, R. P. Urbanek, and J. A. Barzen. 2013. A hierarchical nest survival model integrating incomplete temporally varying covariates. Ecology and Evolution 3:4439–4447.

Frederiksen, M., T. Anker-Nilssen, H. Schekkerman, V. Dierschke, M. Parsons, S. Marra, and I. Mitchell. 2024. Model-based assessment of marine bird population status using monitoring of breeding productivity and abundance. Ibis 166:940–950.

Fujiwara, M., and H. Caswell. 2002. Estimating population projection matrices from multistate mark–recapture data. Ecology 83:3257–3265.

Gaillard, J.-M., M. Festa-Bianchet, N. G. Yoccoz, A. Loison, and C. Toïgo. 2000. Temporal variation in fitness components and population dynamics of large herbivores. Annual Review of Ecology, Evolution, and Systematics 31:367–393.

Gelman, A., and D. B. Rubin. 1992. Inference from iterative simulation using multiple sequences. Statistical Science 7:457–472.

Gimenez, O., J.-D. Lebreton, R. Choquet, and R. Pradel. 2018. R2ucare: An R package to perform goodness-of-fit tests for capture–recapture models. Methods in Ecology and Evolution 9:1749–1754.

Hooten, M. B., and N. T. Hobbs. 2015. A guide to Bayesian model selection for ecologists. Ecological Monographs 85:3–28.

Horswill, C., M. J. Wood, and A. Manica. 2022. Temporal change in the contribution of immigration to population growth in a wild seabird experiencing rapid population decline. Ecography 2022:e05846.

Jacox, M. G., C. A. Edwards, E. L. Hazen, and S. J. Bograd. 2018. Coastal upwelling revisited: Ekman, Bakun, and improved upwelling indices for the U.S. West Coast. Journal of Geophysical Research: Oceans 123:7332–7350.

Jenouvrier, S., C. Barbraud, and H. Weimerskirch. 2003. Effects of climate variability on the temporal population dynamics of Southern Fulmars. Journal of Animal Ecology 72:576–587.

Johns, M., P. Warzybok, R. Bradley, J. Jahncke, M. Lindberg, and G. Breed. 2017. Age, timing, and a variable environment affect double brooding of a long-lived seabird. Marine Ecology Progress Series 564:187–197.

Johns, M. E., P. Warzybok, R. W. Bradley, J. Jahncke, M. Lindberg, and G. A. Breed. 2018. Increased reproductive investment associated with greater survival and longevity in Cassin's Auklets. Proceedings of the Royal Society B: Biological Sciences 285:20181464.

Johns, M. E., P. Warzybok, J. Jahncke, M. Lindberg, and G. A. Breed. 2020. Oceanographic drivers of winter habitat use in Cassin's Auklets. Ecological Applications 30:e02068.

Johns, M. E. 2020. The effects of individual and environmental heterogeneity on long-term population dynamics of Cassin's Auklets (Ptychoramphus aleuticus). University of Alaska Fairbanks.

Johns, M. E., P. Warzybok, J. Jahncke, P. Doak, M. Lindberg, and G. A. Breed. 2022. Episodes of high recruitment buffer against climate-driven mass mortality events in a North Pacific seabird population. Journal of Animal Ecology 91:345–355.

Jones, T., J. K. Parrish, W. T. Peterson, E. P. Bjorkstedt, N. A. Bond, L. T. Ballance, V. Bowes, J. M. Hipfner, H. K. Burgess, J. E. Dolliver, K. Lindquist, J. Lindsey, H. M. Nevins, R. R. Robertson, J. Roletto, L. Wilson, T. Joyce, and J. Harvey. 2018. Massive mortality of a planktivorous seabird in response to a marine heatwave. Geophysical Research Letters 45:3193–3202.

Jones, T., J. K. Parrish, P. MacCready, L. T. Ballance, D. W. Bradley, H. K. Burgess, J. E. Dolliver, J. T. Harvey, T. Joyce, K. Lindquist, J. Lindsey, H. M. Nevins, J. Roletto, L. Wilson, and C. Wright. 2025. Assessing total mortality following seabird wrecks given variable data quantity and quality: the Cassin's auklet die-off. Canadian Journal of Fisheries and Aquatic Sciences 82:1–22.

Kass, R. E., and A. E. Raftery. 1995. Bayes factors. Journal of the American Statistical Association 90:773–795.

Kendall, W. L., and J. D. Nichols. 2002. Estimating state-transition probabilities for unobservable states using capture–recapture/resighting data. Ecology 83:3276–3284.

Kuo, L., and B. Mallick. 1998. Variable selection for regression models. Sankhyā: The Indian Journal of Statistics, Series B (1960–2002) 60:65–81.

Lahoz-Monfort, J. J., M. P. Harris, S. Wanless, S. N. Freeman, and B. J. T. Morgan. 2017. Bringing it all together: multi-species integrated population modelling of a breeding community. Journal of Agricultural, Biological and Environmental Statistics 22:140–160.

Laurenson, K., M. J. Wood, T. R. Birkhead, M. D. K. Priestley, R. B. Sherley, A. L. Fayet, T. Guilford, B. J. Hatchwell, and S. C. Votier. 2025. Long-term multi-species demographic studies reveal divergent negative impacts of winter storms on seabird survival. Journal of Animal Ecology 94:139–153.

Lee, D. E., N. Nur, and W. J. Sydeman. 2007. Climate and demography of the planktivorous Cassin's Auklet Ptychoramphus aleuticus off northern California: Implications for population change. Journal of Animal Ecology 76:337–347.

Lee, D. E., P. M. Warzybok, and R. W. Bradley. 2012. Recruitment of Cassin's Auklet (Ptychoramphus aleuticus): Individual age and parental age effects. The Auk 129:124–132.

Lewontin, R. C., and D. Cohen. 1969. On population growth in a randomly varying environment. Proceedings of the National Academy of Sciences 62:1056–1060.

Link, W. A., and R. J. Barker. 2006. Model weights and the foundations of multimodel inference. Ecology 87:2626–2635.

Lunn, N. J., S. Servanty, E. V. Regehr, S. J. Converse, E. Richardson, and I. Stirling. 2016. Demography of an apex predator at the edge of its range: impacts of changing sea ice on polar bears in Hudson Bay. Ecological Applications 26:1302–1320.

Manuwal, D. A. 1974. The natural history of Cassin's Auklet (Ptychoramphus aleuticus). The Condor 76:421–431.

Messié, M., and F. P. Chavez. 2017. Nutrient supply, surface currents, and plankton dynamics predict zooplankton hotspots in coastal upwelling systems. Geophysical Research Letters 44:8979–8986.

Mills, J. A., J. W. Yarrall, J. M. Bradford-Grieve, M. J. Uddstrom, J. A. Renwick, and J. Merilä. 2008. The impact of climate fluctuation on food availability and reproductive performance of the planktivorous Red-Billed Gull Larus novaehollandiae scopulinus. Journal of Animal Ecology 77:1129–1142.

Montevecchi, W. A., P. M. Regular, J.-F. Rail, K. Power, C. Mooney, K. J. N. D'Entremont, S. Garthe, L. Guzzwell, and S. I. Wilhelm. 2021. Ocean heat wave induces breeding failure at the southern breeding limit of the Northern Gannet Morus bassanus. ICES Journal of Marine Science 78:2992–3001.

Morris, W. F., and D. F. Doak. 2004. Buffering of life histories against environmental stochasticity: accounting for a spurious correlation between the variabilities of vital rates and their contributions to fitness. The American Naturalist 163:579–590.

National Oceanic and Atmospheric Administration (NOAA). 2024. California Current IEA indicators. Integrated Ecosystem Assessment, NOAA Fisheries. https://www.integratedecosystemassessment.noaa.gov/regions/california-current/california-current-iea-indicators (Accessed 13 May 2023).

Nur, N., and W. Sydeman. 2009. Survival, breeding probability and reproductive success in relation to population dynamics of Brandt's Cormorants Phalacrocorax penicillatus. Bird Study 46:S92–S103.

Paleczny, M., E. Hammill, V. Karpouzi, and D. Pauly. 2015. Population trend of the world's monitored seabirds, 1950–2010. PLOS ONE 10:e0129342.

Pfister, C. A. 1998. Patterns of variance in stage-structured populations: evolutionary predictions and ecological implications. Proceedings of the National Academy of Sciences 95:213–218.

Pradel, R. 2005. Multievent: An extension of multistate capture-recapture models to uncertain states. Biometrics 61:442–447.

Pyle, P. 2001. Age at first breeding and natal dispersal in a declining population of Cassin's Auklet. Journal of Field Ornithology 72:354–363.

Pyle, P., W. J. Sydeman, and M. Hester. 2001. Effects of age, breeding experience, mate fidelity and site fidelity on breeding performance in a declining population of Cassin's Auklets. Journal of Animal Ecology 70:1088–1097.

R Core Team. 2024. R: A language and environment for statistical computing. R Foundation for Statistical Computing, Vienna, Austria.

Reed, T. E., M. P. Harris, and S. Wanless. 2015. Skipped breeding in Common Guillemots in a changing climate: restraint or constraint? Frontiers in Ecology and Evolution 3:1–9.

Regehr, H., and W. Montevecchi. 1997. Interactive effects of food shortage and predation on breeding failure of Black-Legged Kittiwakes: Indirect effects of fisheries activities and implications for indicator species. Marine Ecology Progress Series 155:249–260.

Renner, H. M., J. F. Piatt, M. Renner, B. A. Drummond, J. S. Laufenberg, and J. K. Parrish. 2024. Catastrophic and persistent loss of common murres after a marine heatwave. Science 386:1272–1276.

Rotella, J. J., W. A. Link, T. Chambert, G. E. Stauffer, and R. A. Garrott. 2012. Evaluating the demographic buffering hypothesis with vital rates estimated for Weddell seals from 30 years of mark–recapture data. Journal of Animal Ecology 81:162–173.

Sæther, B.-E., and Ø. Bakke. 2000. Avian life history variation and contribution of demographic traits to the population growth rate. Ecology 81:642–653.

Sandvik, H., K. E. Erikstad, and B.-E. Sæther. 2012. Climate affects seabird population dynamics both via reproduction and adult survival. Marine Ecology Progress Series 454:273–284.

Schmidt, A. E., K. E. Dybala, L. W. Botsford, J. M. Eadie, R. W. Bradley, and J. Jahncke. 2015. Shifting effects of ocean conditions on survival and breeding probability of a long-lived seabird. PLOS ONE 10:e0132372.

Smith, D. H. V., S. J. Converse, K. W. Gibson, A. Moehrenschlager, W. A. Link, G. H. Olsen, and K. Maguire. 2011. Decision analysis for conservation breeding: Maximizing production for reintroduction of whooping cranes. The Journal of Wildlife Management 75:501–508.

Sydeman, W. J., R. W. Bradley, P. Warzybok, J. Jahncke, K. D. Hyrenbach, V. Kousky, J. A. Perlwitz, and M. D. Shulz. 2006. Planktivorous auklet Ptychoramphus aleuticus responses to ocean climate, 2005: Unusual atmospheric blocking? Geophysical Research Letters 33:L22S09.

Tomita, N., Y. Niizuma, M. Takagi, M. Ito, and Y. Watanuki. 2009. Effect of interannual variations in sea-surface temperature on egg-laying parameters of Black-Tailed Gulls (Larus crassirostris) at Teuri Island, Japan. Ecological Research 24:157–162.

Valpine, P. de, D. Turek, C. J. Paciorek, C. Anderson-Bergman, D. T. Lang, and R. Bodik. 2017. Programming with models: Writing statistical algorithms for general model structures with NIMBLE. Journal of Computational and Graphical Statistics 26:403–413.

Villellas, J., D. F. Doak, M. B. García, and W. F. Morris. 2015. Demographic compensation among populations: what is it, how does it arise and what are its implications? Ecology Letters 18:1139–1152.

Votier, S. C., B. J. Hatchwell, A. Beckerman, R. H. McCleery, F. M. Hunter, J. Pellatt, M. Trinder, and T. R. Birkhead. 2005. Oil pollution and climate have wide-scale impacts on seabird demographics. Ecology Letters 8:1157–1164.

Wallace, S. J., S. G. Wolf, R. W. Bradley, A. L. Harvey, and V. L. Friesen. 2015. The influence of biogeographical barriers on the population genetic structure and gene flow in a coastal Pacific seabird. Journal of Biogeography 42:390–400.

Warlick, A. 2022. Understanding the effects of environmental variability on demography in species with complex life histories through integrated population modeling. University of Washington Libraries, Seattle, Washington, USA.

Weegman, M. D., T. W. Arnold, R. G. Clark, and M. Schaub. 2021. Partial and complete dependency among data sets has minimal consequence on estimates from integrated population models. Ecological Applications 31:e2258.

Winant, C. D., E. P. Dever, and M. C. Hendershott. 2003. Characteristic patterns of shelf circulation at the boundary between central and southern California. Journal of Geophysical Research: Oceans 108:3021.

Wolf, S. G., W. J. Sydeman, J. M. Hipfner, C. L. Abraham, B. R. Tershy, and D. A. Croll. 2009. Range-wide reproductive consequences of ocean climate variability for the seabird Cassin's Auklet. Ecology 90:742–753.

Young, L., and L. T. Ballance. 2023. Ecology of marine birds. In L. Young and E. VanderWerf, editors. Conservation of marine birds. Academic Press, San Diego, California, USA.

3.8 Tables and Figures

Table 3.1 Hypotheses on the relationship between oceanographic conditions and auklet adult survival and breeding probabilities, and covariates used to test hypotheses in survival model. The code used to reference the hypotheses in the text is included in parentheses under the corresponding hypothesis name.

Hypothesis name	**Hypothesis description**	**Covariate**
Annual effect on survival hypothesis ("annual survival")	Adult survival in year *t* to *t*-1 is driven by Pacific Ocean basin-wide oceanographic conditions throughout the course of the year, reflecting a consistent, year-round sensitivity to large-scale processes.	Oceanic Niño Index (ONI), July in year *t-1* to June in year *t*
Southern winter effect on survival hypothesis ("southern winter")	Adult survival in year *t* to *t*-1 is driven by southern winter conditions, reflecting a sensitivity to overwintering conditions and a tendency to remain in the southern California current during winter.	Biologically Effective Upwelling Transport Index (BEUTI) at 34°N, October of year *t-1* to January of year *t*
Northern winter effect on survival hypothesis ("northern winter")	Adult survival in year *t* to *t*-1 is driven by northern winter conditions, reflecting a sensitivity to overwintering conditions and a tendency to remain in the northern California current during winter.	BEUTI at 36°N, October of year *t-1* to January of year *t*
Annual effect on breeding hypothesis ("annual breeding")	Breeding probability in year *t* is driven by Pacific Ocean basin-wide oceanographic conditions throughout the course of the prior year, reflecting cumulative, long-term effects on decisions to initiate breeding	ONI, April in year *t*-1 to March in year *t*
Pre-season effect on breeding hypothesis ("pre-season breeding")	Breeding probability in year *t* is driven by conditions just prior to breeding at the breeding grounds, reflecting short-term effects on decisions regarding whether to initiate breeding	BEUTI at 34°N, January of year *t* to March of year *t*

Table 3.2 Demographic parameters (name, symbol, definition) estimated in the integrated population model across the study period (1999 – 2022). Each parameter represents a key demographic process influencing auklet population dynamics, including stage-specific survival and breeding transitions. Parameter symbols are consistent with those presented in the model description (section 3.3.5) and figures.

Parameter name	**Parameter symbol**	**Definition**
Fecundity	f	Probability that a breeding pair fledges a chick in year *t*
Adult survival	ϕ	Probability that an adult survives from year *t* to *t*+1
Juvenile survival	$\phi_{juvenile}$	The probability that a juvenile (yearlings, fledglings, pre-breeders) survives from year *t* to *t*+1
Pre-breeder transition	$\psi_{newbreeder}$	Probability of a pre-breeder aged 2 and 3 transitioning to a first-time breeding state
Breeder-breeder breeding transition	ψ_{II}	Probability of an adult breeding in year *t* if they bred in year *t*-1
Skipper-breeder breeding transition	ψ_{OI}	Probability of an adult breeding in year *t* if they did not breed (i.e., "skipped") in year *t*-1

Table 3.3 Bayes Factors (BF) for each covariate in the survival model, indicating relative support for the covariate as a predictor of adult survival and breeding transition probabilities. BFs < 3 indicate no support, while BF > 150 indicate very strong support. See Table 3.1 for detailed hypothesis descriptions.

Hypothesis name	**BF**
Annual survival	0.467
Southern winter	38296.87
Northern winter	0.226
Annual breeding	0.259
Pre-season breeding	0.510

Table 3.4 Posterior model weights for top 10 of 32 candidate survival model sampled in the analysis. Oceanographic covariates hypotheses in the model set included three covariate hypotheses on annual survival probabilities (*annual survival* hypothesis, *southern winter* hypothesis, *northern winter* hypothesis) and three covariate hypotheses on breeding transition probabilities (*annual breeding* hypothesis, *pre-season breeding* hypothesis). See Table 3.1 for detailed hypothesis descriptions.

Model	**Weight**
southern winter	0.283
southern winter + pre-season breeding	0.159
annual survival + southern winter	0.137
southern winter + annual breeding	0.087
annual survival + southern winter + pre-season breeding	0.069
southern winter + northern winter	0.060
southern winter + northern winter + pre-season breeding	0.037
annual survival + southern winter + annual breeding	0.037
annual survival + southern winter + northern winter	0.032
southern winter + annual breeding + pre-season breeding	0.031

Table 3.5 Posterior mean estimates and 95% Bayesian credible intervals (BCIs) for parameters included in the integrated population model. Estimates are included separately by island when parameters were modeled as island-specific; otherwise, a single estimate is shown for both islands combined. See Table 3.2 for definitions of demographic parameters.

Parameter	**Scorpion Rock**	**Prince Island**
	Mean (95% BCI)	
Fecundity f	0.430 (0, 0.761)	0.401 (0, 0.682)
Adult survival ϕ	0.810 (0.542, 0.939)	0.788 (0.520, 0.912)
Juvenile survival $\phi_{juvenile}$	0.624 (0.281, 0.889)	
Pre-breeder transition $\psi_{newbreeder}$	0.633 (0.162, 0.979)	
Repeat breeding probability ψ_{II}	0.288 (0.123, 0.518)	0.791 (0.657, 0.957)
Return breeding probability ψ_{OI}	0.165 (0.079, 0.291)	0.254 (0.084, 0.445)
Southern winter coefficient $\beta_{southern\_winter}$	-0.557 (-0.799, -0.338)	
Observation error σ	0.439 (0.316, 0.602)	
Detection probability p	0.285 (0, 0.892)	0.361 (0, 0.895)

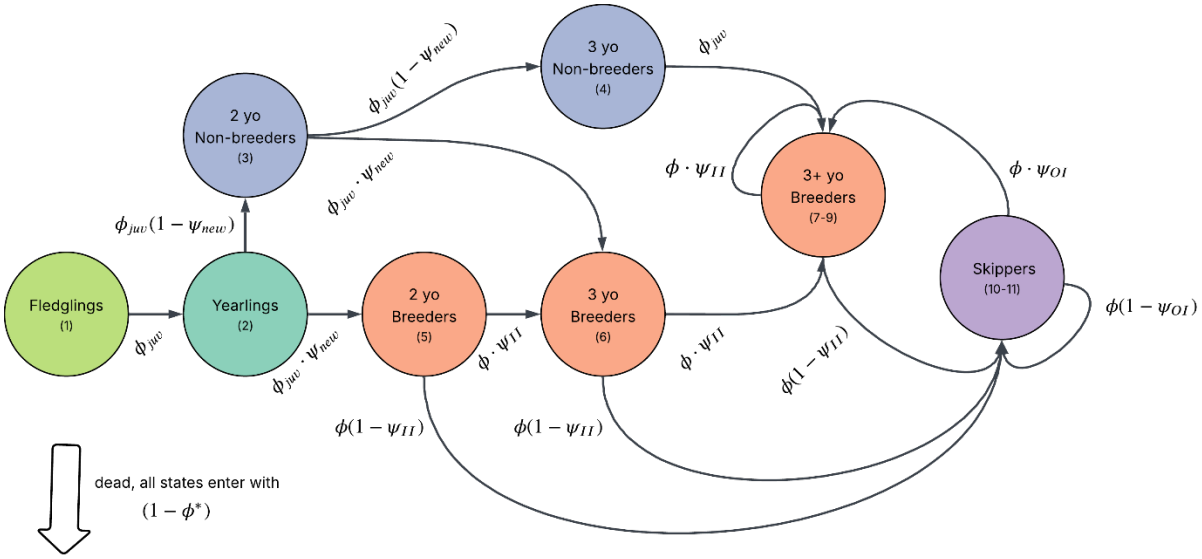

Figure 3.1 State-transition diagram used in integrated population model. The model includes 11 discrete life history stages grouped into biologically meaningful categories: fledglings (stage 1), yearlings (stage 2), non-breeders (stages 3-4), breeders (stages 5-9), and skippers (stages 10-11). Transitions between stages are governed by survival probabilities for adults ϕ and juveniles ϕ_{juv} and state transition probabilities ψ, including recruitment of pre-breeders to breeders ψ_{new}, the probability of a breeder remaining as a breeder if they bred in the previous year ψ_{II}, and the probability of a skipper returning as a breeder ψ_{OI}. Individuals die with probability $1-\phi^*$, with the corresponding adult or juvenile survival rate depending on the life stage. See Table 3.2 for definition of demographic parameters. Here, the symbol for juvenile survival, $\phi_{juvenile}$, and the pre-breeder transition, $\psi_{newbreeder}$, have been shortened to ϕ_{juv} and ψ_{new}, respectively, due to space constraints.

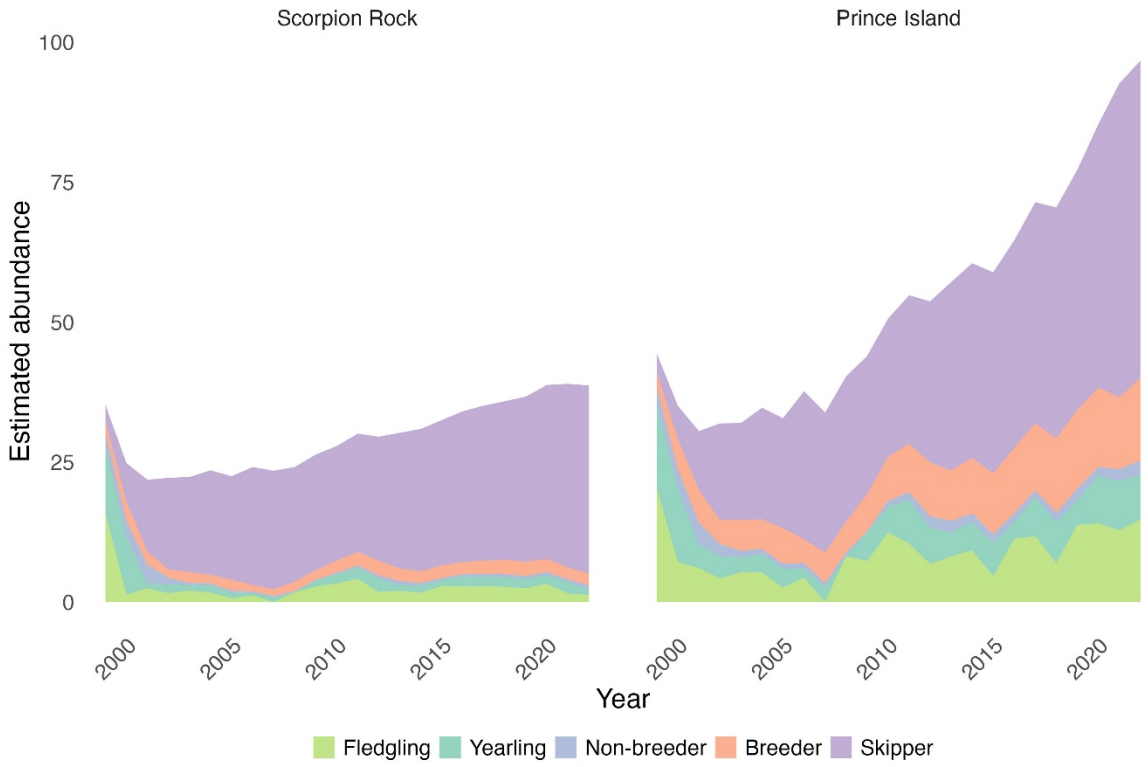

Figure 3.2 Estimated population structure and abundance of auklets at Scorpion Rock and Prince Island from 1999 – 2022. Stacked area plots show the posterior mean abundance of each stage (estimated number of auklets, identified by color in the legend) as estimated by the integrated population model.

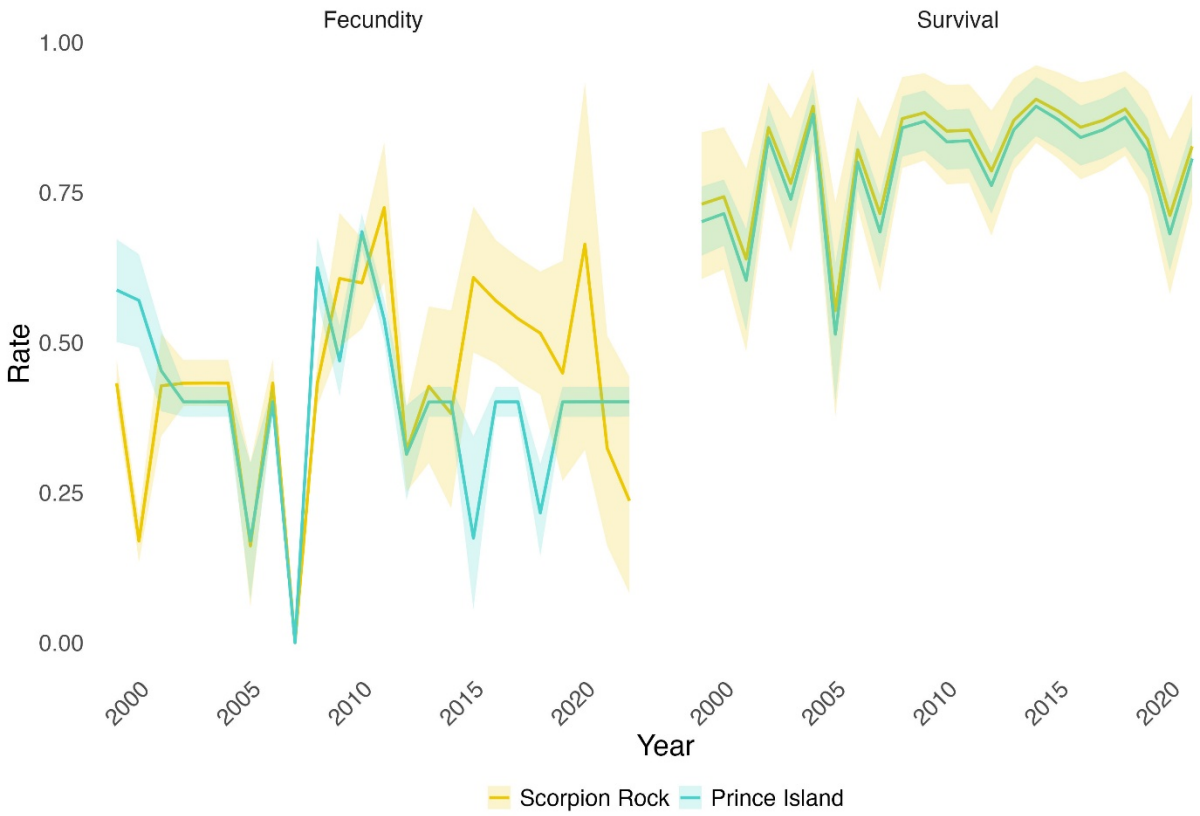

Figure 3.3 Time series of fecundity and adult survival for auklet colonies at Scorpion Rock (yellow) and Prince Island (blue). Shaded bands represent 95% credible intervals from the integrated population model posterior distributions. Survival estimates represent annual adult survival from year *t* to *t*+1 and are plotted at the starting year of the interval (e.g., 1999 = survival from 1999 to 2000). Fecundity reflects the mean number of fledglings produced per breeding pair in year *t* and is plotted in the year observed.

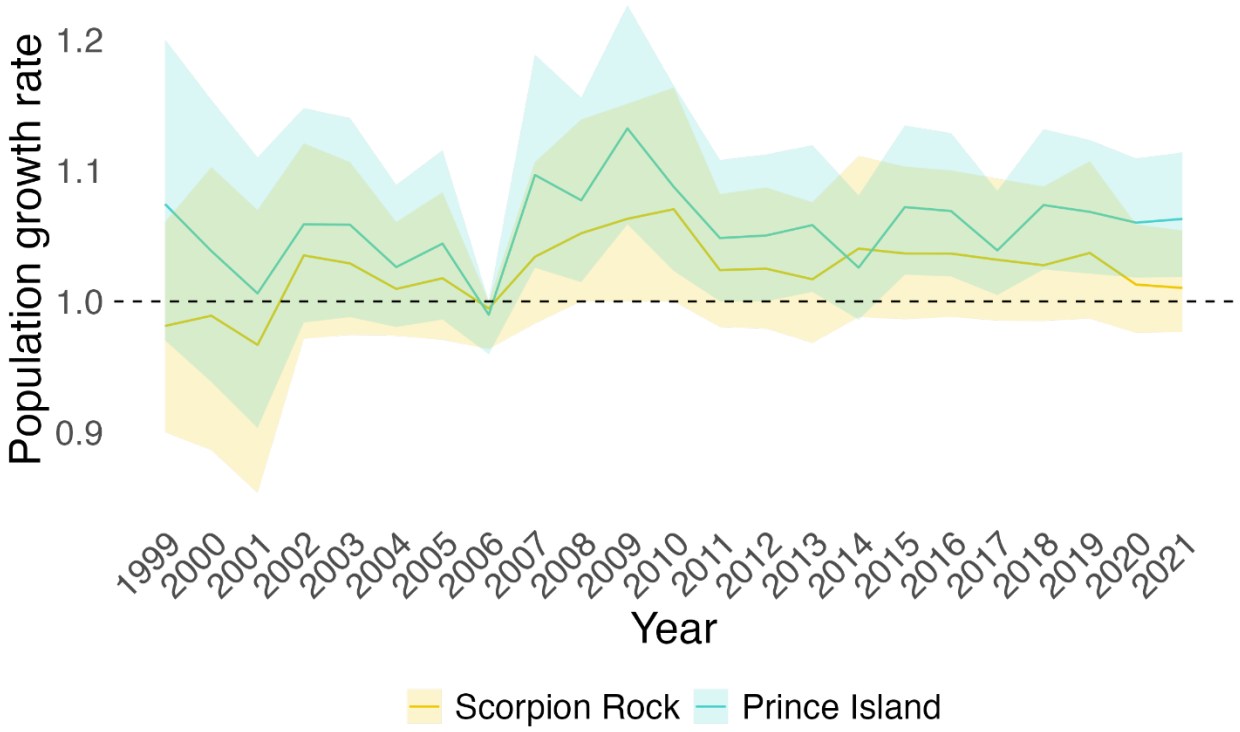

Figure 3.4 Annual population growth rate $\bar{\lambda}$ of auklets at Scorpion Rock (yellow) and Prince Island (blue), 1999 – 2022. Lines represent the posterior mean annual population growth rate for each island, as estimated by the integrated population model, with shaded bands indicating the 95% Bayesian credible interval. The horizontal dashed line at $\lambda = 1.0$ represents stable growth (i.e., neither decreasing nor increasing).

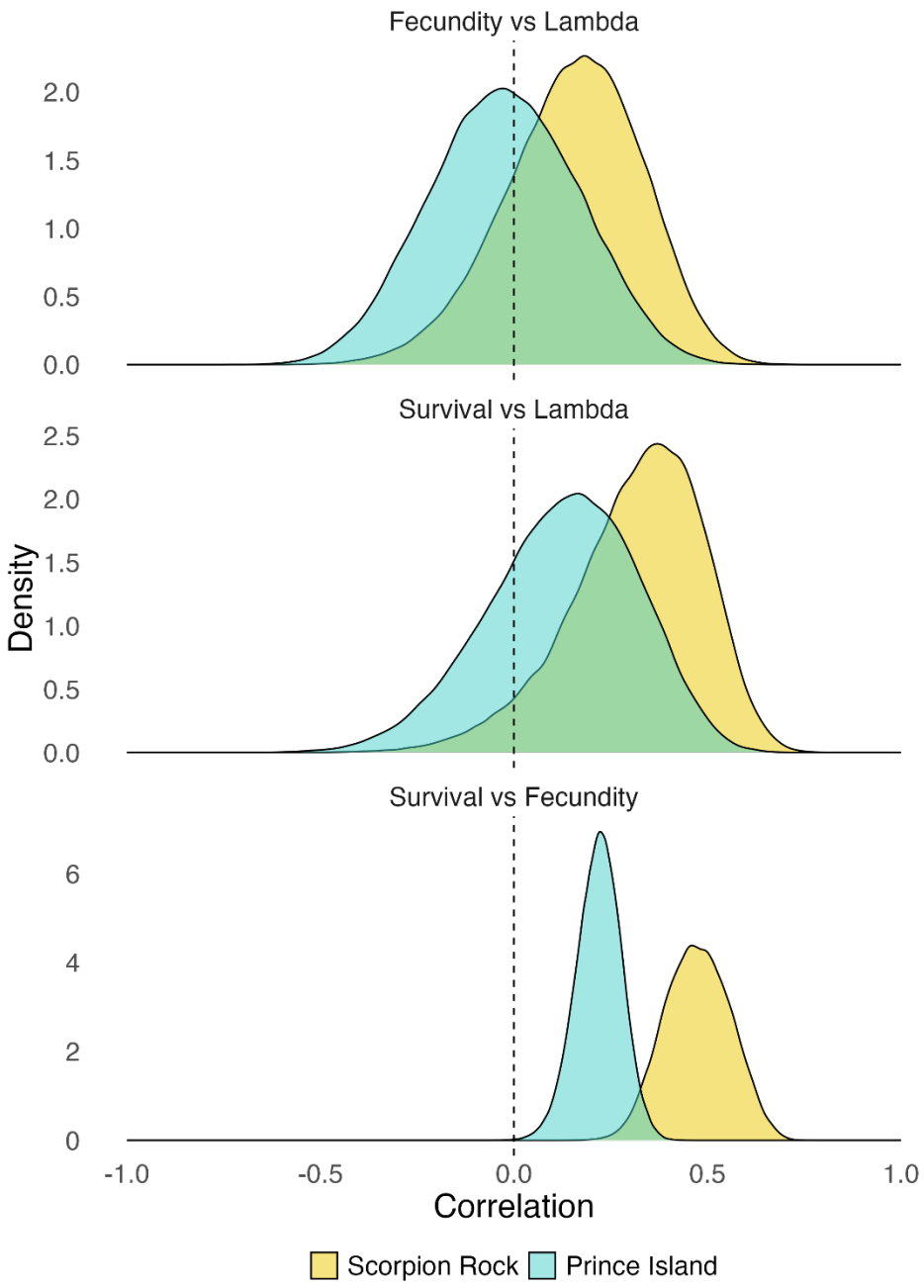

Figure 3.5 Posterior distributions of correlations among demographic parameters and population growth rate (lambda, $\bar{\lambda}$) for Scorpion Rock (yellow) and Prince Island (blue). Top: Correlation between fecundity in year *t* and $\bar{\lambda}$ in year *t*. Middle: Correlation between adult survival in year *t* to *t*+1 and $\bar{\lambda}$ in year t. Bottom: Correlation between survival and fecundity within the same year *t*.

3.9 APPENDIX 3.1

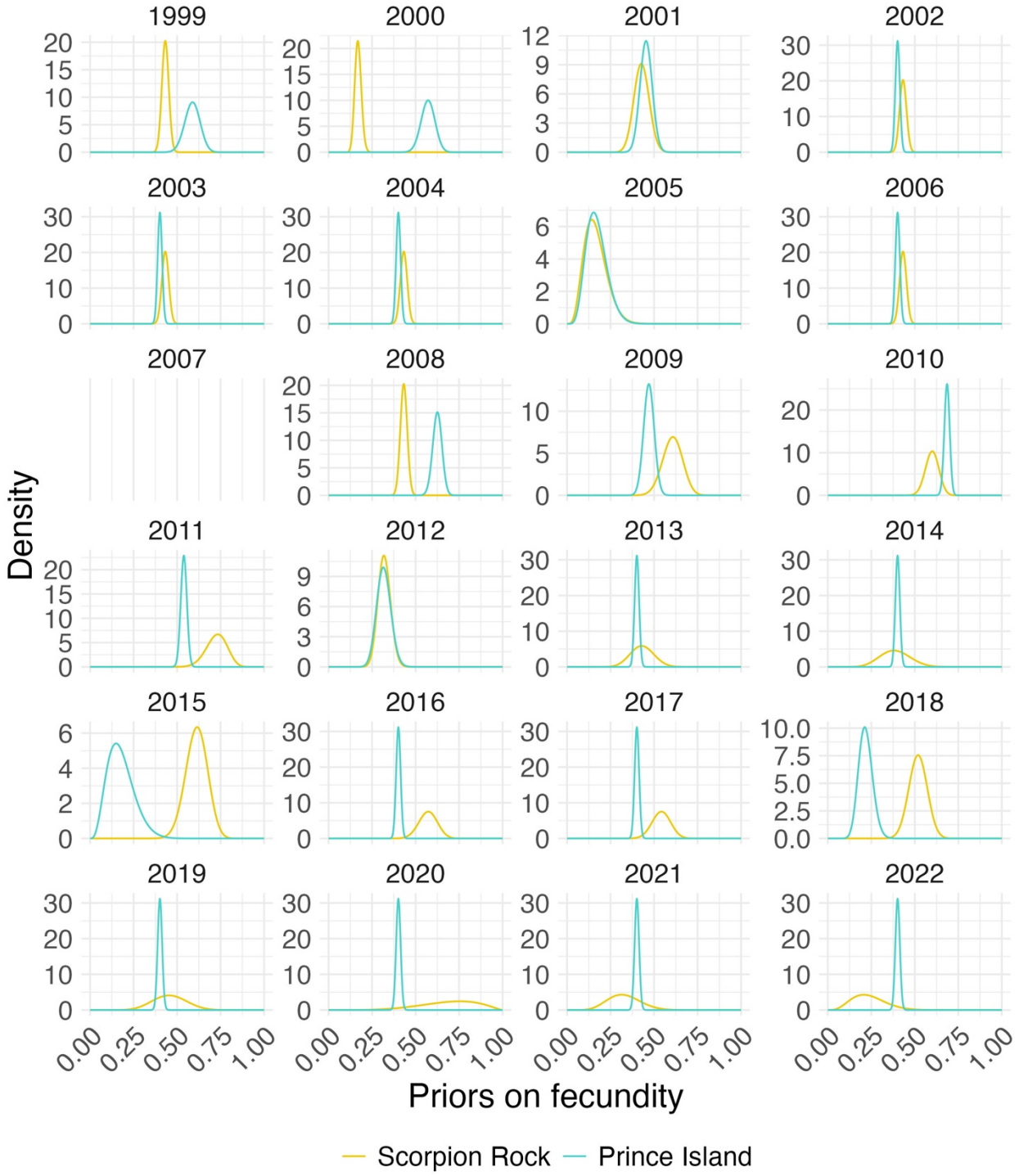

Derived beta distribution priors for island-specific annual fecundity used in the integrated population model, based on posterior samples from the daily nest survival model developed in DuVall (Chapter 2, this dissertation). For each island-year combination with sufficient nest

monitoring data, we calculated the posterior mean and standard deviation of reproductive success (i.e., the proportion of nests that successfully fledged a check), and used the moment-matching method to parameterize corresponding beta distributions. For island-year combinations without monitoring data, the beta distribution was derived from the island-wide mean and standard deviation across all years.

3.10 APPENDIX 3.2

To assess the potential influence of unmodeled temporal variation on survival and breeding transitions, we fit an alternative version of the multistate mark-recapture model that included random time effects on survival and breeding transition probabilities. Specifically, we extended the linear predictors for the survival ($\phi_{island,t}$) and breeding transition probabilities ($\psi^{II}_{island,t}, \psi^{OI}_{island,t}$) to include random time effects. Because of the inconsistent recapture data across years, we grouped years into island-specific time intervals defined by the periods between successive years with banding or recapture effort. We defined nine time intervals for Scorpion Rock and 16 for Prince Island. The equations below show how the random time effects were incorporated into the survival and breeding transition probabilities (see section 3.3.4.2 *Survival model* for a full definition of the model equations):

$$\text{logit}(\phi_{island,t}) = \alpha_0^{\phi} + \alpha_1^{\phi}[I_{island}] + \beta^{\phi}_{annual\_survival} * ONI_t + \beta^{\phi}_{southern\_winter} * winterBEUTI33_t + \beta^{\phi}_{northern\_winter} * winterBEUTI39_t + \varepsilon^{\phi}_{island,time_{island,t}}$$

$$\varepsilon^{\phi}_{island,time_{island,t}} \sim \text{N}(0, \sigma^2_{\phi,island})$$

$$\text{logit}(\psi^{II}_{island,t}) = \alpha^{\psi}_{0,II} + \alpha^{\psi}_1[I_{island}] + \beta^{\psi}_{annual\_breeding} * ONI_{t-1} + \beta^{\psi}_{prebreeding} * preBEUTI33_t, + \varepsilon^{\psi^{II}}_{island,time_{island,t}}$$

$$\text{logit}(\psi^{OI}_{island,t}) = \alpha^{\psi}_{0,OI} + \alpha^{\psi}_1[I_{island}] + \beta^{\psi}_{annual\_breeding} * ONI_{t-1} + \beta^{\psi}_{prebreeding} * preBEUTI33_t, + \varepsilon^{\psi^{OI}}_{island,time_{island,t}}$$

$$\varepsilon^{\psi^{II}}_{island,time_{island,t}} \sim \text{N}(0, \sigma^2_{\psi^{II},island}), \varepsilon^{\psi^{OI}}_{island,time_{island,t}} \sim \text{N}(0, \sigma^2_{\psi^{OI},island})$$

We assigned weakly informative priors to the variance parameters for the random effects, specifying inverse-gamma distributed priors on the variance scale via gamma priors on the precision (inverse variance) parameters:

$$\sigma^{-2}_{\phi,island}, \sigma^{-2}_{\psi^{II},island}, \sigma^{-2}_{\psi^{OI},island} \sim \text{Gamma}(1,1)$$

We implemented the same model selection and fitting procedures described for the main model, using indicator variable selection and Bayes Factor to assess support for covariates (see section 3.3.4.2 *Survival model*). When we included random time effects in the linear predictors for survival and breeding transitions, none of the covariates received support based on Bayes Factor (BF) values (Table A3.2.1) All covariates had BF estimates <2, indicating low evidence for their inclusion when accounting for unmeasured temporal variation. Likewise, the posterior model weights were distributed across several models in the candidate set (Table A3.2.2). The top-weighted model included only the *pre-breeding season* hypothesis (10.5% of the posterior weight). However, model weights were relatively evenly distributed for the top 10 models, with no single model receiving overwhelming support, and the null model still accounting for 4.5% of the posterior weight. These findings contrast with the primary model results (section 3.4.1), in which the *southern winter* hypothesis covariate received strong support (BF = 324.20) and was included in the top inferential model.

Table A3.2.1. Bayes Factors (BF) for each covariate in the survival model, indicating relative support for the covariate as a predictor of adult survival and breeding transition probabilities. BFs < 3 indicate no support, while BF > 150 indicate very strong support.

Hypothesis name	**BF**
Annual survival	0.304
Southern winter	0.796

Northern winter	0.432
Annual breeding	1.098
Pre-season breeding	1.798

Table A3.2.2. Posterior model weights for top 10 of 32 candidate survival model sampled in the analysis. Oceanographic covariates hypotheses in the model set included three covariate hypotheses on annual survival probabilities (*annual survival* hypothesis, *southern winter* hypothesis, *northern winter* hypothesis) and three covariate hypotheses on breeding transition probabilities (*annual breeding* hypothesis, *pre-season breeding* hypothesis).

Model	**Weight**
pre-season breeding	0.105
annual breeding + pre-season breeding	0.093
southern winter + pre-season breeding	0.079
southern winter + annual breeding + pre-season breeding	0.073
annual breeding	0.067
southern winter + annual breeding	0.049
NULL	0.045
northern winter + pre-season breeding	0.043
northern winter + annual breeding + pre-season breeding	0.038
southern winter + northern winter + pre-season breeding	0.032

3.11 APPENDIX 3.3

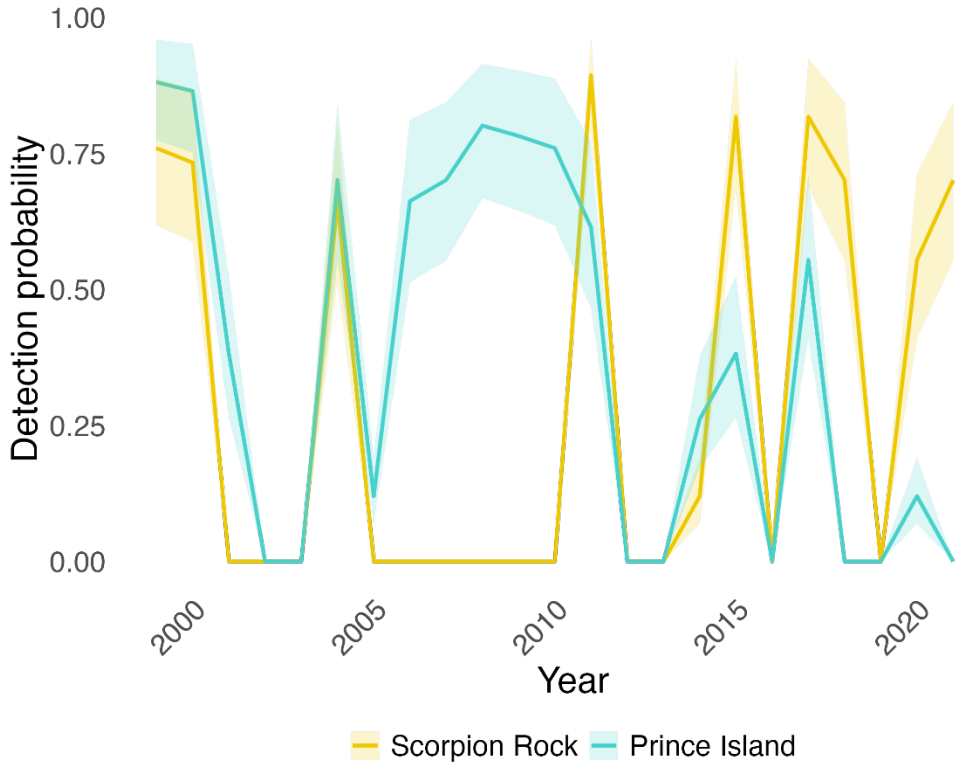

Estimated annual detection probabilities for breeding individuals at Scorpion Rock (yellow) and Prince Island (blue), modeled as a function of monitoring effort (in log-transformed effort days). Years with no effort (e.g., no nest monitoring visits or attempts to capture/recapture individuals) were assigned a detection probability of zero, resulting in intermittent gaps in the estimates. See Eq. 14 and section 3.3.4.2 for more details.

Chapter 4. Disentangling Marine and Terrestrial Drivers of Nest Survival for a Rare Seabird

Publication history: This study was co-authored with Jim A. Howard, David M. Mazurkiewicz, and Sarah J. Converse. This analysis may be expanded in the future, at which point additional co-authors would be invited. At the time this dissertation was published, this chapter was not in review with a journal.

4.1 Abstract

Understanding the drivers of reproductive success in species that span terrestrial and marine realms is critical for informing conservation, especially when management options are limited. On a small island in southern California, USA, reproductive success of a threatened seabird is influenced by marine conditions as well as a terrestrial climate-driven trophic cascade involving endemic mice and owl populations. Here, the major cause of nest failure for Scripps's Murrelets (*Synthliboramphus scrippsi*) is egg predation by mice and, in some years, it is substantial enough to cause a population decline. Mouse abundance is driven by rainfall pulses, along with their major predator, owls. When mouse abundances peak in response to conditions, owl abundance follows and owls prey-switch to adult murrelets when mice populations fall sharply. The presence of owls also exerts a positive indirect influence on murrelet nest survival by modifying mouse foraging behavior, leading to reduced egg predation rates. Given the endemic status of mice and the complex dynamic between mice, owls, and murrelets, management options to conserve murrelets are limited. One promising management intervention is the trapping and translocation of mice from murrelet nesting areas, which has been shown to reduce egg depredation rates. However, it is expensive and labor-intensive to implement. In lieu of consistent data on owl and mouse populations, we sought to identify weather variables

associated with high rates of nest failure that could serve as early warning signs of a high-risk year when management interventions are warranted. We developed a Bayesian multistate nest survival model to evaluate how fine-scale weather conditions, ocean productivity, and nest habitat affect nest survival across six monitoring plots from 1988 – 2019. Daily nest survival was positively associated with increased spring temperature and precipitation, but negatively associated with winter precipitation, particularly when lagged by one year. Nest survival was higher in plots dominated by native shrub habitat as compared to crevice habitat, suggesting that vegetative growth may provide protective cover from owl predation and alternative foraging resources for mice. Our results suggest that habitat restoration and seasonal weather monitoring can be used to strategically guide murrelet conservation efforts.

4.2 Introduction

Species that move across ecological boundaries, known as multi-realm species, depend on the integrity of multiple ecosystems (e.g., terrestrial, freshwater, marine) throughout their lives (Hermoso et al. 2021). As climate change drives divergent and sometimes decoupled changes across these systems, multi-realm species may face compounding threats and require multi-pronged management strategies to persist in the face of these risks. Seabirds exemplify this group: they forage at sea, breed on land, and depend on aerial pathways to connect these realms. For seabirds, reproductive success is a demographic process that tends to be particularly sensitive to environmental variability and change, and it depends not only on the availability and accessibility of prey in dynamic oceanic environments but also on conditions in terrestrial nesting habitats (Young and Ballance 2023).

On Santa Barbara Island, a small oceanic island in the Southern California Bight, USA (Figure 1.1), the reproductive success of the threatened Scripps's Murrelet (*Synthliboramphus*

scrippsi; hereafter murrelet) is influenced by both marine prey availability and a climate-driven terrestrial trophic cascade. Murrelets return to land to breed in late winter to early spring, where their eggs are vulnerable to predation by endemic Island Deer Mice (*Peromyscus maniculatus elusus*; hereafter mouse) and adults face predation by nocturnal Barn Owls (*Tyto alba*; hereafter owl; Thomsen and Green 2016, Thomsen et al. 2018). Mice on the island exhibit boom-bust population dynamics, where abundance rises sharply following high-rainfall years driven by large-scale climatic forces such as the El Niño – Southern Oscillation (Drost and Fellers 1991, Thomsen et al. 2018). As their major predator, owl abundance closely tracks that of mice. However, when mouse populations crash, owls switch to preying on murrelets, leading to substantial adult mortality – up to 15 times more murrelets may be killed following mouse declines (Thomsen and Green 2016; Thomsen et al. 2018). Paradoxically, owls can also exert a positive indirect effect on murrelet egg survival by suppressing mouse activity through a behaviorally mediated effect; mice forage less under owl predation risk, reducing egg depredation on murrelet nests (Thomsen and Green 2016). Still, mice remain the primary cause of nest failure, depredating up to 70% of murrelet eggs in some years (Drost and Lewis 1995, Nur et al. 2013, Thomsen and Green 2019). During drought years, the reduction in reproductive success due to increased egg predation by mice is enough to produce a declining population growth rate for murrelets (Thomsen and Green 2019).

Murrelet reproductive success is also influenced by oceanic conditions that likely reflect prey abundance (Thomsen and Green 2019). Murrelets are generalist foragers, consuming a variety of prey concentrated at ocean convergence lines (Hamilton et al. 2004), where they appear to forage opportunistically on euphausiids, northern anchovy (*Engraulis mordax*), juvenile driftfish (Nomeidae), and medusafish (Centrolophidae). Despite their broad diet,

murrelets have a brief nesting period of just over a month, making it advantageous to time breeding at peak prey abundance when they are incubating and have limited foraging ranges. Like many seabird species, murrelets may abandon nests when foraging conditions are poor, prioritizing their own survival instead (Young and Ballance 2023). However, temporary egg neglect is common, especially in early incubation (Murray et al. 1980), making it difficult to distinguish between a nest that failed due to egg predation versus a nest that was abandoned and then was depredated. Nevertheless, it is likely that in years of low ocean productivity, murrelets are more prone to abandon nests altogether.

Murrelets are already experiencing a declining population trend (Burkett et al. 2003, Nur et al. 2013) that is expected to worsen under future climate change scenarios (Thomsen and Green 2019) and conservation actions are likely necessary to stabilize the population. While the ecological processes influencing murrelet reproductive success are well-documented, conservation options are limited. Direct manipulation of marine prey availability is not feasible, and direct management interventions in the terrestrial realm to reduce predation on murrelets and their eggs are complicated by the island's trophic dynamics. The eradication of an endemic subspecies is also not tenable, and it could exacerbate adult murrelet predation by owls if their major food source is removed.

One promising management intervention is the targeted trapping and translocation of mice out of murrelet nesting areas, which has been shown to reduce egg depredation (Millus et al. 2007). However, such efforts are highly labor- and time-intensive and thus infeasible to implement annually; therefore, identifying high-risk years when these interventions are most likely to be beneficial would support more strategic use of limited management resources. Unfortunately, such forecasting is hindered by a lack of consistent, timely, and reliable

monitoring data on mouse and owl populations. Biannual owl transect surveys are not collected regularly due to a reduced on-island presence of CHIS park staff and partner organizations. Similarly, long-term mouse monitoring grids are currently suspended due to methodological issues. The original reference sites are no longer representative of broader island conditions, as vegetation types have changed over time, undermining their ability for assessing population size and trends (NPS unpublished data).

Given these constraints, there is a pressing need for improved understanding of the fine-scale weather conditions that reliably predict murrelet reproductive outcomes. These proxies could serve as early warning signals in lieu of predator population data to guide the strategic use of scarce management resources for this rare and threatened seabird. With this in mind, we undertook an analysis of reproductive success in murrelets on Santa Barbara Island. Our objective for this analysis was to identify seasonal weather conditions, such as the amount and timing of precipitation, associated with elevated levels of nest failure. Identifying weather cues that are associated with higher predation risk could provide a more cost-effective, proactive means of informing targeted management actions when conditions are warranted.

Through our analysis, we sought to expand upon previous work on a single monitoring plot (Thomsen and Green 2019) by examining differences in nest survival across multiple plots. These additional plots differed in habitat composition (e.g., ranging from native shrub to rocky crevice and manmade structures) and therefore offered the opportunity to explore whether habitat type influences the relationship between weather conditions and nest failure. Given recent investment and continued interest in native habitat restoration on the California Channel Islands, we were particularly interested in determining the role of native shrub habitat in supporting murrelet nest survival. As a further expansion of previous work, we used a multistate nest

survival model that explicitly accounts for nest exposure time (the number of days a nest is under observation and at risk of failing or succeeding; Mayfield 1961), allowing us to estimate survival probabilities more accurately across variable monitoring intervals. Previous assessments relied on mean apparent nest success (i.e., the proportion of total eggs hatched across all observed nest attempts; Thomsen and Green 2019) and were not designed to account for variation in exposure time. Because the apparent nest success approach assumes equal detection probability of successful and failed nests, it can overestimate reproductive success, particularly in cases of intermittent or incomplete monitoring.

We developed a set of hypotheses to evaluate in our analysis (Table 4.1), including four hypotheses that link fine-scale seasonal weather variability to nest survival during the egg stage. Given that mouse abundance, and consequently owl abundance, are closely correlated with rainfall (Drost and Feller 1991, Thomsen et al. 2018), we hypothesized that nest survival would be lower in years with wetter winters, when increased precipitation from November to February is expected to stimulate vegetation growth and lead to subsequent increases in mouse abundance and, in turn, egg predation. Higher mouse abundance may also support larger owl populations, leading to adult murrelet predation when mouse populations decline and further reducing nest survival. Recognizing time lags between precipitation, vegetation response, and mouse/owl abundance (Thomsen et al. 2018), we evaluated this hypothesis at two time scales: (1) precipitation during the winter immediately preceding the breeding season (*winter precipitation* hypothesis), and (2) precipitation during the prior winter (*previous winter precipitation* hypothesis). We also considered a *spring precipitation* hypothesis, in which increased precipitation in the spring (March to May) drives continued vegetative growth, which provides alternative prey resources for mice during the breeding period, increasing nest survival. In

parallel, we tested a *spring temperature* hypothesis, positing that higher temperatures in March to May lead to decreased water resources and forage opportunities, resulting in increased mouse predation on murrelet eggs, reducing nest survival. We were specifically interested in how combinations of seasonal conditions (e.g., a wet winter followed by a wet spring or hot spring) may drive increased nest and adult predation of murrelets. We also examined two hypotheses on marine productivity, which considered the influence of ocean productivity on murrelet breeding at different time scales, the pre-breeding season and breeding season. Specifically, we expected higher nest survival in years with strong upwelling just prior to the breeding season (*pre-breeding season upwelling* hypothesis), which would shape prey availability during the breeding season, leading to reduced rates of abandonment under favorable marine foraging conditions and increased nest survival. We also hypothesize that strong upwelling during the breeding season (*breeding season upwelling* hypothesis) will create favorable marine foraging conditions, leading to reduced rates of nest abandonment and increased nest survival. Finally, we considered a *habitat type* hypothesis that evaluated whether variation in nest survival could be explained by dominant nest habitat. We hypothesized that murrelets nesting in native shrub habitat have increased nest survival compared to murrelets nesting in predominantly artificial areas or areas dominated by rocky crevice habitat. We posited two potential mechanisms: (1) native shrub habitat may reduce aerial predation on adult murrelets by providing protective cover from owls, and (2) it may reduce egg predation by increasing alternative forage availability for mice through the establishment of perennial native shrubs.

4.3 METHODS

4.3.1 STUDY AREA AND POPULATION

Scripps's murrelets are listed as threatened in the state of California (California Natural Diversity Database 2025). They have a small global population (~7000 – 8000 breeding pairs; Karnovsky et al. 2005) and a restricted breeding distribution limited to approximately 12 islands or island groups off southern California and northwestern Baja California, Mexico (Birt et al. 2012). Many colonies are vulnerable to threats including mammalian predators or human disturbance (e.g., year-round human presence, military operations). One of the largest and most-studied breeding colonies is within Channel Islands National Park (CHIS) at Santa Barbara Island (Carter et al. 1991), a small island (2.6 km^2) composed almost entirely of volcanic rock and located approximately 64 kilometers southwest of Los Angeles, California (Figure 1.1). The murrelet breeding population here is estimated to be 475 – 650 breeding pairs, about 20% of the global breeding population (D. Whitworth, personal communication, 2018, as cited in Thomsen and Green 2019). There is no permanent surface water on the island and it has a Mediterranean climate characterized by warm dry summers and cool wet winters (Davidson et al. 2019). Plant communities include exotic annual grasslands (e.g., *Avena* spp., *Bromus* spp.) and native scrub vegetation (coreopsis [*Leptosyne*], boxthorn [*Lycium*], and cactus scrub [*Opuntia*, *Cylindropuntia*], as well as other shrub species; Rodriguez et al. 2012, Jaques et al. 2015). Non-native vegetation covers a substantial portion of the island; approximately 42% is covered with non-native grasses and another 21% is dominated by annual crystalline iceplant (*Mesembryanthemum crystallinum*) and cheeseweed (*Malva parviflora*; Davidson et al. 2019).

Murrelets typically nest in rocky crevices and under shrubs, where females lay a single egg and then return approximately eight days later to lay a second egg (Murray et al. 1983).

During the interim, the first egg is often left unattended, making it especially vulnerable to predation by mice (Murray et al. 1980). After both eggs are laid, incubation is shared by both sexes and lasts approximately 34 days. However, irregular nest attendance during this period can also expose eggs to predation. Upon hatching, chicks typically depart the nest at night within 1-2 days, often accompanied by their parents (Murray et al. 1983).

4.3.2 NEST MONITORING

During the breeding season (circa February to July), murrelet nests were monitored in several established plots on Santa Barbara Island (Figure 4.1). The six plots with the most consistent nest monitoring were Arch Point North Cliffs (APNC), Bunkhouse (BH), Cat Canyon (CC), Dock (DOCK), Landing Cove (LACO), and Nature Trail (NTP). Monitoring plots differed in their nest habitat composition (i.e., natural shrub habitat, artificial habitat, rocky crevice habitat), facilitating comparison of nest survival across habitat types. APNC and CC are both composed primarily of rocky crevice habitat. BH and DOCK are both composed of primarily manmade structures (i.e., artificial) that provide nesting habitat (e.g., underneath the CHIS housing deck, under the dock structure and wood pilings), and LACO and NTP consist of primarily native shrub nesting habitat. We characterized habitat based on the surrounding area within the monitoring plot, rather than the actual structure of the nest because plot- and nest-scale habitats are highly correlated (e.g., most nests within a predominantly rocky crevice habitat are rocky crevice nests).

The historical monitoring effort over time varied by plot. At CC, monitoring has been ongoing since 1975. Regular monitoring at BH, DOCK, and LACO began in 2007, while APNC has been monitored since 2010 (Harvey et al. 2013). Monitoring at NTP has been ongoing since

the 1980s but was discontinued in 2008 due to the continued presence of California brown pelicans (*Pelecanus occidentalis californicus*) in the area (Harvey et al. 2012).

Within each plot, nest sites were tagged with unique identification codes and inspected with a flashlight for evidence of breeding activity, such as an incubating adult, egg(s)/eggshell(s), or in rare circumstances, chick(s). Depredated eggshells can be distinguished from hatched eggshells by the presence of yolk and a shiny inner membrane. Due to the brief nestling period (1 – 2 days), fledging was typically inferred from the presence of hatched eggshells containing a dry, papery membrane. In some cases, more than two eggs were observed in a nest site; these were believed to reflect multiple nest attempts by two or more breeding pairs at a site. Because we could not reliably separate these overlapping attempts into independent encounter histories, such cases were excluded from the analysis. These events were infrequent and occurred at low frequency across years, and their exclusion is unlikely to have affected overall model results.

While annual nest monitoring has largely remained consistent at Santa Barbara Island since the 1980s, effort has varied by year due to funding and logistical constraints. In addition, the absence of a centralized and standardized database has resulted in nest records being dispersed across multiple formats and locations, creating challenges in compiling, integrating, and analyzing data. Due to these limitations, we limited our analysis to years with sufficient monitoring and data accessibility within the period 1988 – 2019, with a gap in data from 1998 – 2009 (see Table 4.2 for total number of nest attempts monitored by plot and year). Survey effort (i.e., the number of days between nest observations) ranged from 2 to 35 days.

We analyzed 1274 nest attempts across 23 breeding seasons in a 32-year period (1988 – 2019; Table 4.2, Figure 4.2). Most observations came from CC monitoring plot (n = 473),

followed by LACO (234), DOCK (230), APNC (140), NTP (138), and BH (59). Crevice habitat was the most common habitat type (n = 613), followed by native shrub (372) and artificial habitat (289).

4.3.3 COVARIATE DATA

To incorporate weather covariates that reflected our hypotheses (see Table 4.1 for all hypotheses), we extracted historical monthly precipitation (inches) and temperature (degrees Fahrenheit) data for Santa Barbara Island (33.47°N, 119.04°W) using the WestWide Drought Tracker (WWDT), a gridded climate data product developed by the Western Regional Climate Center at the Desert Research Institute and the University of Idaho (Abatzoglou et al. 2017). WWDT provides 4 km resolution climate data derived from the Parameter-elevation Relationships on Independent Slopes Model (PRISM; Daly et al. 2008). PRISM integrates station data, a digital elevation model, and various spatial datasets to generate monthly temperature and precipitation grids across the continental United States. For the *winter precipitation* hypothesis, we averaged total precipitation over November of year *t*-1 through February of year *t*. For the previous winter precipitation hypotheses, we used the same time window shifted back one year (November of year *t*-2 through February of year *t*-1). For the *spring precipitation* and *spring temperature* hypotheses, we averaged values from March through May of year *t*. To incorporate a covariate that reflected marine conditions, we used the daily Biologically Effective Upwelling Transport Index (BEUTI) at 33°N, which estimates the vertical nitrate flux associated with coastal upwelling (Jacox et al. 2018). For marine conditions during the breeding season, we averaged monthly variables across April to June in year *t*. For the *habitat type* hypothesis, we used a categorical variable with three levels, each represented by two

monitoring plots: native shrub habitat (LACO, NTP), artificial habitat (BH, DOCK), and crevice habitat (APNC, CC).

All continuous covariates were Z-scored (i.e., standardized to have a mean of 0 and a standard deviation of 1) prior to inclusion in the model to facilitate interpretation and comparison of effect sizes (see Figure 4.3 for time series plots of covariates during the study period). We also verified that continuous covariates were not strongly collinear ($|r| < 0.5$).

4.3.4 Daily nest survival model

To test our hypotheses, we implemented a multistate daily nest survival model within a Bayesian framework. This modeling approach builds on the Mayfield method (Mayfield 1961) and extends recent developments in nest survival modeling (e.g., Dinsmore et al. 2002, Rotella et al. 2004) by incorporating unknown nest age and latent state transitions (see also Warlick 2022, Bratt 2023). By modeling survival on a daily scale, the model accounts for exposure time (Mayfield 1961), with the likelihood reflecting the actual number of days that a nest was under observation and at risk of transitioning to failure (i.e., not surviving), allowing for more accurate estimation of survival probabilities across irregular or incomplete monitoring periods.

The true state of nest n at survey day d, $z_{n,d}$, was modeled as categorical random variable governed by a transition probability matrix, $\boldsymbol{\theta_{n,d}}$, which is conditional on the state at the previous time step:

$$z_{n,d}|z_{n,d-1} \sim \text{Categorical}(\boldsymbol{\theta_{n,d}}) \quad (20)$$

where $\boldsymbol{\theta_{n,d}}$ is a state transition matrix structured as:

$$\begin{bmatrix} & \boldsymbol{egg} & \boldsymbol{chick} & \boldsymbol{dead} \\ \boldsymbol{egg} & \phi_{n,d}(1-\psi_{n,d}) & \phi_{n,d}(\psi_{n,d}) & 1-\phi_{n,d} \\ \boldsymbol{chick} & 0 & 1 & 0 \\ \boldsymbol{dead} & 0 & 0 & 1 \end{bmatrix}$$

(21)

Here, $\phi_{n,d}$ represents the daily survival probability in the egg state, and $\psi_{n,d}$ represents the conditional probability of transitioning from egg(s) to chick(s), given survival. We conditioned upon observation of an egg(s) at the nest site, and we assumed that nest state was observed without error (i.e., observation reflects the true state of the nest on any given survey day). By restricting survey effort to less than the median incubation period (the mid-point between the minimum and maximum days to hatch; 35 days), we reduced the possibility of missing hatched eggshells; otherwise, we could mistakenly assume nest failure. Observations of one or two eggs were grouped into the "egg" state, while observations of one or two chicks (or evidence of hatching) were grouped into the "chick" state. The overall hatching probability (i.e., probability that a nest transitions from the egg state to the chick state) is derived as the egg stage-specific daily nest survival probability raised to the number of incubation days.

The transition probability from egg to chick was modeled as age-dependent, such that these transitions were only allowed during a biologically realistic window of incubation (set to 27 to 44 days; Murray et al. 1983). Within this interval, we modeled the prior probability of transitioning as equal across days, i.e.,

$$\psi_{n,d} \sim Dirichlet\ (min_e : max_e),$$

(22)

where min_e is the minimum egg age at hatching and max_e is the maximum egg age at hatching. We modeled latent nest age by modeling the age at first observation, $\alpha_{n,first_n}$, as a random variable, with age thereafter deterministic, i.e.,

$$\alpha_{n,first_n} \sim Dirichlet(1 : max_e),$$
$$\alpha_{n,first_n+1} = \alpha_{n,first_n} + 1.$$

(23)

4.3.5 HYPOTHESIS TESTING

To test the effects of covariates on daily egg-stage survival, we modeled survival probability $\phi_{n,d}$ for nest *n* on day *d* as a function of covariates that reflected our hypotheses:

$$logit(\phi_{n,d}) = \beta_0 + \beta_{prevWinterPrecip} * prevWinterPrecip_n + \beta_{winterPrecip} * winterPrecip_n + \beta_{springPrecip} * springPrecip_n + \beta_{springTemp} * springTemp_n + \beta_{preUpwelling} * preUpwelling_n + \beta_{breedUpwelling} * breedUpwelling_n + \beta_{habitat}[habitat_n] + \delta_y$$

$$\delta_y \sim N(0, \sigma_y)$$

(24)

where β_0 is an egg state-specific intercept term and $\beta_{prevWinterPrecip}$, $\beta_{winterPrecip}$, $\beta_{springPrecip}$, $\beta_{springTemp}$, $\beta_{preUpwelling,}$ $\beta_{breedUpwelling,}$ and $\beta_{habitat}$ are coefficients reflecting our hypotheses on *previous winter precipitation*, *winter precipitation*, *spring precipitation*, *spring temperature*, *pre-breeding season upwelling*, *breeding season upwelling*, and *habitat type*. While all other covariates were continuous, the categorical habitat type $\beta_{habitat}$ covariate had three levels: native shrub (reference level), artificial, and crevice. The covariate was coded using a corner constraint, such that the coefficient for the reference level was fixed at 0, and the other levels are estimated in reference to this category. To account for repeated measures and residual variation, we included a random effect for year (δ_y) that was normally distributed with a mean of 0 and a standard deviation (σ_y) assigned a uniform(0, 5) prior. All fixed-effect coefficients were assigned normal(0,1) priors. We recognized that our hypotheses were not necessarily mutually exclusive, so instead of undertaking model selection, and given

the size of the dataset, we fit a single model and drew inference based on the relative size of the effects and whether their 95% Bayesian credible interval limits excluded 0.

4.3.6 Model fitting and implementation

Models were fit using NIMBLE (Valpine et al. 2017) executed through R (R Core Team 2024). We ran 10,000 iterations across three independent Markov chains after discarding the first 5,000 samples, for a total of 30,000 samples. We assessed convergence of the chains by visually inspecting trace plots and based on Brooks-Gelman-Rubin statistics $\hat{R}$ <1.1 (Gelman and Rubin 1992, Brooks and Roberts 1998). All materials and code developed for the analysis can be found on GitHub (https://github.com/ameliaduvall/Dissertation_Chapter4).

4.4 Results

The estimated mean daily nest survival probability for the egg state on the logit scale was β_0 = 3.079 (95% Bayesian credible interval [BCI]: 2.816, 3.324; Table 4.3). Back transformed to the probability scale, this corresponds to a daily survival probability of 0.956 (95% BCI: 0.944, 0.965), which reflects the estimated probability of an egg(s) surviving one day in the egg state. Over the median incubation period of 35 days, this equates to an estimated 21% probability of an egg(s) surviving the hatching period to the chick state (i.e., hatching probability).

Among the weather covariates, spring temperature, $\beta_{springTemp}$, had the strongest positive association with nest survival, with a mean posterior estimate of 0.177 and 88.4% of the posterior weight greater than 0 [95% BCI: -0.157, 0.471]; Table 4.3, Figure 4.4). Springtime precipitation also had a positive relationship with nest survival but with greater uncertainty ($\beta_{springPrecip}$ = 0.056 [95% BCI: -0.200, 0.308] and 66.8% of the posterior weight greater than 0). In contrast, higher precipitation during the winter in the year prior to breeding

($\beta_{prevWinterPrecip}$ = -0.140 [95% BCI: -0.417, 0.149], 84.5% of the posterior weight less than 0) and, to a lesser effect with greater uncertainty, during the most recent winter ($\beta_{winterPrecip}$ = -0.021 [95% BCI: -0.250, 0.214], 56.8% of the posterior weight less than 0) were associated with decreased nest survival.

Simulated hatching probabilities under contrasting weather scenarios revealed variation in hatching probability (Figure 4.5). The lowest estimated hatching probability (~20%) occurred under two consecutive wet winters followed by a dry and cold spring (i.e., worst case scenario). Conversely, the highest hatching probability (~28%) occurred under two dry winters followed by a wet and warm spring (i.e., best case scenario).

Posterior estimates on the effect of upwelling on nest survival revealed contrasting patterns (Table 4.3, Figure 4.4). Upwelling during the pre-breeding season had a stronger, and negative, relationship with nest survival ($\beta_{preUpwelling}$ = -0.493 [95% BCI: -0.835, -0.172], 99.9% of the posterior weight less than 0). In contrast, we found a weaker, and positive, relationship between upwelling and nest survival during the breeding season ($\beta_{breedUpwelling}$ = 0.105 [95% BCI: -0.126, 0.339]), with 82.3% of the posterior distribution above zero.

Finally, coefficient estimates from habitat covariates indicated that nests in crevice habitat had lower daily nest survival compared to those in native shrub habitat, which served as the reference habitat type ($\beta_{habitat[crevice]}$ = -0.556 [95% BCI: -0.731, -0.384]; Table 4.3, Figure 4.4). For artificial habitat, we were unable to detect a difference in nest survival as compared to native shrub habitat ($\beta_{habitat[artificial]}$ = 0.008 (95% BCI: -0.188, 0.207).

4.5 Discussion

We developed a daily nest survival model that accounts for nest exposure time to evaluate fine-scale weather drivers of reproductive success and to assess the influence of marine conditions and nesting habitat on murrelets at Santa Barbara Island. We found strong evidence that nesting habitat plays a role in daily nest survival, alongside key winter and spring weather conditions. Our results can be used to inform management interventions aimed at improving reproductive outcomes for murrelets at one of their largest breeding colonies.

Monitoring plots dominated by native shrub habitat (LACO, NTP) exhibited higher daily nest survival compared to those characterized primarily by crevice habitat (APNC, CC), while the estimated effect of artificial habitat (BH, DOCK), relative to native shrub, was ambiguous. This finding largely supports our *habitat type* hypothesis that native shrub habitat provides alternative forage resources for mice and protective cover for murrelets from owls, leading to increased nest survival. During the spring, deer mice consume lepidopteran larvae (e.g., moth and butterfly caterpillars; NPS unpublished data), and many native Lepidoptera caterpillars depend on native plants (Powell 2005). As a result, native shrub habitat could offer greater foraging opportunities for mice, potentially reducing their reliance on murrelet eggs. Additionally, the increased structural cover provided by native shrubs may also reduce the risk of adult murrelet depredation by owls, although we lack direct empirical evidence of this interaction and it requires future study. While some artificial habitat features may support nesting in limited contexts, covering the island with artificial structures is neither ecologically nor logistically feasible. Thus, the observed benefits of native shrub habitat emphasize the importance of conserving and restoring native vegetation as a more sustainable and ecologically integrated strategy for supporting murrelet reproductive success. Future studies examining spatial variation

in mouse diet composition and abundance across habitat types could also clarify the ecological pathways through which native shrub habitat influences murrelet survival.

Our results are particularly noteworthy considering the extensive habitat degradation at Santa Barbara Island. Historical accounts indicate that the island was once covered with dense scrub vegetation prior to the 1890s (Davidson et al. 2019). Since then, large-scale vegetation changes were brought on by a series of anthropogenic disturbances, including farming, fire, and the introduction of non-native herbivores such as rabbits and sheep (Davidson et al. 2019). Early naturalist reports (e.g., Howell 1917), soil surveys (United States Department of Agriculture Natural Resources Conservation Service 2007), and faunal remains (Collins et al. 2018) all collectively suggest that Santa Barbara Island used to host far greater seabird abundances (Davidson et al. 2019). Habitat loss is a well-documented driver of seabird declines at other breeding grounds, seen in other species such as penguins (Trathan et al. 2015) and the closely related Marbled Murrelet (*Brachyeamphus marmoratus*), which nests in old-growth forests increasingly lost to the timber industry (Betts et al. 2020). In recognition of the habitat-associated decline in seabirds at Santa Barbara Island, a multi-year restoration project was initiated in 2007 with funds from the Montrose Settlements Restoration Program to restore shrub habitat for nesting seabirds. However, logistical challenges posed by the remote nature of the island, coupled with funding limitations, curtailed most of the program in 2016. Our findings offer the first quantitative evidence that native shrub habitat can benefit seabird reproductive success here, underscoring the conservation value of habitat restoration on degraded islands.

Our results suggest support for our *breeding season upwelling* hypothesis, but not the *pre-breeding season upwelling* hypothesis (Table 4.1, Figure 4.4). We expected a positive relationship between upwelling in the pre-breeding season and nest survival, believing this

would lead to greater marine productivity and prey availability during the breeding season, and thus a reduced likelihood of nest abandonment. The negative relationship between upwelling in the pre-breeding season (January to March of year *t*) may be explained, in part, because upwelling in the California Current tends to be lowest in the winter, peaking in the spring and summer (Bograd et al. 2009). Instead of reflecting marine productivity, BEUTI upwelling indices during the winter could be reflecting storminess, conditions that may aggravate foraging success for seabirds, but this warrants further examination. As we expected, greater upwelling during the breeding season (April to June of year *t*) was associated with higher nest survival – again, reflecting greater prey availability and more foraging resources, leading to reduced rates of nest abandonment. Upwelling strength in the springtime has also been associated with increased breeding effort for another alcid in the California Current, the Cassin's Auklet (*Ptychoramphus aleuticus*; Johns et al. 2022). However, because auklets feed at lower trophic levels than murrelets (Adams et al. 2004, Hamilton et al. 2004), they are more likely to experience rapid benefits in prey availability following increased upwelling. Regardless of the role of marine conditions on murrelet nest survival, there are no direct management actions available to enhance prey availability for murrelets. Notably, the effect of breeding season upwelling on nest survival was relatively weak compared to most weather variables (Figure 4.4), highlighting the greater role of terrestrial-based drivers on murrelet nest survival (Thomsen and Green 2019).

Most of our weather-related hypotheses were supported by the results (Table 4.1, Figure 4.4); however, 95% credible intervals for all coefficients overlapped with 0. Increased winter precipitation was associated with reduced nest survival, likely due to cascading effects on vegetative growth that elevate mouse and owl populations, ultimately increasing predation risk

for murrelets (Thomsen et al. 2018). The effect of precipitation during the previous winter (*previous winter precipitation* hypothesis) was stronger than that of precipitation in the winter immediately preceding the breeding season (*winter precipitation* hypothesis), consistent with earlier findings of a one-year time lag between vegetative growth and mouse population responses (Thomsen et al. 2018). We also found support for our *spring precipitation* hypothesis, which posits that increased rainfall in the spring provides alternative foraging resources for mice, thereby reducing egg predation and increasing nest survival. An additional potential mechanism of increased nest survival in high spring precipitation years is that sustained mouse populations during wet springs may divert owl predation away from adult murrelets, further contributing to higher nest survival rates. The strongest effect size observed for our weather variables was for *spring temperature*, but the direction of the effect was opposite to our hypothesis. We had anticipated that higher spring temperatures would reduce water availability on this island without any permanent water resources as well as foraging opportunities for mice, leading to increased egg predation and, ultimately, greater adult murrelet predation by owls due to a decline in mouse populations. Instead, we observed a strong positive relationship between increased springtime temperatures and nest survival. This unexpected result warrants further investigation, including an assessment of potential threshold effects (see below). One possible explanation is that warmer spring temperatures may stimulate vegetative growth, indirectly enhancing alternative prey availability for mice. Alternatively, increased temperatures could influence mouse behavior or energetic demands in ways that reduce their reliance on murrelet eggs.

Through our analysis, we identified weather conditions that would warrant deploying expensive management interventions to improve murrelet egg survival. If CHIS managers observe two consecutive wet winters, followed by a cold dry spring (relative to mean weather

conditions), we anticipate a reduction in murrelet nest survival and overall hatching probability (Figure 4.5). Under these conditions, we recommend using management interventions, such as trapping and translocation of mice from murrelet breeding colonies (Millus et al. 2007), to prevent substantial declines in murrelet nest survival by egg depredation. Additionally, these management interventions may be of greater benefit at breeding colonies already associated with reduced nest survival, such as those with primarily crevice habitat (APNC, CC). Although owl home range sizes are relatively small (0.06 – 1.12 km^2) and they do not appear to use the entire island (Thomsen et al. 2014), a key assumption underlying mouse removal strategies is that owls will locate the translocated mice and/or continue to rely on mouse populations in unaffected areas, rather than shift their diet towards murrelets in locations where mice have been removed. While short-term management actions to directly reduce owl predation on adult murrelets are limited, our finding that nest survival for murrelets is higher in native shrub habitat warrants further investigation on the potential protective mechanism of vegetative structure from owl predation. This is also particularly important given that adult mortality may have disproportionally negative effects on overall population viability (Sæther and Bakke 2000).

Our results should be interpreted with several important caveats. First, variable monitoring effort, in particular extended survey intervals, may have increased the likelihood of missing evidence of successful hatching, leading to an underestimation of daily nest survival rates and overall reproductive success. While eggshell fragments (e.g., hatched or depredated eggshells) are frequently observed at nest sites, they are not always present. However, mice are more likely to carry away depredated eggshells (NPS unpublished data), so we believe the assumption of nest failure in this case is warranted. Second, we did not distinguish between nests with one egg and those with two eggs during the egg stage, despite suspected differences in

survival. Specifically, nests with only one egg may experience lower survival due to temporary neglect prior to the laying of the second egg (Murray et al. 1980). By combining one- and two-egg stages, we may have underestimated average egg-stage survival, particularly if losses are more common during the early, single-egg period. Third, we modeled the relationship between nest survival and weather covariates as linear, although we acknowledge that non-linear relationships or thresholds may exist. For example, nest survival may decline sharply once temperatures exceed a biologically meaningful limit or if precipitation is extensive enough to cause damage to nesting habitat. In addition, potential interactive effects among weather covariates (e.g., a stronger or weaker effect under certain precipitation and temperature combinations) are not captured in our additive framework, potentially obscuring synergistic or antagonistic influences on nest survival that could be important. Finally, we recognize our model is a simplified representation of a highly complex system of interactions between owls, mice, murrelets, and terrestrial and marine climate conditions. Ideally, long-term monitoring data of predator populations will be collected and will allow for more mechanistic inference and targeted management. However, given logistical constraints, our aim was to provide actionable insights based on abiotic weather drivers to guide the timing of management interventions under limited resource conditions.

By identifying weather conditions that can reliably predict reduced nest survival, our analysis provides CHIS a framework to anticipate high-risk breeding years and to inform the deployment of costly, but effective, management interventions to conserve the threatened Scripps's Murrelet. Specifically, we leveraged the availability of abiotic weather data to identify combinations of seasonal conditions that lead to reduced murrelet nest survival due to climate-driven predator-prey dynamics where direct monitoring of predator populations is not available.

We also underscored the importance of nest habitat in murrelet nest survival, particularly the apparent benefits of native shrub habitat. Future research areas should investigate potential mechanisms underlying this pattern, including differences in mouse abundance and diet between degraded and intact habitats, and the role of vegetative structure in reducing aerial predation risk for murrelets.

4.6 Acknowledgements

We acknowledge the Montrose Trustee Council, whose funding and support were critical to the collection of these data. We thank and acknowledge the many individuals who have contributed to this work. Any use of trade, firm, or product names is for descriptive purposes only and does not imply endorsement by the U.S. Government.

4.7 References

Abatzoglou, J. T., D. J. McEvoy, and K. T. Redmond. 2017. The West Wide Drought Tracker: Drought monitoring at fine spatial scales. Bulletin of the American Meteorological Society 98:1815–1820.

Adams, J., J. Y. Takekawa, and H. R. Carter. 2004. Stable foraging areas and variable chick diet in Cassin's Auklets (Ptychoramphus aleuticus) off southern California. Canadian Journal of Zoology 82:1578–1595.

Betts, M. G., J. M. Northrup, J. A. B. Guerrero, L. J. Adrean, S. K. Nelson, J. L. Fisher, B. D. Gerber, M.-S. Garcia-Heras, Z. Yang, D. D. Roby, and J. W. Rivers. 2020. Squeezed by a habitat split: Warm ocean conditions and old-forest loss interact to reduce long-term occupancy of a threatened seabird. Conservation Letters 13:e12745.

Birt, T. P., H. R. Carter, D. L. Whitworth, A. McDonald, S. H. Newman, F. Gress, E. Palacios, J. S. Koepke, and V. L. Friesen. 2012. Rangewide population genetic structure of Xantus's Murrelet (Synthliboramphus hypoleucus). Auk 129:44–55.

Bograd, S. J., I. Schroeder, N. Sarkar, X. Qiu, W. J. Sydeman, and F. B. Schwing. 2009. Phenology of coastal upwelling in the California Current. Geophysical Research Letters 36.

Bratt, A. E. 2023. From mark-resight to management: Bayesian hierarchical models for endangered bird populations. University of Washington Libraries, Seattle, Washington, USA.

Brooks, S. P., and G. O. Roberts. 1998. Convergence assessment techniques for Markov chain Monte Carlo. Statistics and Computing 8:319–335.

Burkett, E. E., N. A. Rojek, A. E. Henry, M. J. Fluharty, L. Comrack, P. R. Kelly, A. C. Mahaney, and K. M. Fien. 2003. Report to the California Fish and Game Commission: Status review of Xantus's Murrelet (Synthliboramphus hypoleucus) in California. California Department of Fish and Game, Habitat Conservation Planning Branch Status Report 2003-03. 96 pp. + appendices.

California Natural Diversity Database. 2025. State and federally listed endangered and threatened animals of California. California Department of Fish and Wildlife, Sacramento, California, USA.

Carter, H. R., G. J. McChesney, D. L. Jaques, C. S. Strong, M. W. Parker, J. E. Takekawa, D. L. Jory, and D. L. Whitworth. 1992. Breeding populations of seabirds in California, 1989–1991. Volume I – Population estimates. Unpublished draft final report. U.S. Fish and Wildlife Service, Northern Prairie Wildlife Research Center, Dixon, California.

Collins, P. W., A. F. Ainis, J. Rodriguez, S. Ceniceros, J. L. Sperati, R. B. Guttenberg, S. K. Thomsen, and R. L. Vellanoweth. 2018. Faunal and floral deposits from Barn Owl Cave: A proxy for natural and anthropogenic change on Santa Barbara Island during the past ~1,500 years. Unpublished report prepared by the Santa Barbara Museum of Natural History, Santa Barbara, California, for the National Park Service and Montrose Settlements Restoration Program. 94 pp.

Daly, C., M. Halbleib, J. I. Smith, W. P. Gibson, M. K. Doggett, G. H. Taylor, J. Curtis, and P. P. Pasteris. 2008. Physiographically sensitive mapping of climatological temperature and precipitation across the conterminous United States. International Journal of Climatology 28:2031–2064.

Davidson, A. D., A. K. McEachern, T. J. Coonan, W. T. Bean, A. J. Armstrong, and B. R. Hudgens. 2019. Natural resource condition assessment: Channel Islands National Park. Natural Resource Report NPS/CHIS/NRR—2019/1899. National Park Service, Fort Collins, Colorado, USA.

Dinsmore, S. J., G. C. White, and F. L. Knopf. 2002. Advanced techniques for modeling avian nest survival. Ecology 83:3476–3488.

Drost, C. A., and G. M. Fellers. 1991. Density cycles in an island population of deer mice, Peromyscus maniculatus. Oikos 60:351–364.

Drost, C. A., and D. B. Lewis. 1995. Xantus's Murrelet (Synthliboramphus hypoleucus). Pages 1–23 in A. Poole and F. Gill, editors. The birds of North America. The Academy of Natural Sciences, Philadelphia, Pennsylvania, USA, and The American Ornithologists' Union, Washington, D.C., USA.

Gelman, A., and D. B. Rubin. 1992. Inference from iterative simulation using multiple sequences. Statistical Science 7:457–472.

Hamilton, C. D., H. R. Carter, and R. T. Golightly. 2004. Diet of Xantus's Murrelets in the Southern California Bight. The Wilson Bulletin 116:152–157.

Harvey, A. L., C. E. Hand, and S. A. Auer. 2012. Scripps's Murrelet reproductive performance on Santa Barbara Island, California in 2008–2009. Unpublished report, California Institute of Environmental Studies, Davis, California, USA.

Hermoso, V., R. P. Vasconcelos, S. Henriques, A. F. Filipe, and S. B. Carvalho. 2021. Conservation planning across realms: Enhancing connectivity for multi-realm species. Journal of Applied Ecology 58:644–654.

Howell, A. B. 1917. Birds of the islands off the coast of Southern California. Cooper Ornithological Club, Pacific Coast Avifauna 12:127.

Jacox, M. G., C. A. Edwards, E. L. Hazen, and S. J. Bograd. 2018. Coastal upwelling revisited: Ekman, Bakun, and improved upwelling indices for the U.S. West Coast. Journal of Geophysical Research: Oceans 123:7332–7350.

Jacques, M. E., A. A. Yamagiwa, D. M. Mazurkiewicz, A. L. Harvey, and A. Little. 2015. Seabird habitat restoration on Santa Barbara Island, California: 2007–2014 data report. Unpublished report, California Institute of Environmental Studies. 242 pp.

Johns, M. E., P. Warzybok, J. Jahncke, P. Doak, M. Lindberg, and G. A. Breed. 2022. Episodes of high recruitment buffer against climate-driven mass mortality events in a North Pacific seabird population. Journal of Animal Ecology 91:345–355.

Karnovsky, N. J., L. B. Spear, H. R. Carter, D. G. Ainley, K. D. Amey, L. T. Ballance, K. T. Briggs, R. G. Ford, G. L. Hunt Jr., C. Keiper, J. W. Mason, K. H. Morgan, R. L. Pitman, and C. T. Tynan. 2005. At-sea distribution, abundance and habitat affinities of Xantus's Murrelets. Marine Ornithology 33:89–104.

Mayfield, H. 1961. Nesting success calculated from exposure. The Wilson Bulletin 73:8.

Millus, S. A., P. Stapp, and P. Martin. 2007. Experimental control of a native predator may improve breeding success of a threatened seabird in the California Channel Islands. Biological Conservation 138:484–492.

Murray, K. G., K. Winnett-Murray, and G. L. Hunt Jr. 1980. Egg neglect in Xantus' Murrelet. Proceedings of the Colonial Waterbird Group 3:11.

Murray, K. G., K. Winnett-Murray, Z. A. Eppley, G. L. Hunt, and D. B. Schwartz. 1983. Breeding biology of the Xantus' Murrelet. The Condor 85:12–21.

Nur, N., A. L. Harvey, S. K. Thomsen, R. Bradley, and J. Jahncke. 2013. Modeling the population level impacts of Barn Owls on Scripps's Murrelet population trends on Santa Barbara Island. Unpublished report prepared for the National Fish and Wildlife Foundation. Point Blue Conservation Science, Petaluma, California, USA. PRBO Contribution Number 1969.

Powell, J. A. 2005. Assessment of inventory effort for Lepidoptera (Insecta) and the status of endemic species on Santa Barbara Island, California. Pages 351–371 in D. K. Garcelon and C. A. Schwemm, editors. Proceedings of the Sixth California Islands Symposium. Institute for Wildlife Studies, Arcata, California, USA.

R Core Team. 2024. R: A language and environment for statistical computing. R Foundation for Statistical Computing, Vienna, Austria.

Rodriguez, D., T. Sajar, T. Handley, and A. K. McEachern. 2012. Draft Santa Barbara Island vegetation mapping project. Technical report to Channel Islands National Park. 84 pp.

Rotella, J. J., S. J. Dinsmore, and T. L. Shaffer. 2004. Modeling nest–survival data: A comparison of recently developed methods that can be implemented in MARK and SAS. Animal Biodiversity and Conservation 27:187–205.

Sæther, B.-E., and Ø. Bakke. 2000. Avian life history variation and contribution of demographic traits to the population growth rate. Ecology 81:642–653.

Thomsen, S. K., C. E. Kroeger, P. H. Bloom, and A. L. Harvey. 2014. Space use and home-range size of Barn Owls on Santa Barbara Island. Monographs of the Western North American Naturalist 7:339–347.

Thomsen, S. K., and D. J. Green. 2016. Cascading effects of predation risk determine how marine predators become terrestrial prey on an oceanic island. Ecology 97:3530–3537.

Thomsen, S. K., D. M. Mazurkiewicz, T. R. Stanley, and D. J. Green. 2018. El Niño/Southern Oscillation-driven rainfall pulse amplifies predation by owls on seabirds via apparent competition with mice. Proceedings of the Royal Society B: Biological Sciences 285:20181161.

Thomsen, S. K., and D. J. Green. 2019. Predator-mediated effects of severe drought associated with poor reproductive success of a seabird in a cross-ecosystem cascade. Global Change Biology 25:1642–1652.

Trathan, P. N., P. García-Borboroglu, D. Boersma, C.-A. Bost, R. J. M. Crawford, G. T. Crossin, R. J. Cuthbert, P. Dann, L. S. Davis, S. De La Puente, U. Ellenberg, H. J. Lynch, T. Mattern, K. Pütz, P. J. Seddon, W. Trivelpiece, and B. Wienecke. 2015. Pollution, habitat loss, fishing, and climate change as critical threats to penguins. Conservation Biology 29:31–41.

United States Department of Agriculture Natural Resources Conservation Service. 2007. Soil survey of Channel Islands National Park, California. Available at: http://soils.usda.gov/survey/printed_surveys/ (accessed 8 January 2014).

Valpine, P. de, D. Turek, C. J. Paciorek, C. Anderson-Bergman, D. T. Lang, and R. Bodik. 2017. Programming with models: Writing statistical algorithms for general model structures with NIMBLE. Journal of Computational and Graphical Statistics 26:403–413.

Warlick, A. 2022. Understanding the effects of environmental variability on demography in species with complex life histories through integrated population modeling. University of Washington Libraries, Seattle, Washington, USA.

Young, L., and L. T. Ballance. 2023. Ecology of marine birds. In L. Young and E. VanderWerf, editors. Conservation of marine birds. Academic Press, San Diego, California, USA.

4.8 Tables and Figures

Table 4.1 Hypotheses on weather (*previous winter precipitation* hypothesis, *winter precipitation* hypothesis, *spring precipitation* hypothesis, *spring temperature* hypothesis), marine, and habitat (*habitat type* hypothesis) drivers of Scripps's Murrelet nest survival, and covariates used to test each hypothesis in the daily nest survival model.

Hypothesis name	**Hypothesis description**	**Covariate**
Previous winter precipitation hypothesis	Increased precipitation during the previous winter drives vegetative growth and leads to a delayed (1 year) increase in mouse populations and owl populations, resulting in higher egg and adult predation during the breeding season, leading to decreased nest survival.	WestWide Drought Tracker (WWDT) island-specific monthly precipitation, November in year *t*-2 to February in year *t-1*
Winter precipitation hypothesis	Increased precipitation during the winter immediately preceding the breeding season drives vegetative growth and a short-lag increase in mouse and owl populations, resulting in higher egg and adult predation during the breeding season, leading to decreased nest survival.	WWDT island-specific monthly precipitation, November in year *t*-1 to February in year *t*
Spring precipitation hypothesis	Increased precipitation in the spring drives continued vegetative growth, which provides alternative prey resources for mice during the breeding period and sustains mouse populations, leading to increased nest survival.	WWDT island-specific monthly precipitation, March to May in year *t*
Spring temperature hypothesis	Increased temperature in the spring reduces water resources and forage opportunities, resulting in increased mouse predation on murrelet eggs and decreased mouse populations, leading to decreased nest survival.	WWDT island-specific monthly temperature, March to May in year *t*
Pre-breeding season upwelling hypothesis	Strong upwelling in the months prior to the breeding season leads to favorable marine foraging conditions during the breeding season in which murrelets are less likely to abandon their nests, leading to increased nest survival.	Biologically Effective Upwelling Transport Index (BEUTI) at 33°N, January to March in year *t*
Breeding season upwelling hypothesis	Strong upwelling during the breeding season leads to favorable marine foraging conditions in which murrelets are less likely to abandon their nests, leading to increased nest survival.	BEUTI at 33°N, April to June in year *t*
Habitat type hypothesis	Native shrub habitat provides protective cover for murrelets from owls and	Habitat categorical variable (artificial, crevice, native shrub)

	alternative forage availability for mice, leading to increased nest survival.	

Table 4.2 Number of Scripps's Murrelet monitored nest attempts by year (1988 – 2019) and plot (n = 6) at Santa Barbara Island. Years or plots without any monitoring data are indicate by a dash (-). Nest attempts are summed across plots for each year and bolded and italicized in the last column, Total.

Year	**Arch Point North Cliffs**	**Bunkhouse**	**Cat Canyon**	**Dock**	**Landing Cove**	**Nature Trail**	**Total**
1988	-	-	9	-	-	16	***25***
1989	-	-	11	-	-	6	***17***
1990	-	-	15	-	-	8	***23***
1991	-	-	38	-	-	13	***51***
1992	-	-	27	-	-	4	***31***
1993	-	-	23	-	-	13	***36***
1994	-	3	21	-	-	18	***42***
1995	-	-	17	1	-	7	***25***
1996	-	-	12	15	-	19	***46***
1997	-	-	11	14	-	16	***41***
1998	-	-	28	2	-	18	***48***
1999	-	-	-	-	-	-	***0***
2000	-	-	-	-	-	-	***0***
2001	-	-	-	-	-	-	***0***
2002	-	-	-	-	-	-	***0***
2003	-	-	-	-	-	-	***0***
2004	-	-	-	-	-	-	***0***
2005	-	-	-	-	-	-	***0***
2006	-	-	-	-	-	-	***0***
2007	-	-	-	-	-	-	***0***
2008	-	-	-	-	-	-	***0***
2009	-	5	10	12	3	-	***30***
2010	35	9	46	22	43	-	***155***
2011	22	16	47	23	8	-	***116***
2012	1	8	40	30	61	-	***140***
2013	19	5	17	31	36	-	***108***
2014	14	2	17	19	22	-	***74***
2015	13	3	27	14	21	-	***78***
2016	17	3	28	18	29	-	***95***
2017	10	3	17	10	-	-	***40***
2018	5	1	6	11	9	-	***32***

2019	4	1	6	8	2	-	***21***

Table 4.3 Parameter mean estimates and lower and upper 95% Bayesian credible interval bounds from Scripps's Murrelet daily nest survival model. See Eq. 24 for a full description of the parameters and section 4.3.3 for information on covariate data. All parameters are reported on the logit scale.

Parameter	**Mean**	**Lower 95% Credible Interval**	**Upper 95% Credible Intervals**
β_0	3.079	2.816	3.324
$\beta_{prevWinterPrecip}$	-0.140	-0.417	0.149
$\beta_{winterPrecip}$	-0.021	-0.250	0.214
$\beta_{springPrecip}$	0.056	-0.200	0.308
$\beta_{springTemp}$	0.177	-0.157	0.471
$\beta_{preUpwelling}$	-0.493	-0.835	-0.172
$\beta_{breedUpwelling}$	0.105	-0.126	0.339
$\beta_{artificial}$	0.008	-0.188	0.207
$\beta_{crevice}$	-0.556	-0.731	-0.384
δ_y	0.503	0.325	0.768

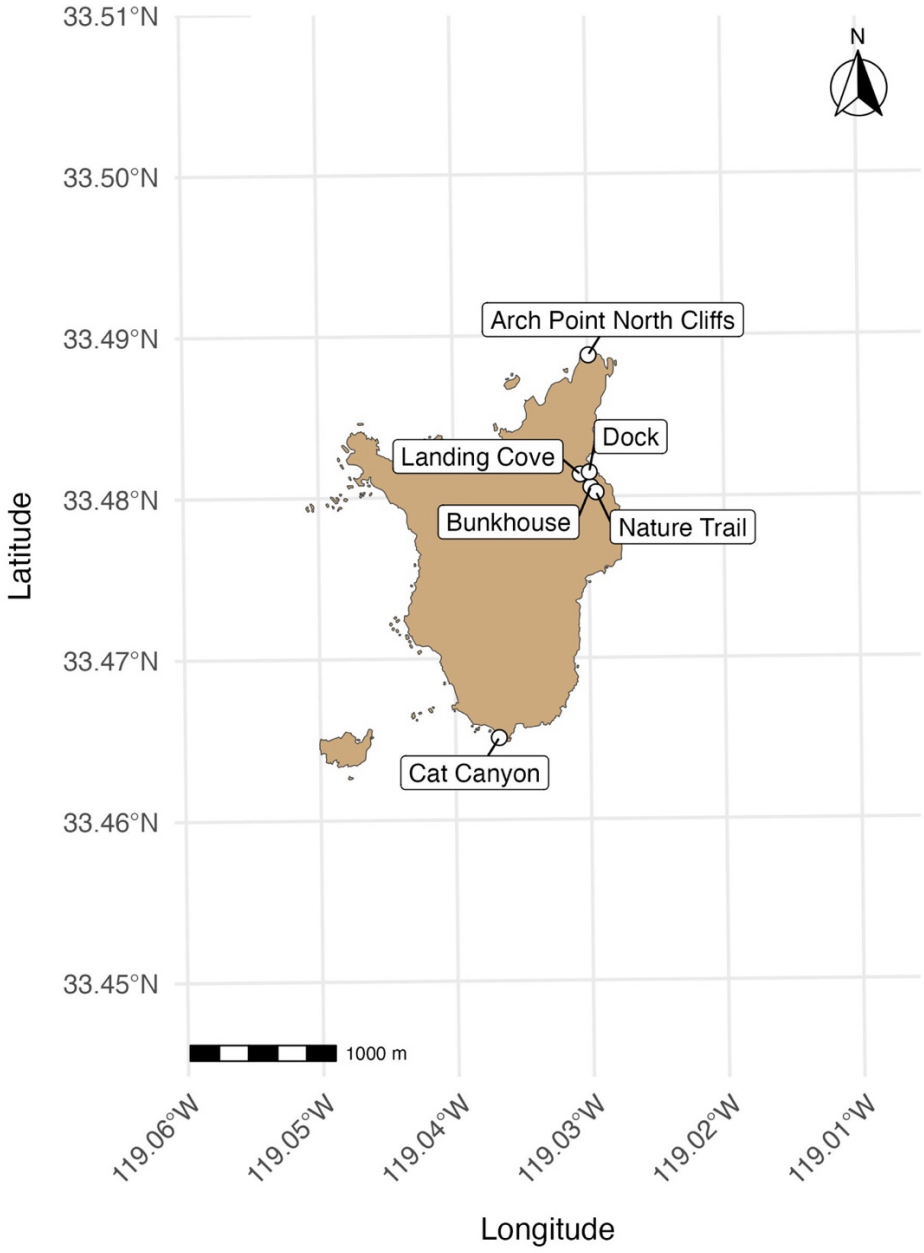

Figure 4.1 Santa Barbara Island, Channel Islands National Park with the locations of long-term Scripps's Murrelet nest monitoring plots (n = 6): Arch Point North Cliffs, Bunkhouse, Cat Canyon, Dock, Landing Cove, and Nature Trail.

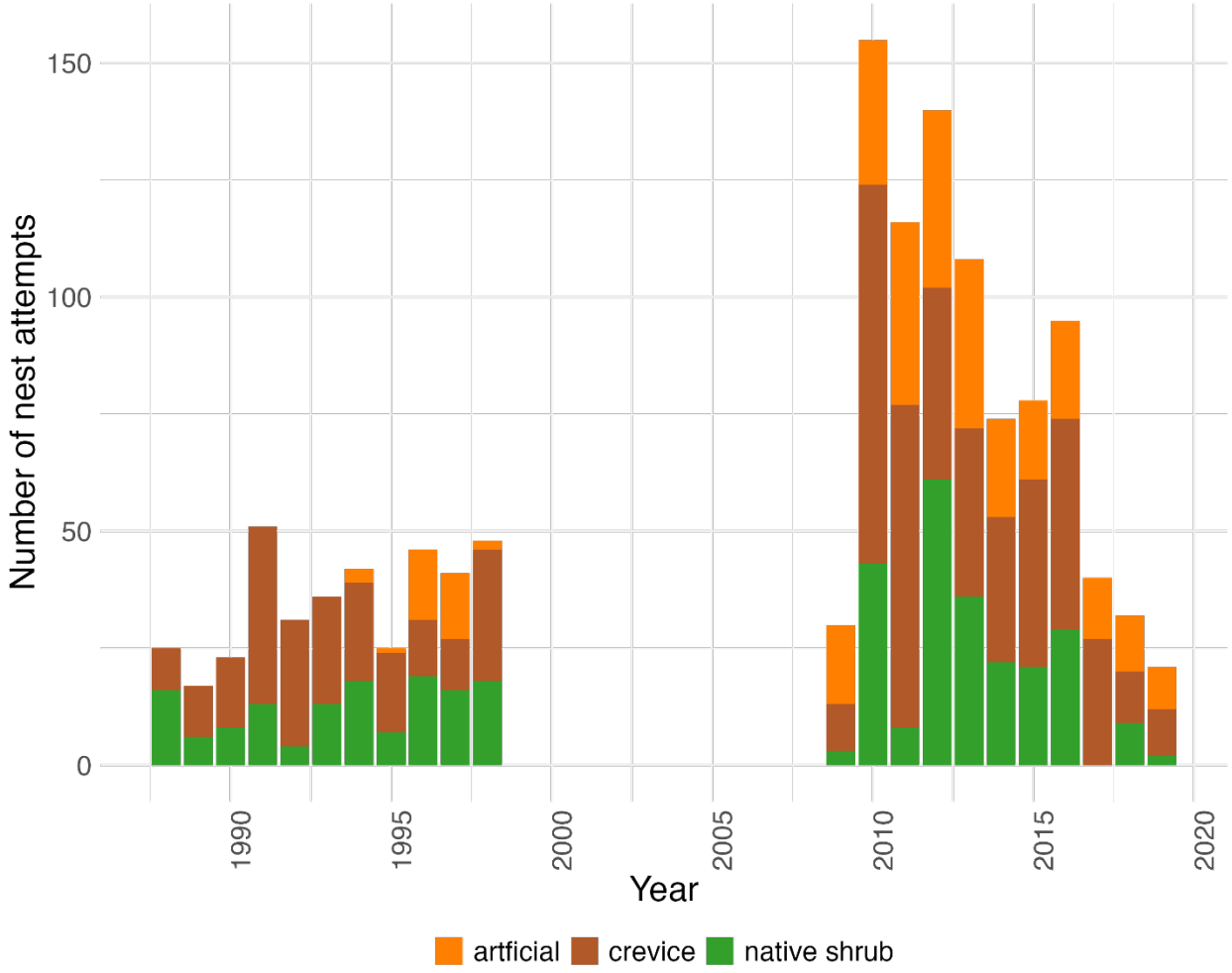

Figure 4.2 Scripps's Murrelet nest attempts at six monitoring plots on Santa Barbara Island over the study period, 1988 – 2019. Bars indicate the total number of monitored nest attempts, partitioned and colored by general nesting habitat: artificial/manmade habitat (orange), rocky crevice habitat (brown), and native shrub habitat (green).

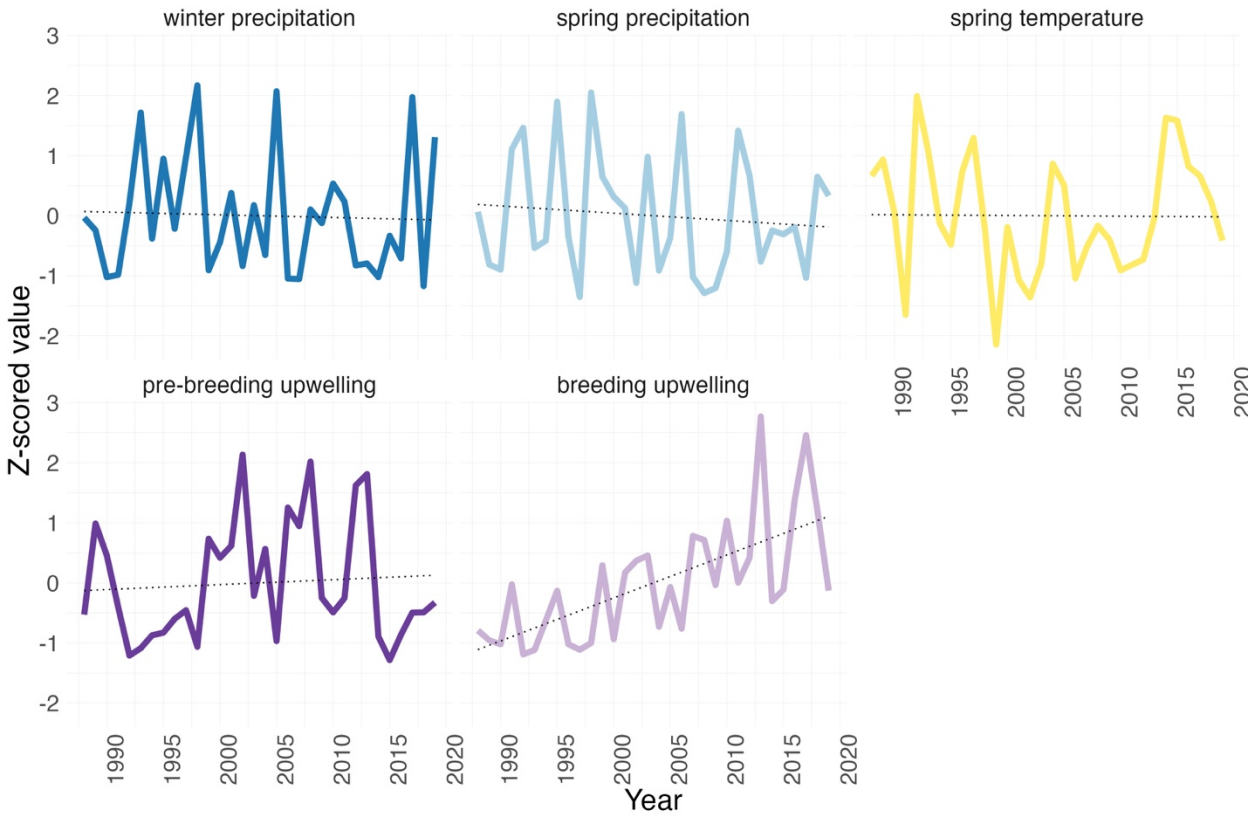

Figure 4.3 Time series of continuous covariates used in the daily nest survival model. Values are z-scored within each covariate. Dotted lines represent linear trends over the time series period, 1988 – 2019. Variables include: *winter precipitation* (November in year *t*-1 to February in year *t*), *spring precipitation* (March to May in year *t*), *spring temperature* (March to May in year *t*), *pre-breeding season upwelling* (as measured by the Biologically Effective Upwelling Transport Index [Jacox et al. 2018]; January to March in year *t*), and *breeding season upwelling* (April to June in year *t*). See section 4.3.3 and Table 4.1 for more information on covariate data and hypotheses tested using covariate data. Note that we do not plot the covariate for the *previous winter precipitation* hypothesis since it is the same as the data for the winter precipitation hypothesis but lagged by one year.

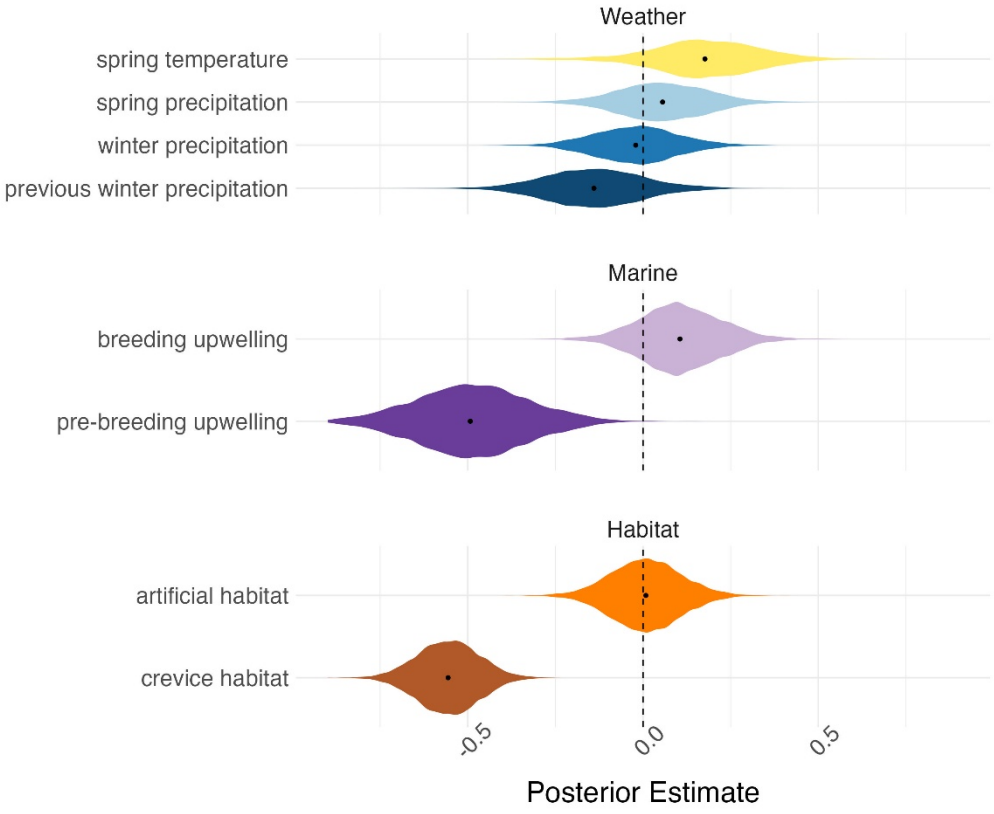

Figure 4.4 Posterior distributions of covariate effects on Scripps's Murrelet daily nest survival across six monitoring plots at Santa Barbara Island, 1988 – 2019. Plot are faceted by covariate type: weather (previous winter precipitation, winter precipitation, spring precipitation, spring temperature), marine (pre-breeding upwelling, breeding upwelling), and habitat (artificial habitat, crevice habitat). Note that covariate results for nesting habitat type variables are relative to the reference habitat type, native shrub habitat. Violin plots show the estimated effect sizes (posterior distributions) for each covariate, with black dots identifying the posterior means. Violin plots to the left of the dashed line (x = 0) indicates a negative relationship with daily nest survival; plots to the right indicate a positive relationship.

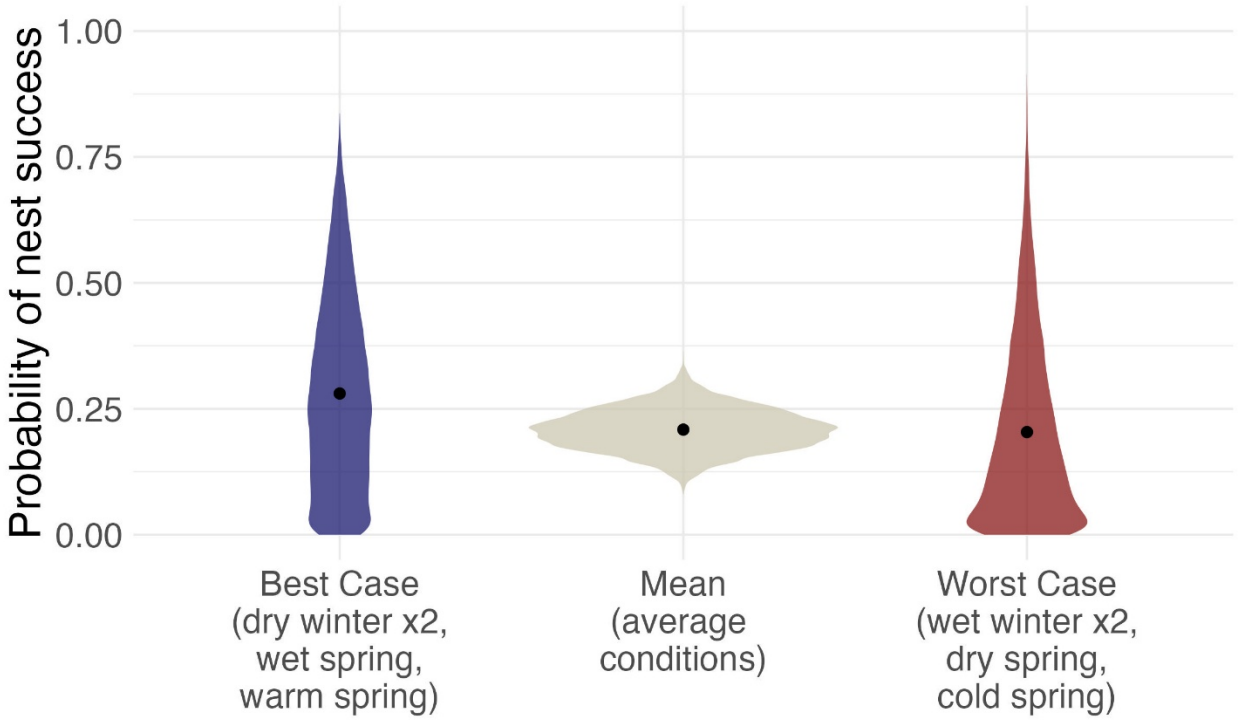

Figure 4.5 Posterior distribution of predicted hatching probability under three contrasting weather scenarios. Scenarios are created using standardized values (±2 standard deviations) for covariates reflecting *previous winter precipitation*, *winter precipitation*, *spring precipitation*, and *spring temperature*. The "Best Case" scenario reflects a dry previous winter, a dry recent winter, and warm and wet spring – conditions associated with higher nest survival. The "Worst Case" scenario reflects a wet previous winter, a wet recent winter, and a dry and cold spring – conditions associated with lower nest survival. The "Mean" scenario uses average conditions across all weather covariates (with the mean set to 0). Black dots indicate posterior means.

Chapter 5. Use of Constructed Value of Information to Identify Critical Uncertainties in Marine Bird Conservation

Publication history: This study was co-authored with David M. Mazurkiewicz and Sarah J. Converse. Workshop participants and experts, listed in Appendix 5.1 and Table 5.3, will be invited to be co-authors on the final publication. At the time this dissertation was published, this chapter was not in review with a journal.

5.1 Abstract

Wildlife managers must often make conservation decisions under substantial uncertainty about the magnitude of threats, the response of populations, and the effectiveness of potential management actions. Structured decision making (SDM) and value of information frameworks offer systematic approaches to prioritize research and monitoring that are most likely to improve conservation outcomes. Here, we applied a structured decision-making process and constructed value of information (CVOI) analysis to identify and prioritize critical uncertainties affecting seabird and shorebird conservation at Channel Islands National Park (CHIS) in California, USA. Through expert elicitation, we evaluated 28 threat hypotheses across six priority marine bird species, scoring the magnitude of uncertainty, the relevance of each threat to management decisions, and the reducibility of each uncertainty through research or monitoring. We found that threats from recreation, native predators, offshore wind development, invasive plant species, invasive black rats, new invasive species, and disease were consistently ranked among the highest priorities across all or most species, suggesting opportunities for cross-species management actions. Our results highlight key information gaps where targeted research and monitoring would yield the greatest conservation benefit and emphasize the importance of

tailoring seabird management strategies to species-specific vulnerabilities while building resilience across the broader marine bird community at CHIS. This study demonstrates the utility of CVOI as a tool for guiding conservation planning in complex, data-limited systems and provides a framework that can be adapted to similar ecosystems globally.

5.2 Introduction

Wildlife managers are often tasked with making difficult decisions under uncertainty. Across ecosystems, conservation actions must be planned and implemented without full knowledge of the nature and extent of threats, the efficacy of available management strategies, or amid incomplete or conflicting information. Moreover, collecting new information to reduce uncertainty can be costly, time-consuming, and subject to diminishing returns. As a result, there is a critical need to apply structured approaches that explicitly incorporate uncertainty into conservation decision making.

Structured decision making (SDM) offers a formal framework to support transparent, objective-driven conservation decisions in complex and uncertain contexts. SDM emphasizes the clear articulation of management objectives, the systematic evaluation of alternative management actions, and the explicit consideration of uncertainty throughout the decision-making process (Runge et al. 2020; Hemming et al. 2022). Within the SDM framework, value of information (VOI) analysis offers a quantitative approach to assess whether, and to what extent, reducing uncertainty would lead to improved management actions (Runge et al. 2011, Canessa et al. 2015, Williams and Johnson 2015). VOI can be used not only to prioritize which research and monitoring efforts are likely to yield the greatest conservation benefit given stated objectives, but also to identify uncertainties where additional information would be unlikely to alter

management decisions. In this way, VOI helps managers strategically allocate limited resources, focusing attention on the most consequential information gaps.

Constructed value of information (CVOI) is a recent extension of VOI that is well-suited for data-poor, complex systems where traditional VOI analyses are infeasible, such as when the number of management alternatives would overwhelm expert elicitation (Runge et al. 2023). CVOI relies on expert judgment to prioritize uncertainties based on their level of uncertainty (*magnitude of uncertainty*), the relevance of the uncertainty to decision making (*relevance*), and the ability to learn about the uncertainty through targeted research and monitoring (*reducibility*). Overall, it allows managers to identify research and monitoring needs with the greatest potential to improve management outcomes in the future (Runge et al. 2023). It has been used to prioritize uncertainties regarding climate effects on migratory birds (Rushing et al. 2020), habitat management effects on Eastern Black Rail (*Laterallus jamaicensis jamaicensis*) populations on the Atlantic Coast (Lawson et al. 2022), the use of prescribed fire to benefit rails and ducks in the U.S. Gulf of Mexico (Stantial et al. 2023), and uncertainties regarding stagnant growth in a reintroduced population of hihi (Stitchbird, *Notiomystis cincta*) in New Zealand (Sipe 2023). In the first three examples, the authors refer to CVOI as qualitative value of information (i.e., QVOI) but use a similar method (Runge et al. 2023).

The need to integrate decision analysis into conservation is especially urgent with seabird management. Seabird populations have dropped by nearly 70% over the past century, driven by a convergence of threats including invasive species, fisheries bycatch, habitat degradation, and climate change (Paleczny et al. 2015; Dias et al. 2019). These long-lived species depend on both marine and terrestrial environments for breeding, foraging, and survival, rendering them particularly vulnerable to complex and interacting threats. Despite increased recognition of these

challenges, substantial uncertainty remains regarding the mechanisms underlying seabird declines and the effectiveness of management interventions. This uncertainty complicates conservation planning and highlights the need to identify which threats most critically affect population viability, and which actions are most likely to improve outcomes, especially under limited resource availability.

Channel Islands National Park (CHIS), located in the Southern California Bight, USA, encompasses land on five of the eight California Channel Islands (Anacapa, Santa Barbara, Santa Cruz, San Miguel, and Santa Rosa; Figure 1.1). The park supports some of the most ecologically significant marine bird colonies in the region. Positioned at the confluence of the nutrient-rich California Current and the warmer Southern California countercurrent, the park hosts a unique assemblage of northern and southern breeding seabirds not found anywhere else in the world (Hunt Jr. et al. 1980). Nearly 99% of Southern California's breeding seabirds nest on these islands, which also serve as key breeding, wintering, and migratory stopover habitats for shorebirds. At least 15 seabird and two shorebird species currently breed within the park, and this number appears to be increasing as species shift their ranges in response to climate-driven changes in marine conditions (Howard et al. 2024).

CHIS was designated in the early 1980s as a National Park Service Prototype Monitoring Park, with seabirds identified as a "vital sign" of ecosystem health (Cameron et al. 2005). A Seabird Monitoring Handbook, published in 1983 and updated in 1988, established priorities for long-term data collection on a subset of priority marine species (Ingram et al. 1983; Lewis et al. 1988). However, gaps in staffing and funding have led to discontinuities in monitoring, and updated demographic data are lacking for several key species with globally significant populations at CHIS, such as the California Brown Pelican (*Pelecanus occidentalis californicus*),

Ashy Storm-Petrel (*Hydrobates homochroa*), and Scripps's Murrelet (*Synthliboramphus scrippsi*). Although the park has undertaken substantial conservation efforts (e.g., predator control, habitat restoration, and seasonal colony protections), these actions are resource-intensive, and uncertainty remains about both population trajectories and the effectiveness of current management actions. To ensure long-term viability of seabird populations, monitoring and conservation efforts must be strategically targeted at high-priority sites where they can provide the greatest return on investment.

Here, we applied SDM to seabird conservation planning at CHIS. Through expert elicitation and CVOI analysis, we identified and prioritized critical uncertainties regarding threats to six priority marine bird species. Through this process, we sought to rank hypotheses on threats to priority species based on their potential impact and the feasibility of resolving uncertainty and to highlight research and monitoring priorities with the greatest expected benefit. This framework not only informs local management but also provides a scalable approach for addressing conservation challenges for seabirds and other species in similarly complex systems.

5.3 Methods

5.3.1 Participants and workshop format

Problem framing was conducted through a collaborative three-day workshop at CHIS headquarters in Ventura, California, USA, led by SJ Converse and AJ DuVall (1-3 November 2022). Participants included managers and scientific experts (Appendix 5.1). While the ultimate decision maker in this context was CHIS, we included several managers with jurisdiction on the California Channel Islands and its adjacent waters, including the U.S Fish and Wildlife Service, the Channel Islands National Marine Sanctuary, the U.S. Navy, and The Nature Conservancy. The workshop was front-loaded with a brief informational session over Zoom on 25 October

2022, in which workshop facilitators explained the structure and goals, and allowed participants to ask questions and provide input on content and outcomes. We approached the workshop with an SDM lens and guided workshop activities using the PrOACT framework: (1) Define the problem; (2) identify objectives; (3) define alternative actions to be taken; (4) evaluate consequences of actions; and (5) assess trade-offs among alternative actions (Hammond et al. 1999). The first three steps (known as problem setup) were prototyped during the workshop and finalized through post-workshop discussions (Garrard et al. 2017).

5.3.2 Problem definition

The statement of the decision problem, as defined by workshop participants, was as follows: *CHIS needs to formalize their Seabird Monitoring & Management Plan to manage a dynamic suite of over 15 seabird species over five remote islands. Management of seabirds is impeded by uncertainties regarding population trends, demographic processes underlying trends, threats, and the availability of management actions to address those threats, which may vary by species or species group. Monitoring, a key part of the Seabird Program, can help to address uncertainties and improve management. Thus, CHIS is bringing together a panel of experts and stakeholders to help identify coupled management and monitoring priorities for the CHIS Seabird Program to carry it into the coming decades. These priorities must be developed in recognition of the fact that available resources are uncertain, and are composed of limited base resources, periodic short-term project resources, and the contributions of partners to monitoring and managing seabirds; and the need to regularly revisit and update the priorities as conditions change*.

5.3.3 Objectives

CHIS managers, aided by conversations with workshop participants, identified the following strategic (high-level) objectives for the Seabird Program: (1) understand, maintain, restore, and protect natural processes and systems that lead to viability and resilience of seabird species and their ecological roles; (2) connect the public to the global, regional, ecological, and cultural significance of seabirds through communication and experience; and, (3) achieve and maintain a robust Seabird Program supported by stable and adequate resources to ensure continuity of the program.

Additional discussions led to the identification of a fundamental objective to maximize abundance of priority breeding species (Table 5.1). Workshop attendees identified eight priority species based on the global importance of CHIS to that species, and the potential of CHIS to support that species in a changing climate: Ashy Storm-Petrel (ASSP), California Brown Pelican (BRPE), Cassin's Auklet (*Ptychoramphus aleuticus*; CAAU), Guadalupe Murrelet (*Synthliboramphus hypoleucus*; GUMU), Leach's Storm-Petrel (*Hydrobates leucorhous*; LHSP), Scripps's Murrelet (SCMU), Western Gull (*Larus occidentalis*; WEGU), and Western Snowy Plover (*Anarhynchus nivosus nivosus*; WSPL). Note that one shorebird species (WSPL) is also included due to its status as Threatened under the U.S. Endangered Species Act (U.S. Fish and Wildlife Service 1993). Recognizing that ASSP and SCMU could act as a proxy for LHSP and GUMU, respectively, these species were removed to reduce the list to six priority species.

5.3.4 Alternatives

Workshop participants identified 28 threat hypotheses related to the six priority species (Table 5.2). Hypotheses included both present and anticipated threats to priority species and were grouped across eight threat categories: disturbance (n = 2 hypotheses), fisheries (2),

harmful native species interactions (3), human infrastructure (4), invasive species (3), pollution (3), projected climate change impacts (8), and toxins/diseases/parasites (3). For each hypothesis and across all species, participants identified the mechanism of impact and the demographic parameters affected (e.g., reproductive success, juvenile survival, and/or adult survival). Where possible, workshop attendees also identified management actions that could be taken if the given hypothesis were true; over forty potential management actions were identified (Appendix 5.2). We further contextualized each management action by including the following information for each: (1) management authority (i.e., does CHIS have the authority to manage the threat?); (2) management feasibility (i.e., are there precedents for effectively managing the threat?); and, (3) management timing (i.e., can the threat be effectively mitigated through action in a single defined timeframe or will the threat require ongoing, perpetual management?).

5.3.5 CVOI ANALYSIS

To identify research and monitoring needs with the greatest potential to improve management outcomes, we used expert elicitation to calculate CVOI. To identify research and monitoring needs with the greatest potential to improve management outcomes, we used expert elicitation to calculate CVOI. We recruited a group of seabird experts based on their knowledge of the priority species and/or the Channel Islands or a similar geographic area; they further needed a minimum of 5 years' experience working either with the priority species or in the islands (Table 5.3).

For each species and hypothesis, experts scored the three CVOI components (*magnitude of uncertainty*, *relevance*, and *reducibility*; Rushing et al. 2020, Runge et al. 2023). CVOI is calculated as the product of *magnitude of uncertainty* and *relevance* and then plotted against *reducibility* to identify priorities (Rushing et al. 2020). Highest priority classes have high CVOI

and high *reducibility*; high priority classes have high CVOI and low *reducibility*; medium priority classes have low CVOI and high *reducibility*; and low priority classes have low CVOI and low *reducibility*. Hypothesis priority rankings were assigned based on their position within quadrants defined by the median values of CVOI and *reducibility* scores for each species.

Experts rated each metric on a ratio scale from 0 to 4 using a standardized rubric, where, for example, a score of 1 if half as large as a score of 2, and a score of 2 is half as large as a score of 4 (Sipe 2023; see Table 5.4 for detailed questions and scoring rubric). For *magnitude of uncertainty*, experts were asked to score "the degree of uncertainty in the validity of the hypothesis, while considering the degree to which the hypothesis is currently operating on the hypothesis as well as the degree of uncertainty regarding the impact of the threat on the hypothesis." A score of 0 represented low uncertainty; a score of 4 represented high uncertainty. To make the *relevance* metric more tractable mentally, we parsed it into two components: *relevance (a)*, the relevance of threat hypothesis to the population in question, and *relevance (b)*, the relevance of management actions to reduce the effect of the threat hypothesis on the population in question (Sipe 2023). For *relevance (a)*, experts were asked to score, contingent upon the hypothesis being true, "the degree to which it is having an impact on the population, while considering (1) the extent of the threat on the hypothesized demographic parameter(s), (2) the sensitivity of the population trend to the hypothesized demographic parameter(s), and (3) the overall effect, given 1 and 2, on the population trend (i.e., the mean rate of growth or decline in the population across time)." Experts were asked to answer conditional on the expected levels of the threat over the next 30 years. For potential threats, experts were asked to score the question qualitatively as the threat risk, which is defined as product of the likelihood of the threat occurring over the next 30 years and the potential magnitude of its impact. A score of 0

represented a low relevance; a score of 4 represented a high relevance. For *relevance (b)*, experts were asked to score, contingent upon the hypothesis being true, "the degree to which management actions, listed or otherwise, have the potential to reduce the effect of this hypothesis on the population, while considering the availability of management actions (listed or otherwise) to address the threat as well as the likelihood that management actions would/could be fully and effectively implemented." A score of 0 represented a low potential of management actions, while a score of 4 represented a high potential. Finally, for *reducibility*, experts were asked to score, "the potential to reduce uncertainty regarding the validity of the hypothesis, i.e., to reduce uncertainty regarding whether this hypothesis is having an effect on the population and to what degree, while considering the costs, logistics, and feasibility of designing an experimental or observational study that could lead to meaningful results within a relevant management timeframe of 30 years." A score of 0 represented a low potential to reduce uncertainty, and a score of 4 represented a high potential. Narrative definitions for scores for each component can be found in Table 5.4.

To determine the overall *relevance* score, we multiplied *relevance (a)* by *relevance (b)* and rescaled the product to a 0 to 4 scale. Given the large number of elements for each expert to score, along with the recognition that some hypotheses were not relevant for some priority species, we asked experts to first score *relevance (a)*, the relevance of the threat hypothesis to the population in question. If experts did not think the hypothesis was relevant for that particular species, they ceased scoring for that particular hypothesis and species and moved onto the next question. In this case, the CVOI score for this particular hypothesis and species was automatically a 0, since a *relevance (a)* score of 0—indicating that the hypothesis was not relevant for that species—would nullify all other subsequent non-zero scores for *relevance (b)*

and *magnitude of uncertainty*. In this scenario, experts also did not provide scores for *reducibility*; thus, in cases of expert disagreement on relevance (i.e., if some but not all experts scored *relevance (a)* as 0), we had fewer scores on *reducibility*.

We used a modified Delphi process to elicit expert judgements for each CVOI component (Hemming et al. 2018). First, we held two remote expert elicitation overview sessions (18 March 2024 and 25 March 2024) to review the decision context, share and discuss the alternative hypotheses, introduce the concept of CVOI, and work through practice questions. Shortly after, we held another remote meeting (11 April 2024) to review the CVOI framework, scoring rubric, and timeline and to provide instructions for experts to complete their scores. We also compiled and made available an annotated bibliography of relevant literature on threats to priority species. Experts completed their round 1 scores independently over a two-week period using a fillable scoring spreadsheet. We summarized and shared results from round 1 scores and held a remote discussion meeting (26 April 2024) to discuss the results with experts and clarify any lingering linguistic uncertainty (Regan et al. 2002). We also created an interactive web-based discussion board, where experts could share additional resources and comment on preliminary round 1 results. Then we updated the materials as needed and experts completed a second and final round of scoring over a two-week period.

5.3.6 Sensitivity analysis

To test the robustness of expert responses to individual variation and to calculate standard errors, we bootstrapped the elicited responses for CVOI and *reducibility*. For each species and hypothesis, we resampled, with replacement, the elicited CVOI and *reducibility* scores from each expert with replacement 1000 times. Then, we calculated the mean and standard error for each component using the 1000 sets of scores. Bootstrapped responses were also used to calculate the

sensitivity of priority ranking to between-expert variation for each species and hypothesis by determining the percentage of bootstrapped responses that remained in the mean priority ranking category (highest, high, medium, and low priority). We considered the priority ranking to be robust to expert-to-expert variation if >90% of the bootstrapped samples retained the mean priority ranking; moderately sensitive if <90% but >75% of the bootstrapped samples retained the mean priority ranking; and highly sensitive if <75% of the bootstrapped samples retained the mean priority ranking.

5.3.7 Personal confidence

Due to the range in subject matter explored in this analysis, experts expressed a desire to caveat their scoring responses with a measure of their *personal confidence*. Experts can perform better if allowed to assess their own confidence in their responses (Speirs-Bridge et al. 2010); however, eliciting expert uncertainty on a constructed scale poses unique cognitive challenges, so our approach was experimental. During the second round, experts scored their *personal confidence* for each hypothesis and species on a ratio scale of 0 to 2. A score of 0 indicated experts were least confident in their response for this hypothesis and species; a score of 1 indicated experts were moderately confident in their response; and a score of 2 indicated that experts were most confident in their response (see Table 5.4 for scoring rubric). To explore the impact of *personal confidence* on the priority ranking of hypotheses, we conducted a separate analysis where we weighted the bootstrapped expert scores by their *personal confidence*; a score of 2 received 100% weighting, a score of 1 received 50% weighting, and a score of 0 received 0.01% weighting. Here, we refer to these results as "linear confidence," as compared to "full confidence," which weighs each expert's response equally. We were particularly interested in whether accounting for *personal confidence* changed our results.

All analyses were conducted in R (v4.4.1; R Core Team 2024). Materials and code developed for the analysis can be found on GitHub (https://github.com/ameliaduvall/Dissertation_Chapter5).

5.4 Results

We elicited scores for *relevance (a)*, *relevance (b)*, *magnitude of uncertainty*, and *reducibility* from 12 experts for six species across 28 hypotheses. We also elicited scores for *personal confidence* for each species and hypothesis combination, which we present separately at the end of this section. Below, we present the bootstrapped results for CVOI and *reducibility*, hypothesis priority ranking, and sensitivity by each species.

5.4.1 Ashy Storm-Petrel

For ASSP, eight highest priority (high CVOI, high *reducibility*) hypotheses were identified (Table 5.5, Figure 5.1): Recreation (H2; moderately sensitive, 83.20% of bootstrapped samples retained the priority ranking), Native Predators (H5; robust, 93.60%), Offshore Wind (H9; robust, 100%), Invasive Plants (H12; highly sensitive, 61.30%), Black Rats (H13; robust, 99.10%), New Invasive Species (H14; moderately sensitive, 84.10%), Sea Level Rise (H18; highly sensitive, 64.60%), and Disease (H27; highly sensitive, 55.10%).

The high priority threat hypotheses (high CVOI, low *reducibility*) were Fishery Equipment (H3; moderately sensitive, 76.30%), Overfishing (H4; moderately sensitive, 87.20%), Oil Platforms (H8; highly sensitive, 47.20%), Artificial Light (H11; highly sensitive, 49.50%), Contaminants (H17; highly sensitive, 38.70%), and Storm Events (H24; highly sensitive, 46.00%).

The medium priority threat hypotheses (low CVOI, high *reducibility*) were Residual DDT (H16; moderately sensitive, 76.70%), Sea Surface Temperature (H20; highly sensitive, 55.80%), Precipitation (H21; highly sensitive, 26.10%), Ambient Temperature (H22; highly sensitive, 54.00%), and Marine Heat Waves (H23; highly sensitive, 66.40%).

The low priority threat hypotheses (low CVOI, low *reducibility*) were Seabird Colonization (H7; moderately sensitive, 81.40%), Shipping Traffic (H10; highly sensitive, 42.50%), Oil Spills (H15; moderately sensitive, 81.20%), Marine Productivity (H19; highly sensitive, 65.20%), Wind (H25; robust, 93.10%), Harmful Algal Blooms (H26; moderately sensitive, 85.80%), and Parasites (H28; moderately sensitive, 85.20%). Experts unanimously agreed that two hypotheses were not relevant for the Ashy Storm-Petrel: Overflights (H1) and Pinnipeds (H6).

5.4.2 California Brown Pelican

For BRPE, ten highest priority (high CVOI, high *reducibility*) hypotheses were identified (Table 5.6, Figure 5.2): Overflights (H1; robust, 99.30% of bootstrapped samples retained the priority ranking), Recreation (H2; robust, 99.60%), Fishery Equipment (H3; highly sensitive, 68.40%), Native Predators (H5; highly sensitive, 59.40%), Offshore Wind (H9; robust, 99.50%), Invasive Plants (H12; robust, 98.70%), Black Rats (H13; moderately sensitive, 89.00%), New Invasive Species (H14; moderately sensitive, 85.20%), Ambient Temperature (H22; highly sensitive, 28.80%), and Disease (H27; moderately sensitive, 80.70%).

The high priority threat hypotheses (high CVOI, low *reducibility*) were Overfishing (H4; moderately sensitive, 79.70%), Shipping Traffic (H10; highly sensitive, 61.70%), Contaminants (H17; highly sensitive, 36.90%), and Precipitation (H21; highly sensitive, 58.50%).

The medium priority threat hypotheses (low CVOI, high *reducibility*) were Pinnipeds (H6; robust, 95.50%), Seabird Colonization (H7; highly sensitive, 68.805), Residual DDT (H16; moderately sensitive, 86.80%), and Sea Level Rise (H18; highly sensitive, 55.80%).

The low priority threat hypotheses (low CVOI, low *reducibility*) were Oil Platforms (H8; moderately sensitive, 80.50%), Artificial Light (H11; moderately sensitive, 83.10%), Oil Spills (H15; highly sensitive, 65.30%), Marine Productivity (H19; highly sensitive, 73.90%), Sea Surface Temperature (H20; highly sensitive, 55.80%), Marine Heat Waves (H23; moderately sensitive, 76.70%), Storm Events (H24; highly sensitive, 29.60%), Wind (H25; robust, 99.50%), Harmful Algal Blooms (H26; highly sensitive, 68.20%), and Parasites (H28; moderately sensitive, 84.90%).

5.4.3 Cassin's Auklet

For CAAU, seven highest priority (high CVOI, high *reducibility*) hypotheses were identified (Table 5.7, Figure 5.3): Recreation (H2; highly sensitive, 62.80% of bootstrapped samples retained the priority ranking), Native Predators (H5; moderately sensitive, 84.90%), Offshore Wind (H9; moderately sensitive, 86.60%), Invasive Plants (H12; moderately sensitive, 76.30%), Black Rats (H13; robust, 98.70%), New Invasive Species (H14; moderately sensitive, 85.10%), and Disease (H27; highly sensitive, 44.40%).

The high priority threat hypothesis (high CVOI, low *reducibility*) were Fishery Equipment (H3; highly sensitive, 62.10%), Overfishing (H4; robust, 92.20%), Oil Platforms (H8; highly sensitive, 48.50%), Artificial Light (H11; moderately sensitive, 81.70%), Contaminants (H17; highly sensitive, 35.10%), Precipitation (H21; highly sensitive, 24.50%), and Storm Events (H24; highly sensitive, 40.90%).

The medium priority threat hypotheses (low CVOI, high *reducibility*) were Pinnipeds (H6; robust, 96.30%), Residual DDT (H16; highly sensitive, 69.30%), Sea Level Rise (H18; highly sensitive, 43.60%), Marine Productivity (H19; highly sensitive, 45.50%), Sea Surface Temperature (H20; highly sensitive, 56.20%), Ambient Temperature (H22; highly sensitive, 52.30%), and Marine Heat Waves (H23; highly sensitive, 56.10%).

The low priority threat hypotheses (low CVOI, low *reducibility*) were Seabird Colonization (H7; moderately sensitive, 83.70%), Shipping Traffic (H10; highly sensitive, 52.50%), Oil Spills (H15; robust, 90.50%), Wind (H25; robust, 94.70%), Harmful Algal Blooms (H26; robust, 92.00%), and Parasites (H28; robust, 93.90%). Experts unanimously agreed that one hypothesis was not relevant for the Cassin's Auklet: Overflights (H1).

5.4.4 Scripps's Murrelet

For SCMU, ten highest priority (high CVOI, high *reducibility*) hypotheses were identified (Table 5.8, Figure 5.4): Recreation (H2; moderately sensitive, 84.40% of bootstrapped samples retained the priority ranking), Native Predators (H5; highly sensitive, 74.10%), Offshore Wind (H9; robust, 100.00%), Artificial Light (H11; highly sensitive, 66.20%), Invasive Plants (H12; moderately sensitive, 77.00%), Black Rats (H13; robust, 99.90%), New Invasive Species (H14; moderately sensitive, 89.60%), Sea Level Rise (H18; highly sensitive, 58.50%), Precipitation (H21; highly sensitive, 58.20%), and Disease (H27; highly sensitive, 41.50%).

The high priority threat hypotheses (high CVOI, low *reducibility*) were Fishery Equipment (H3; moderately sensitive, 75.50%), Overfishing (H4; highly sensitive, 68.90%), Oil Platforms (H8; highly sensitive, 31.70%), and Storm Events (H24; highly sensitive, 34.90%).

The medium priority threat hypotheses (low CVOI, high *reducibility*) were Pinnipeds (H6; robust, 100.00%), Residual DDT (H16; moderately sensitive, 75.80%), Sea Surface

Temperature (H20; moderately sensitive, 76.40%), and Marine Heat Waves (H23; moderately sensitive, 76.60%).

The low priority threat hypotheses (low CVOI, low *reducibility*) were Seabird Colonization (H7; highly sensitive, 66.00%), Shipping Traffic (H10; highly sensitive, 46.70%), Oil Spills (H15; highly sensitive, 69.00%), Contaminants (H17; highly sensitive, 32.50%), Marine Productivity (H19; highly sensitive, 56.70%), Ambient Temperature (H22; highly sensitive, 45.30%), Wind (H25; moderately sensitive, 89.10%), Harmful Algal Blooms (H26; moderately sensitive, 88.10%), and Parasites (H28; moderately sensitive, 84.30%). Experts unanimously agreed that one hypothesis was not relevant for the Scripps's Murrelet: Overflights (H1).

5.4.5 Western Gull

For WEGU, nine highest priority (high CVOI, high *reducibility*) hypotheses were identified (Table 5.9, Figure 5.5): Overflights (H1; robust, 96.60% of bootstrapped samples retained the priority ranking), Recreation (H2; robust, 96.60%), Fishery Equipment (H3; highly sensitive, 50.30%), Native Predators (H5; highly sensitive, 68.20%), Offshore Wind (H9; robust, 97.80%), Black Rats (H13; robust, 98.10%), New Invasive Species (H14; moderately sensitive, 85.60%), Ambient Temperature (H22; highly sensitive, 42.50%), and Disease (H27; highly sensitive, 43.80%).

The high priority threat hypotheses (high CVOI, low *reducibility*) were Overfishing (H4; moderately sensitive, 84.40%), Oil Platforms (H8; highly sensitive, 52.40%), Artificial Light (H11; moderately sensitive, 87.20%), Contaminants (H17; highly sensitive, 44.50%), and Precipitation (H21; highly sensitive, 48.80%).

The medium priority threat hypotheses (low CVOI, high *reducibility*) were Pinnipeds (H6; robust, 99.20%), Invasive Plants (H12; highly sensitive, 56.50%), Residual DDT (H16; highly sensitive, 58.90%), Sea Level Rise (H18; highly sensitive, 58.00%), and Storm Events (H24; highly sensitive, 31.80%).

The low priority threat hypotheses (low CVOI, low *reducibility*) were Seabird Colonization (H7; moderately sensitive, 87.30%), Shipping Traffic (H10; highly sensitive, 67.60%), Oil Spills (H15; moderately sensitive, 76.70%), Marine Productivity (H19; moderately sensitive, 75.00%), Sea Surface Temperature (H20; highly sensitive, 54.50%), Marine Heat Waves (H23; highly sensitive, 63.60%), Wind (H25; robust, 99.00%), Harmful Algal Blooms (H26; highly sensitive, 73.70%), and Parasites (H28; highly sensitive, 79.90%).

5.4.6 Western Snowy Plover

For WSPL, ten highest priority (high CVOI, high *reducibility*) hypotheses were identified (Table 5.10, Figure 5.6): Overflights (H1; robust, 96.90% of bootstrapped samples retained the priority ranking), Recreation (H2; robust, 100.00%), Native Predators (H5; robust, 99.90%), Pinnipeds (H6; robust, 96.40%), Invasive Plants (H12; robust, 91.00%), Black Rats (H13; robust, 97.30%), New Invasive Species (H14; robust, 94.20%), Sea Level Rise (H18; highly sensitive, 65.60%), Precipitation (H21; highly sensitive, 45.90%), and Disease (H27; highly sensitive, 72.30%).

The high priority threat hypotheses (high CVOI, low *reducibility*) were Artificial Light (H11; highly sensitive, 62.80%), Oil Spills (H15; highly sensitive, 49.50%), Contaminants (H17; mean highly sensitive, 29.90%), and Storm Events (H24; highly sensitive, 52.50%).

The medium priority threat hypotheses (low CVOI, high *reducibility*) were Offshore Wind (H9; highly sensitive, 41.70%), Residual DDT (H16; robust, 90.60%), Ambient

Temperature (H22; highly sensitive, 56.90%), and Marine Heat Waves (H23; highly sensitive, 55.00%).

The low priority threat hypotheses (low CVOI, low *reducibility*) were Fishery Equipment (H3; highly sensitive, 64.90%), Overfishing (H4; robust, 91.70%), Seabird Colonization (H7; robust, 99.40%), Oil Platforms (H8; robust, 99.20%), Shipping Traffic (H10; robust, 100.00%), Marine Productivity (H19; highly sensitive, 65.70%), Sea Surface Temperature (H20; highly sensitive, 55.60%), Wind (H25; moderately sensitive, 88.70%), Harmful Algal Blooms (H26; highly sensitive, 66.60%), and Parasites (H28; moderately sensitive, 79.50%).

5.4.7 Personal Confidence

In general, *personal confidence* did not consistently affect the threat hypothesis priority ranking across species (Appendix 5.3a – Appendix 5.3f), with two exceptions. The Storm Events Hypothesis (H24) increased from a lower priority ranking to a higher priority ranking for five species (BRPE, CAAU, SCMU, WEGU, WSPL) when *personal confidence* was considered. The Disease Hypothesis (H27) dropped from a higher priority ranking to a lower priority ranking for four species (CAAU, SCMU, WEGU, WSPL).

Personal confidence varied by hypothesis but generally averaged around 1.0 (*moderately confident in their response for this hypothesis and species*). Confidence was highest for New Invasive Species (H14; mean *personal confidence* score = 1.73) and lowest for Parasites (H28; 0.46; Figure 5.7). *Personal confidence* was consistent across species, with mean personal confidence by species above 1.0 (Figure 5.8). *Personal confidence* was highest for BRPE (1.37) and lowest for WSPL (1.08).

5.5 Discussion

We developed a decision framework using CVOI that identifies and prioritizes critical uncertainties about seabird and shorebird conservation management at CHIS in California, USA. By using SDM and CVOI, we generated 28 current and emerging threat hypotheses across six priority species, and we identified the most pressing hypotheses to address to effectively conserve priority species at CHIS. In addition to focusing on the California Channel Islands and the priority breeding species here, our multi-species analysis is unique in that it prioritizes threats that have both a high degree of impact and can likely be reduced through targeted management actions.

Across all priority species, general trends emerged in terms of ranking of threat hypotheses, but variation across species suggests that conservation initiatives are likely to be most effective if tailored for specific species. However, five threat hypotheses were ranked as highest priority across all six species: Recreation Hypothesis (H2), Native Predators Hypothesis (H5), Black Rats Hypothesis (H13), New Invasive Species Hypothesis (H14), and Disease (H27). Two other hypotheses were ranked as highest priority for five of the six species: Offshore Wind Hypothesis (H9; ASSP, BRPE, CAAU, SCMU, WEGU) and Invasive Plants Hypothesis (H12; ASSP, BRPE, CAAU, SCMU, WSPL). These seven threat hypotheses represent uncertainties that could be resolved for multiple species, potentially resulting in cost-savings and benefitting a suite of priority species as well as other breeding seabirds at CHIS.

Of these highest priority hypotheses across multiple species, the Offshore Wind (H9) and Black Rats (H13) hypotheses were robust to between-expert variation for most species (Tables 5.5 – 5.10). As such, they represent hypotheses that were highest priority across multiple species and judged consistently so by experts. Management options vary widely for these two

hypotheses. The Offshore Wind Hypothesis represented a potential future threat, as offshore wind energy infrastructure has not yet been developed on the west coast of the U.S. Preventing offshore wind energy development was the only management action identified as available to address this threat, but CHIS does not have direct management authority to address offshore wind installations (A18, Appendix 5.2). However, five of the six priority species have been identified as vulnerable to potential adverse impacts from offshore wind energy in this region in terms of population vulnerability (ASSP, BRPE), collision vulnerability (BRPE, WEGU), and/or displacement vulnerability (CAAU, SCMU; Kelsey et al. 2018).

The Black Rats Hypothesis (H13) represented a present threat but with a more limited spatial scale. Black rats are currently present on only one island within CHIS, San Miguel Island, and two other islands within the California Channel Islands archipelago, Santa Catalina Island and San Clemente Island. They were eradicated from Anacapa Island in 2002 (Howald et al. 2010) and have never been documented on the other CHIS islands. Invasive rats are among the leading drivers of seabird extinction and endangerment across the globe, with small burrow-nesting seabirds particularly susceptible to predation (Jones et al. 2008), such as the ASSP and SCMU. Management actions that were identified for this hypothesis were: eradicate black rats (A23, one-off action), control black rat populations (A24, continuous action), and install predator-proof artificial habitat (A26, continuous action; Appendix 5.2). Eradications are preferrable to rat control in terms of ecological benefit and long-term cost (Pascal et al. 2006), but they are costly, risky, and can fail (Holmes et al. 2015). Eradication is also complicated at San Miguel Island by the presence of an island endemic mammal, the island fox (*Urocyon l. littoralis*). In addition, eradication require vigilance against reinvasion (see New Invasive Species Hypothesis below).

Another hypothesis that was robust to between-expert variation for at least three species was the Recreation Hypothesis (H2); it was robust for BRPE, WEGU, and WSPL, but moderately sensitive for ASSP and SCMU, and highly sensitive for CAAU (Tables 5.5 – 5.10). The variation in sensitivity may reflect differences in nest site exposure to human activity: surface-nesting species (BRPE, WEGU, WSPL) tend to nest in open, accessible areas that are more likely to be frequented by recreating humans, increasing the risk of disturbance. In contrast, burrow- and crevice-nesting species (ASSP, CAAU, SCMU) typically use more concealed nest sites, which may offer some natural protection from disturbance. However, ASSP and SCMU nest in dry sea caves that are closed to the public, but susceptible to disturbance as they are not consistently patrolled and trespassing is known to occur (NPS unpublished data). Several management actions were identified to address this hypothesis, including increase enforcement of a drone ban (A2), focus visitation in less sensitive areas (A3), increase public education and outreach on disturbance impacts (A4), increase enforcement of closures (A5), and increase signage of closures (A6). Some of these actions are one-off actions (A3, A6) while others would require ongoing management effort (A2, A4, A5; Appendix 5.2).

The remaining highest priority hypotheses were more sensitive to between-expert variation. The Native Predators Hypothesis (H5) was robust for two species (ASSP, WSPL), but highly sensitive to between-expert variation for three species (BRPE, SCMU, WEGU) and moderately sensitive for one (CAAU). Native predator species such as the Common Raven (*Corvus corax*) and Island Spotted Skunk (*Spilogale gracilis amphiala*) are documented predators for ASSP (McIver et al. 2018) and SCMU (NPS unpublished data). Egg predation via the endemic island deer mice (*Peromyscus maniculatus*) is a major cause of reduced nest success for SCMU, enough to cause a declining population growth rate in drought years when nest

predation is increased (Thomsen and Green 2018). Experts identified several relevant management actions: install predator-proof artificial habitat (A11), remove known predators (A12), and remove mammalian predators from breeding colonies (A13). For each of these actions, CHIS has the management authority to manage the threat and there are precedents for effectively managing the threat. Action A11 is a one-off action, but A12 and A13 would require ongoing effort by CHIS (Appendix 5.2).

The priority ranking of the Invasive Plants Hypothesis (H12) was robust for two species (BRPE, WSPL) and highly sensitive (ASSP) or moderately sensitive (CAAU, SCMU) to between-expert variation for others (note that it was a medium priority threat hypothesis and highly sensitive for WEGU). In recent decades, CHIS has undertaken extensive habitat restoration efforts to combat invasive plant species, including the targeted removal (A21, reduce cover of invasive plant species) of iceplant (*Mesembryanthemum* and *Carpobrotus* spp.) and Cape Ivy (*Delairea odorata*) at Anacapa Island and several acres of native habitat restoration (A22, restore native habitat; Appendix 5.2) on East Anacapa and Santa Barbara islands (NPS unpublished data). However, the impact of these efforts on seabird demography has not been quantified and effectively managing invasive plants as a threat requires persistent, ongoing action.

Another anticipated future threat that was a highest priority across all priority species was the New Invasive Species Hypothesis (H14). It was moderately sensitive for most species (ASSP, BRPE, CAAU, SCMU, WEGU) and robust for one (WSPL) to between-expert variation. A single management action was identified for this hypothesis: increase biosecurity measures and monitoring (A27; Appendix 5.2). Biosecurity programs exist across the Channel Islands (Boser et al. 2014, Matos et al. 2018) and a joint biosecurity program was developed between

CHIS, The Nature Conservancy, and the U.S. Navy in 2014 to prevent, detect, and respond to new non-native species introductions. Biosecurity requires sustained, ongoing effort.

Finally, the Disease Hypothesis (H27) was most sensitive to between-expert variation across species (highly sensitive for ASSP, CAAU, SCMU, WEGU, WSPL and moderately sensitive for BRPE). To date, there are no documented major seabird disease outbreaks at CHIS, but in recent years, highly pathogenic avian influenza (HPAI) has emerged as a major threat to wild birds in North America (Ramey et al. 2022). High mortality rates have been observed for Northern Gannets (*Morus bassanus*) in eastern Canada (Avery-Gomm et al. 2024), Peruvian Pelicans (*Pelecanus thagus*) in Peru (Leguia et al. 2023), Sandwich Terns (*Thalasseus sandvicensis*) in northwestern Europe (Knief et al. 2024), and elsewhere. We identified one potential management action to address this threat, to administer HPAI vaccinations (A40; Appendix 5.2), but at present there is no widely available vaccine specifically approved for use in wild seabirds.

CVOI consistently had higher variance across all species and hypotheses as compared to *reducibility*. This higher variance could in part be due to the greater complexity of CVOI, given that it requires judgements across three components (*relevance (a)*, *relevance (b)*, and *magnitude of uncertainty*). However, it also suggests a lack of consensus and greater uncertainty regarding the impact of current and anticipated future threats on priority species and the ability to address them via management actions as compared to the feasibility of reducing uncertainty regarding the validity of the hypotheses.

A novel aspect of our analysis was our exploration of the impact of *personal confidence* on expert judgements regarding CVOI and *reducibility*. We elicited *personal confidence* scores for each species and hypothesis from experts because some expressed discomfort in their

expertise for specific hypotheses and species, and thus a desire to caveat their responses. Most research on expert judgement has focused on the role of overconfidence, such as the tendency of those who exhibit high *personal confidence* to overinflate their ability and be less inclined to seek or value alternative expert judgments (e.g., Kruger and Dunning 1999), or the tendency of people to underestimate their uncertainty (e.g., Soll and Klayman 2004). Methods exist to allow experts to express uncertainty in their quantitative judgments, such as the four-point elicitation format (Speirs-Bridge et al. 2010, Hemming et al. 2018), which asks experts to provide a lower plausible bound, an upper plausible bound, a best estimate, and a degree of belief, and can be used to calculate a statistical distribution. Currently, best practices for eliciting expert uncertainty in CVOI applications are not described, and special challenges exist in expressing uncertainty on a constructed scale. Our approach was to evaluate whether weighting responses by *personal confidence* influenced our outcomes. On average, our experts rated themselves as moderately confident in their responses and we were able to identify areas where experts were least confident in their judgment, which may suggest gaps in expertise in our selection of experts. The generally inconsistent patterns in how weighting responses by *personal confidence* affected our results suggests that gaps occur around specific interactions between threats and species, rather than for a particular threat or a particular species.

Our analysis contributes to the conservation of marine avifauna at CHIS by assessing the numerous hypothesized threats to species and identifying those which are most beneficial to address to conserve priority species as well as other sympatric species. We recognize that funding is limited to initiate additional research and monitoring at CHIS, but when resources do become available, knowing how to allocate will be critical. Because the scope of the analysis and results extends across the California Channel Islands, we encourage CHIS to partner with other

land managers within the archipelago to develop a comprehensive seabird conservation strategy and seek funding collaboratively. While the scope of the analysis was geographically limited, we believe results are relevant to similar ecosystems and this framework can be adapted for application in other regions to enhance global seabird conservation efforts. Finally, our work advances the CVOI literature by providing a case study on its use for conservation planning in a multi-species context while also considering the role of *personal confidence* of experts on our results.

5.6 Acknowledgements

We are grateful for support from the U.S. Geological Survey Natural Resources Preservation Program for this work. We thank the workshop participants and experts listed in Appendix 5.1 and Table 5.3 for their time, knowledge, insights, and contributions. We also thank Hannah Sipe for her contributions, guidance, and review of this chapter. Any use of trade, firm, or product names is for descriptive purposes only and does not imply endorsement by the U.S. Government.

5.7 References

Avery-Gomm, S., T. Barychka, M. English, R. A. Ronconi, S. I. Wilhelm, J. Rail, T. Cormier, M. Beaumont, C. Bowser, T. V. Burt, S. M. Collins, S. Duffy, J. A. Giacinti, S. Gilliland, J. Giroux, C. Gjerdrum, M. Guillemette, K. E. Hargan, M. Jones, A. Kennedy, L. Kusalik, S. Lair, A. Lang, R. A. Lavoie, C. Lepage, G. McPhail, W. A. Montevecchi, G. J. Parsons, J. F. Provencher, I. Rahman, G. J. Robertson, Y. Seyer, C. Soos, C. R. E. Ward, R. Wells, and J. Wight. 2024. Wild bird mass mortalities in eastern Canada associated with the Highly Pathogenic Avian Influenza A(H5N1) virus, 2022. Ecosphere 15:e4980.

Boser, C. L., C. Cory, K. R. Faulkner, J. M. Randall, J. J. Knapp, and S. A. Morrison. 2014. Strategies for biosecurity on a nearshore island in California. Monographs of the Western North American Naturalist 7:412–420.

Cameron, J. L., R. Sauvajot, D. Kamradt, and L. Lee. 2005. Mediterranean Coast Network Vital Signs Monitoring Plan. National Park Service. 102 pp.

Canessa, S., G. Guillera-Arroita, J. J. Lahoz-Monfort, D. M. Southwell, D. P. Armstrong, I. Chadès, R. C. Lacy, and S. J. Converse. 2015. When do we need more data? A primer on calculating the value of information for applied ecologists. Methods in Ecology and Evolution 6:1219–1228.

Dias, M. P., R. Martin, E. J. Pearmain, I. J. Burfield, C. Small, R. A. Phillips, O. Yates, B. Lascelles, P. G. Borboroglu, and J. P. Croxall. 2019. Threats to seabirds: A global assessment. Biological Conservation 237:525–537.

Garrard, G. E., S. A. Bekessy, and M. A. McCarthy. 2017. Rapid prototyping for conservation decision making. Pages 46–55 in V. Maltby, J. R. Bennett, and G. S. Cumming, editors.

Solution scanning in conservation: A decision support toolkit. Cambridge University Press.

Hammond, J. S., R. L. Keeney, and H. Raiffa. 1999. Smart choices: A practical guide to making better decisions. Harvard Business School Press.

Hemming, V., M. A. Burgman, A. M. Hanea, M. F. McBride, and B. C. Wintle. 2018. A practical guide to structured expert elicitation using the IDEA protocol. Methods in Ecology and Evolution 9:169–180.

Hemming, V., A. E. Camaclang, M. S. Adams, M. Burgman, K. Carbeck, J. Carwardine, I. Chadès, L. Chalifour, S. J. Converse, L. N. K. Davidson, G. E. Garrard, R. Finn, J. R. Fleri, J. Huard, H. J. Mayfield, E. M. Madden, I. Naujokaitis-Lewis, H. P. Possingham, L. Rumpff, M. C. Runge, D. Stewart, V. J. D. Tulloch, T. Walshe, and T. G. Martin. 2022. An introduction to decision science for conservation. Conservation Biology 36:e13868.

Holmes, N. D., R. Griffiths, M. Pott, A. Alifano, D. Will, A. S. Wegmann, and J. C. Russell. 2015. Factors associated with rodent eradication failure. Biological Conservation 185:8–16.

Howald, G., C. J. Donlan, K. R. Faulkner, S. Ortega, H. Gellerman, D. A. Croll, and B. R. Tershy. 2010. Eradication of black rats Rattus rattus from Anacapa Island. Oryx 44:30–40.

Howard, J. A., A. J. DuVall, D. M. Pereksta, D. M. Mazurkiewicz, A. J. Searcy, P. J. Capitolo, and T. M. Russell. 2024. Northern breeding range expansion of two Sula species at Sutil Island, California, USA. Western North American Naturalist 84(3):223–231.

Hunt, G. L., Jr., R. L. Pitman, and H. L. Jones. 1980. Distribution and abundance of seabirds breeding on the California Channel Islands. Pages 443–459 in D. M. Power, editor. The California Islands: Proceedings of a multidisciplinary symposium. Santa Barbara Museum of Natural History, Santa Barbara, California.

Ingram, T., D. B. Lewis, F. Gress, G. L. Hunt, Jr., and D. W. Anderson. 1983. Seabird Monitoring Handbook, Channel Islands National Park. Unpublished report, University of California, Irvine, California.

Jones, H. P., B. R. Tershy, E. S. Zavaleta, D. A. Croll, B. S. Keitt, M. E. Finkelstein, and G. R. Howald. 2008. Severity of the effects of invasive rats on seabirds: a global review. Conservation Biology 22:16–26.

Kelsey, E. C., J. J. Felis, M. Czapanskiy, D. M. Pereksta, and J. Adams. 2018. Collision and displacement vulnerability to offshore wind energy infrastructure among marine birds of the Pacific Outer Continental Shelf. Journal of Environmental Management 227:229–247.

Knief, U., T. Bregnballe, I. Alfarwi, M. Z. Ballmann, A. Brenninkmeijer, S. Bzoma, A. Chabrolle, J. Dimmlich, E. Engel, R. Fijn, K. Fischer, B. Hälterlein, M. Haupt, V. Hennig, C. Herrmann, R. in ‘t Veld, E. Kirchhoff, M. Kristersson, S. Kühn, K. Larsson, R. Larsson, N. Lawton, M. Leopold, S. Lilipaly, L. Lock, R. Marty, H. Matheve, W. Meissner, P. Morrison, S. Newton, P. Olofsson, F. Packmor, K. T. Pedersen, C. Redfern, F. Scarton, F. Schenk, O. Scher, L. Serra, A. Sibille, J. Smith, W. Smith, J. Sterup, E. Stienen, V. Strassner, R. G. Valle, R. S. A. van Bemmelen, J. Veen, M. Vervaeke, E. Weston, M. Wojcieszek, and W. Courtens. 2024. Highly pathogenic avian influenza

causes mass mortality in Sandwich Tern Thalasseus sandvicensis breeding colonies across north-western Europe. Bird Conservation International 34:e6.

Kruger, J., and D. Dunning. 1999. Unskilled and unaware of it: How difficulties in recognizing one's own incompetence lead to inflated self-assessments. Journal of Personality and Social Psychology 77:1121–1134.

Lawson, A. J., K. Kalasz, M. C. Runge, A. C. Schwarzer, M. L. Stantial, M. Woodrey, and J. E. Lyons. 2023. Application of qualitative value of information to prioritize uncertainties about Eastern Black Rail population recovery. Conservation Science and Practice 5:e12732.

Leguia, M., A. Garcia-Glaessner, B. Muñoz-Saavedra, D. Juarez, P. Barrera, C. Calvo-Mac, J. Jara, W. Silva, K. Ploog, L. Amaro, P. Colchao-Claux, C. K. Johnson, M. M. Uhart, M. I. Nelson, and J. Lescano. 2023. Highly pathogenic avian influenza A (H5N1) in marine mammals and seabirds in Peru. Nature Communications 14:5489.

Lewis, D. B., F. Gress, T. Ingram, G. L. Hunt, Jr., and D. W. Anderson. 1988. Seabird Monitoring Handbook, Channel Islands National Park. Unpublished report, Channel Islands National Park, Ventura, California.

Matos, J., A. Little, K. Broome, E. Kennedy, F. A. M. Sánchez, M. Latofski-Robles, R. Irvine, C. Gill, A. Espinoza, G. Howald, K. Olthof, M. Ball, and C. L. Boser. 2018. Connecting island communities on a global scale: Case studies in island biosecurity. Western North American Naturalist 78:959–972.

McIver, W. R., H. R. Carter, A. L. Harvey, D. M. Mazurkiewicz, J. A. Howard, P. L. Martin, and J. W. Mason. 2018. Avian and skunk predation of Ashy Storm-Petrels at Santa Cruz Island, California. Western North American Naturalist 78:421–440.

Paleczny, M., E. Hammill, V. Karpouzi, and D. Pauly. 2015. Population trend of the world's monitored seabirds, 1950–2010. PLOS ONE 10:e0129342.

Pascal, M., O. Lorvelec, V. Bretagnolle, and J.-M. Culioli. 2008. Improving the breeding success of a colonial seabird: a cost–benefit comparison of the eradication and control of its rat predator. Endangered Species Research 4:267–276.

R Core Team. 2024. R: A language and environment for statistical computing. R Foundation for Statistical Computing, Vienna, Austria.

Ramey, A. M., N. J. Hill, T. J. DeLiberto, S. E. J. Gibbs, M. C. Hopkins, A. S. Lang, R. L. Poulson, D. J. Prosser, J. M. Sleeman, D. E. Stallknecht, and X.-F. Wan. 2022. Highly pathogenic avian influenza is an emerging disease threat to wild birds in North America. The Journal of Wildlife Management 86:e22171.

Regan, H. M., M. Colyvan, and M. A. Burgman. 2002. A taxonomy and treatment of uncertainty for ecology and conservation biology. Ecological Applications 12:618–628.

Runge, M. C., S. J. Converse, and J. E. Lyons. 2011. Which uncertainty? Using expert elicitation and expected value of information to design an adaptive program. Biological Conservation 144:1214–1223.

Runge, M. C., S. J. Converse, J. E. Lyons, and D. R. Smith, editors. 2020. Structured decision making: case studies in natural resource management. Johns Hopkins University Press, Baltimore, Maryland.

Runge, M. C., C. S. Rushing, J. E. Lyons, and M. A. Rubenstein. 2023. A simplified method for value of information using constructed scales. Decision Analysis 20:220–230. https://doi.org/10.1287/deca.2023.0474.

Rushing, C. S., M. Rubenstein, J. E. Lyons, and M. C. Runge. 2020. Using value of information to prioritize research needs for migratory bird management under climate change: a case study using federal land acquisition in the United States. Biological Reviews 95:1109–1130.

Sipe, H.A., 2023. Exploring complexity, uncertainty, and risk in avian reintroduction decisions through structured decision making. PhD dissertation, University of Washington, Seattle, Washington, USA.

Soll, J. B., and J. Klayman. 2004. Overconfidence in interval estimates. Journal of Experimental Psychology: Learning, Memory, and Cognition 30:299–314.

Speirs-Bridge, A., F. Fidler, M. McBride, L. Flander, G. Cumming, and M. Burgman. 2010. Reducing overconfidence in the interval judgments of experts. Risk Analysis 30:512–523.

Stantial, M. L., A. J. Lawson, A. M. V. Fournier, P. J. Kappes, C. S. Kross, M. C. Runge, M. S. Woodrey, and J. E. Lyons. 2023. Qualitative value of information provides a transparent and repeatable method for identifying critical uncertainty. Ecological Applications 33:e2824.

Thomsen, S. K., and D. J. Green. 2019. Predator-mediated effects of severe drought associated with poor reproductive success of a seabird in a cross-ecosystem cascade. Global Change Biology 25:1642–1652.

U.S. Fish and Wildlife Service. 1993. Endangered and threatened wildlife and plants; determination of threatened status for the Pacific Coast population of the western snowy plover. Federal Register 58:12864–12874.

Williams, B. K., and F. A. Johnson. 2015. Value of information and natural resources decision-making. Wildlife Society Bulletin 39:488–496.

5.8 Tables and Figures

Table 5.1 Breeding marine species at Channel Islands National Park. Species are noted with an X if they were included in the original 1983 monitoring plan as well as if they were selected as a priority species due to their conservation status for this analysis.

Common name	Alpha code	Scientific name	Breeding status	1983 plan	Priority species
Ashy Storm-Petrel	ASSP	*Hydrobates homochroa*	Confirmed		X
Black Oystercatcher	BLOY	*Haematopus bachmani*	Confirmed		
Black Storm-Petrel	BLSP	*Hydrobates melania*	Confirmed		
Blue-footed Booby	BFBO	*Sula nebouxii*	Confirmed		
Brandt's Cormorant	BRAC	*Urile penicillatus*	Confirmed		
California Brown Pelican	BRPE	*Pelecanus occidentalis californicus*	Confirmed	X	X
Cassin's Auklet	CAAU	*Ptychoramphus aleuticus*	Confirmed	X	X
Cocos Booby	COBO	*Sula brewsteri*	Confirmed		
Common Murre	COMU	*Uria aalge*	Confirmed		
Double-Crested Cormorant	DCCO	*Nannopterum auritus*	Confirmed	X	
Guadalupe Murrelet	GUMU	*Synthliboramphus hypoleucus*	Confirmed		
Leach's Storm-Petrel	LHSP	*Hydrobates leucorhous*	Confirmed		
Pelagic Cormorant	PECO	*Urile pelagicus*	Confirmed	X	
Pigeon Guillemot	PIGU	*Cepphus columba*	Confirmed		
Rhinoceros Auklet	RHAU	*Cerorhinca monocerata*	Suspected/ Historic		
Scripps's Murrelet	SCMU	*Synthliboramphus scrippsi*	Confirmed	X	X
Tufted Puffin	TUPU	*Fratercula cirrhata*	Historic		
Western Gull	WEGU	*Larus occidentalis*	Confirmed	X	X
Western Snowy Plover	WSPL	*Anarhynchus nivosus nivosus*	Confirmed	X	X

Table 5.2 Alternative threat hypotheses (n = 28) evaluated for six priority species across eight threat categories. Each hypothesis is identified by a number and includes the hypothesized driver(s) of population change.

Hypothesis number	Hypothesis name	Hypothesis description
Disturbance		
1	Overflights	Low overflights disturb breeding colonies and reduce reproductive success.
2	Recreation	Recreation causes disturbance to breeding colonies and reduces reproductive success.
Fisheries		
3	Fishery Equipment	Commercial and recreational fishery equipment entangles/entraps individuals and reduces juvenile survival and/or adult survival.
4	Overfishing	Overfishing from commercial and recreational fisheries reduces foraging availability and/or quality, which reduces reproductive success, juvenile survival and/or adult survival.
Harmful native species interactions		
5	Native Predators	Native predators (island deer mouse, island spotted skunk, island fox, common raven, barn owl, peregrine falcon) predate eggs, chicks, and/or breeding adults, which reduces reproductive success and/or adult survival.
6	Pinnipeds	Pinnipeds displace breeding habitat and/or reduce breeding habitat quality, which reduces reproductive success.
7	Seabird Colonization	Colonization of new seabird species increases competition for breeding habitat and/or prey, which reduces reproductive success.
Human infrastructure		
8	Oil Platforms	Oil platforms increase predation risk by creating at-sea roosting habitat for aerial predators, which reduces juvenile survival and/or adult survival.
9	Offshore Wind	Offshore wind energy infrastructure displaces foraging habitat and/or increases collision risk, which reduces reproductive success, juvenile survival and/or adult survival.

10	Shipping Traffic	Shipping traffic displaces foraging habitat and reduces reproductive success.
11	Artificial Light	Artificial light at night exposes individuals to novel predation and/or increases collision risk with structures, which reduces juvenile survival and/or adult survival.
Invasive species		
12	Invasive Plants	Invasive plants decrease the breeding habitat availability and/or quality, which reduces reproductive success and/or adult survival via increased predation risk.
13	Black Rats	Black rats predate eggs and chicks at San Miguel Island, which reduces reproductive success.
14	New Invasive Species	New introductions of invasive and non-native animals predate eggs, chicks, and/or breeding adults, which reduces reproductive success and/or adult survival.
Pollution		
15	Oil Spills	Oil spills on foraging grounds increase fouling risk, which reduces juvenile survival and/or adult survival.
16	Residual DDT	Residual DDT in the marine environment bioaccumulates/biomagnifies in the foraging food web, which decreases eggshell thickness and reduces reproductive success.
17	Contaminants	Contaminants (heavy metals, microplastics, macroplastics) accumulate in foraging food webs, which reduces reproductive success, juvenile survival and/or adult survival.
Projected climate change impacts		
18	Sea Level Rise	Sea level rise reduces breeding habitat availability and/or quality, which reduces reproductive success.
19	Marine Productivity	Decreased marine productivity impacts abundance and distribution of prey, which reduces reproductive success, juvenile survival and/or adult survival.
20	Sea Surface Temperature	Increased sea surface temperatures impact abundance and distribution of prey, which reduces reproductive success, juvenile survival and/or adult survival.

21	Precipitation	Altered precipitation regimes reduce native plant breeding habitat availability and/or quality, which reduces reproductive success and/or adult survival via increased predation risk.
22	Ambient Temperature	Increased ambient temperatures lead to higher rates of heat stress, which reduces reproductive success.
23	Marine Heat Waves	Marine heat waves (periods of usually five days or more of warmer sea-surface temperatures than the 90th percentile) alter prey abundance and distribution, which reduces reproductive success, juvenile survival and/or adult survival.
24	Storm Events	Increased frequency and severity of storm events reduce breeding habitat availability and/or quality, which reduces reproductive success and/or adult survival via increased predation risk.
25	Wind	Altered wind regimes reduce foraging efficacy, which reduces reproductive success, juvenile survival and/or adult survival.
Toxins/diseases/parasites		
26	Harmful Algal Blooms	Harmful algal blooms, which produce the neurotoxins domoic acid and saxitoxin, reduce juvenile survival and/or adult survival.
27	Disease	Disease outbreaks, such as highly pathogenic avian influenza (HPAI), reduce reproductive success, juvenile survival and/or adult survival.
28	Parasites	Parasite loading reduces reproductive success, juvenile survival and/or adult survival.

Table 5.3. Experts that participated in expert elicitation (n = 12). Four individuals did not attend the November 2022 workshop.

Name	Position	Organization
Dan Robinette	Senior Biologist/Coastal Program Leader	Point Blue Conservation Science
David Mazurkiewicz	Wildlife Biologist	Channel Islands National Park
David Pereksta	Avian Biologist	Bureau of Ocean Energy Management
Jim Howard	Seabird Biologist	California Institute of Environmental Studies
Josh Adams [a]	Research Ecologist	Western Research Ecological Center, U.S. Geological Survey
Katy Carter [a]	Operations and Development Manager	California Institute of Environmental Studies
Marc Romano	Coordinator	Pacific Seabird Program, U.S. Fish and Wildlife Service
Mike Johns [a]	Senior Marine Ecologist	Point Blue Conservation Science
Mike Parker	Executive Director	California Institute of Environmental Studies
Nick Holmes	Lead Scientist	The Nature Conservancy
Russell Bradley	Director	Santa Rosa Island Research Center, California State University Channel Islands
Yuliana Bedolla [a]	Director of the Marine Birds Project	Grupo de Ecología y Conservación de Islas

[a] Did not attend November 2022 workshop.

Table 5.4 Scoring rubric for *relevance (a)*, *relevance (b)*, *magnitude of uncertainty*, and *reducibility* for constructed value of information (CVOI) expert elicitation. *Relevance* is calculated as *relevance (a)* multiplied by *relevance (b)* and rescaled to 0 – 4. CVOI is the product of *magnitude of uncertainty* and *relevance*. We also include a scoring rubric for *personal confidence*.

Relevance (a)	
If this hypothesis is true, how much of an impact is it having on the population? Consider 1) the extent of the threat on the hypothesized demographic parameter(s), 2) the sensitivity of population trend to the hypothesized demographic parameters, and 3) the overall effect, given 1 and 2, on the population trend (i.e., the mean rate of growth or decline in the population across time). Answer conditional on levels of the threat over the coming 30 years when evaluating this. For threats that are potential (i.e., are not currently present), score this question as the threat risk, which is the product of the likelihood of the threat occurring and the potential magnitude of its impact.	
0	Even if true, this hypothesis has no to very little impact on the population.
1	If true, this hypothesis has a small to moderate impact on the population, with an impact that is approximately 25% compared to the total range of variability in population trend.
2	If true, this hypothesis has a moderate impact on the population, with an impact that is approximately 50% compared to the total range of variability in population trend.
3	If true, this hypothesis has a moderate to large impact on the population, with an impact that is approximately 75% compared to the total range of variability in population trend.
4	If true, this hypothesis has a large impact on the population, with an impact as large as the total range of variability in population trend.
Relevance (b)	
If this hypothesis is true, what is the potential of management actions, listed or otherwise, to reduce the effect of this hypothesis on the population? Consider the availability of management actions (listed or otherwise) to address the threat as well as the likelihood that management actions would/could be fully and effectively implemented.	
0	Management actions will have no to very little impact on the hypothesized effect.
1	Management actions will reduce the hypothesized effect on the population by approximately 25%.
2	Management actions will reduce the hypothesized effect on the population by approximately 50%.
3	Management actions will reduce the hypothesized effect on the population by approximately 75%.
4	Management actions will mostly or completely reduce the hypothesized effect.
Magnitude of uncertainty	
How uncertain are you about the validity of this hypothesis? Consider the degree to which you think this hypothesis is currently operating on the population as well as your uncertainty regarding the impact of this threat on the population.	
0	There is little to no uncertainty regarding whether this hypothesis is true or false, based on current knowledge, theory, personal experience, or other rationale.

1	There is low to moderate uncertainty regarding whether this hypothesis is true or false.
2	There is moderate uncertainty regarding whether this hypothesis is true or false.
3	There is moderate to high uncertainty regarding whether this hypothesis is true or false.
4	There is little to no information currently available to discern whether this hypothesis is true or false.
Reducibility	
What is the potential to reduce uncertainty regarding the validity of this hypothesis, i.e., to reduce uncertainty regarding whether this hypothesis is having an effect on the population and to what degree? Consider the costs, logistics, and feasibility of designing an experimental or observational study that could lead to meaningful results within a relevant management timeframe of 30 years. Answer this question independent of the magnitude of uncertainty; in other words, answer this question assuming you do not know the effect of the hypothesis on the population.	
0	The uncertainty about this hypothesis is unlikely to be reduced within a relevant management timeframe due to the expected cost, logistics, and ability to obtain necessary data.
1	The uncertainty about this hypothesis could be reduced by approximately 25% within a relevant management timeframe based on the expected cost, logistics, and ability to obtain necessary data.
2	The uncertainty about this hypothesis could be reduced by approximately 50% within a relevant management timeframe based on the expected cost, logistics, and ability to obtain necessary data.
3	The uncertainty about this hypothesis could be reduced by approximately 75% within a relevant management timeframe based on the expected cost, logistics, and ability to obtain necessary data.
4	The uncertainty about this hypothesis could be mostly or completely reduced within a relevant management timeframe based on the expected cost, logistics, and ability to obtain necessary data.
Personal confidence	
What is your personal level of confidence, given your expertise and experience, in scoring this hypothesis for this particular species?	
0	I am the least confident in my response for this hypothesis and species.
1	I am moderately confident in my response for this hypothesis and species.
2	I am most confident in my response for this hypothesis and species.

Table 5.5 Ashy Storm-Petrel (ASSP): Mean and estimated standard error (SE) for CVOI (constructed value of information; *relevance* * *magnitude of uncertainty*) and *reducibility* and percentage of 1,000 bootstrapped samples falling into each priority quadrat for each threat hypothesis (n = 28). Priority quadrats were assigned based on the median CVOI and *reducibility* scores across hypotheses. NA indicates experts unanimously agreed the hypothesis was not relevant for this species. Highest priority hypothesis names are bolded and italicized (n = 8); bolded percentages represent the priority ranking of each hypothesis.

Hypothesis number	Hypothesis name	CVOI	Reducibility	Percentage of bootstrapped samples in each quadrat			
				Highest priority	High priority	Medium priority	Low priority
1	Overflights	NA	NA	NA	NA	NA	NA
2	***Recreation***	2.73 (0.65)	2.70 (0.20)	**83.20%**	0.00%	16.80%	0.00%
3	Fishery Equipment	3.72 (1.25)	1.68 (0.38)	13.80%	**76.30%**	1.20%	8.70%
4	Overfishing	5.36 (1.69)	1.63 (0.34)	10.70%	**87.20%**	0.30%	1.80%
5	***Native Predators***	4.53 (1.60)	3.46 (0.24)	**93.60%**	0.00%	6.40%	0.00%
6	Pinnipeds	NA	NA	NA	NA	NA	NA
7	Seabird Colonization	1.53 (0.68)	1.25 (0.29)	0.00%	18.60%	0.00%	**81.40%**
8	Oil Platforms	2.68 (1.44)	1.87 (0.26)	15.30%	**47.20%**	8.70%	28.80%
9	***Offshore Wind***	7.92 (1.41)	2.55 (0.20)	**100.00%**	0.00%	0.00%	0.00%
10	Shipping Traffic	2.15 (1.00)	1.68 (0.44)	8.50%	38.80%	10.20%	**42.50%**
11	Artificial Light	5.16 (2.13)	2.01 (0.26)	43.60%	**49.50%**	3.40%	3.50%
12	***Invasive Plants***	2.40 (0.86)	2.57 (0.19)	**61.30%**	0.00%	38.70%	0.00%
13	***Black Rats***	10.00 (3.01)	3.00 (0.35)	**99.10%**	0.70%	0.20%	0.00%
14	***New Invasive Species***	5.31 (2.52)	2.68 (0.36)	**84.10%**	4.50%	11.10%	0.30%
15	Oil Spills	0.91 (0.63)	1.67 (0.37)	0.70%	4.60%	13.50%	**81.20%**
16	Residual DDT	1.19 (0.76)	2.54 (0.43)	10.60%	1.40%	**76.70%**	11.30%
17	Contaminants	2.17 (1.06)	1.83 (0.28)	10.40%	**38.70%**	11.70%	39.20%
18	***Sea Level Rise***	3.35 (1.36)	2.28 (0.28)	**64.60%**	15.90%	15.60%	3.90%
19	Marine Productivity	0.00 (0.00)	1.92 (0.32)	0.00%	0.00%	34.80%	**65.20%**
20	Sea Surface Temperature	0.00 (0.00)	2.08 (0.29)	0.00%	0.00%	**55.80%**	44.20%
21	Precipitation	0.35 (0.32)	2.03 (0.70)	0.00%	0.00%	**26.10%**	73.90%

22	Ambient Temperature	1.49 (0.76)	2.33 (0.46)	16.30%	5.50%	**54.00%**	24.20%
23	Marine Heat Waves	0.00 (0.00)	2.18 (0.31)	0.00%	0.00%	**66.40%**	33.60%
24	Storm Events	3.27 (1.63)	1.93 (0.36)	27.50%	**46.00%**	9.20%	17.30%
25	Wind	0.00 (0.00)	1.65 (0.26)	0.00%	0.00%	6.90%	**93.10%**
26	Harmful Algal Blooms	1.12 (0.95)	1.46 (0.27)	0.00%	12.90%	1.30%	**85.80%**
27	***Disease***	2.65 (1.04)	2.29 (0.29)	**55.10%**	12.40%	26.40%	6.10%
28	Parasites	0.33 (0.21)	1.78 (0.26)	0.00%	0.00%	14.80%	**85.20%**

Table 5.6 California Brown Pelican (BRPE): Mean and estimated standard error (SE) for CVOI (constructed value of information; *relevance * magnitude of uncertainty*) and *reducibility* and percentage of 1,000 bootstrapped samples falling into each priority quadrat for each threat hypothesis (*n* = 28). Priority quadrats were assigned based on the median CVOI and *reducibility* scores across hypotheses. NA indicates experts unanimously agreed the hypothesis was not relevant for this species. Highest priority hypothesis names are bolded and italicized (*n* = 8); bolded percentages represent the priority ranking of each hypothesis.

Hypothesis number	Hypothesis name	CVOI	Reducibility	Percentage of bootstrapped samples in each quadrat			
				Highest priority	High priority	Medium priority	Low priority
1	***Overflights***	4.78 (1.50)	3.29 (0.29)	**99.30%**	0.10%	0.60%	0.00%
2	***Recreation***	4.95 (1.54)	3.19 (0.21)	**99.60%**	0.00%	0.40%	0.00%
3	***Fishery Equipment***	2.37 (1.00)	2.49 (0.22)	**68.40%**	7.30%	21.30%	3.00%
4	Overfishing	8.29 (2.27)	2.00 (0.26)	20.30%	**79.70%**	0.00%	0.00%
5	***Native Predators***	2.10 (0.93)	2.87 (0.51)	**59.40%**	6.90%	30.50%	3.20%
6	Pinnipeds	0.68 (0.38)	2.67 (0.27)	1.80%	0.00%	**94.50%**	3.70%
7	Seabird Colonization	0.41 (0.28)	2.51 (0.44)	0.00%	0.00%	**67.60%**	32.40%
8	Oil Platforms	1.03 (0.72)	2.00 (0.00)	0.00%	19.50%	0.00%	**80.50%**
9	***Offshore Wind***	6.13 (1.15)	2.83 (0.25)	**99.50%**	0.50%	0.00%	0.00%
10	Shipping Traffic	2.15 (1.03)	1.65 (0.46)	6.20%	**61.70%**	3.30%	28.80%
11	Artificial Light	1.11 (0.54)	1.49 (0.25)	0.00%	16.90%	0.00%	**83.10%**
12	***Invasive Plants***	2.99 (0.65)	2.83 (0.17)	**98.70%**	0.00%	1.30%	0.00%
13	***Black Rats***	4.01 (2.55)	4.00 (0.00)	**89.00%**	0.00%	11.00%	0.00%
14	***New Invasive Species***	6.40 (2.28)	2.61 (0.36)	**85.20%**	13.50%	1.30%	0.00%
15	Oil Spills	1.05 (0.71)	1.82 (0.40)	3.30%	18.00%	13.40%	**65.30%**
16	Residual DDT	0.00 (0.00)	2.68 (0.39)	0.00%	0.00%	**87.60%**	12.40%
17	Contaminants	1.69 (0.74)	2.10 (0.26)	17.90%	**36.90%**	14.40%	30.80%
18	Sea Level Rise	0.83 (0.37)	2.41 (0.55)	1.30%	1.20%	**57.20%**	40.30%
19	Marine Productivity	0.00 (0.00)	2.00 (0.31)	0.00%	0.00%	26.10%	**73.90%**
20	Sea Surface Temperature	0.00 (0.00)	2.16 (0.28)	0.00%	0.00%	44.20%	**55.80%**
21	Precipitation	3.96 (1.70)	2.11 (0.33)	34.80%	**58.50%**	1.90%	4.80%
22	***Ambient Temperature***	1.66 (0.76)	2.28 (0.26)	**28.80%**	20.30%	28.80%	22.10%

23	Marine Heat Waves	0.00 (0.00)	2.00 (0.31)	0.00%	0.00%	23.30%	**76.70%**
24	Storm Events	1.51 (0.58)	2.20 (0.40)	17.10%	25.30%	28.00%	**29.60%**
25	Wind	0.00 (0.00)	1.64 (0.26)	0.00%	0.00%	0.50%	**99.50%**
26	Harmful Algal Blooms	1.20 (0.96)	1.66 (0.30)	0.50%	27.90%	3.40%	**68.20%**
27	***Disease***	2.71 (1.01)	2.65 (0.26)	**80.70%**	4.40%	14.20%	0.70%
28	Parasites	0.51 (0.25)	2.00 (0.24)	0.00%	0.00%	15.10%	**84.90%**

Table 5.7 Cassin's Auklet (CAAU): Mean and estimated standard error (SE) for CVOI (constructed value of information; *relevance* * *magnitude of uncertainty*) and *reducibility* and percentage of 1,000 bootstrapped samples falling into each priority quadrat for each threat hypothesis (n = 28). Priority quadrats were assigned based on the median CVOI and *reducibility* scores across hypotheses. NA indicates experts unanimously agreed the hypothesis was not relevant for this species. Highest priority hypothesis names are bolded and italicized (n = 8); bolded percentages represent the priority ranking of each hypothesis.

Hypothesis number	Hypothesis name	CVOI	Reducibility	Percentage of bootstrapped samples in each quadrat			
				Highest priority	High priority	Medium priority	Low priority
1	Overflights	NA	NA	NA	NA	NA	NA
2	***Recreation***	3.71 (0.77)	2.31 (0.33)	**62.80%**	32.20%	3.50%	1.50%
3	Fishery Equipment	3.01 (0.74)	1.78 (0.46)	15.40%	**62.10%**	3.70%	18.80%
4	Overfishing	5.08 (1.59)	1.56 (0.39)	4.10%	**92.20%**	0.30%	3.40%
5	***Native Predators***	3.88 (1.30)	2.89 (0.35)	**84.90%**	3.00%	11.80%	0.30%
6	Pinnipeds	0.37 (0.22)	3.02 (0.48)	0.00%	0.00%	**96.30%**	3.70%
7	Seabird Colonization	1.73 (0.68)	1.16 (0.36)	0.00%	16.30%	0.00%	**83.70%**
8	Oil Platforms	2.69 (1.43)	1.88 (0.27)	7.20%	**48.50%**	5.30%	39.00%
9	***Offshore Wind***	5.03 (1.53)	2.45 (0.23)	**86.60%**	9.70%	3.60%	0.10%
10	Shipping Traffic	2.39 (1.03)	1.48 (0.45)	3.20%	41.00%	3.30%	**52.50%**
11	Artificial Light	6.04 (1.85)	1.90 (0.26)	16.40%	**81.70%**	0.50%	1.40%
12	***Invasive Plants***	3.55 (1.09)	2.54 (0.24)	**76.30%**	7.00%	15.40%	1.30%
13	***Black Rats***	7.82 (2.48)	3.12 (0.38)	**98.70%**	0.90%	0.40%	0.00%
14	***New Invasive Species***	6.75 (2.86)	2.72 (0.40)	**85.10%**	10.50%	4.10%	0.30%
15	Oil Spills	1.02 (0.65)	1.62 (0.40)	0.10%	2.50%	6.90%	**90.50%**
16	Residual DDT	1.48 (0.71)	2.48 (0.43)	8.60%	1.90%	**69.30%**	20.20%
17	Contaminants	2.77 (1.29)	2.11 (0.35)	25.90%	**35.10%**	19.30%	19.70%
18	Sea Level Rise	2.39 (1.00)	2.49 (0.34)	38.00%	7.10%	**43.60%**	11.30%
19	Marine Productivity	0.00 (0.00)	2.18 (0.33)	0.00%	0.00%	**45.50%**	54.50%
20	Sea Surface Temperature	0.00 (0.00)	2.27 (0.32)	0.00%	0.00%	**56.20%**	43.80%
21	Precipitation	2.49 (1.00)	2.15 (0.33)	22.00%	**24.50%**	24.50%	29.00%
22	Ambient Temperature	1.98 (0.69)	2.37 (0.35)	16.50%	7.50%	**52.30%**	23.70%

23	Marine Heat Waves	0.00 (0.00)	2.28 (0.30)	0.00%	0.00%	**56.10%**	43.90%
24	Storm Events	2.92 (1.14)	2.01 (0.39)	22.40%	**40.90%**	12.60%	24.10%
25	Wind	0.00 (0.00)	1.70 (0.28)	0.00%	0.00%	5.30%	**94.70%**
26	Harmful Algal Blooms	1.15 (0.95)	1.52 (0.29)	0.20%	6.60%	1.20%	**92.00%**
27	***Disease***	2.67 (1.07)	2.39 (0.29)	**44.40%**	12.10%	34.30%	9.20%
28	Parasites	0.36 (0.23)	1.75 (0.29)	0.00%	0.00%	6.10%	**93.90%**

Table 5.8 Scripps's Murrelet (SCMU): Mean and estimated standard error (SE) for CVOI (constructed value of information; *relevance * magnitude of uncertainty*) and *reducibility* and percentage of 1,000 bootstrapped samples falling into each priority quadrat for each threat hypothesis (n = 28). Priority quadrats were assigned based on the median CVOI and *reducibility* scores across hypotheses. NA indicates experts unanimously agreed the hypothesis was not relevant for this species. Highest priority hypothesis names are bolded and italicized (n = 8); bolded percentages represent the priority ranking of each hypothesis.

Hypothesis number	Hypothesis	CVOI	Reducibility	Percentage of bootstrapped samples in each quadrat			
				Highest priority	High priority	Medium priority	Low priority
1	Overflights	NA	NA	NA	NA	NA	NA
2	***Recreation***	3.65 (0.81)	2.30 (0.25)	**84.40%**	7.30%	8.00%	0.30%
3	Fishery Equipment	3.73 (0.96)	1.59 (0.36)	14.40%	**75.50%**	1.50%	8.60%
4	Overfishing	6.50 (1.60)	1.79 (0.31)	31.00%	**68.90%**	0.00%	0.10%
5	***Native Predators***	3.47 (1.35)	3.26 (0.30)	**74.10%**	0.00%	25.90%	0.00%
6	Pinnipeds	0.24 (0.17)	2.00 (0.00)	0.00%	0.00%	**100.00%**	0.00%
7	Seabird Colonization	2.14 (0.97)	1.25 (0.34)	0.60%	31.10%	2.30%	**66.00%**
8	Oil Platforms	2.86 (1.45)	1.89 (0.25)	23.20%	**31.70%**	18.10%	27.00%
9	***Offshore Wind***	7.43 (1.29)	2.64 (0.24)	**100.00%**	0.00%	0.00%	0.00%
10	Shipping Traffic	2.15 (1.01)	1.67 (0.46)	9.00%	23.20%	21.10%	**46.70%**
11	***Artificial Light***	5.11 (1.90)	2.08 (0.24)	**66.20%**	26.20%	5.60%	2.00%
12	***Invasive Plants***	3.78 (1.58)	2.50 (0.19)	**77.00%**	0.10%	22.90%	0.00%
13	***Black Rats***	9.17 (2.54)	2.90 (0.32)	**99.90%**	0.10%	0.00%	0.00%
14	***New Invasive Species***	7.38 (3.33)	2.57 (0.37)	**89.60%**	4.60%	5.40%	0.40%
15	Oil Spills	1.34 (0.98)	1.67 (0.39)	2.20%	8.30%	20.50%	**69.00%**
16	Residual DDT	1.52 (1.04)	2.38 (0.39)	10.20%	1.30%	**75.80%**	12.70%
17	Contaminants	2.46 (1.23)	1.90 (0.27)	17.70%	24.70%	25.10%	**32.50%**
18	***Sea Level Rise***	3.13 (1.37)	2.31 (0.25)	**58.50%**	5.10%	33.10%	3.30%
19	Marine Productivity	0.00 (0.00)	1.91 (0.32)	0.00%	0.00%	43.30%	**56.70%**
20	Sea Surface Temperature	0.00 (0.00)	2.16 (0.28)	0.00%	0.00%	**76.40%**	23.60%
21	***Precipitation***	3.42 (1.40)	2.22 (0.27)	**58.20%**	12.00%	25.50%	4.30%
22	Ambient Temperature	1.09 (0.39)	2.00 (0.35)	0.10%	0.00%	54.60%	**45.30%**

23	Marine Heat Waves	0.00 (0.00)	2.17 (0.29)	0.00%	0.00%	**76.60%**	23.40%
24	Storm Events	3.05 (1.45)	1.90 (0.36)	24.20%	**34.90%**	18.50%	22.40%
25	Wind	0.00 (0.00)	1.60 (0.29)	0.00%	0.00%	10.90%	**89.10%**
26	Harmful Algal Blooms	1.03 (0.93)	1.50 (0.29)	0.30%	5.90%	5.70%	**88.10%**
27	***Disease***	2.55 (0.88)	2.27 (0.26)	**41.50%**	4.90%	47.80%	5.80%
28	Parasites	0.34 (0.21)	1.66 (0.27)	0.00%	0.00%	15.70%	**84.30%**

Table 5.9 Western Gull (WEGU): Mean and estimated standard error (SE) for CVOI (constructed value of information; *relevance* * *magnitude of uncertainty*) and *reducibility* and percentage of 1,000 bootstrapped samples falling into each priority quadrat for each threat hypothesis (n = 28). Priority quadrats were assigned based on the median CVOI and *reducibility* scores across hypotheses. NA indicates experts unanimously agreed the hypothesis was not relevant for this species. Highest priority hypothesis names are bolded and italicized (n = 8); bolded percentages represent the priority ranking of each hypothesis.

Hypothesis number	Hypothesis	CVOI	Reducibility	Percentage of bootstrapped samples in each quadrat			
				Highest priority	High priority	Medium priority	Low priority
1	***Overflights***	3.84 (0.93)	3.20 (0.30)	**96.60%**	0.30%	3.10%	0.00%
2	***Recreation***	4.99 (1.60)	3.17 (0.24)	**96.60%**	0.00%	3.40%	0.00%
3	***Fishery Equipment***	2.51 (0.74)	2.33 (0.28)	**50.30%**	22.80%	18.70%	8.20%
4	Overfishing	5.13 (1.20)	2.00 (0.24)	15.50%	**84.40%**	0.00%	0.10%
5	***Native Predators***	2.48 (0.77)	3.12 (0.38)	**68.20%**	0.50%	30.70%	0.60%
6	Pinnipeds	0.82 (0.43)	2.99 (0.35)	0.40%	0.00%	**99.20%**	0.40%
7	Seabird Colonization	1.25 (0.45)	1.35 (0.60)	0.10%	4.20%	8.40%	**87.30%**
8	Oil Platforms	2.33 (0.89)	1.87 (0.27)	7.80%	**52.40%**	4.70%	35.10%
9	***Offshore Wind***	4.99 (1.15)	2.81 (0.28)	**97.80%**	1.80%	0.40%	0.00%
10	Shipping Traffic	1.64 (0.63)	1.66 (0.45)	2.60%	22.30%	7.50%	**67.60%**
11	Artificial Light	3.32 (0.85)	1.87 (0.21)	6.00%	**87.20%**	0.30%	6.50%
12	Invasive Plants	1.99 (0.70)	2.78 (0.21)	43.40%	0.00%	**56.50%**	0.10%
13	***Black Rats***	8.06 (2.27)	2.99 (0.34)	**98.10%**	1.60%	0.30%	0.00%
14	***New Invasive Species***	4.99 (1.67)	2.66 (0.37)	**85.60%**	10.50%	3.50%	0.40%
15	Oil Spills	1.05 (0.70)	1.84 (0.38)	1.60%	6.50%	15.20%	**76.70%**
16	Residual DDT	1.76 (0.97)	2.72 (0.38)	30.50%	3.70%	**58.90%**	6.90%
17	Contaminants	3.14 (1.58)	2.15 (0.29)	29.50%	**44.50%**	11.00%	15.00%
18	Sea Level Rise	0.99 (0.43)	2.39 (0.54)	0.90%	0.30%	**58.00%**	40.80%
19	Marine Productivity	0.00 (0.00)	2.01 (0.31)	0.00%	0.00%	25.00%	**75.00%**
20	Sea Surface Temperature	0.00 (0.00)	2.17 (0.28)	0.00%	0.00%	45.50%	**54.50%**
21	Precipitation	3.39 (1.25)	2.20 (0.28)	37.00%	**48.80%**	5.80%	8.40%
22	***Ambient Temperature***	2.33 (0.83)	2.39 (0.27)	**42.50%**	17.40%	29.60%	10.50%

23	Marine Heat Waves	0.00 (0.00)	2.11 (0.33)	0.00%	0.00%	36.40%	**63.60%**
24	Storm Events	1.97 (0.97)	2.20 (0.45)	22.90%	18.80%	**31.80%**	26.50%
25	Wind	0.00 (0.00)	1.61 (0.29)	0.00%	0.00%	1.00%	**99.00%**
26	Harmful Algal Blooms	1.19 (0.96)	1.74 (0.24)	1.30%	23.30%	1.70%	**73.70%**
27	***Disease***	2.14 (0.88)	2.54 (0.28)	**43.80%**	7.60%	41.70%	6.90%
28	Parasites	0.32 (0.21)	2.11 (0.25)	0.00%	0.00%	29.10%	**70.90%**

Table 5.10 Western Snowy Plover (WSPL): Mean and estimated standard error (SE) for CVOI (constructed value of information; *relevance * magnitude of uncertainty*) and *reducibility* and percentage of 1,000 bootstrapped samples falling into each priority quadrat for each threat hypothesis (*n* = 28). Priority quadrats were assigned based on the median CVOI and *reducibility* scores across hypotheses. NA indicates experts unanimously agreed the hypothesis was not relevant for this species. Highest priority hypothesis names are bolded and italicized (*n* = 8); bolded percentages represent the priority ranking of each hypothesis.

Hypothesis number	Hypothesis	CVOI	Reducibility	Percentage of bootstrapped samples in each quadrat			
				Highest priority	**High priority**	**Medium priority**	**Low priority**
1	***Overflights***	3.07 (1.02)	3.00 (0.37)	**96.90%**	0.80%	2.30%	0.00%
2	***Recreation***	7.23 (1.95)	3.00 (0.19)	**100.00%**	0.00%	0.00%	0.00%
3	Fishery Equipment	0.92 (0.47)	0.67 (0.27)	0.00%	35.10%	0.00%	**64.90%**
4	Overfishing	0.58 (0.37)	1.00 (0.71)	0.00%	8.30%	0.00%	**91.70%**
5	***Native Predators***	5.33 (1.30)	3.17 (0.32)	**99.90%**	0.10%	0.00%	0.00%
6	***Pinnipeds***	2.73 (0.83)	2.81 (0.36)	**96.40%**	1.90%	1.70%	0.00%
7	Seabird Colonization	0.24 (0.24)	2.00 (0.00)	0.00%	0.60%	0.00%	**99.40%**
8	Oil Platforms	0.42 (0.27)	1.32 (0.27)	0.00%	0.80%	0.00%	**99.20%**
9	Offshore Wind	1.07 (0.55)	2.34 (0.27)	29.40%	12.20%	**41.70%**	16.70%
10	Shipping Traffic	0.17 (0.16)	1.00 (0.00)	0.00%	0.00%	0.00%	**100.00%**
11	Artificial Light	1.38 (0.72)	1.76 (0.21)	0.00%	**62.80%**	0.00%	37.20%
12	***Invasive Plants***	2.79 (1.36)	2.90 (0.24)	**91.00%**	0.00%	9.00%	0.00%
13	***Black Rats***	6.26 (2.65)	3.13 (0.41)	**97.30%**	1.20%	1.50%	0.00%
14	***New Invasive Species***	7.44 (3.16)	2.67 (0.37)	**94.20%**	5.40%	0.40%	0.00%
15	Oil Spills	1.62 (1.39)	1.73 (0.41)	14.40%	**49.50%**	7.50%	28.60%
16	Residual DDT	0.33 (0.22)	2.59 (0.40)	0.20%	0.00%	**90.60%**	9.20%
17	Contaminants	1.16 (0.51)	2.00 (0.25)	20.40%	**29.90%**	23.80%	25.90%
18	***Sea Level Rise***	1.67 (0.57)	2.27 (0.30)	**65.60%**	19.40%	12.50%	2.50%
19	Marine Productivity	0.00 (0.00)	1.91 (0.36)	0.00%	0.00%	34.30%	**65.70%**
20	Sea Surface Temperature	0.00 (0.00)	2.00 (0.31)	0.00%	0.00%	44.40%	**55.60%**
21	***Precipitation***	2.21 (1.48)	2.18 (0.36)	**45.90%**	28.80%	14.40%	10.90%
22	Ambient Temperature	0.81 (0.38)	2.19 (0.25)	13.30%	6.80%	**56.90%**	23.00%

23	Marine Heat Waves	0.00 (0.00)	2.12 (0.37)	0.00%	0.00%	**55.00%**	45.00%
24	Storm Events	3.11 (1.46)	1.99 (0.34)	41.10%	**52.50%**	2.90%	3.50%
25	Wind	0.00 (0.00)	1.67 (0.32)	0.00%	0.00%	11.30%	**88.70%**
26	Harmful Algal Blooms	0.57 (0.47)	1.86 (0.32)	3.40%	8.00%	22.00%	**66.60%**
27	***Disease***	1.85 (0.90)	2.45 (0.27)	**72.30%**	5.40%	21.40%	0.90%
28	Parasites	0.17 (0.16)	1.76 (0.35)	0.00%	0.00%	20.50%	**79.50%**

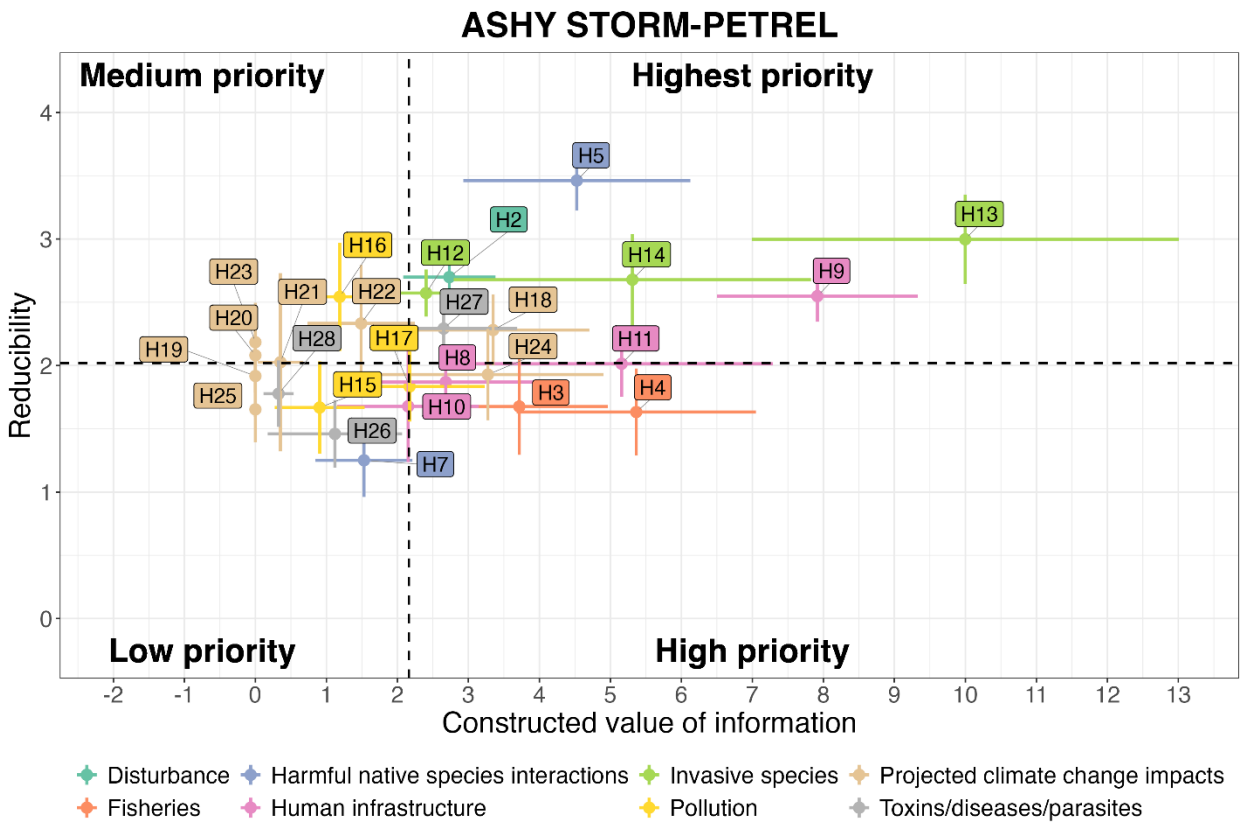

Figure 5.1 Ashy Storm-Petrel (ASSP): Mean CVOI (constructed value of information; x-axis) and *reducibility* (y-axis) for each alternative threat hypothesis (n = 28). Each point represents the mean across experts with the horizontal bars representing estimated standard error for CVOI and the vertical bars representing estimated standard error for *reducibility*. Hypotheses are labeled by the hypothesis number, and colored based on the threat category shown in the legend. The vertical dashed black bar represents the median *reducibility* across all hypotheses for this species; the horizontal dashed black bar represents the median CVOI across all hypotheses for this species. See Table 5.2 for hypothesis names and descriptions.

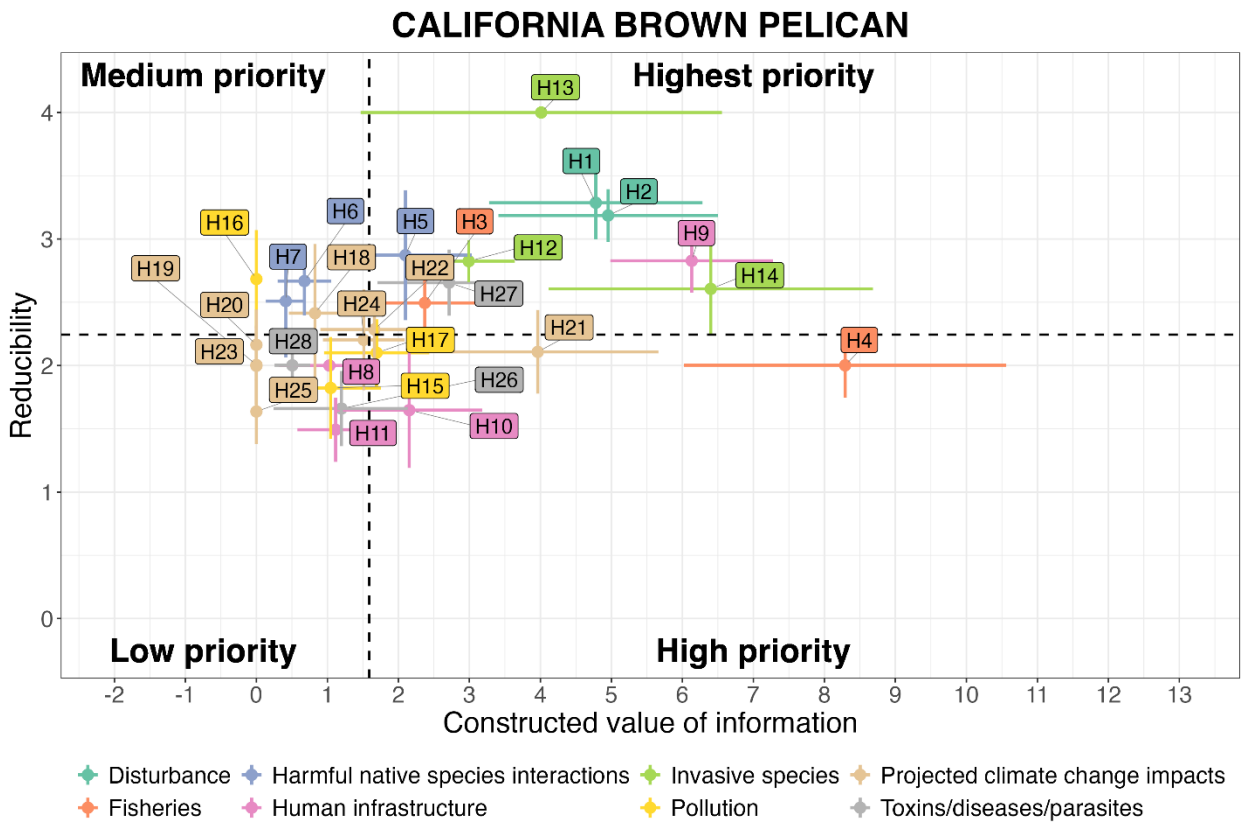

Figure 5.2 California Brown Pelican (BRPE): Mean CVOI (constructed value of information; x-axis) and *reducibility* (y-axis) for each alternative threat hypothesis (n = 28). Each point represents the mean across experts with the horizontal bars representing estimated standard error for CVOI and the vertical bars representing estimated standard error for *reducibility*. Hypotheses are labeled by the hypothesis number, and colored based on the threat category shown in the legend. The vertical dashed black bar represents the median *reducibility* across all hypotheses for this species; the horizontal dashed black bar represents the median CVOI across all hypotheses for this species. See Table 5.2 for hypothesis names and descriptions.

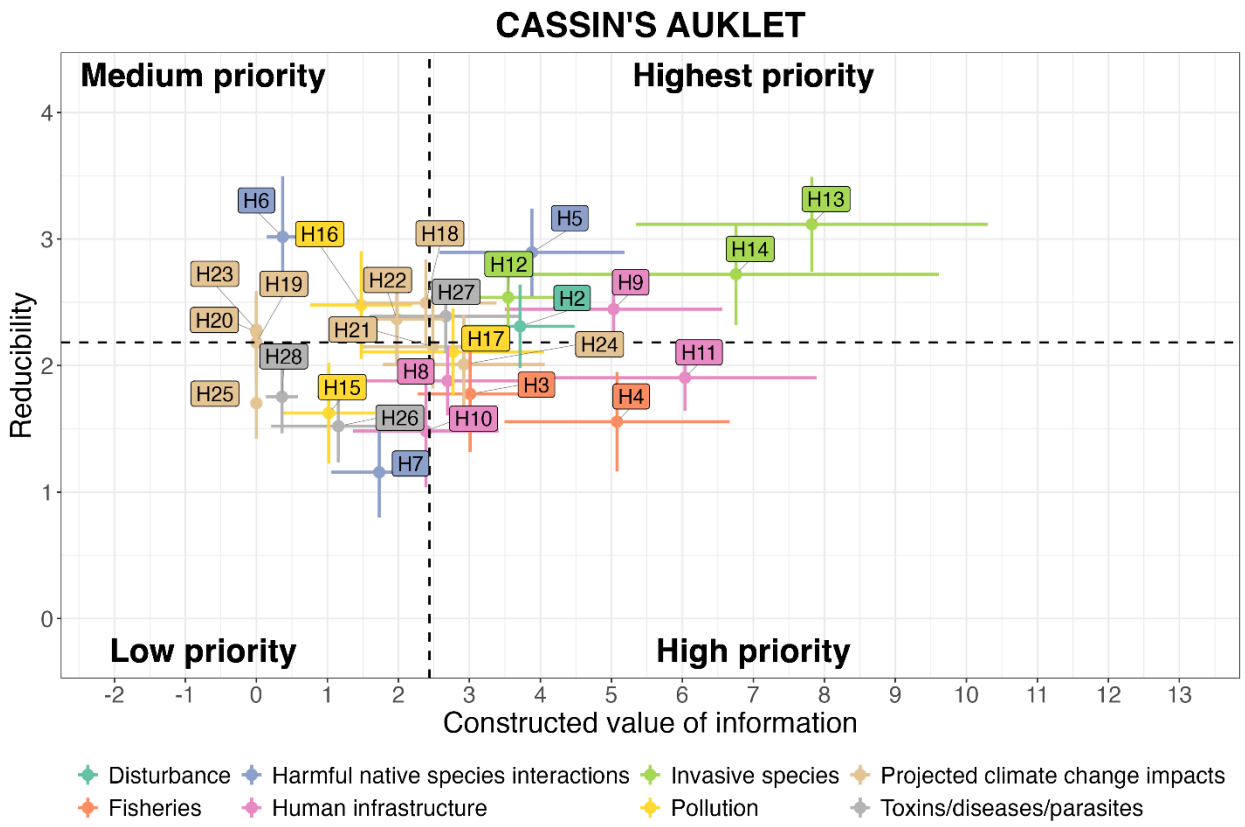

Figure 5.3 Cassin's Auklet (CAAU): Mean CVOI (constructed value of information; x-axis) and *reducibility* (y-axis) for each alternative threat hypothesis (n = 28). Each point represents the mean across experts with the horizontal bars representing estimated standard error for CVOI and the vertical bars representing estimated standard error for *reducibility*. Hypotheses are labeled by the hypothesis number, and colored based on the threat category shown in the legend. The vertical dashed black bar represents the median *reducibility* across all hypotheses for this species; the horizontal dashed black bar represents the median CVOI across all hypotheses for this species. See Table 5.2 for hypothesis names and descriptions.

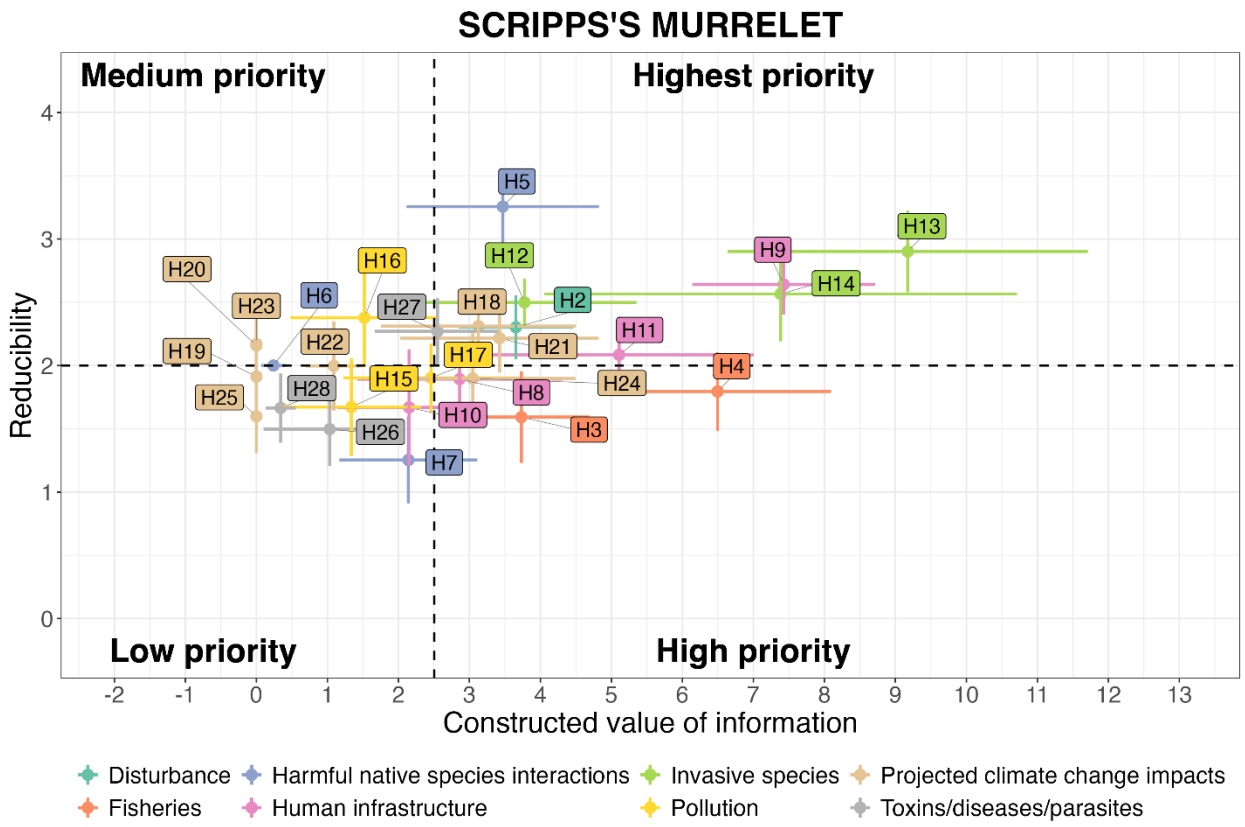

Figure 5.4 Scripps's Murrelet (SCMU): Mean CVOI (constructed value of information; x-axis) and *reducibility* (y-axis) for each alternative threat hypothesis (n = 28). Each point represents the mean across experts with the horizontal bars representing estimated standard error for CVOI and the vertical bars representing estimated standard error for *reducibility*. Hypotheses are labeled by the hypothesis number, and colored based on the threat category shown in the legend. The vertical dashed black bar represents the median *reducibility* across all hypotheses for this species; the horizontal dashed black bar represents the median CVOI across all hypotheses for this species. See Table 5.2 for hypothesis names and descriptions.

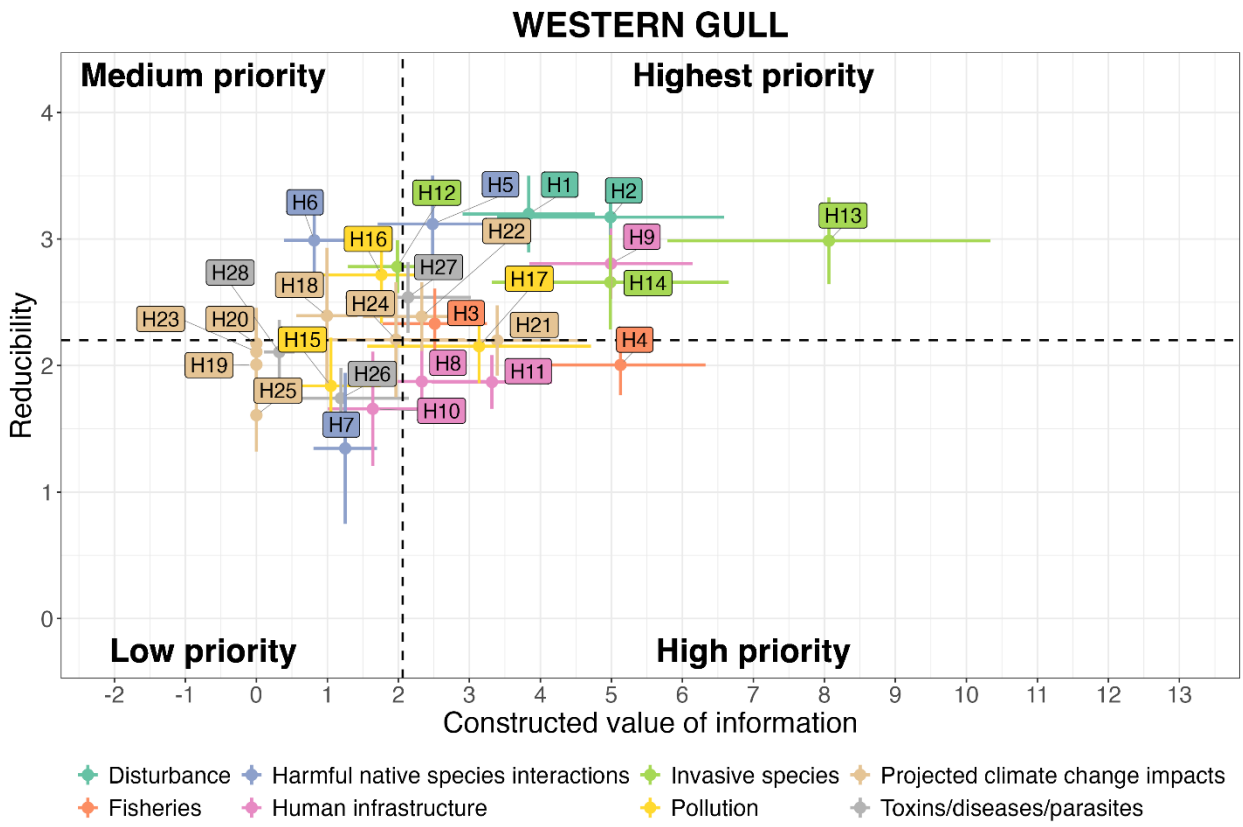

Figure 5.5 Western Gull (WEGU): Mean CVOI (constructed value of information; x-axis) and *reducibility* (y-axis) for each alternative threat hypothesis (n = 28). Each point represents the mean across experts with the horizontal bars representing estimated standard error for CVOI and the vertical bars representing estimated standard error for *reducibility*. Hypotheses are labeled by the hypothesis number, and colored based on the threat category shown in the legend. The vertical dashed black bar represents the median *reducibility* across all hypotheses for this species; the horizontal dashed black bar represents the median CVOI across all hypotheses for this species. See Table 5.2 for hypothesis names and descriptions.

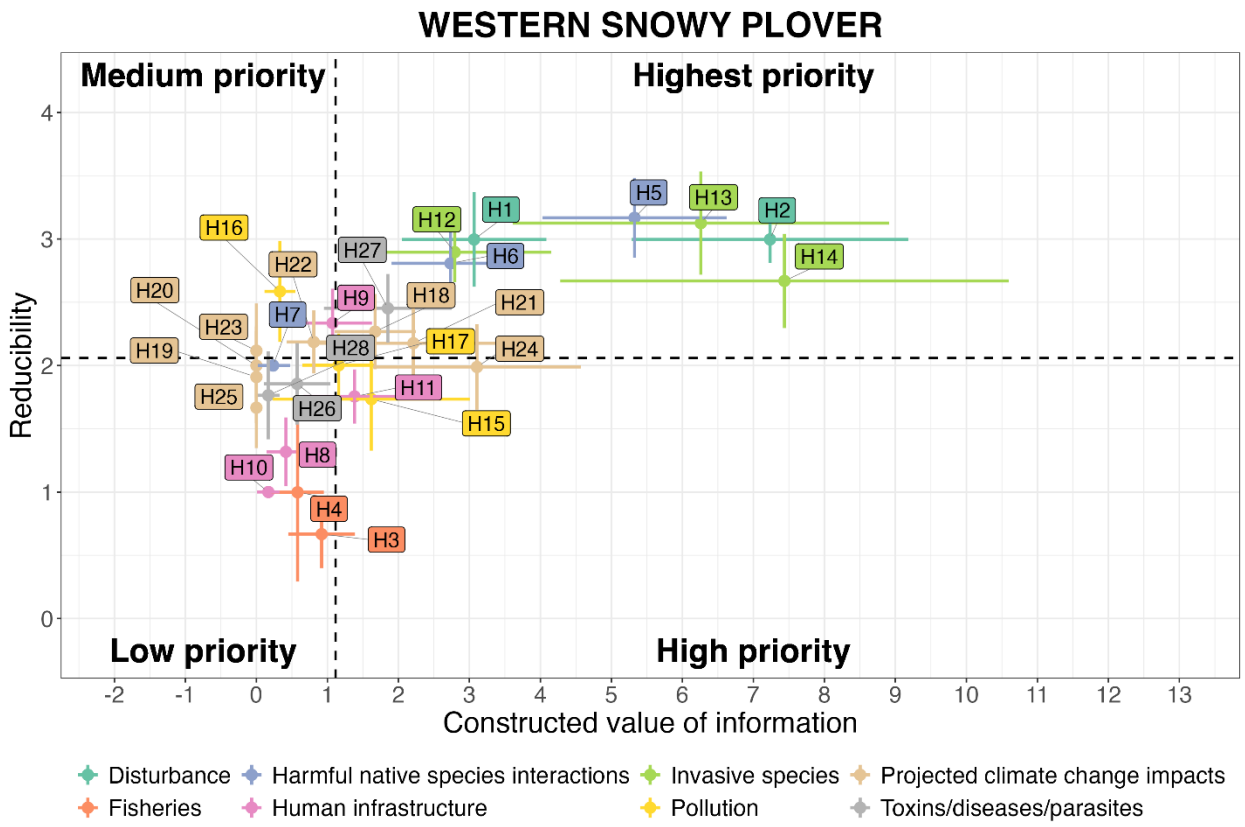

Figure 5.6 Western Snowy Plover (WSPL): Mean CVOI (constructed value of information; x-axis) and *reducibility* (y-axis) for each alternative threat hypothesis (n = 28). Each point represents the mean across experts with the horizontal bars representing estimated standard error for CVOI and the vertical bars representing estimated standard error for *reducibility*. Hypotheses are labeled by the hypothesis number, and colored based on the threat category shown in the legend. The vertical dashed black bar represents the median *reducibility* across all hypotheses for this species; the horizontal dashed black bar represents the median CVOI across all hypotheses for this species. See Table 5.2 for hypothesis names and descriptions.

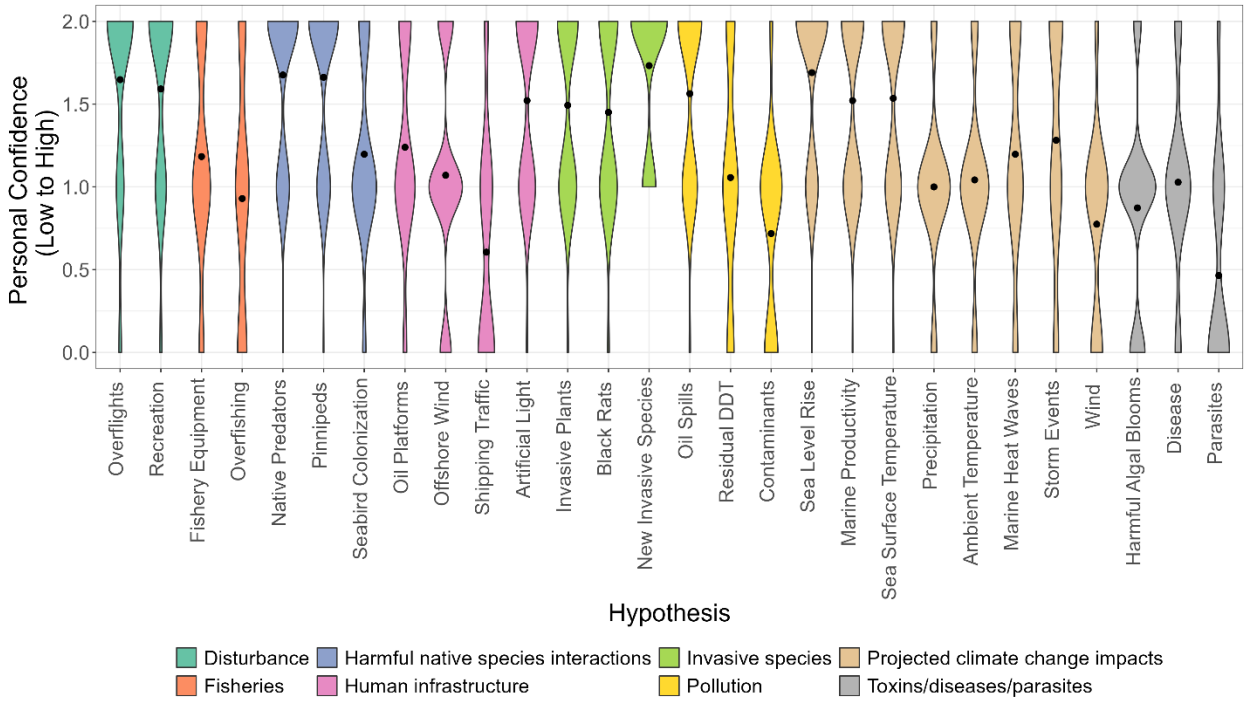

Figure 5.7 *Personal confidence* by hypothesis across all priority species. Hypotheses are on the x-axis and *personal confidence* scores on the y-axis, from low *personal confidence* to high *personal confidence*. Violin plots for each hypothesis are colored by threat category, shown in the legend below. Mean *personal confidence* by hypothesis is represented by a black dot.

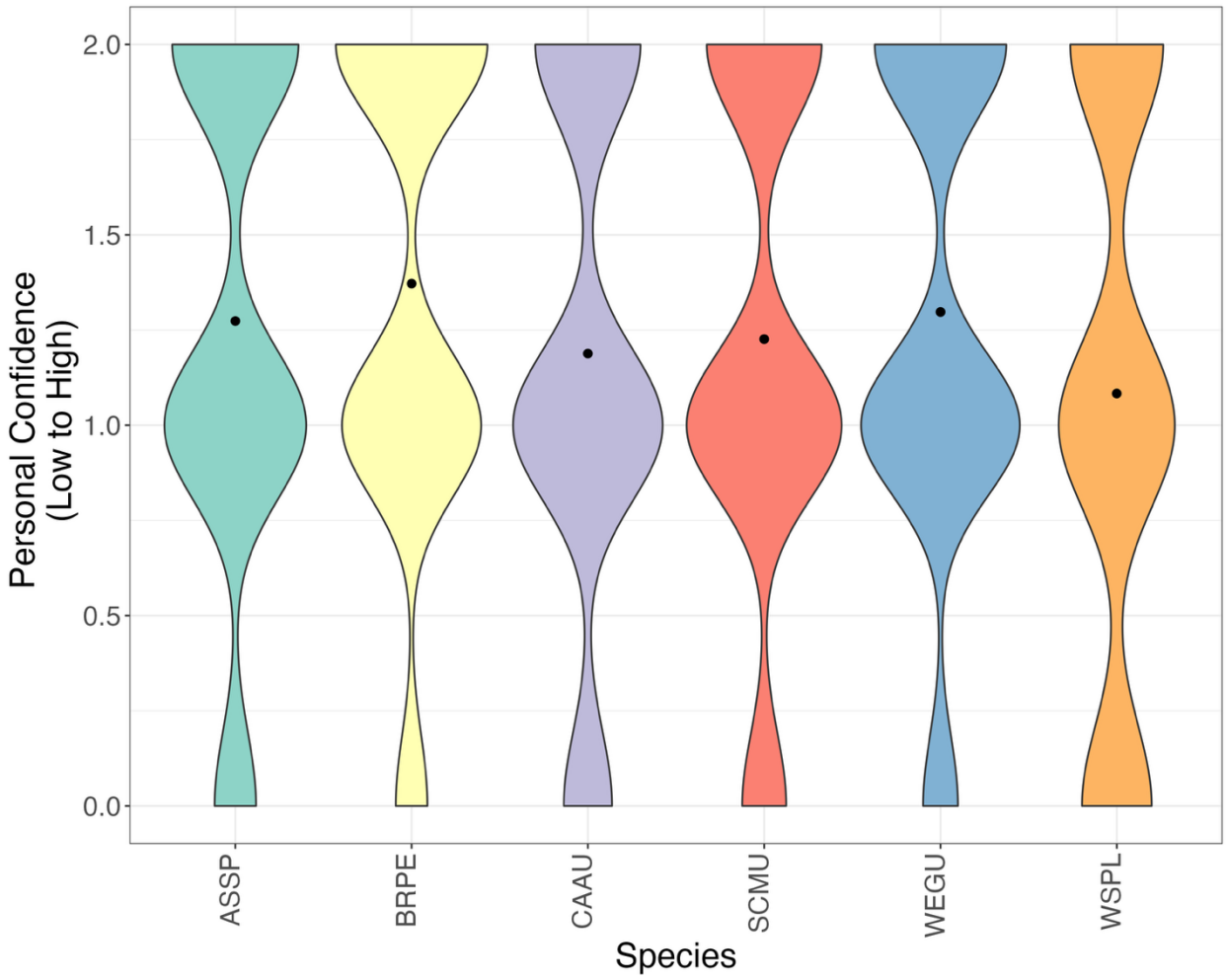

Figure 5.8 *Personal confidence* by priority species across all hypotheses. Species codes are on the x-axis (ASSP = Ashy Storm-Petrel, BRPE = California Brown Pelican, CAAU = Cassin's Auklet, SCMU = Scripps's Murrelet, WEGU = Western Gull, and WSPL = Western Snowy Plover) and *personal confidence* scores on the y-axis, from low *personal confidence* to high *personal confidence*. Mean *personal confidence* by priority species is represented by a black dot.

5.9 APPENDIX 5.1

Workshop attendees at Channel Islands National Park headquarters in Ventura, California, USA from 1-3 November 2022. Attendees are classified by role: Decision analysts help to structure, analyze, and guide the decision-making process; managers are those who have authority for decision-making; and experts are those who provided judgments. In some cases, participants held multiple roles.

Name	Organization	Role
Amelia DuVall	School of Aquatic and Fishery Sciences, University of Washington	Decision analyst
Andrew Dennhardt	Ventura Fish & Wildlife Office, U.S. Fish and Wildlife Service	Manager
Annie Little	Channel Islands National Park	Manager
Craig Stuart	Channel Islands National Marine Sanctuary	Manager
Dan Robinette	Point Blue Conservation Science	Expert
David Mazurkiewicz	Channel Islands National Park	Manager, Expert
David Pereksta	Bureau of Ocean Energy Management	Expert
Jim Howard	California Institute of Environmental Studies	Expert
Keith Lombardo	NPS Southern California Research Learning Center	Manager
Ken Convery	Channel Islands National Park	Manager
Marc Romano	Pacific Seabird Program, U.S. Fish and Wildlife Service	Expert
Martin Ruane	Environmental Division, Naval Base Ventura County	Expert
Mike Parker	California Institute of Environmental Studies	Expert
Nick Holmes	The Nature Conservancy	Manager, Expert
Russell Bradley	Santa Rosa Island Research Center, California State University Channel Islands	Expert
Sarah Converse	U.S. Geological Survey, Washington Cooperative Fish and Wildlife Research Unit, School of Environmental and Forest Sciences & School of Aquatic and Fishery Sciences, University of Washington	Decision analyst
Scott Sillett	Smithsonian Migratory Bird Center	Expert
Stacey Ostermann-Kelm	NPS Inventory & Monitoring Division, Mediterranean Coast Network	Manager

5.10 APPENDIX 5.2

Alternative management actions (n = 41) identified to address alternative threat hypotheses. Actions are grouped by threat categories and described according to management authority (i.e., whether Channel Islands National Park has the jurisdiction to implement the action), management feasibility (i.e., whether effective implementation has precedent), and management timing (i.e., whether the action requires one-time or ongoing implementation).

Code	Potential management action	Management authority	Management feasibility	Management timing
		Disturbance		
A1	Increase flight height limits.	No	Yes	One-off Action
A2	Increase enforcement of drone ban.	Yes	Yes	Continuous Action
A3	Focus visitation in less sensitive areas.	Yes	Yes	One-off Action
A4	Increase public education and outreach on disturbance impacts.	Yes	Yes	Continuous Action
A5	Increase enforcement of closures.	Yes	Yes	Continuous Action
A6	Increase signage of closures.	Yes	Yes	One-off Action
		Fisheries		
A7	Ban or reduce number of lobster traps.	Partial	Yes	One-off Action
A8	Ban or reduce number of squid boats.	Partial	Yes	One-off Action
A9	Increase public education and outreach on entanglement risk.	Partial	Yes	Continuous Action
A10	Reduce catch limits for forage fish.	No	Yes	One-off Action
		Harmful native species interactions		
A11	Install predator-proof artificial habitat.	Yes	Yes	One-off Action
A12	Remove known predators.	Yes	Yes	Continuous Action

A13	Remove mammalian predators from breeding colonies.	Yes	Yes	Continuous Action
A14	Remove pinnipeds from breeding grounds.	Yes	Yes	Continuous Action
A15	Fence off nesting areas from pinniped use.	Yes	Yes	One-off Action
A16	Deter colonization of new species.	Yes	Yes	Continuous Action
Human infrastructure				
A17	Reduce or relocate oil development.	No	Yes	One-off Action
A18	Prevent offshore wind energy development.	No	Yes	One-off Action
A19	Reduce shipping traffic.	No	Yes	One-off Action
A20	Use non-disruptive lights on squid boats.	No	Yes	One-off Action
Invasive species				
A21	Reduce cover of invasive plant species.	Yes	Yes	Continuous Action
A22	Restore native habitat.	Yes	Yes	Continuous Action
A23	Eradicate black rats.	Yes	Yes	One-off Action
A24	Control black rat populations.	Yes	Yes	Continuous Action
A25	Improve enforcement of dog ban.	Yes	Yes	Continuous Action
A26	Install predator-proof artificial habitat.	Yes	Yes	Continuous Action
A27	Increase biosecurity measures and monitoring.	Yes	Yes	Continuous Action
Pollution				
A28	Update information on colony information and foraging areas to relevant agencies.	Yes	Yes	One-off Action
A29	Expand resources/training/certifications at CHIS to respond to oil spills.	Yes	Yes	Continuous Action
A30	Remove remaining DDT barrels from marine environment.	No	Unknown	One-off Action
A31	Remove heavy metals from marine environment.	No	Unknown	Continuous Action

A32	Remove micro-plastics from marine environment.	No	Unknown	Continuous Action
A33	Remove macro-plastics from marine environment.	No	Unknown	Continuous Action
Projected climate change impacts				
A34	Create breeding habitat on high ground.	Yes	Yes	One-off Action
A35	Restore native habitat.	Yes	Yes	Continuous Action
A36	Mitigate drought via desalination and sprinklers.	Yes	Unknown	Continuous Action
A37	Install fencing to block sand movement.	Yes	Unknown	One-off Action
A38	Translocate individuals to more suitable habitat.	Partial	Yes	One-off Action
Toxins/diseases/parasites				
A39	Mitigate nearshore nutrification to ocean.	No	Yes	Continuous Action
A40	Administer HPAI vaccinations.	Yes	Unknown	One-off Action
A41	Administer anti-parasite medication.	Yes	Unknown	One-off Action

5.11 APPENDIX 5.3

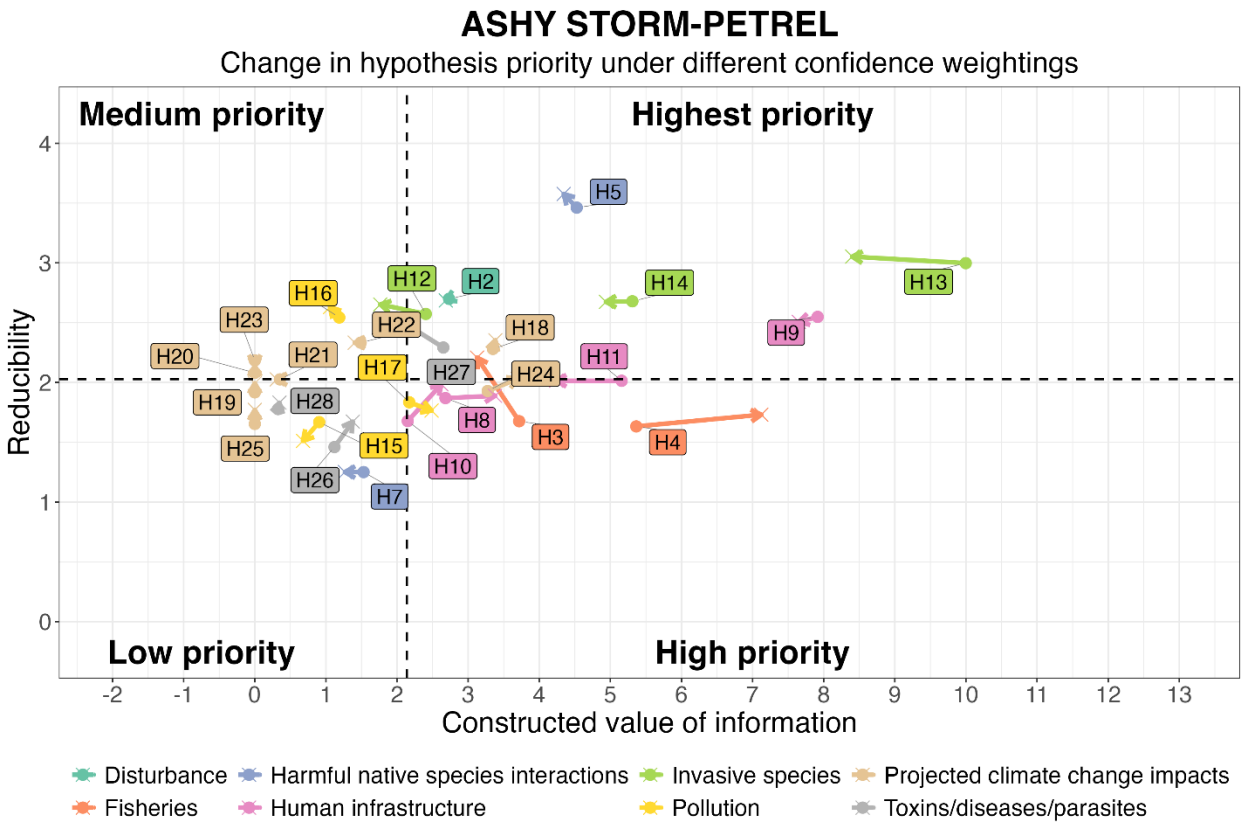

Appendix 5.3a Ashy Storm-Petrel (ASSP): Shifts in hypothesis prioritization under two confidence-weighting schemes: full personal confidence and linear personal confidence. Points represent mean constructed value of information (CVOI; x-axis) and mean *reducibility* (y-axis) for each hypothesis under full (circles) and linear (X) confidence weighting. Arrows indicate the direction and magnitude of change in prioritization between weighting methods. Dashed lines denote the median values of CVOI and *reducibility* across all hypotheses. Quadrants are annotated to indicate relative priority levels.

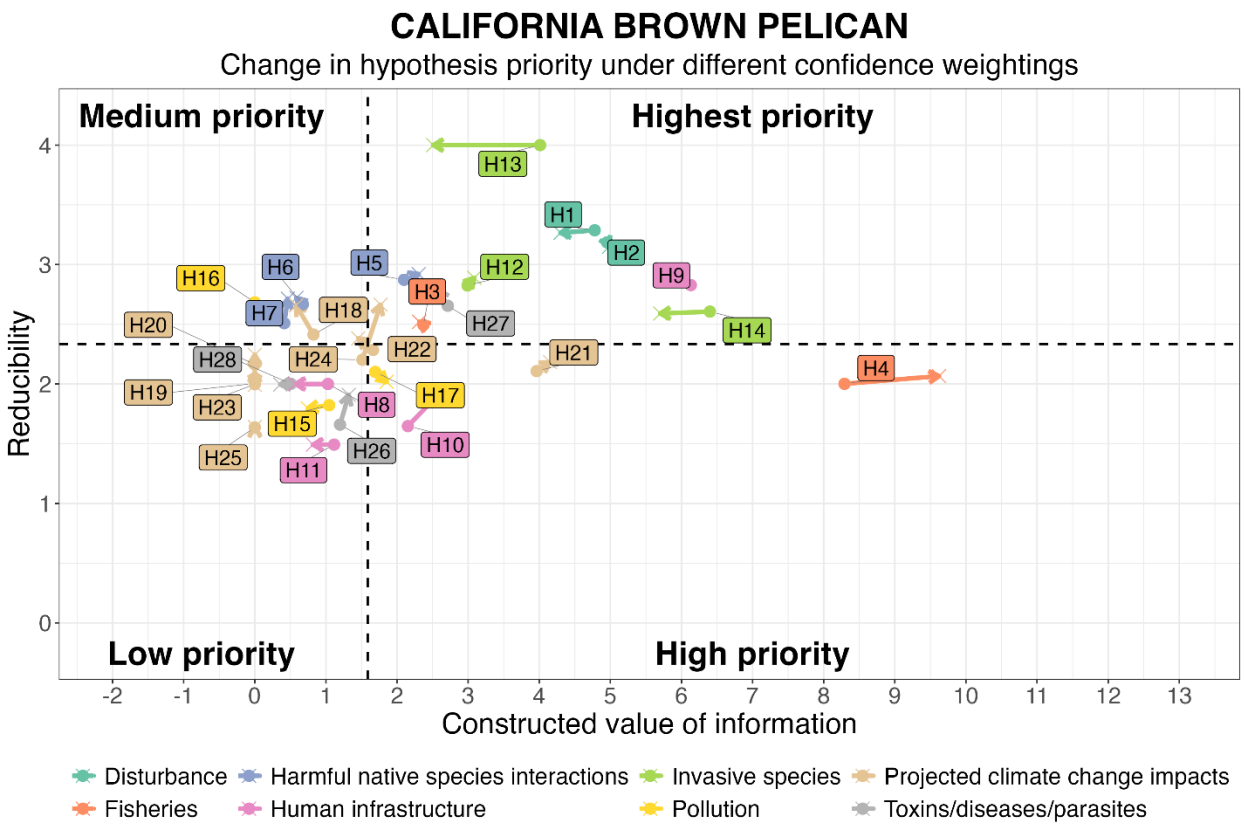

Appendix 5.3b California Brown Pelican (BRPE): Shifts in hypothesis prioritization under two confidence-weighting schemes: full personal confidence and linear personal confidence. Points represent mean constructed value of information (CVOI; x-axis) and mean *reducibility* (y-axis) for each hypothesis under full (circles) and linear (X) confidence weighting. Arrows indicate the direction and magnitude of change in prioritization between weighting methods. Dashed lines denote the median values of CVOI and *reducibility* across all hypotheses. Quadrants are annotated to indicate relative priority levels.

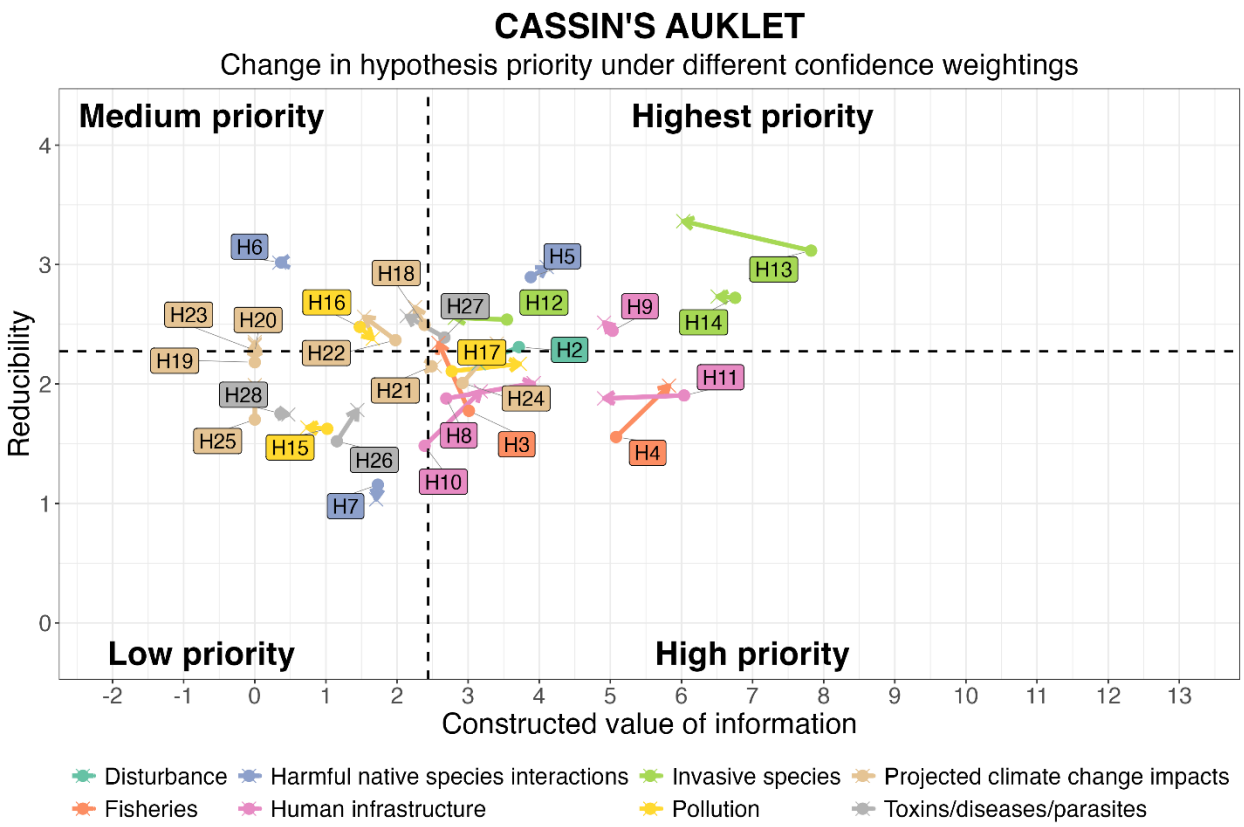

Appendix 5.3c Cassin's Auklet (CAAU): Shifts in hypothesis prioritization under two confidence-weighting schemes: full personal confidence and linear personal confidence. Points represent mean constructed value of information (CVOI; x-axis) and mean *reducibility* (y-axis) for each hypothesis under full (circles) and linear (X) confidence weighting. Arrows indicate the direction and magnitude of change in prioritization between weighting methods. Dashed lines denote the median values of CVOI and *reducibility* across all hypotheses. Quadrants are annotated to indicate relative priority levels.

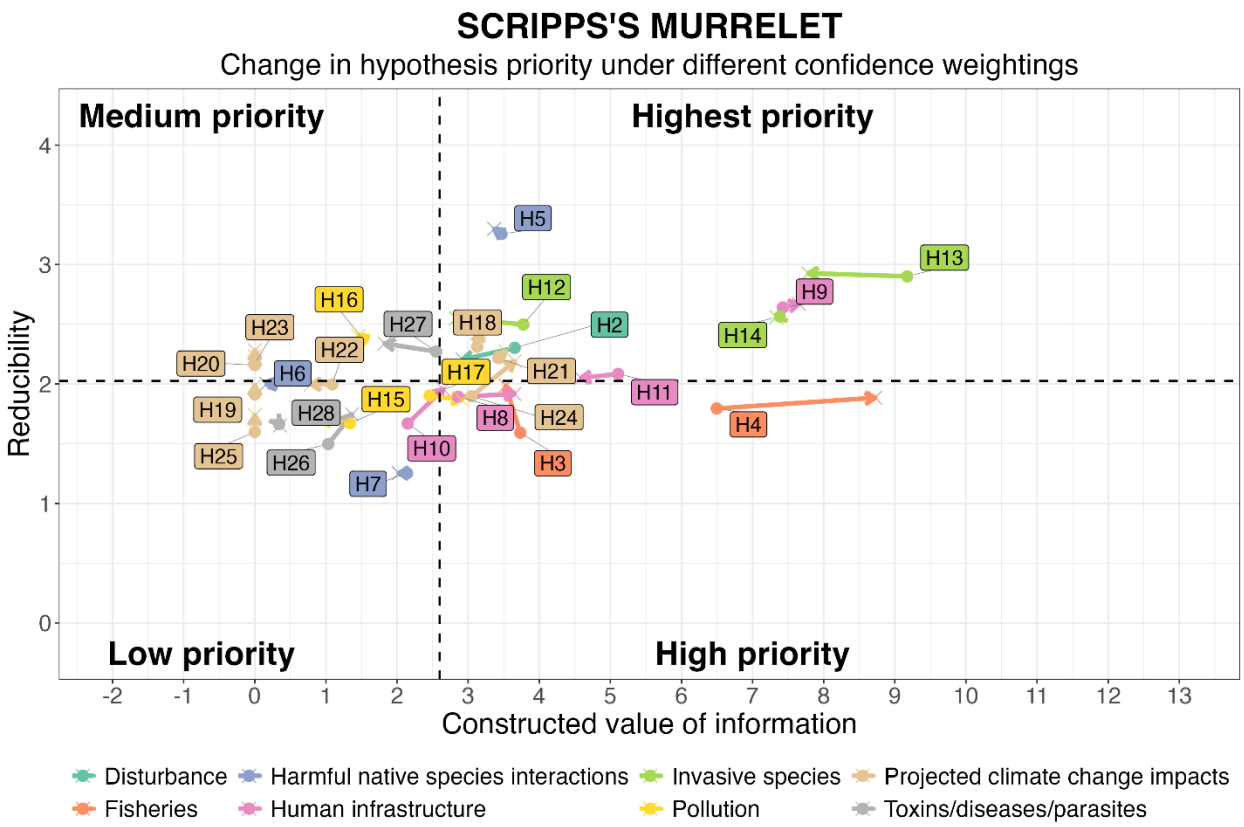

Appendix 5.3d Scripps's Murrelet (SCMU): Shifts in hypothesis prioritization under two confidence-weighting schemes: full personal confidence and linear personal confidence. Points represent mean constructed value of information (CVOI; x-axis) and mean *reducibility* (y-axis) for each hypothesis under full (circles) and linear (X) confidence weighting. Arrows indicate the direction and magnitude of change in prioritization between weighting methods. Dashed lines denote the median values of CVOI and *reducibility* across all hypotheses. Quadrants are annotated to indicate relative priority levels.

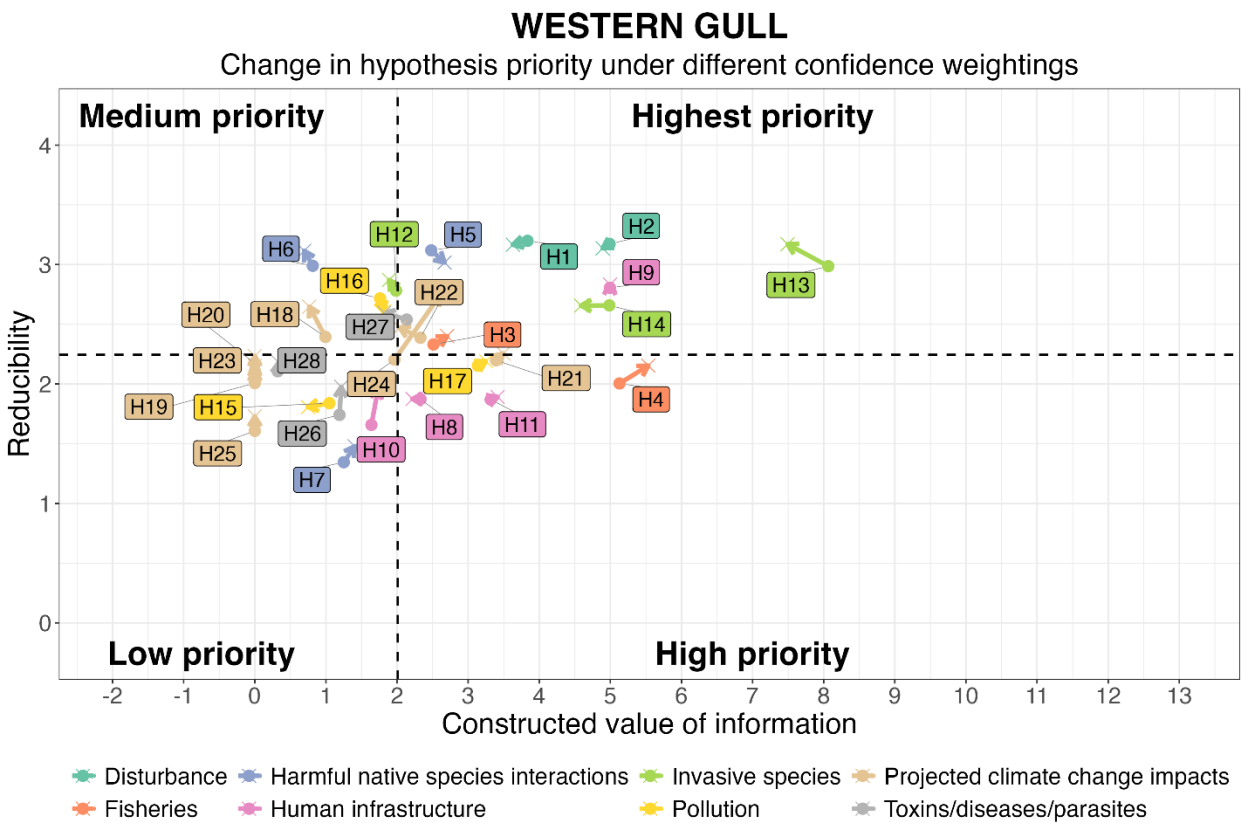

Appendix 5.3e Western Gull (WEGU): Shifts in hypothesis prioritization under two confidence-weighting schemes: full personal confidence and linear personal confidence. Points represent mean constructed value of information (CVOI; x-axis) and mean *reducibility* (y-axis) for each hypothesis under full (circles) and linear (X) confidence weighting. Arrows indicate the direction and magnitude of change in prioritization between weighting methods. Dashed lines denote the median values of CVOI and *reducibility* across all hypotheses. Quadrants are annotated to indicate relative priority levels.

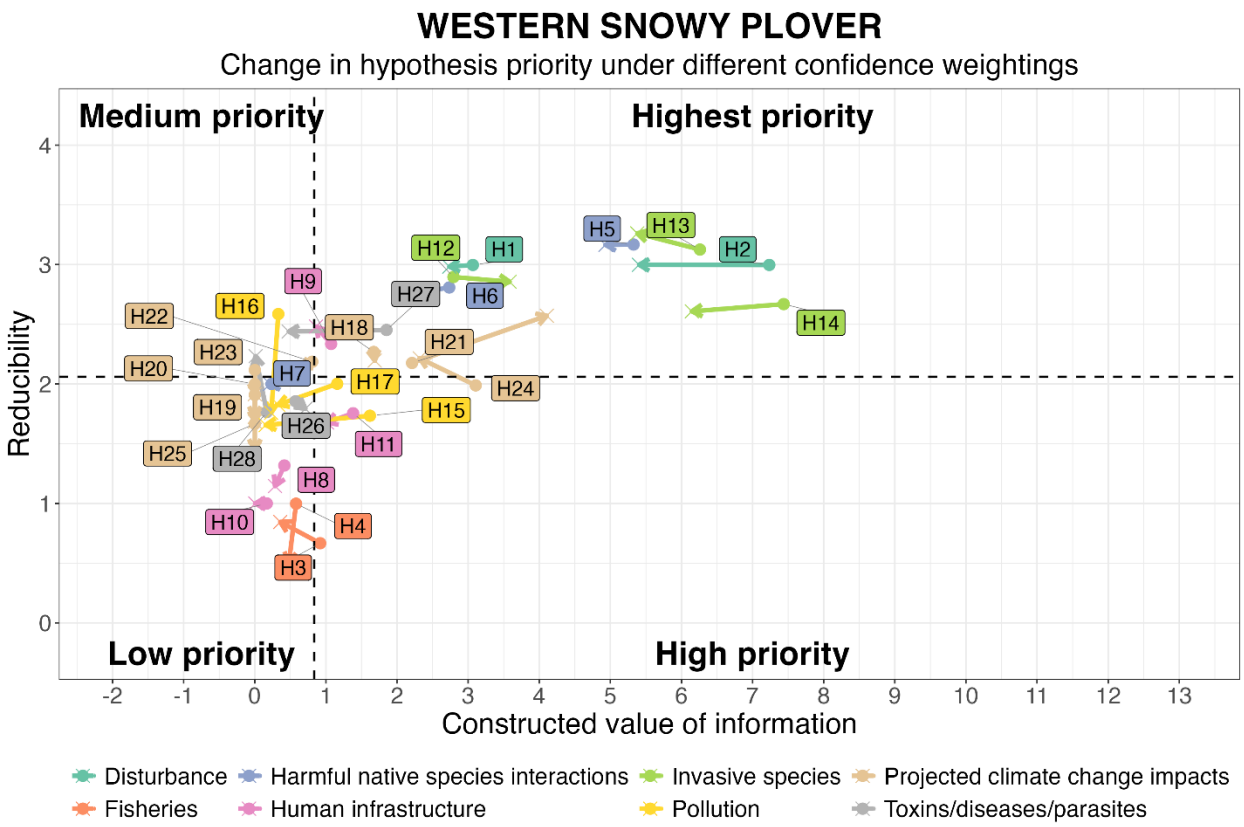

Appendix 5.3f Western Snowy Plover (WSPL): Shifts in hypothesis prioritization under two confidence-weighting schemes: full personal confidence and linear personal confidence. Points represent mean constructed value of information (CVOI; x-axis) and mean *reducibility* (y-axis) for each hypothesis under full (circles) and linear (X) confidence weighting. Arrows indicate the direction and magnitude of change in prioritization between weighting methods. Dashed lines denote the median values of CVOI and *reducibility* across all hypotheses. Quadrants are annotated to indicate relative priority levels.